NOVEL MESOPOROUS SILICATES AS INDOOR AIR POLLUTANT SCAVENGERS

Claire J. Robertson

Supervisor: Dr Lorraine T. Gibson

Department of Pure and Applied Chemistry
University of Strathclyde

A thesis submitted to the Department of Pure and Applied Chemistry, University of Strathclyde, in part fulfilment of the requirements for the degree of Doctor of Philosophy.

May 2008

Acknowledgements

Firstly I would not have been able to carry out this research if was not for the support and guidance of Dr Lorraine Gibson. If I had to start again tomorrow I wouldn't swap you for anybody else.

I would also like to thank the many people who have been involved in the project at various stages:

To Claire Watt for her initial hard work in getting the project started and giving me a platform to build upon.

To Jim Tate at the National Museum of Scotland for taking time out and allowing the use of their ESEM.

To all at Glantreo and University College Cork who made my visit so worthwhile. Special thanks go to John Hanrahan, Joe Tobin and Aiofe Burke for taking time out to help me use the XRD, TEM, SEM and BET.

To Jim Druzik and Herant Khanjian at the Getty Conservation Institute for their time and advice.

A special thanks to all at Strathclyde University and Glasgow University who helped during the project; Brian Cooksey Jack Brown, Dawn Wallace, John Reglinski, Allison Drummond, Barbara Balfour, Kate Reid, Gavin Bain, Margaret Adams, David McKay, and Justin Hargreaves.

To all the PhD students and post docs past and present (Ann, Andrew, Claire, Pamela, Nicci, David & Kenny). We've shared many a late night, some of which

weren't even alcohol related! The long hours spent in the office have been a pleasure mainly due to the hilarious topics of conversation (apologies to Dave and Kenny for putting up with the count down to NY). To all the final year project students who have contributed to the project over the three years (Stephanie, Victoria, Marianne and Simon).

To Russell, you have an incredible talent to make me forget about work when things aren't going well. Most of the time this has involved you dragging me to the beach and me then subsequently freezing the outer extremities of my body. But hey at least this gave me something else to curse about! On a more serious note a big thank you for your constant and unwavering support. And Mum & Dad for letting me doss under their roof for the past three years.

Abstract

A mesoporous silicate has been developed for the removal of volatile organic compounds (VOCs). The indoor air pollutants of interest were formaldehyde, toluene, ethylbenzene, o-xylene, cumene and dichlorobenzene. The indoor air pollutants were actively sampled onto (i) Tenax filled sampling tubes and subsequently analysed by thermal desorption gas chromatography mass spectrometry or (ii) chemically modified C_{18} silica cartridges analysed by high performance liquid chromatography ultraviolet spectroscopy. A pollutant atmosphere suitable for testing the sorbents chambers were created in-house.

Mesoporous silicates were synthesised to control the surface area, pore size and pore volume of the material. Several preparation methods were used to produce the final mesoporous silicate sorbent. The mesoporous silicates were mainly synthesised using tetraethyl orthosilicate as a precursor with either a quaternary ammonia silicate or triblock copolymer as the organic template synthesising MCM-41 and SBA-15, respectively. A selection of the successfully synthesised mesoporous silicates were modified with propyl amine to investigate the possibility of formaldehyde chemisorption. Material characterisation was performed using powder x-ray diffraction, transmission electron microscopy, scanning electron microscopy, nitrogen adsorption and elemental analysis. Sorbents were selected for adsorption efficiency testing based on the characterisation results. The synthesised mesoporous sorbent VOC and formaldehyde adsorption efficiencies were then compared with commercially available sorbents. It was observed that the commercial sorbents were inefficient at adsorbing both the formaldehyde and the selected VOCs. The modified

sorbents adsorbed formaldehyde strongly compared to the unmodified parent sorbent. However when using the modified mesoporous silicate an unwanted release of toluene was also recorded. Simulated closed environments were generated with the selected VOCs. SBA-15 was efficient in reducing the VOC chamber concentration over a period of 2 hours. SBA-15 adsorbed ethylbenzene, cumene and dichlorobenzene with efficiency rates of 89.4, 99.9 and 97.7 %, respectively. The adsorption efficiency for toluene was reduced at 35.4 %.

Table of Contents

1. INTRODUCTION

1.1. Indoor air pollution

Throughout our daily lives we spend a large majority of time indoors, whether that is at work or at home. It is therefore imperative that our quality of life is not impeded by poor indoor quality air. Air pollution has many sources and is often associated with industrial and transportation related emissions. However indoor air pollution can be caused by household products and materials. To ensure good quality air the levels of indoor air pollutants should be restricted to a minimum level either though prevention or removal.

1.2. Volatile organic compounds

Volatile organic compounds (VOCs) are the largest group of pollutants in the indoor environment and, on average, concentrations can be 10 times higher than outdoor levels.[1, 2] Several hundred VOCs with boiling points between 50-260 °C have been identified in indoor air. VOCs can be defined as organic compounds that have a high enough vapour pressure under normal conditions to vaporize and enter the atmosphere. Included in this category of pollutants are aromatic hydrocarbons, halogenated hydrocarbons, aldehydes and ketones. VOC classification has been extended to include very volatile organic compounds and semi volatile organic compounds which are classified with boiling points between <0-50 °C and 240-400 °C, respectively.[3] The presence of VOCs in indoor air is caused by their emission from building materials, paints, adhesives, furniture, carpets and household products.[4]

1.2.1. Effects of VOCs in indoor air in relation to human health

To improve energy loss in some buildings, air exchange rates are reduced with an increased use of air conditioning systems. The reduction of air exchange with outdoor air has led to increasing levels of indoor-generated VOCs within indoor environments. Higher levels of VOCs within enclosed work place environments has been an associated factor with a condition named 'sick building syndrome' (SBS), first defined by the World Health Organisation in 1982.[5] Further contributing factors to SBS include poor lighting and contamination of heating ventilation and air conditioning systems. Victims of SBS often experience a range of symptoms from fatigue, headaches, eye nose and throat irritation, dry cough, dry skin, dizziness and nausea.[6] The symptoms observed from exposure to low level air pollutants are not indicative of any one air pollutant.[7] Furthermore indoor air can contain hundreds of different compounds in a wide range of concentrations.[7]

The levels at which VOCs are deemed damaging to humans depends on several factors. First the levels at which individual VOCs become irritants to humans is individual-based, therefore can vary widely. Individuals can become sensitised to VOCs after long periods of exposure. The evaluation of health effects caused by complex VOC mixtures is difficult. The effects of pollutants may be additive (Effect mix= Effect A + Effect B), synergistic (Effect mix > Effects of A and Effect B), antagonistic (Effect mix < Effect A + Effect B) or even independent from each other.[3] Pollutant compounds may interact and cause unexpected toxic effects which could not be expected from the known toxicity of individual components.[7]

1.3. Formaldehyde

One of the simplest VOCs associated with SBS is methanal, commonly known as formaldehyde, its chemical structure is shown in Figure 1.1.[8] It is the simplest of an organic group of chemicals called aldehydes.[8] Aldehydes are molecules containing a carbonyl (C=O) group with a hydrogen bound to the carbon atom.[9, 10] Formaldehyde is often encountered as formalin,[9] this is a colourless aqueous solution 37-50 % of formaldehyde containing methanol as a stabilizer.[11]

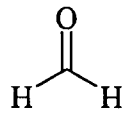

Figure 1.1: Chemical structure of Formaldehyde

Formaldehyde is an important industrial starting material and is produced worldwide on a large scale by catalytic, vapour phase oxidation of methanol.[8] It is used as a monomer for "Bakelite" or "Formica", trademark names for formaldehyde phenol polymer and formaldehyde urea polymer.[11] Formaldehyde is often used as a preservative or insulation and can be used in resins, wood products, particle board, plywood, construction materials, cosmetics, adhesives, paints, drug products and a variety of products around the home. [8, 12]

1.3.1. Formaldehyde in the museum environment

The presence of indoor air pollutants has a detrimental impact on items of cultural importance. Display cabinets are often used in museums to exhibit objects and to protect them from theft, physical damage, humidity, temperature variations and lighting.[13-15] Often, museum display cabinets are made from wood because of its

pleasing visual appeal and its ability to act as a humidity buffer by absorbing and releasing moisture. The cabinets are normally well sealed with low air exchange rates.[16] However wood and wood-related cabinets can also be detrimental to the items on display if the materials used to construct the cabinet emit pollutants. The presence of acetic acid is detrimental to many cultural items on display. Free acetic acid is present in woods and further acetic acid can be produced from the hydrolysis of acetyl groups in the hemicellulose component of wood, see Figure 1.2.[17] Softer woods such as pine contain fewer hemicelluloses and are therefore a better choice than hardwoods for cabinet construction.[16] The rate of acetic acid release is influenced by the temperature and relative humidity of the surrounding environment.[18] [19] Formic acid is also emitted from woods although at a much lower rate compared to acetic acid. It is thought that formic acid may form from formate esters present within the wood or from the splitting of pyruvic acid during the metabolic process.

where x is the sugar unit, either pentoses or hexoses.

Figure 1.2: production of acetic acid from hemicellulose in woods

With the associated problems with the production of the acetic acid and formic acid from hard woods cabinets alternative materials were sought for the construction of museum display cabinets. Particle board and wood chip based materials were considered viable alternatives. However particle boards are constructed with the use of formaldehyde based resins e.g. urea or phenol formaldehyde.[20] Unfortunately,

these materials also produce a volatile emission in the form of formaldehyde. The formaldehyde is produced through the reverse hydrolysis of the synthesis method used to produce the initial resin. The amount of formaldehyde released depends on the ratio of urea to formaldehyde present. Moreover formaldehyde is often added in excess to ensure adequate cross linking of the resin.[16] Reducing the mole ratio of formaldehyde to urea, reduces the free formaldehyde present therefore formaldehyde emission reduces.[21] Formaldehyde can also be released and form formic acid through the Canizzaro reaction, see Figure 1.3, whereby formaldehyde is oxidised by water.[8]

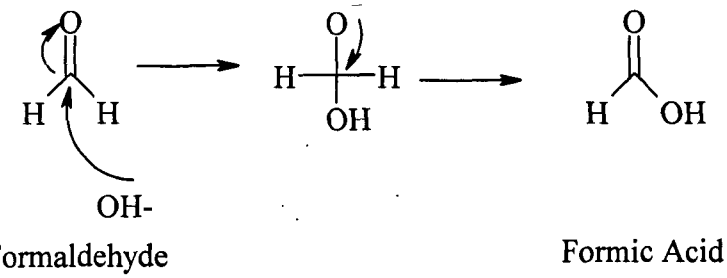

Figure 1.3: Canizzaro reaction

The sealed displays units allow the formaldehyde concentration to accumulate to levels whereby they become dangerous to the artefacts housed within them. In some instances the problem is further exacerbated when items on display themselves emit pollutants.[15, 22] When high concentrations of formaldehyde exist certain materials have been known to deteriorate. The extent of the degradation is dependent upon i) exposure time, ii) pollutant concentration iii) the composition/type of material exposed iv) temperature and v) relative humidity.[15]

The first documented degradation of materials on display was reported in 1899. Byne[23] reported on the deterioration of marine shells in public museums and commented on a "grey efflorescence both tasting and smelling strongly of vinegar, covers the whole surface like a powder, rising doubtless from the interior, and specimens are almost irretrievably ruined". The deterioration "occurs principally amongst shells kept in drawers in the dark, where air is confined and seldom changed". Byne came to the conclusion that the main cause of the corrosion was as a result of butyric acid upon the calcium carbonate of shells and that the presence of butyric acid was derived from the decay of the pieces of animals left in shells. Byne determined the action of acetic acid on the shells was solely due to the gum used to attach the shells on display and this played a minor role in the degradation compared to the butyric acid. Later this was more accurately attributed by Nicholls as the effect of acetic acid from wooden cabinets.[24] Since Byne's discovery there have been many instances of artefact degradation attributed to pollutants generated within museum enclosures.

To investigate the damage caused by formaldehyde Streigel[25] created an environment inside a dynamic exposure chamber using a permeation device. Glass, shells, ceramics glazes, metal and alloys were exposed to a formaldehyde concentration of 1226 $\mu g\ m^{-3}$. The items were removed after a period of 100 days and analysed for signs of degradation. The surface of the glasses and ceramic showed no signs of degradation, however the exposure of glass is expected to result in the formation of sodium formate.[26] The shells were examined by surface microscopy and signs of efflorescence were noted. Metals were the most susceptible to degradation after the

exposure to formaldehyde. After 30 days 44 % of the metals studied showed conclusive signs of degradation, after 100 days 78 % of the metals showed definitive degradation. Based on visual observations the sensitivity of metals to formaldehyde is lead > bronze> brass> zinc> copper> sterling silver> silver. The rate of corrosion is dependent on the relative humidity of the environment.[26] [19] It has been reported that formaldehyde effects protein based materials like gelatine, animal glue and casein due to crosslinking which results in brittleness, denaturing and loss of elasticity.[26]

1.4. Sampling methods for indoor air pollutants

Sampling methods, required to detect indoor air pollutants, can occur in two different modes: active or passive. Active sampling involves extracting a known volume of air from the chosen atmosphere through a trapping device using a pump. Passive sampling methods are based on the diffusion of the pollutants through a concentration gradient to a trapping medium. The movement of the pollutant is described by Fick's first law of diffusion, which states that the flux of the pollutant is proportional to the concentration gradient in the sampling unit.[27] This method of sampling is often time consuming and sampling times are often in the region of days or weeks (compared to minutes or hours used in active sampling methods) giving time weighted average concentrations. However, passive sampling does have the advantage that no mechanical equipment is required to pump the sample of air to the sorbent. This method is therefore preferred for sampling within the museum environment due to a number of advantages such as: a lack of noise during sampling, ease of introduction of passive samplers into display units, as well as being a low cost method of analysis.[27]

When sampling indoor air a large number of pollutants can be potentially absorbed onto the sampling sorbent if a non-specific trapping medium is used. Trapping mediums can be chemically modified to trap specific pollutants of interest, e.g. doping silica cartridges with 2-4 dinitrophenylhydrazine (2,4- DNPH) to trap aldehydes, or potassium hydroxide for the detection of acetic and formic acid.[28] Once the sample has been successfully trapped from the selected polluted areas further sample treatment may be required to remove the trapped analytes from the sorbent before chromatographic analysis and determination of the pollutants present. Normally either solvent or thermal desorption is required as a pre-treatment method prior to analysis. With solvent desorption a suitable solvent is used to strip the analyte from the sorbent. An aliquot of the solvent desorbed sample is then analysed by a chromatographic technique.[29] Carbon disulfide is an example of a solvent used for desorption of analytes from activated charcoal, the analysis is preformed by gas chromatography (GC) flame ionisation detection (FID).[29] Baya *et al*[30] used acetone to solvent desorb VOCs from Tenax and Anasorb CMS (carbon molecular sieve). Occupational health and safety administration (OSHA) for the US Department of Labour uses active sampling in conjunction with solvent desorption methods for the detection of methanol and ethanol (OSHA methods 91 & 100). Here the sorbent used is Anasorb 747 with a mixture dimethylformide and carbon disulfide as the solvent used for desorption.[31, 32] The OSHA method 52 for the detection and quantification of formaldehyde uses toluene to solvent desorb formaldehyde from Amberlite XAD-2 resin coated in hydroxymethyl piperdine.[33]

During thermal desorption (TD) the sorbent is subject to increased temperatures, which decreases the sorbent-sorbate interaction strength thereby releasing the analytes for analysis. TD offers the advantage of the analysis of the whole sample rather than a re-diluted portion.[27] TD therefore offers higher sensitivity[3] and the absence of a solvent front that may interfere with chromatographic analysis of the eluted components.[27] A further advantage of TD, when post-analysis of eluted components is performed by gas chromatography, is that the eluted components are already in the gas phase before entering the chromatograph. There are also some disadvantages to the method of TD. The range of compounds available for use with TD is limited by the thermal stability of the sorbent and that the entire sample is consumed during a single analysis.

1.4.1. Common sampling methods for VOCs

For VOC detection sorbent sampling is the preferred method of sampling in combination with gas chromatography analysis as it offers sensitivity, selectivity and is convenient when thermal desorption is used.[27] When Tenax TA is used to actively sample VOCs, flow rates vary from 80 to 250 mL min^{-1} with thermal desorption temperatures between 250 and 300 °C.[34-38] To separate and analyse VOCs the methods generally used are gas chromatography mass spectrometry (GCMS)[2, 34-37, 39-41] or gas chromatography flame ionisation detection (GCFID)[38, 42-45]. The most common type of column used for the separation of non polar VOCs consists of 5% diphenyl 95% polydimethylsiloxane and are encountered under trade names such as DB-5, MDN-5S, CP-Sil 8, 5 % Ph Me silicone, SMS Elite.[34-36, 46, 47] It has been recommended by Mohave *et al*[3] that a GC column used to analyse non polar VOCs should not contain more than 8 % phenyl silicone. Alternative columns can be used

when separating polar VOCs such as HP 624 which contains 6 % cyanopropylphenyl.[42] Column parameters also vary with column lengths between 25 and 60 m, internal diameters of either 0.25 or 0.30 mm and a stationary phase film thickness within the range of 0.25 to 1.8 μm.[34-36, 42, 45, 47, 48] Oven heating programmes vary, although in general the starting temperature is around 40°C, followed by either one or two temperature ramps to approximately 220 °C, a temperature which may be held for a short period of time.[2, 35, 37, 38, 40-42, 44, 45, 49] Detection of the analytes is commonly by mass spectrometry[2, 34-37, 41] (scans are performed for a m/z range of 30-500) or FID.[38, 42, 44, 45, 49]

1.4.1.1. VOC concentrations in indoor air

The concentration of VOCs indoors depends on the source emission rate(s), the air exchange rate, the sorption properties of the room and potential chemical reactions.[50] The concentration of VOCs present show some seasonal variation[51, 52] in some cases the concentration of VOCs present in the winter is up to three times higher than in the summer.[2] The number of VOCs present in indoor air can be extremely high. A study of 26 houses identified over 200 compounds and 54 of these were identified as aromatic hydrocarbons.[34] A recent study showed the distribution of VOCs in air as 15% aromatic hydrocarbons, 10% aliphatic hydrocarbons, 16% terpenes, 15% alcohols, 12% aldehydes and 15% were unidentified compounds.[36] With a large amount of VOCs present it is not always practical to identify each individual analyte present on every sample. Often the total level of VOCs present is given by the term total volatile organic compounds (TVOC). TVOC levels are often incomparable in

the literature due to the different combinations present which contribute to the TVOC concentration. Therefore it is important to clearly define the specified range of VOCs included in the term TVOC. In a study by Hippelien[36] looking at VOC concentrations in indoor air. The three highest recurring VOCs present were toluene, ethylbenzene and o-xylene at 100%, 96.2% and 97.5%, respectively. In the study by Kostiainen[34] cumene and 1,2 dichlorobenzene occurred in 96 and 92 % of the houses studied, however the concentration at which these VOCs where present was lower then toluene. Typical levels of toluene ethylbenzene and xylene are between 10-100, 1-10 and 1-10 $\mu g\ m^{-3}$, respectively.[2,34,36,40,47,51,53,54] In comparison outdoor concentrations of toluene, ethylbenzene and o-xylene ranged upwards from 0.52, <0.01 and 0.1 $\mu g\ m^{-3}$, respectively.[53] From the literature obtained toluene, ethylbenzene and xylene where present in 100% of the buildings termed as sick. In houses that were designated as 'sick' the concentration of toluene, ethylbenzene and o-xylene ranged from 4.6 -2326, 2.25-747 and 1.74-1101 $\mu g\ m^{-3}$, respectively.[34] The VOCs selected for this study were toluene, ethylbenzene, o-xylene, cumene and dichlorobenzene. The physical properties of the VOCs studied are given in Table 1.1

Table 1.1: Physical properties of the VOCs studied[55]

	Boiling Point / °C	Vapour Density •	Liquid Density / g mL^{-1}	Molecular Weight	Vapour Pressure/ N m^{-2} at 20°C
Toluene	111	3.14	0.87	92.14	2933
Ethylbenzene	136	3.66	0.87	106.17	1105 ♦
o-Xylene	137-140	3.7	0.88	106.17	1067
Cumene	152	4.1	0.86	120.20	1067
Dichlorobenzene	39.8	2.9	1.30	147	133 ♦

• *vapour density relative to air*

♦ *vapour pressure taken at 25 °C*

1.4.2. Sampling methods for formaldehyde vapour

Formaldehyde vapour detection is most often associated with the use of a derivitisation agent from which the levels of formaldehyde can be quantified. A common derivitisation agent is 2,4-DNPH. When exposed to formaldehyde a hydrazone derivative is formed known as formaldehyde-dinitrophenylhydrazine or f-DNPH (NIOSH Method 2016).[56] This reaction is not specific to formaldehyde as both aldehydes and ketones will undergo the same reaction. To sample the formaldehyde in the atmosphere using 2,4-DNPH a solid support is required in which the 2,4-DNPH is loaded or doped onto e.g. filter paper or silica. Both passive and active sampling can be utilised using this method in the form of passive sampling tubes and cartridges filled silica functionalised with C_{18}, respectively. The reacted and un-reacted 2,4-DNPH are removed from the support medium through solvent desorption with acetonitrile. Quantitative determination of f-DNPH is possible through UV-vis as the molecule contains a chromophore. High performance liquid chromatography is essential for this analysis to separate the reacted and unreacted dinitrophenylhydrazine and because the reaction is not specific to formaldehyde. Solid phase microextraction fibres coated with the trapping reagent *o*-(2,3,4,5,6-pentafluorobenzyl)hydroxylamine hydrochlororide (PFBHA) can be used to trap formaldehyde vapour through the production of the stable formaldehyde –PFBHA oxime. The production of the oxime is proportional to the formaldehyde vapour present and is detected by GC-FID.[57, 58]

An alternative colourimetric method for the detection of formaldehyde is the use of chromotropic acid (NIOSH Method 3500).[59] On exposure to formaldehyde the solution of heated 1 % w/v chromotropic acid in concentrated sulphuric acid (97 % w/v) a purple species is produced in solution. Recently sol-gels doped with Schiffs reagent have been used as a new colourimetric sensor to detect formaldehyde. Sol-gels provide a solid support which acidified pararosaniline and sodium sulfate can be doped. When exposed to formaldehyde the doped sol-gels change colour from yellow to purple. The colour change can be measured directly using a bench top spectrometer or a portable hand held UV-vis spectrometer.[60]

In 2005 a novel colourimetric sensor was developed by Kawamura *et al*[61], where an acidic solution of 4 amino hydrazine 5 mercapto-1,2,4 triazole mixed on a 1:1 ratio with a potassium hydroxide aqueous solution. This solution was then deposited on a glass filter chip. When exposed to formaldehyde a colour change to purple was recorded with a photodiode LED combination at 540 nm. Advantages of this technique were: an extremely fast response time of 3 minutes, the stability in a range of relative humidities and a limit of detection of 0.04 ppm. When this method was compared with the traditional 2,4-DNPH method similar detection results were obtained. This method of detection of formaldehyde has been incorporated into a hand held formaldehyde sensor.

The detection of formaldehyde is not solely by colourimetric methods. In 1997 Thomas et al. [62] used thermal desorption gas chromatography mass spectrometry to

detect formaldehyde based on the reaction with 2-hydroxymethylpiperidine to produce the volatile derivative hexahydrooxazolo[3,4-α]pyridine. Active sampling was used to pass formaldehyde over a denuder tube coated with the derivitisation reagent. The denuder tube was connected to a Tenax filled sampling tube which would subsequently trap the volatile hexahydrooxazolo[3,4-α]pyridine. Through thermal desorption gas chromatography mass spectrometry quantitative detection was obtained.

The main methods for the detection and quantification has mainly involved colourimetric and chromatographic techniques. Alternative novel methods for the detection of formaldehyde include electric sensors, piezo electric crystals, laser induced photo acoustic spectroscopy and fluorescent methods.

Helaleh *et al*[63] developed a fluorimetric method for the detection of gaseous formaldehyde. A trapping reagent of hydralazine in boric acid was used to form a droplet at the end of a stainless steel capillary, onto which formaldehyde would be adsorbed from the air. The product produced from the reaction was s-triazolo[3,4-a] phthalazine, a highly fluorescent compound, with an excitation wavelength of 236 nm and an emission wavelength of 389 nm.

Dirksen *et al*[64] first used NiO thin films as an electric sensor in 2001, a 0.4 μm film of NiO on an aluminium substrate with silver paste electrodes attached to the NiO surface. On exposure to formaldehyde the voltage increase was linear at 0.825 mV ppm^{-1}. However the limit of detection was above the recommended levels

outlined by OSHA and NIOSH. In 2007 Lee *et al*[65] enhanced the detection limit of the sensor to 0.9 ppm through a micro-hotplate used to heat the thin film. However the use of NiO films to detect formaldehyde is based on the oxidation reaction of formaldehyde on the NiO surface which produces formic acid as the final product. The formation of formic acid makes this method unsuitable as a detection method in a museum environment.

In 1983 piezo electric crystals were investigated as formaldehyde detectors.[66] The crystal was coated in formaldehyde dehydrogenase which in the presence of nicotinamide adenine dinucleotide catalysed the reaction of formaldehyde to formic acid. Thereby increasing the mass on the crystal and decreasing the frequency of vibration of the crystal. Linear responses were obtained from 10 ppb to 10 ppm. The enzyme coating was specific to formaldehyde with little responses obtained for other small aldehydes and alcohols. Recently, Feng at al[67] developed a formaldehyde sensor that incorporated a molecular imprinted polymer and a quartz crystal balance. In using a molecular imprinted polymer a cavity was produced in the polymer that would accept a formaldehyde molecule. As the mass increases through the trapping of formaldehyde the resonant frequency of the quartz crystal balance decreases. The linear range of the technique was between 1.25-14.25 μM. However acetic ether and acetone gave similar responses as formaldehyde.

1.4.2.1. Museum sampling methods used for the detection and quantification of formaldehyde

To determine if a material is suitable for use in a museum enclosure small sections of the material are tested for the release of harmful vapours. The simplest of these tests

involves the use of metal strips or coupons. In the Oddy test[13,68] the suspect material, along with a polished strip of metal, is placed inside a sealed glass test tube or conical flask. The test tube is then heated to 60 °C for a period of 28 days, after which the metal coupon is visually examined for degradation to determine if the material is suitable for museum enclosures. A similar method is used to determine if an enclosure is detrimental to sensitive materials, through the exposure of polished strips of metal within the enclosure. Polished strips of copper, lead and silver normally used. If corrosion is observed then the enclosure is deemed detrimental to sensitive materials.[22] The corrosion of lead indicates the presence of organic carbonyl pollutants such as formaldehyde. However in situations where the concentration of the pollutants is low the use of the coupon test is not sensitive enough.[22] The use of metal coupons do not allow for the identification of the pollutants nor the pollutant concentration levels.[22, 69] Therefore passive and active sampling is required in enclosures.

Active sampling can be used in conjunction with Dräeger tubes. Dräeger tubes contain specific chemicals which undergo a colour change when the target pollutant is present. The Dräeger tube are externally marked and depending on the depth to which the colour change occurs in the sorbent bed gives an approximate concentration.[70] The use of Dräeger tubes are more suited to higher formaldehyde concentration levels and not suitable for museum levels.[69, 71]

Passive sampling tubes have been developed for the monitoring of formaldehyde, acetic and formic acid concentration.[28, 72] To sample formaldehyde acidified

2,4-DNPH solution is impregnated onto a filter paper disc and placed inside the end cap of the passive sampling tube, 7cm length with a 1.1 cm diameter. The passive samplers are placed inside the display cabinets for a period of 28 days. After exposure the filter disc is place in acetonitrile and the f-DNPH is solvent desorbed and analysed by HPLC.[72]

1.4.2.2. Formaldehyde concentrations in the museum environment

The concentrations of organic carbonyl pollutant present within a museum enclosure is dependant on the age and type of material from which the pollutant is emitted and the air exchange present within the enclosure ('leaky' display cabinets have more air exchanges, and so a reduction in pollutant concentration). The concentration units used to quantify the pollutants present are often quoted in parts per billion (ppb) or micrograms per metre cubed ($\mu g\ m^{-3}$). The concentration of formaldehyde within museum environments range from 0.24 $\mu g\ m^{-3}$ to 1717 $\mu g\ m^{-3}$.[19, 69, 71, 73, 74] Formaldehyde concentrations in museums greater than 61.25 $\mu g\ m^{-3}$ are often associated with sites of low circulation such as display cases.[69] In comparison the formaldehyde concentration in a museum environment outside of a display case has been measured at 16 $\mu g\ m^{-3}$.[19]

1.5. Extraction of indoor air pollutants

1.5.1. Sorbents used for VOCs

The type of sorbent used for extraction depends on the nature of the VOC mixture studied. Sorbents used for pollutant extraction can be classified into four different categories: inorganic, elemental carbon, organic polymers and graphitized organic

polymers. The sorbent used depends on the type of compounds targeted; a selection of sorbents are given in Table 1.2. Inorganic sorbents are used to collect polar organic compounds which are adsorbed strongly to the sorbent. However these sorbents are hydrophilic and tend to collect water on the adsorption sites which eventually become saturated with water. Activated carbons have a strong sorbate bonding. Activated carbon is inert and porous graphite can be described as "graphite plates". Imperfections on the plate's structure leads to the formation of a skeleton which comprises of voids. The voids provide the sites used for adsorption.[75] Organic polymers such as Tenax, Amberlite and Chromosorb 106 are hydrophobic and do not have the same associated moisture problems as other sorbents. Carbon molecular sieves e.g Anasorb CMS and zeolites (microporous aluminosilicate) trap molecules based on the size and polarity of the absorbate molecule entering their internal cavities. Molecules can be held by physical and chemical bonding. The cavity inside the zeolite can be modified to target molecules with specific dimensions and polarities. Zeolites have an added advantage over activated carbons as they do not have the same handling problems and can be used in specific situations were colour is important.[75] Tenax is the most often used and best evaluated sorbent for VOC sampling.[3] To monitor a large mixture of VOCs multiple sorbents are required to cover the wide range of VOCs. To extract VOCs from the indoor environment filtration of air can be achieved with the use of activated carbon filters.

Table 1.2: A selection of sorbents used for the adsorption of VOCs [29, 76, 77 78, 79]

Sorbent Name	Composition	Surface Area $m^2 g^{-1}$	Target Compounds	Advantages	Disadvantages
Silica Gel	Inorganic	300-800	Non-Polar hydrocarbons	Can be coated with derivatizing agents	Water vapour is strongly adsorbed
Activated Charcoal	Activated Carbon	800-1000	Wide Range	Microporous, adsorption enhanced by activation	Residual inorganic ash content
Anasorb 747	Activated Carbon	1000	Less volatile & polar compounds	Regular porosity , low ash content	Hydrophillic
Carbotrap	Graphitised carbon black	100	C_5 –C_{12} hydrocabons	Relatively hydrophobic	Low surface area, non-porous
Tenax TA	Porous polymer (poly(2,6-diphenyl-p-phenylene oxide))	35	Non-polar compounds	Inert, macroporous, high thermal stability, hydrophobic	Low surface area, not suitable for low-weight molecular weight organic acids
Amberlite XAD-2	Porous polymer (styrene-divinyl benzene copolymer)	300	Semi volatile molecules	Hydrophobic, often used as a support for deivatizing agents	Reacts with strong oxidising agents at room temperature
Chromosorb 106	Porous polymer (polystyrene)	700-800	More volatile & polar VOCs	Used for higher concentration samples, hydrophobic	Not suitable for low concentration sampling. Lower thermal stability than Tenax
Carboxen 564	Graphitised carbon black	400	Many VOCs C_2-C_5	High porosity, enhanced storage stability for reactive compounds	Not thermally stable at high temperatures
Anasorb CMS	Carbon Molecular Sieves	1700	Very volatile organic compounds	High capacity for small molecules	Hydrophilic

1.5.2. Removal of formaldehyde from museum air

To reduce the formaldehyde concentration within a display case four measures can be taken

i) restrict the emission of formaldehyde therefore inhibiting the pollutant mass accumulation

ii) remove formaldehyde through filtration or trapping

iii) eliminate the source of the pollutant within the cabinet where possible

iv) increased ventilation to avoid build up of formaldehyde.

To inhibit the movement of pollutants from the cabinet materials barrier methods can be used such metal foils and polyester sheeting e.g Marvelseal 360[15] Moistop 622[74] and Melinex®[19]. Grzywacz and Tennent[74] used metal barrier foil to line an old and a new plywood display case. The formaldehyde concentration measured within the new case was 51.3 $\mu g\ m^{-3}$ whereas the formaldehyde concentration in the old case was 136 $\mu g\ m^{-3}$. Barrier methods reduce the formaldehyde concentration but do not eliminate the emission of formaldehyde.[19] Despite metal foils effectiveness at reducing the formaldehyde concentration the adhesive backing used to adhere to the surface may be corrosive and full surface coverage is difficult.[26]

Efforts have been made to seal the woods to inhibit the formaldehyde emission with a polyurethane coating however this was unsuccessful.[80] In some cases pollutants released by the wood products can slowly diffuse through the barrier and then reach a significant level.[26] Therefore it is more effective to avoid products that release harmful pollutants than to seal them.[15]

Heating ventilation and air conditioning (HVAC) systems provide a stable and uniform climate.[15] HVAC systems may contain filter systems for gaseous adsorption. Activated carbon, and activated alumina impregnated with sodium bicarbonate are good filters for the removal of acetic acid but are poor for the removal of formaldehyde.[15] Indeed most of the sorbents used in filters have a medium to poor rating for the adsorption of formaldehyde. MicroChamber products which consist of molecular traps, (zeolites and activated carbon) cast into a paper matrix containing alkaline buffers.[75] The microchamber product was developed as a more effective way to trap and neutralise pollutant molecules.[81] The presence of MicroChamber within an enclosure increased the retained strength of a 30 year old book when subjected to 88 hours of accelerated aging at 100 °C in both acidic and alkaline conditions.[82] Activated carbon filters have been employed to reduce formaldehyde vapours in museum cases.[26, 80] However carbon filters will only absorb 10 % of their weight in formaldehyde, require constant monitoring and after saturation they become a secondary source of formaldehyde.[80] Similar problems are associated with silica gels.[26] Crucially it is difficult to determine when the sorbent media become saturated. Filter systems used to reduce internally generated pollutants can be passive, active or externally active whereby positive pressure is used inside the enclosure to force air outside the enclosure.[15] However the preferred choice is an internally active air filtration system.

The Getty Conservation Institute created a specialised formaldehyde catalysed charcoal cartridge for use in museums. The formaldehyde eliminator was used as an

active mitigation method. During laboratory tests chamber enclosures were created with concentrations as high as 1700 μg m^{-3}. When the formaldehyde eliminator was used as a mitigation method the chamber enclosure was less than 0.24 μg m^{-3}.[69]

1.6. Aims and objectives

The aim of this project was to overcome problems associated with current sampling and prevention strategies for indoor air pollutants. Mesoporous silicate based sorbents, containing large surface areas and specific pore sizes, were synthesised as a new type of indoor air pollution scavengers. In order to test the efficiency of the new materials for the extraction of formaldehyde vapour and VOCs, a number of tasks were undertaken. There are 5 main objectives associated with this research.

1. Environmental chambers are required to provide environments with known concentrations of formaldehyde vapours or selected VOCs (toluene, ethylbenzene, o-xylene, cumene and dichlorobenzene). Static and dynamic systems will be assessed and validated for the pollutants of interest. Calibration experiments will include the use of direct injection and spiked Tenax tubes.

2. Several materials will be synthesised as potential air pollutant sorbents:
    a. MCM-41 silicates
    b. SBA-15
    c. Commercially available materials (Purakol, Purafil and Puracarb).
3. Several chemical modification methods will be used to alter the surface characteristics of selected materials (e.g., MCM-41 and SBA-15) to aid the extraction efficiency of formaldehyde vapour from air.

4. Sorbents will be characterised by assessing their physical and chemical nature using techniques such as scanning electron microscopy, transmission electron microscopy, x-ray diffractometry, nitrogen adsorption isotherms and microanalysis.

5. Sorbents will then be used to extract target pollutants from air by determination of pollutant extraction efficiencies in active sampling mode. Tests will also be performed in a simulated museum enclosure.

1.7. References

1. *Clean Air At Work: New Trends is Assesment and measurement for the 1990's*, Royal Society of Chemistry, 1992.

2. M. Rehwagen, U. Schlink and O. Herbarth, *Indoor Air*, 2003, **13**, 283-291.

3. L. Molhave, G. Clausen, B. Berglund, J. De Ceaurriz, A. Kettrup, T. Lindvall, M. Maroni, A. C. Pickering, U. Risse, H. Rothweiler, B. Seifert and M. Younes, *Indoor Air*, 1997, **7**, 225-240.

4. J. D. Spengler and J. A. Samet, *Indoor Air Pollution: A Health Perspective*, The Johns Hopkins University Press, Baltimore, 1991.

5. WHO, *Indoor Air pollutants: exposure and health effects*, World Health Organisation, Copenhagen, 1982.

6. *Sick Building Syndrome: causes, effects and control*, London Hazards Centre Trust, London, 1990.

7. L. Molhave, *Indoor Air*, 2003, **13**, 12-19.

8. McMurry J., *Organic Chemistry*, 5th edn., Brookes and Cole, Pacific Grove, California, 2000.

9. D. Ebbing and S. Gammon, *General Chemistry*, 6th edn., Houghton Mifflin Company, Boston, 1999.

10. H. Hart, L. Craine and D. Hart, *Organic chemistry, A short course*, 10th edn., Houghton Mifflin and Company, Boston, 1999.

11. *Dictionary of Science*, 4th edn., Oxford University Press, 1999.

12. http://www.epa.gov/iaq/formalde.html, *United States Environmental Protection Agency*, Accessed October 19th, 2007.

13. W. A. Oddy, *Museum Journal*, 1973, **73**, 27-28.

14. G. Thomson, *The Museum Environment*, second edn., Butterworths, 1986.

15. J. Tétreault, *Airborne Pollutants in Museums, Galleries, and Archives: Risk Assesment, Control Strategies, and Preservation Management*, Canadian Conservation Insitute, Ottawa, 2003.

16. J. Greenfield, *Building a Better Case*, Art Conservation Centre at the University of Denver, 1992.

17. P. C. Arni, G. C. Cochrane and J. D. Gray, *Journal of Applied Chemistry*, 1965, **15**, 463.

18. P. C. Arni, G. C. Cochrane and J. D. Gray, *Journal of Applied Chemistry*, 1965, **15**, 305-313.

19. D. Thickett, S. Bradley and Lee L., Proceedings of the International Conference on Metals Conservation, France, 1998.

20. G. E. Myers, Wood adhesives in 1985: Status and needs. Proceedings 47344, Madison, WI, May 14-16 1985.

21. G. E. Myers, *Forest Products Journal*, 1984, **34**, 35.

22. C. M. Grzywacz and N. H. Tennent, Preservation of Collections Assesment, Evaluation and Mitigation Strategies, 24th Annual AIC Meeting Norfolk, Virginia, 10-11 June 1996.

23. L. S. G. Byne, *Journal of Conchology*, 1899, **9**, 172.

24. J. R. Nicholls, *Journal of the Society of Chemical Industry*, 1934, **53**, 1077-1078.

25. M. F. Striegel, Postprints of the AIC Objects Specialty Group Meeting , AIC Washigton D.C, Alberquerque, 8th June 1991.

26. P. Hatchfield and J. M. Carpenter, *The International Journal of Museum Management and Curatorship*, 1986, **5**, 183-188.

27. T. Salthammer, *Organic Indoor Air Pollutants: Occurence, Measurement, Evaluation*, Wiley-VCH, Weinheim; New York, 1999.

28. L. T. Gibson, B. G. Cooksey, D. Littlejohn and N. H. Tennent, *Analytica Chimica Acta*, 1997, **341**, 11-19.

29. M. Harper, *Journal of Chromatography A*, 2000, **885**, 129-151.

30. M. P. Baya and P. A. Siskos, *The Analyst*, 1996, **121**, 303-307.

31. A. Vinu, K. Z. Hossain and K. Ariga, *Journal Of Nanoscience And Nanotechnology*, 2005, **5**, 347-371.

32. *Method 100, U.S. Department of Labour. Occupational Health and Safety Administration,*, http://www.osha.gov/dts/sltc/methods/organic/org100/org100.html, Accessed 1st Nov, 2007.

33. *Method 52, U.S. Department of Labour. Occupational Health and Safety Administration,*, http://www.osha.gov/dts/sltc/methods/organic/org052/org052.html, Accessed 1st Nov, 2007.

34. R. Kostianen, *Atmospheric Environment*, 1995, **29**, 693-702.

35. J. Volden, Y. Thomassen, T. Greibrokk, S. Thorud and P. Molander, *Analytica Chimica Acta*, 2005, **530**, 263-271.

36. M. Hippelein, *Journal Of Environmental Monitoring*, 2004, **6**, 745-752.

37. A. L. Pasanen, S. Lappalainen and P. Pasanen, *The Analyst*, 1996, **121**, 1949-1953.

38. A. Roche, Thevenet. R., V. Jacob, P. Kaluzny, C. Ferrari, Baussand P. and P. Foster, *Atmospheric Environment*, 1999, **33**, 1905-1912.

39. M. Huxham and C. L. P. Thomas, *The Analyst*, 2000, **125**, 825-832.

40. O. O. Kuntasal, D. Karman, D. Wang, S. G. Tuncel and G. Tuncel, *Journal of Chromatography A*, 2005, **1099**, 43-54.

41. M. D. G. Meniconi, R. Parris and C. L. P. Thomas, *The Analyst*, 2003, **128**, 1232-1237.

42. R. A. Hallama, E. Rosenberg and M. Grasserbauer, *Journal of Chromatography A*, 1998, **809**, 47-63.

43. A. L. Sunesson, M. Sundgren, J. O. Levin, K. Eriksson and R. Carlson, *Journal Of Environmental Monitoring*, 1999, **1**, 45-50.

44. K. L. Yang and J. G. Lo, *Chemosphere*, 1998, **36**, 1893-1902.

45. T.-M. Wu, G.-R. Wu, H.-M. Kao and J.-L. Wang, *Journal of Chromatography A*, 2006, **1105**, 168.

46. M. Huxham and C. L. P. Thomas, *LC GC North America*, 1999, **17**, S31-+.

47. J. S. Park and K. Ikeda, *Indoor Air*, 2006, **16**, 129-135.

48. Y. S. Fung and Z. Wu, *The Analyst*, 1996, **121**, 1955-1961.

49. C. Thammakhet, V. Muneesawang, P. Thavarungkul and P. Kanatharana, *Atmospheric Environment*, 2006, **40**, 4589-4596.

50. P. Wolkoff, C. K. Wilkins, P. A. Clausen and G. D. Nielsen, *Indoor Air*, 2005, **16**, 7-19.

51. J. F. Pankow, W. Luo, D. Bender, L. M. Isabelle, J. S. Holllingsworth, C. Chen, W. E. Asher and J. S. Zorogorski, *Atmospheric Environment*, 2003, **37**, 5023-5046.

52. J. L. Adgate, T. R. Church, A. D. Ryan, G. Ramachandran, A. L. Fredrickson, T. H. Stock, M. T. Morandi and K. Sexton, *Environmental Health Perspectives*, 2004, **112**, 1386-1392.

53. C. Godwin and S. Batterman, *Indoor Air*, 2007, **17**, 109-121.

54. K. Sexton, J. L. Adgate, G. Ramachandran, C. Pratt, S. Mongin, T. H. Stock and M. T. Morandi, *Environmental Science and Technology*, 2004, **38**, 423-430.

55. *Material Safety Data Sheets*, Sigma Aldrich.

56. NIOSH, *Manual of Analytical Methods*, 4th edn., US Dept. of Health, Eductaion and Welfare, Method 2016(2), 2003.

57. P. A. Martos and J. Pawliszyn, *Analytical Chemistry*, 1998, **70**, 2311-2320.

58. J. A. Koziel, J. Noah and J. Pawliszyn, *Environmental Science and Technology*, 2001, **35**, 1481 - 1486;.

59. NIOSH, *Manual of Analytical Methods*, 4th edn., US Dept. Health, Education and Welfare, Method 3500(2), 1994.

60. C. Watt, PhD Thesis, '*Development of novel sensors and sorbents to protect items of cultural importance in museum environments*',, Department of Pure and Applied Chemistry, University of Strathclyde, Glasgow G1 1XL, 2004.

61. K. Kawamura, K. Kerman, M. Fujihara, N. Nagatani, T. Hashiba and E. Tamiya, *Sensors and Actuators B*, 2005, **105**, 495-501.

62. C. L. P. Thomas, C. D. M^{c}Gill and R. Towill, *The Analyst*, 1997, **122**, 1471-1476.

63. M. I. H. Helaleh, M. Kumemura, S. Fujii and T. Korenaga, *The Analyst*, 2001, **126**, 104-108.

64. J. A. Dirksen, K. Duval and T. A. Ring, *Sensors And Actuators B-Chemical*, 2001, **80**, 106-115.

65. C. Y. Lee, C. M. Chiang, Y. H. Wang and R. H. Ma, *Sensors And Actuators B-Chemical*, 2007, **122**, 503-510.

66. G. G. Guilbault, *Analytical Chemistry*, 1983, **55**, 1682-1684.

67. L. Feng, Y. J. Liu, X. D. Zhou and J. M. Hu, *Journal Of Colloid And Interface Science*, 2005, **284**, 378-382.

68. L. R. Green and D. Thickett, *Studies in Conservation*, 1995, **40**, 145-152.

69. C. M. G. Druzik and D. C. Stulik, *Western Association Art Conservation Newsletter*, 1991, **13**, 13-16.

70. Dräeger, *Dräeger-Tubes and accuro Pump*, www.draeger.com/ST/internet/pdf/US/detection/brochure_tubes_e.pdf, Accessed 1st Nov 2007.

71. C. M. Grzywacz and D. C. Stulik, American Institute for Conservation Objects Specialty group meeting , Post prints of the 19th Annual Meeting, 1991.

72. L. T. Gibson and A. W. Brokerhof, *Studies in Conservation*, 2001, **46**, 289-303.

73. S. Bradley and D. Thickett, ICOM Committee for Conservation, 12th Triennial Meeting, Lyon, 1999.

74. C. M. Grzywacz and N. H. Tennent, Preventive Conservation Practice, Theory and Research, Preprints of the contributions to the Ottawa Congress, 12-16 September 1994.

75. S. Rempel, *Western Association Art Conservation Newsletter*, 1996, **18**.

76. A. Kumar and I. Viden, *Environmental Monitoring and Assesment*, 2007, **131**, 301-321.

77. M. Harper, *The Analyst*, 1994, **119**, 65-69.

78. Supelco, *Air Monitoring*, http://www.sigmaaldrich.com/Graphics/Supelco/objects/6800/6734.pdf, Accessed 5th Nov, 2007.

79. SKC.Inc, *Anasorb 747*, http://www.skcinc.com/instructions/1385.pdf, Accessed 5th Nov 2007.

80. M. A. Leveque, AIC preprints, 14th Annual meeting, American Institute for Conservation,, Washington D.C, 1986.

81. W. K. Hollinger Jr, in *Preventative Conservation Practice, Theory and Research*, eds. R. Ashok and S. Perry, Ottawa, Editon edn., 1994.

82. W. K. Hollinger Jr and M. G. Vine, *MicroChamber Active Archival Housings Provide Preventative Conservation*, Conservation Resources International, Springfield, Virginia, 1993.

2 THEORY OF INSTRUMENTAL METHODS

2.1 Use of bell chambers to provide known concentrations of volatile organic compounds in air

The polluted atmospheres, used for sampling, were created inside a 22.85 L glass bell chamber by injecting small volumes of liquid VOC's into the chamber and allowing the liquids to volatilise. The chamber was sealed with a silicone stopper. The atmosphere can be sampled by drawing a small volume of polluted air from the chamber onto a conditioned Tenax sampling tube at a specified flow rate, controlled by an air sampling pump. The bell chamber design used is shown in Figure 2.1.

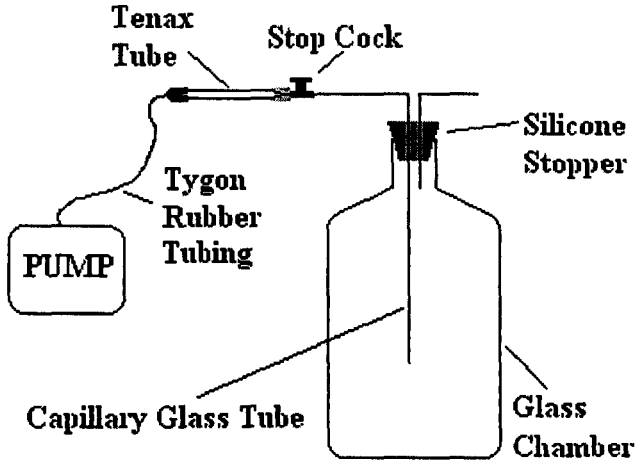

Figure 2.1: Atmospheric Bell Chamber System

To calculate the pollutant concentrations within the bell chamber the densities of each liquid injected were used to convert injection volumes to masses (Equation 2.1). The densities of toluene, ethylbenzene, o-xylene, cumene and dichlorobenzene (DCB) are 0.87, 0.87, 0.88, 0.86 and 1.30 g mL^{-1}, respectively. By multiplying the density (ρ) by the injection volume (V) the total mass (M) injected into the chamber

can be determined. The calculated masses can then be used to calculate the concentration of each analyte in the chamber in units of mg m^{-3} given that the chamber has a known volume. Injection volumes and chamber concentrations varied therefore specific details will be given in the appropriate following sections. To estimate the mass of analyte that can be theoretically trapped on to the Tenax assuming unit sorption probability, the total volume sampled from the chamber was calculated using Equation 2.2. The flow rate of the pump in mL min^{-1} was converted to m^3 s^{-1} for use in Equation 2.2. Given that the sampling time was measured in seconds the volume of air sampled from the chamber was in m^3. The volume of air sampled was then used in Equation 2.3 along with the chamber concentration, in mg m^{-3}, to determine the mass trapped on the Tenax.

$$\rho = \frac{M}{V}$$

Equation 2.1

$$\text{Volume sampled}\left(m^3\right) = \text{Flow rate}\left(m^3 s^{-1}\right) \times \text{Sampling time}\,(s)$$

Equation 2.2

Theoretical mass of VOC trapped on Tenax (mg) = Chamber concentration (mg m^{-3}) × Chamber volume sampled (m^3)

Equation 2.3

2.1.1 Example calculation for the theoretical mass of toluene trapped on a Tenax sampling tube

Toluene has a liquid density of 0.87 g mL^{-1} and a 5 µL volume of a solution of toluene was injected into the chamber. Therefore the mass of toluene injected into

the bell chamber was 4.35 mg. The bell chamber has a volume of 22.85 L, or 0.02285 m^3. Hence the chamber concentration for toluene was 190.4 mg m^{-3}. When the air was collected for 10 s at a pump flow rate of 50 mL min^{-1}, equivalent to 8.3×10^{-7} m^3 s^{-1}, the volume of air sampled was 8.3×10^{-6} m^3. Therefore the theoretical mass trapped on the Tenax for toluene was 1.58 μg. For ethylbenzene, o-xylene, cumene and DCB similar calculations can be performed using their respective densities.

2.2 Dynamic atmospheric chambers for the production of indoor air pollutants

Atmospheric chambers were also used to provide a constant and controlled polluted air stream of VOCs or formaldehyde. The atmospheric chambers consist of a pollutant source, two flow streams and a 20 L sampling chamber as set out in Figure 2.2

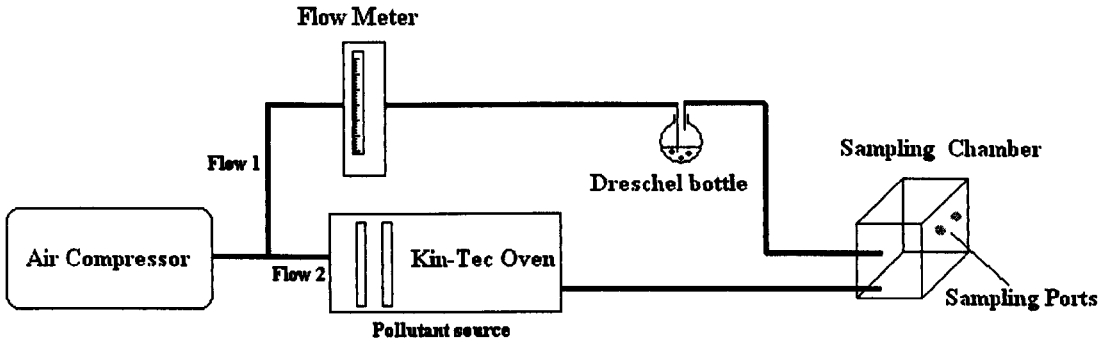

Figure 2.2: Atmospheric chamber system

An initial unpolluted air stream is obtained from an air compressor. This initial flow is split into two streams. Flow 1 provides the sample chamber with humidified air as the controlled air flow enters a dreschel bottle filled with water prior to the sample

chamber. The second flow stream enters a temperature controlled oven (Kin-Tek Laboratories Inc. Model 491M-B.). Inside the oven, flow 2 is further split into a flow which passes over a permeation device, holding the pollutant source, and a diluent flow. Both flows recombine before reaching the sampling chamber. Each permeation device, (Kin-Tek Laboratories Inc.) releases the required pollutant at a specific rate, when heated, into the controlled permeation flow. By varying the air flow rate over the device, the diluent oven flow and the temperature of the oven, the concentration of pollutant reaching the 20 L perspex chamber can be altered. The polluted air flow that reaches the perspex chamber is mixed with the humidified air (Flow 1). Mixing occurs through a holed shelf placed immediately above the inputs of the two streams. By careful control of both flow streams, estimates of the final pollutant concentration and relative humidity within the chamber can be calculated.

2.2.1 The permeation device

Each permeation device emits a specific pollutant type. The concentration within the chamber depends on the specific tube used as each has a different emission rate. The permeation tubes sit inside a glass housing unit which is 'o-ring' sealed, see Figure 2.3. The unit sits inside the oven which is set at a required temperature. The pollutant is emitted through the porous coating of the tube. Each tube has been calibrated by the manufacturer and has a set emission rate (E_R) in ng min^{-1} and K_o value (specific for each pollutant). The K_o value converts the emission rate from weight per minute to volume per minute using Equation 2.4, where MW is the molecular weight of the pollutant. To calculate the concentration of the polluted air stream within the chamber, at a specified temperature, Equation 2.5 was used,[1] where C is the pollutant

concentration in parts per million (ppm) in the flowing air stream (F), in mL min^{-1}, at a specific temperature. A mixing ratio of 1 ppm implies that in 1 million volumes of air the pollutant occupies 1 volume.

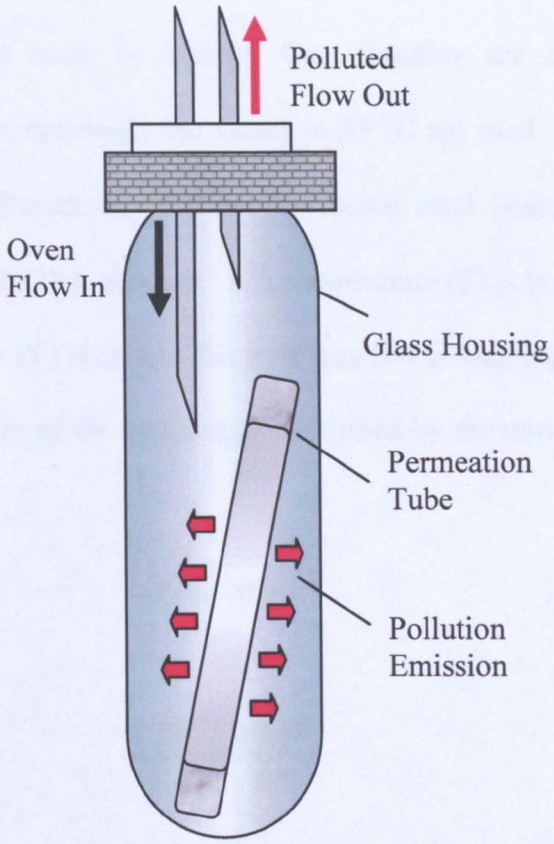

Figure 2.3: Permeation Tube and glass housing

$$K_o = \frac{22.4}{MW}$$

Equation 2.4

$$C = \frac{K_o E}{F1000}$$

Equation 2.5

2.2.2 Conversion of gas units from ppb to μg m^{-3}

Gas concentration units of parts per billion (ppb) and parts per million (ppm) are often used, however they are often also quoted as μg m^{-3} or mg m^{-3}, respectively. To convert the units of ppb (volume/volume) into μg m^{-3} (mass/volume) the gaseous density of the pollutant must be known. Gas densities are dependent upon temperature (T), however, nominally the values at 25 °C are used. To calculate the gaseous density of the pollutant, the ideal gas equation is used, (Equation 2.6) where the gas constant (R) is 0.0821 L atm mol^{-1} K^{-1}, temperature (T) is in °K, pressure (P) is in atm and the volume (V) is in L . The ideal gas law is rearranged as shown in Equation 2.7 and each side of the equation is multiplied by the molecular weight of the pollutant.

$$PV = nRT$$

Equation 2.6

$$\frac{nMW}{V} = \frac{PMW}{RT}$$

Equation 2.7

For n=1 the units of the left hand side of the equation are g L^{-1} which is the unit used for density.

For example consider the conversion of 1 μg m^{-3} of toluene to ppb at 1 atm pressure the gaseous density of toluene was calculated at 298 °K as 3.77 g L^{-1}. Now that the density of toluene is known the units of ppb (v/v) can be converted to μg m^{-3} (m/v). 1 μg m^{-3} of toluene is equal to 1 ng L^{-1} of toluene. To convert the mass (1 ng) to volume, it is divided by the gaseous density as shown below:

$$\text{Volume of toluene in 1 ng} = 1 \text{ ng} / 3.77 \text{ g L}^{-1}$$
$$= 1 \times 10^{-9} \text{ g} / 3.77 \text{ g L}^{-1}$$
$$= 2.65 \times 10^{-10} \text{ L}$$
$$= 0.265 \text{ nL}$$

For toluene 1 ng is equivalent to 0.265 nL, so 1 ng L^{-1} is equal to 0.265 nL L^{-1}. 1 nL in a total volume of 1 L (1×10^9 nL) is a part per billion (ppb). Therefore 1 μg m^{-3} is equivalent to 0.265 ppb. Similar calculations were calculated for 1 μg m^{-3} of ethylbenzene, cumene, dichlorobenzene and formaldehyde giving conversion factors of 0.230, 0.204, 0.166 and 0.815, respectively.

2.2.3 The trapping of formaldehyde on C_{18} cartridges

To trap the formaldehyde from polluted air streams 2,4-DNPH was loaded onto C_{18} cartridges. When 2,4-DNPH traps formaldehyde a hydrazone derivative is formed known as F-DNPH. The mechanism for the reaction is shown in Figure 2.4 and occurs through the nucleophilic attack of the carbonyl followed by a 1,2-elimination of water aided by the presence of acid.[2]

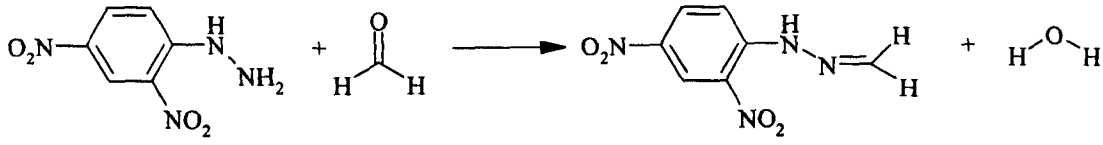

Figure 2.4: Mechanistic Pathway for the reaction of 2,4-DNPH with formaldehyde producing F-DNPH

To determine the concentration of formaldehyde in the polluted atmospheres the trapped F-DNPH was eluted from the C_{18} cartridge. The extract was then analysed by

reverse phase high performance liquid chromatography to determine the mass of F-DNPH held by in the C_{18} cartridge. This mass is then used to calculate the mass of formaldehyde trapped by the cartridge. Quantitative analysis is achieved as one mole of 2,4-DNPH traps one mole of formaldehyde to produce one mole of F-DNPH. The mass of F-DNPH present was calculated using Equation 2.8, this mass was used to calculate the number of moles of formaldehyde present, Equation 2.9. Equation 2.10 was then used to determine the experimental concentration within the chamber.

$$\text{F-DNPH Concentration (ug mL}^{-1}) \times \text{Total elution volume (mL)} = \text{Total Mass of F-DNPH present (ug)}$$

Equation 2.8

$$\frac{\text{Mass F-DNPH (g)}}{\text{FM of F-DNPH}} = \text{nm of F-DNPH} \equiv \text{nm of Formaldehdye} = \frac{\text{Mass of Formaldehyde (g)}}{\text{FM of Formaldehyde}}$$

Equation 2.9

$$\frac{\text{Mass of Formaldehyde trapped (ug)}}{\text{Volume sampled (m}^3) = \text{Flow (m}^3\text{s}^{-1}) \times \text{Time (s)}} = \text{Formaldehyde experimental concentration (ug m}^{-3})$$

Equation 2.10

2.3 Theory of chromatography[3-5]

Chromatography has been defined by the International Union of Pure and Applied Chemistry as "*a physical method of separation in which the components to be separated are distributed between two phases, one of which is stationary while the other moves in a definite direction*". Separation is achieved on chromatographic

columns through differences in physical and chemical properties of the individual components. These differences determine their relative affinities for the stationary phase (SP), either liquids or solids, and the mobile phase (MP), either liquids or gases. If a component has large affinity for the SP then it will migrate through the column slower than a component with a small affinity for the SP. The differences in migration rates allow mixtures of components to be separated before analysis.

2.3.1 High performance liquid chromatography[3, 6]

High performance liquid chromatography can be split into four main categories based solely on separation mechanisms: partition, adsorption, ion exchange and size exclusion chromatography. The type of chromatography required for efficient separation of analytes in a sample depends on the molecular weight and polarity of the analyte. Partition chromatography is the most widely used liquid chromatography method with liquid bonded phase packing dominating, as used in this research. The stationary phase is modified by reacting organosilanes with –OH groups formed on the silica surface. This produces organosiloxanes as shown in Figure 2.5. The R group is often a straight chain octyl- or octyldecyl- group; R groups can also contain amines, ethers, nitriles and aromatic hydrocarbons to introduce a range of polarities. Partition chromatography can be further split into normal and reverse phase chromatography. In reverse phase chromatography the stationary phase is non-polar while the mobile phase is polar, hence the most polar components elutes first. Common stationary and mobile phases in reverse phase chromatography are C_{18} columns and acetonitrile:water, respectively.

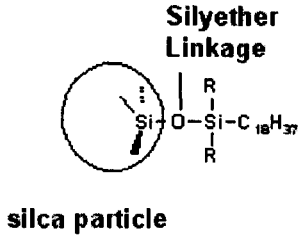

Figure 2.5: Bonded stationary phase on silica particles

With normal phase chromatography the polarities of the stationary phase and mobile phase are the opposite to reversed phase. After the sample has been separated in the chromatographic column the individual analytes are commonly detected by ultraviolet-visible spectroscopy (UV-vis).

2.3.1.1 Ultraviolet-visible spectroscopy[6, 7]

UV spectrometry involves the absorption of radiation, which promotes valence electrons within the molecules from a ground state to a higher excited state (Figure 2.6). The UV – visible spectral region consists of wavelengths between 200-800 nm that can also be represented in the pre-SI Angstrom unit whereby 1 nm is the equivalent to 10 Å. Quantum theory predicts that each molecule will have a unique set of energy levels. Absorption of energy from a photon is only possible when energy from the photon exactly matches the energy difference between the ground state (highest occupied molecular orbital (HOMO)) and the excited state (lowest unoccupied molecular orbital (LUMO)).

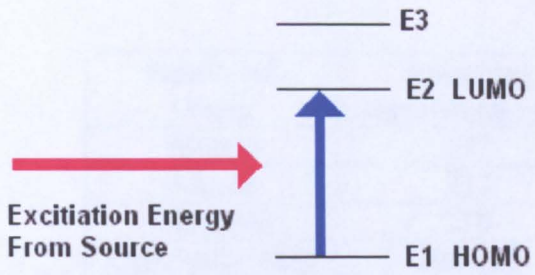

Figure 2.6: UV transitions in energy levels

During the analysis samples are irradiated with UV light of continuing changing wavelengths. When the wavelength corresponds to the energy level required to excite an electron to a higher level, energy is absorbed. The wavelength at which a molecule absorbs depends upon how tightly the electrons are bound. Therefore the wavelength of the absorption is a measure of the separation of the energy levels. Single bond electrons are held more tightly than double or triple bond electrons (termed conjugates). Electrons from double and triple bonds (π-bonds) in organic molecules are relatively easy to excite by radiation. Molecules containing π-bonds separated by a single bond are termed conjugated. Molecular orbital calculations show that the energy difference between the ground state and excited state decreases as the extent of conjugation increases. With a reduced energy gap between the electronic energy levels less energy is needed to promote electrons, therefore, absorption occurs at a longer wavelength. Absorbing wavelengths can be influenced by solvent effects as well as other structural details of the molecule. Unsaturated organic functional groups (chromophores) are extremely useful for UV analysis; some are listed in Table 2.1. along with their absorbing wavelengths.

Table 2.1: Absorption wavelengths of common organic functional groups.

Functional Group	Absorbing wavelength / nm
Alkene	177
Alkyne	217
Aldehyde	210
Carboxylic Acid	200-210
Amine	195
Nitro	210
Nitrite	220-230

There are two important laws that are used in UV spectrometry, Lambert's Law states that "the fraction of incident light absorbed is independent of the intensity of the source". Beer's Law states that "the absorption is proportional to the number of absorbing molecules".

Transmittance and absorbance are the two terms commonly used as quantitative measures of beam attenuation. As the beam of photons I_0 passes through the absorbing medium the intensity of the beam is reduced to I. Transmittance is often displayed as % Transmittance calculated from Equation 2.11. The term absorbance is defined in Equation 2.12 and can be related to concentration using Beer Lambert Law (Equation 2.13). For monochromatic radiation absorbance is proportional to absorptivity, L mol^{-1} cm^{-1} (a), the path length, cm (b) and concentration, mol L^{-1} (c), permitting quantitative analysis.

$$\%T = \frac{I}{I_0} \times 100$$

Equation 2.11

$$A = \log \frac{I_0}{I} = \log \frac{1}{T}$$

Equation 2.12

$$A = a.b.c.$$

Equation 2.13

2.3.2 Gas chromatography[5, 6]

Gas chromatography (GC) is a technique that provides a mechanism to separate volatile, thermally stable analytes in mixtures. The length of time the analyte is retained on the stationary phase is due to the specific interactions it has with the stationary phase. The stationary phase determines the retention and separation of the analytes. Separation primarily occurs through differences in the boiling points of the analytes and the different analytes' relative affinities for the stationary phase. If an analyte has a low boiling point then the proportion of the analytes in the mobile phase is greater, these analytes will move down the column quickly with the carrier gas. Therefore lower boiling point analytes will elute faster than higher boiling point analytes. The solutes that partition most into the stationary phase will be retarded longest and therefore elute later. The mobile phase acts as a carrier for the analytes through the system from the injection port to the detector. The carrier gas does not interact with the stationary phase and is not involved in the chromatographic process. The carrier gas flow rate can affect the bandwidth of the analyte peak through longitudinal diffusion and mass transfer.

Introduction of the sample to the GC is commonly via a microsyringe through a silicone-rubber septum. Sample volumes range from a microlitre to 20 μL. When a smaller sample volume is required a sample splitter is used to limit the volume of sample entering the column and discards the remaining to waste. GC columns consist of two types, packed and capillary, generally constructed of stainless steel, glass or

fused silica. Column lengths vary from 10 to 100 m, which requires them to be coiled in order to be housed in the GC oven. When samples have a broad range of boiling points a temperature programme is used to ramp the temperature of the oven at a controlled rate. After separation the analytes are passed on to the detector. There are many different detectors used in conjunction with GC, these include flame ionization, thermal conductivity, infra red and mass spectrometry. For this research samples where introduced via a thermal desorption unit and detected by mass spectrometry.

2.3.2.1 Gas chromatography sample introduction by thermal desorption[8-10]

Analytes can also be thermally desorbed from the Tenax sampling tube using a commercial thermal desorption unit (TDU) and diverted into the GC for analysis. Analytes are passed on to the column from the sampling tube via a two-stage mechanism as shown in Figure 2.7.

The sorbent filled sample tube is heated to 300 °C and a desorb flow (helium) is used to carry the analytes on to a cold trap where they are readsorbed on to Tenax. The cold trap temperature is operated at -30 °C, using peltier coolers, to preconcentrate the analytes. The trap is then rapidly heated to 300 °C at a rate of 99 °C s^{-1}, causing the analytes to be 'backflushed' from the cold trap onto the GC column in a small 'plug' of vapour. During the 'injection' process of the TDU optional splits can be incorporated into the procedure. The splits are required to permit introduction of a small mass of sample onto the capillary column, in order to prevent overloading which would result in band broadening and poor resolution. Both inlet and outlet

splits are incorporated in the sample desorption method. The split ratio was calculated as shown in Equation 2.14.[8]

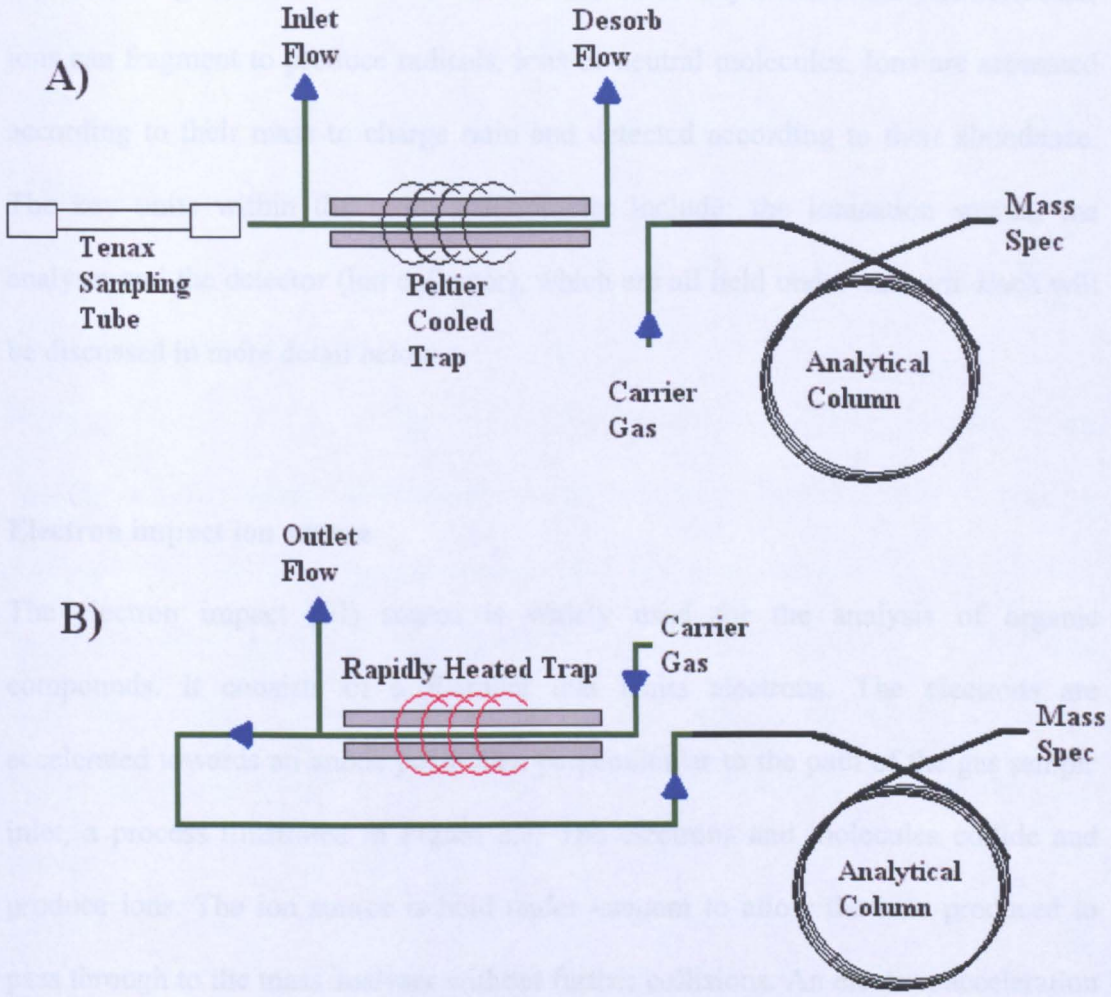

Figure 2.7: Two stage desorption mechanism used in the TDU a) stage one analytes passed from sample tube to cold trap and b) stage two analytes passed from cold trap to column

$$\%\,Analytes\ on\ Column = \frac{(Column\ Flow \times Desorb\ Flow) \times 100}{(Outlet\ Split\ Flow + Column\ Flow) \times (Desorb\ Flow + Inlet\ Split\ Flow)}$$

Equation 2.14

2.3.2.2 Analyte detection by mass spectrometry[11, 12]

Analytes are passed from the GC system to the mass spectrometer (MS) via a heated transfer line. In the MS the ionisation process creates molecular ions, which are formed through the removal of an electron from the analyte molecule. The molecular ions can fragment to produce radicals, ions or neutral molecules. Ions are separated according to their mass to charge ratio and detected according to their abundance. The key units within the mass spectrometer include: the ionisation source, the analyser and the detector (ion collector), which are all held under vacuum. Each will be discussed in more detail below.

Electron impact ion source

The electron impact (EI) source is widely used for the analysis of organic compounds. It consists of a filament that emits electrons. The electrons are accelerated towards an anode positioned perpendicular to the path of the gas sample inlet, a process illustrated in Figure 2.8. The electrons and molecules collide and produce ions. The ion source is held under vacuum to allow the ions produced to pass through to the mass analyser without further collisions. An electron acceleration potential of 70 eV is commonly used to expel an electron from the incoming molecule. Each electron produced from the cathodic filament with an acceleration potential of 70 eV has a wavelength equal to 1.4 Å. For many organic molecules the maximum number of ions are produced at 70 eV. At higher energies there are more fragments produced. The ions and fragment pattern produced allow the identification of the original molecule.

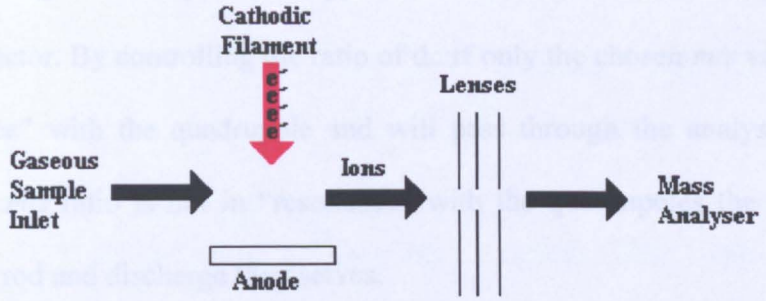

Figure 2.8: Basic electron impact diagram

Quadrupole mass analyser

Mass analysers scan and separate the ions produced according to their mass. In this research a quadrupole mass analyser was used. Quadrupole mass analysers separate ions according to their mass to charge ratio (*m/z*) by utilising the difference in trajectory paths. Quadrupole mass analyser consists of four rods (as seen in Figure 2.9), where opposite pairs of rods have the same potential. Incoming ions are focused at the centre of the four rods. Positive ions will be attracted towards the negative rods.

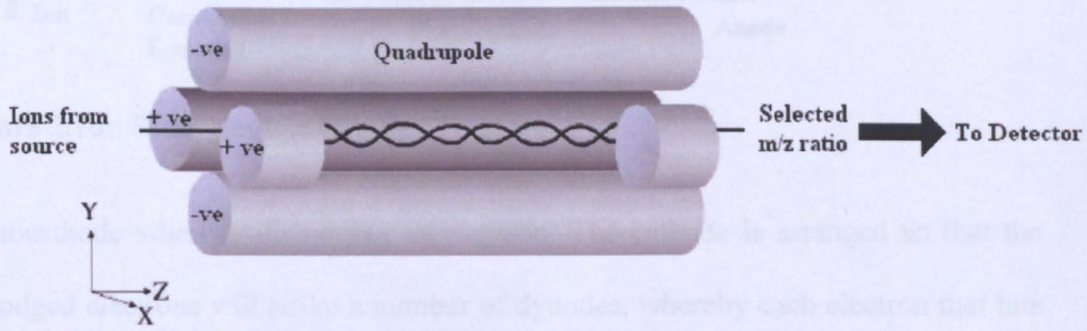

Figure 2.9: Quadrupole rods and ion trajectory path

When an oscillating radio frequency is applied ions undergo a 'cork screw' motion towards the detector. By controlling the ratio of dc:rf only the chosen *m/z* values will be in "resonance" with the quadrupole and will pass through the analyser to the detector. If the *m/z* ratio is not in "resonance" with the quadrupoles the ions will collide with the rod and discharge themselves.

Photomultiplier detectors

A photomultiplier detector is one of a range of detectors such as an electron multiplier or a Faraday cup. Photomultiplier detectors consist of two conversion dynodes, a phosphor plate and a photo-multiplier tube as shown in Figure 2.10. Ions strike the conversion dynode where electrons are emitted. The electrons emitted are accelerated toward the phosphor plate. When the electrons strike the plate a photon is released on the opposite side to the incoming electron. The photons then strike a

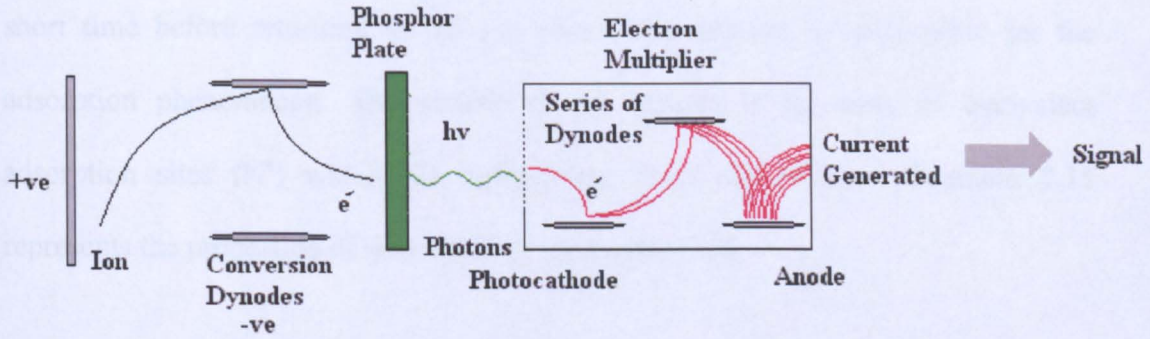

Figure 2.10: Basic photomultiplier diagram

photocathode whereby dislodging an electron. The cathode is arranged so that the dislodged electrons will strike a number of dynodes, whereby each electron that hits the dynode dislodges several more electrons. This cascade effect results in an amplification of the signal in a relatively short period of time. The electrons will

strike the anode where the generation of a current can be used as the signal. Amplification ranges from 10^4 to 10^5.

2.4 Nitrogen adsorption isotherms for characterisation of mesoporous silicates[13 14]

An isotherm is a measure of the molar quantity of gas taken up at a constant temperature by an initially clean solid surface as a function of gas pressure. Nitrogen adsorption isotherms determine the surface area, pore diameter and pore volume of porous materials.

2.4.1 Langmuir theory

Langmuir theory is based on the assumption that gases form only one layer on a solid. When a gas molecule comes into contact with a surface the collision is taken to be inelastic. Therefore the gas molecule remains on the surface of the solid for a short time before returning to the gas phase, this process is responsible for the adsorption phenomenon. The surface of the sorbent is an array of equivalent adsorption sites (N^s) which are independent from each other. Equation 2.15 represents the proportion of sites filled by molecules (N^a).

$$\theta = \frac{N^a}{N^s}$$

Equation 2.15

Equation 2.16 relates the rate at which molecules strike a surface to the rate at which they leave the surface. The quantity of gas adsorbed at pressure P is V_a, the quantity of gas adsorbed when the surface is covered with a monomolecular layer is V_m, and b

is the adsorption coefficient. Equation 2.16 is generally rearranged into its linear form Equation 2.17. When P/V_a is plotted against P, b and V_m are evaluated from the slope and intercept of the line.

$$V_a = \frac{V_m bP}{1+bP}$$

Equation 2.16

$$\frac{P}{V_a} = \frac{1}{V_m b} + \frac{P}{V_m}$$

Equation 2.17

The specific surface area of the sorbent (s) is determined from Equation 2.18 where σ is the area of surface occupied by a single adsorbed gas molecule, N_A is Avogadro constant, m is the mass (g) of the adsorbing sample and V_o is the molar volume of the gas. When nitrogen is the adsorptive gas molecule the equation becomes Equation 2.19, as σ is 16.2×10^{-20} m^2, and V_o is 22414 cm^3.

$$s = \frac{V_m \sigma N_A}{m V_o}$$

Equation 2.18

$$s = \frac{4.35 V_m}{m}$$

Equation 2.19

2.4.2 The Brunauer-Emmett-Teller theory

An advance in Langmuir theory was proposed by Brunauer Emmett and Teller (referred to as BET). BET incorporates the concept of multimolecular layer

adsorption and includes the assumption that the forces active in the condensation of gases are also responsible for the binding energy in multimolecular adsorption. BET equates the rate of condensation of the gas molecules on to the surface layer to the rate of evaporation from that layer and summing for an infinite number of layers giving the Equation 2.20, where C is a constant and P_o is the saturation pressure of the gas.

$$\frac{P}{V_a(P_o - P)} = \frac{1}{V_m C} + \frac{C-1}{V_m C}\left(\frac{P}{P_o}\right)$$

Equation 2.20

A plot of $P/(V_a(P_o-P)$ versus P/P_o should give a straight line where the intercept and slope are equivalent to $1/(V_mC)$ and the slope $(C-1)/V_mC$ respectively which allows the determination of V_m and C. The surface area of the sample is determined from Equation 2.21 and is based on the assumption of close packing at the surface, where σ is the mean area per molecule, M is the molecular weight and ρ is the density of the liquid adsorbate. The area occupied by a single nitrogen molecule is 16.2 $Å^2$ at liquid nitrogen temperature.

$$\sigma = (4)(0.866)\left[\frac{M}{4(2N_A\rho)^{1/2}}\right]^{2/3}$$

Equation 2.21

Isotherms consist of three main stages i) the initial rise due to the adsorbing gas molecules interacting with the most energetic regions of the surface, ii) the mid point due to the formation of multilayers and iii) the end point rise due to the initiation of bulk condensation to a liquid. There are six basic adsorption isotherms and these were classified by International Union of Pure and Applied Chemistry (IUPAC) in

1985 as types I - type VI, shown in Figure 2.11 Isotherm shapes divulge information regarding the structure of the adsorbing material.

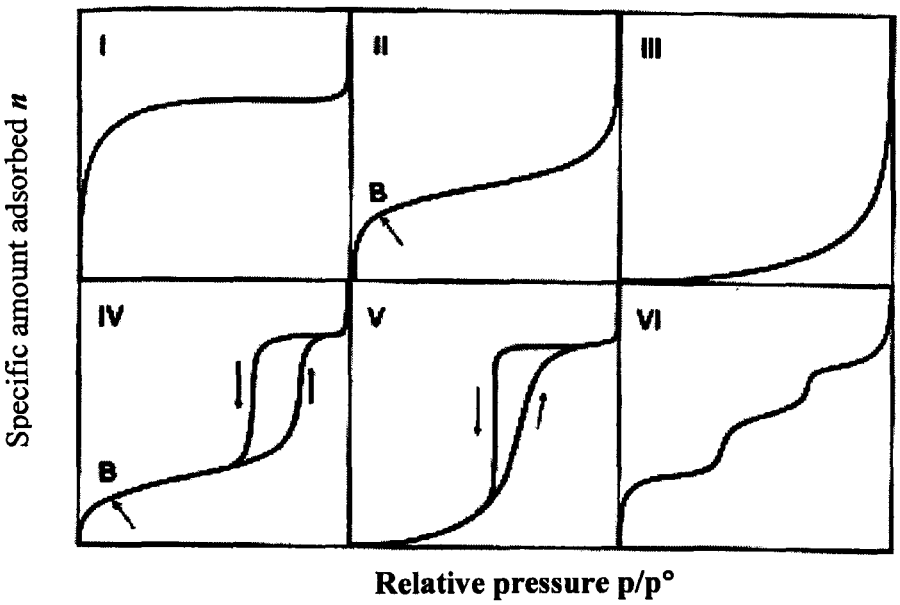

Figure 2.11: Six main types of gas physisorption isotherms, according to the IUPAC classification [13]

Type I isotherm is characteristic of a material which has extremely small pores. Types III and V isotherms arise when occur when the adsorptive molecules have a greater affinity for each other than they do for the solid, therefore these conditions are of no use in surface and pore analysis. A type VI isotherm is symptomatic of a solid material which is non-porous and has an almost completely uniform surface. Isotherm types II and IV are indicative of either nonporous or adsorbents having relatively large pores. The completion of a monolayer coverage is indicated by point B in isotherm types II and IV and the linear portions of the isotherms that follow indicate the start of multilayers. A type IV isotherm contains a hysteresis loop, the lower branch of the isotherm is representative of the gas molecules filling the pores of the adsorbent and the higher branch of the loop is associated with the gas molecules leaving the pores. The filling and emptying of mesopores, and therefore

the hysteresis loop is generally associated with capillary condensation. The IUPAC classifies hysteresis loops into four distinct types see Figure 2.12.

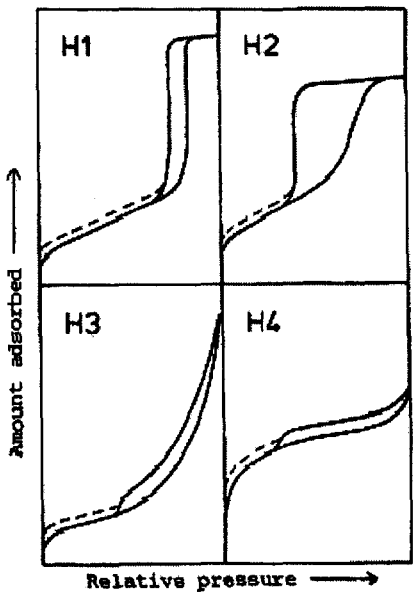

Figure 2.12: IUPAC classification of hysteresis loops

Type H1 has a very narrow loop with very steep parallel adsorption and desorption branches. Type H1 loops are characteristic of adsorbents with narrow pore distribution and are common to MCM-41. A H2 type hysteresis loop has a broad and long adsorption branch while the desorption branch in much steeper. The type H2 hysteresis represents a more complex pore structure and is made up of interconnected network of pores of different size and shape. Unlike hysteresis types H1 and H2, hysteresis types H3 and H4 do not contain a plateau at high relative pressures. Types H3 and H4 are given when the adsorbents contain slit like pores.

2.5 Scanning electron microscopy[15-18]

To determine the surface morphology of materials scanning electron microscopy (SEM) can be used to identify the surface composition of the material and give a

detailed microscopic image of the material. The process involves focussing a high energy beam, typically 30 keV onto the surface of the material, see Figure 2.13.

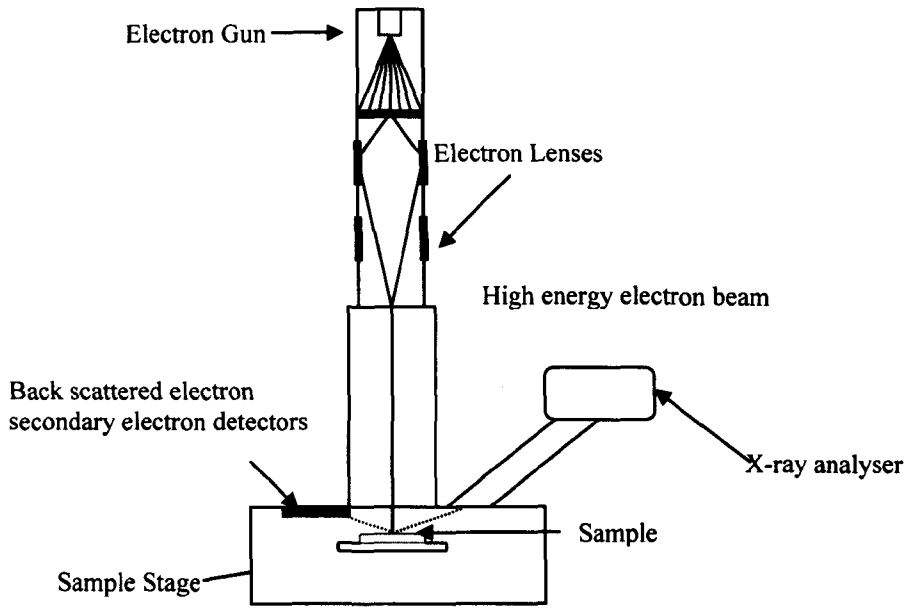

Figure 2.13: Schematic diagram of an SEM

Several types of electron guns exist, the most common is the tungsten thermionic type, consisting of three parts; a tungsten wire filament (cathode), an anode and a Wehnelt cylinder or grid cap. Thermionic emission occurs when heat is supplied to the tungsten filament in order for electrons to escape. The grid cap focuses the randomly directed electrons emitted from the filament. The anode accelerates the electrons towards the lenses through a small aperture to form the electron beam. Electron lenses situated beyond the gun are used to demagnify the image of the crossover of the electron gun to the final spot size on the specimen. The electron path and specimen chamber are under high vacuum. Deflection plates allow the beam to be scanned across the surface and an image of the surface is created. When the high energy electron beam (also known as the primary beam) interacts with the surface of

the material the electrons can be elastically or inelastically scattered. Elastic scattering causes the incident electron to change direction with no loss of kinetic energy a phenomenon known as back scattering. The back scattered electron is an important imaging signal in SEM. When inelastic scattering occurs some of the energy is transferred from the electron to tightly bound inner-shell electrons and loosely bound outer-shell electrons of the atom. An inelastic collision can result in outermost electrons being detached from the specimen atom, see Figure 2.14a, leaving behind an ionised atom with a positive charge. The dislodged electrons have a low kinetic energy and are readily captured by nearby ionised atoms and if they contain enough energy can cause an emission of a secondary electron.

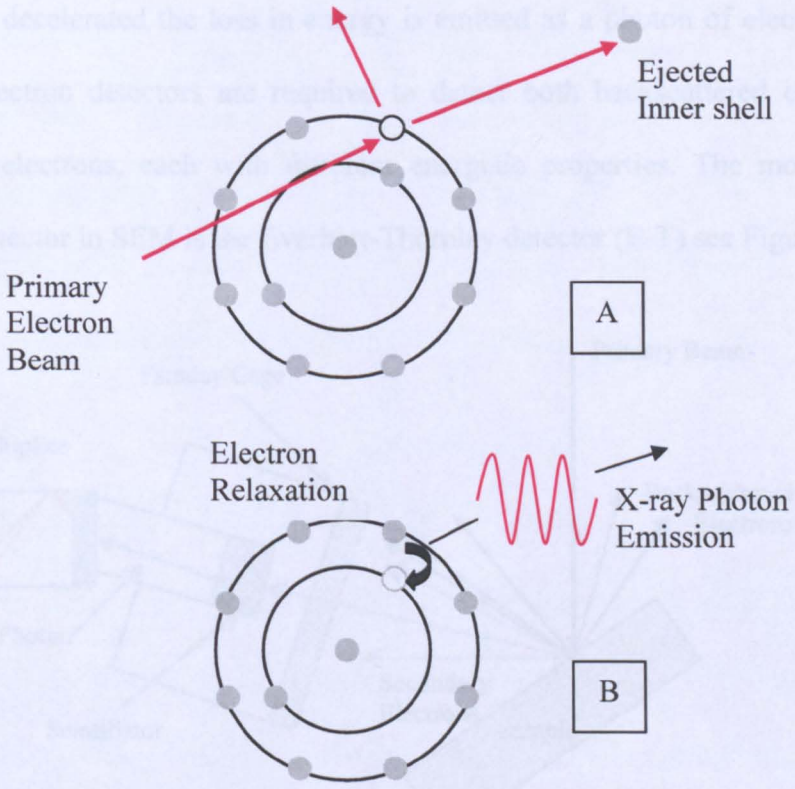

Figure 2.14: Process of secondary ion and x-ray production

The secondary electron can then propagate through the material. If the second electron contains enough kinetic energy it can also undergo inelastic scattering of its own, producing a cascade of electrons. When the electron beam has sufficient energy the interaction with the surface atoms can result in the ejection of a tightly bound inner-shell atomic electron. The ejection of the inner electron leaves the atom in an excited state. To relax the ionised atom the electron vacancy is 'filled' by an electron dropping from one of the outer shells and the excess energy in released as a characteristic x-ray, Figure 2.14b. The energy of the x-rays produced can transfer to another electron which can be further emitted, known as the Auger electron. X-rays are also emitted when the speed of the incident electrons are reduced. When the electron is decelerated the loss in energy is emitted as a photon of electromagnetic energy. Electron detectors are required to detect both backscattered electron and secondary electrons, each with different energetic properties. The most common electron detector in SEM is the Everhart-Thornley detector (E-T) see Figure 2.15.

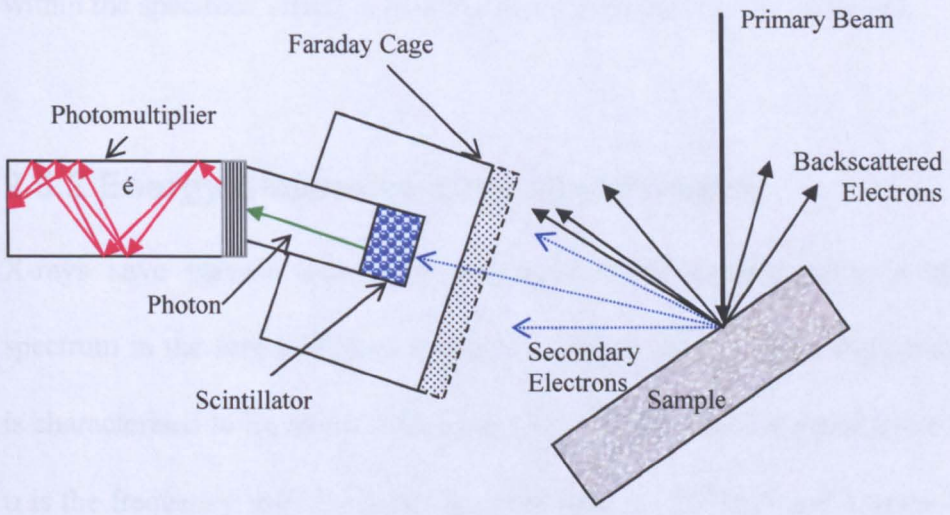

Figure 2.15: Everhart-Thornley Detector

The electron strikes a scintillator material which produces a photon. The photons are transmitted to an electrode within a photomultiplier. At the electrode (photocathode) the photon is converted back to an electron. The electron signal is multiplied through successive electrodes of the photomultiplier. Surrounding the scintillator is a Faraday cage its purpose is to 'attract' the scattered secondary electrons through acceleration in order to strike the scintillator with enough energy to produce a photon.

2.5.1 Environmental scanning electron microscopy

In an environmental SEM, a small pressure limiting aperture exists between the specimen chamber and the gun chamber. This allows the gun to operate at a high vacuum while a poorer vacuum is maintained around the sample. The charge build up on the surface of insulating materials is neutralised by interaction between gas molecules and electrons. Therefore these materials can now be studied without first applying a conductive coating. By varying the pressure, temperature and gas mixture within the specimen chamber a wide range of samples can be observed.

2.5.2 Energy dispersive x-ray spectrometry

X-rays have particle and wave properties. Each element gives a characteristic spectrum in the forms of lines at different energy levels. The energy transition (ΔE) is characterised in Equation 2.22, where h is Planks constant equal to 6.63×10^{-34} Js, υ is the frequency in Hz, c is the speed of light 3×10^{8} ms^{-1} and λ is the wavelength of the x-ray.

$$\Delta E = h\nu = \frac{hc}{\lambda}$$

Equation 2.22

An energy dispersive x-ray spectrometer detector contains a Si(Li) detector crystal which adsorbs each individual x-ray photon and leads to an ejection of a photoelectron. The photoelectron gives up most of its energy to form electron-hole pairs. A charge pulse is formed which is converted to a voltage. Each voltage pulse is proportional to the incoming x-ray photon. Each element gives a characteristic spectrum in the forms of lines at different energy levels. Electrons within an atom occupy specific energy levels, each electron is described by a specific set of quantum numbers. In x-ray spectrometry atomic electrons are arranged into major and minor shells. The major shells are designated K, L, M, N and O and they represent n quantum numbers of 1, 2, 3, 4 and 5, respectively. When a K electron is removed an electron from the L, M, N & O shell fills the existing hole, the excess energy is released as an x-ray, this is known as the K series. When an L electron is removed, the L series is produced. Different series of lines are produced depending on the quantum number of the electron removed. However not all transitions between shells are allowed, therefore selection rules are applicable. The selection rules state that Δn must be greater than zero. When Δn is equal to 1 α lines are produced while β lines are produced when Δn is greater than 1, illustrated in Figure 2.16.

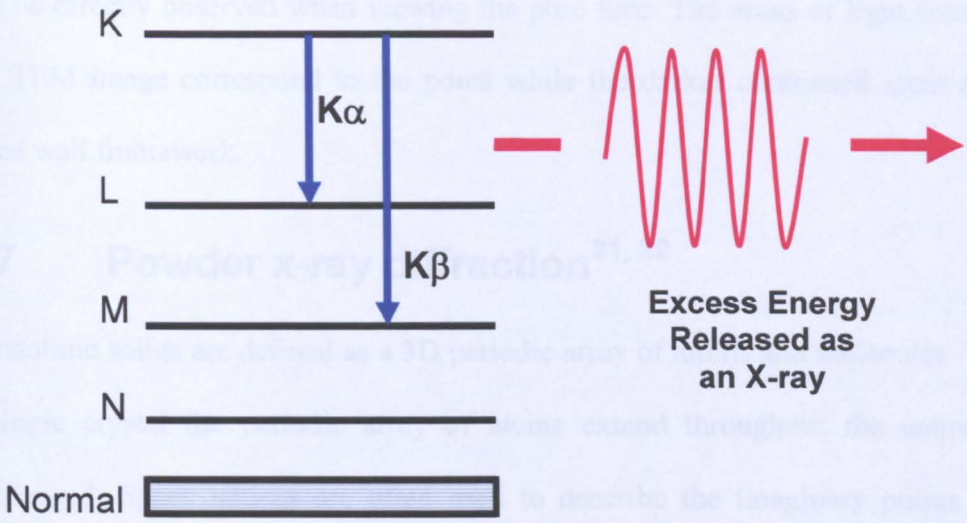

Figure 2.16: Energy level diagram for an atom illustrating the formation of Kα and Kβ x-rays

2.6 Transmission electron microscopy[19, 20]

Transmission electron microscopy (TEM) is a technique which belongs to a family of techniques referred to as electron microscopy. TEM produces magnified images through the use of fast-moving electrons as illumination. TEM makes use of shorter wavelength electron illumination. As with a conventional light microscope a transmission electron microscope contains two-image forming lenses. Electrons are produced from an electron gun within a vacuum. The electrons pass through the sample and are focussed by an objective lens into a magnified image which is enlarged by a projector lens. The image is observed on a fluorescent screen or recorded on a digital camera.

For mesoporous silicates, structural information is obtained by viewing the pore face and perpendicular to the pores (channels). The hexagonal arrangement of mesopores

can be directly observed when viewing the pore face. The areas of light contrast in the TEM image correspond to the pores while the darker contrasted areas are the silica wall framework.

2.7 Powder x-ray diffraction[21, 22]

Crystalline solids are defined as a 3D periodic array of atoms and molecules. Within a single crystal the periodic array of atoms extend throughout the entire solid unchanged. Space lattices are often used to describe the imaginary points which describe the scheme of repetition of a pattern. A unit cell is an imaginary parallel-sided figure that contains one unit of the repeating pattern. The unit cell can be used to generate the whole lattice through translation of the unit cell. The length of the sides in a unit are denoted a, b and c and the angles between them are noted α, β and γ. Each plane of the lattice can be distinguished by the distances at which the intersection of the axes occurs e.g. (1a, 1b, 1c). However the label of the plane is more simply referred to as (1, 1, 1,). If the plane intersects the axes at a fraction or runs parallel to the axes, the reciprocal of the label is used to avoid fractions and ∞, known as Miller indices.

2.7.1 Generation of X-rays for use in PXRD

X-rays are generated within x-ray tubes. Electrons are produced from a heated cathode, and are accelerated through a vacuum to an anode. Electrons are accelerated by a high electric potential between the cathode and anode. When the electrons strike the anode they decelerate and produce radiation. When higher energy electrons strike

the anode electrons from the anode can be released from the atomic orbitals, resulting in the refilling of orbitals by electrons with the generation of characteristic x-rays, as seen in Section 2.5.2. Figure 2.17 shows a common design used in powder diffractometers. A divergent beam of x-rays interact with the sample and a convergent beam of x-rays is diffracted. Before the x-rays reach the detector the x-rays pass through a narrow slit and unwanted wavelengths of x-ray photons are removed by a single crystal monochromator.

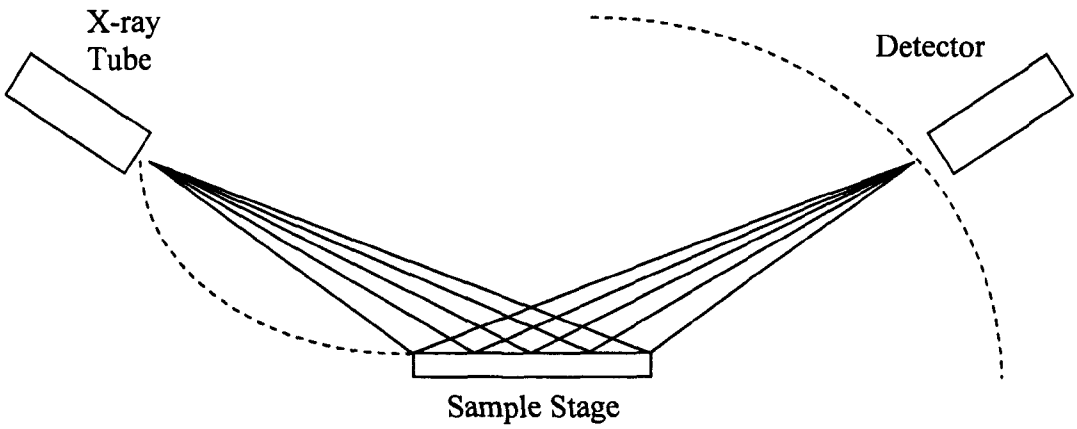

Figure 2.17: Focusing schemes in powder diffraction

Within PXRD the sample consists of many small single crystals at different orientations. The sample is prepared ensuring a flat surface. A conventional scintillation detector is used to measure the intensity of the diffracted x-rays, as covered in the SEM Section 2.5.

2.7.1.1 Construction of diffraction patterns

Diffraction patterns use x-rays to characterise the crystalline solid. When an x-ray encounters a crystal the x-ray can be diffracted. The atoms within the crystal scatter the x-rays. For simplicity in x-ray diffraction the lattice planes can be regarded as a stack of mirrors, separated by the distance d, which reflect the incoming x-rays, as shown in Figure 2.18.

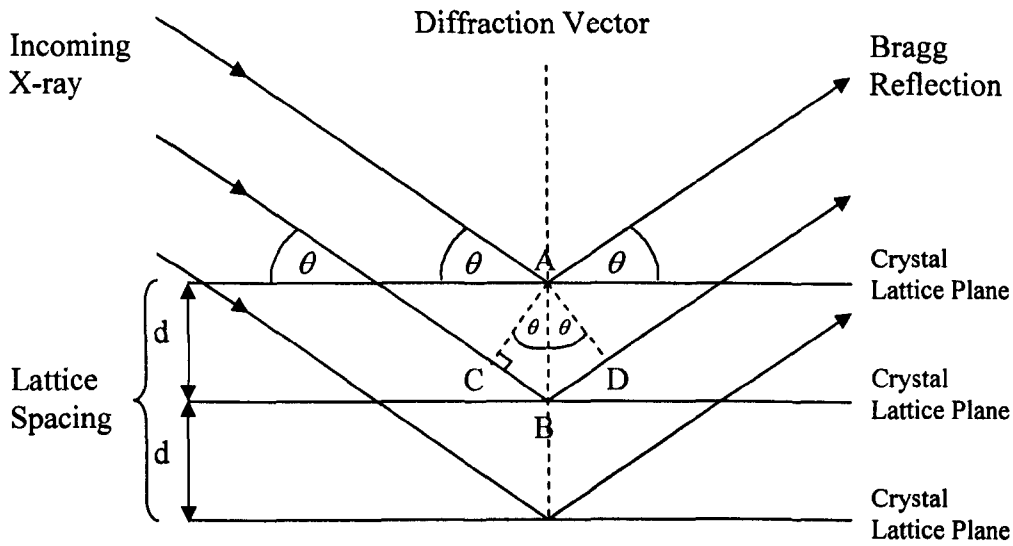

Figure 2.18: Diffraction of x-rays from a crystal set of planes

The difference in path lengths of the two reflected x-rays of wavelength, λ is CB + BD, the length of which depends upon the incoming angle, θ. This path length difference can also be represented as 2d sin θ, where d is equal to the distance AB. Many values of θ do not result in exiting x-rays in the same phase. If the x-rays diffracted by the atom are in the same phase then an amplitude in signal will be recorded, when out of phase there is destructive interference. For constructive interference the path length difference must be an integer (n) of the number of

wavelengths. A diffracted beam will be produced from a given set of planes when Bragg's Law is satisfied, Equation 2.23.

$$n\lambda = 2d\sin\theta$$

Equation 2.23

2.7.1.2 Determination of pore wall thicknesses using PXRD

In ordered mesoporous silicates powder x-ray diffraction is used to determine the thickness of the silica wall. The distance between the crystal lattice planes, d, can be used with hexagonally ordered mesoporous silicates as shown in Figure 2.19. From the figure the distance a, represents the pore diameter and pore wall thickness, given that d is determined through Braggs Law. The distances a and d make a right angled triangle by which given d, a can be calculated via Equation 2.24.

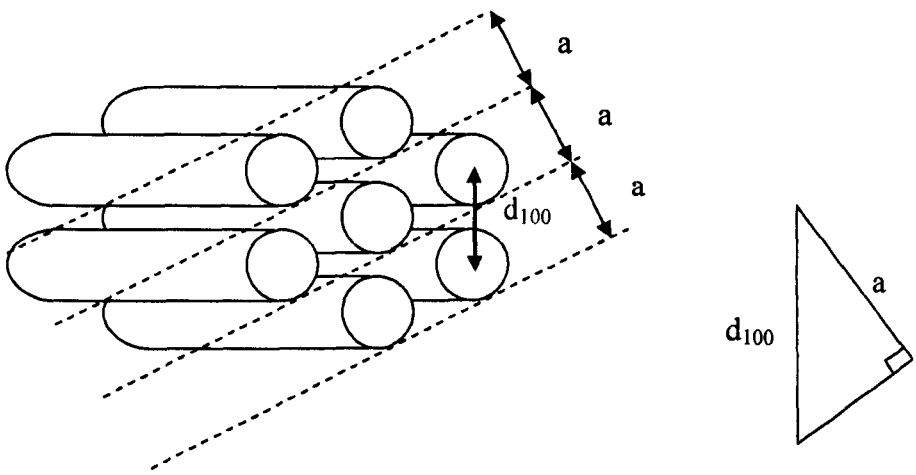

Figure 2.19: X-ray diffraction and the determination of pore wall thicknesses

$$d = \frac{\sqrt{3}}{2}a$$

Equation 2.24

With the pore diameter determined through nitrogen adsorption the pore wall thickness is determined by the subtraction of pore diameter from the distance a.

2.8 References

1. Kin-TeK Laboraotries Inc., *Model 491M-B Operation Manual.*

2. L. T. Gibson and A. W. Brokerhof, *Studies in Conservation*, 2001, **46**, 289-303.

3. A. Braithwaite and F. J. Smith, *Chromatographic methods*, 5th edn., Blackie Academic & Professional, London; New York 1996.

4. V. Meyer, *Practical High Performance Liquid Chromatography*, 3rd edn., John Wiley & Sons, Chichester, 1998.

5. E. Heftmann, *Chromatography : fundamentals and applications of chromatography and related differential migration methods. Part A:fundamentals and techniques*, 6th edn., Elsevier, Amsterdam: New York, 2004.

6. D. A. Skoog, D. M. West and F. J. Holler, *Fundamentals of Analytical Chemistry*, 7th edn., Saunders College Publishing, 1996.

7. T. Frost, B. J. Clark and M. A. Russell, *Ultra-Violet Spectrometry: practicle techniques, instrumentation and data handling*, 1st edn., Chapman & Hall, London, 1993.

8. PerkinElmer, *TDU Manual.*

9. M. Harper, *J. Chromatogr. A*, 2000, **885**, 129-151.

10. T. Salthammer, *Organic Indoor Air Pollutants: Occurence, Measurement, Evaluation*, Wiley-VCH, Weinheim; New York, 1999.

11. E. De Hoffmann, J. Charette and V. Stroobant, *Mass Spectrometry Principles and Applications*, John Wiley & Sons, 1996.

12. PerkinElmer, *TurboMass Gold GC/MS: Hardware guide*

13. F. Rouquerol, J. Rouquerol and K. Sing, *Adsorption by powders and porous solids: principles, methodology and applications*, Academic Press, San Diego, 1999.

14. Webb P.A. and Orr C., *Analytical Methods in Fine Particle Technology*, Micromertics Instrument Corporation, Norcross, 1997.

15. J. I. Goldstein, D. E. Newbury, P. Echlin, D. C. Joy, C. E. Lyman, C. Fiori, E. Lifshin and A. D. Romig, *Scanning Electron Microscopy and X-ray Microanalysis: a text for biologists, material scientists and geologists*, 2nd edn., Plenum Publishing Corporation, New York, 1992.

16. J. O'Connor, B. Sexton and R. Smart, *Surface Analysis Methods in Materials Science*, 2nd edn., Springer-Verlag Berlin, 2003.

17. R. A. Pethrick and D. L. Littlejohn, *13.913 Surface Analysis and X-Ray Techniques (Undergraduate Lecture Notes)*, University of Strathclyde, 2004.

18. J. M. Walls, *Methods of surface analysis*, Cambridge University Press, Cambridge, 1989.

19. X.-F. Zhang. and Z. Zhang, *Progress in Transmission Electron Microscopy 2: Applications in Materials Science*, Springer-Verlag, Berlin, 2001.

20. I. M. White, *The principles and practice of electron microscopy*, 2nd edn., Cambridge University Press, Cambridge, 1997.

21. P. W. Atkins, *Physical Chemistry*, 6th edn., Oxford University Press, Oxford, 1998.

22. B. E. Warren, *X-ray Diffraction*, Dover Publications, New York, 1990.

3 SAMPLING VALIDATION

The main aim of the research project is to synthesise novel mesoporous materials that can extract indoor air pollutants from contaminated environments. As part of the procedure, it is necessary to test the extraction efficiency of the new materials for the pollutants of interest; volatile organic compounds (VOCs) and formaldehyde vapour. As there were no in-house valid active sampling methods of analysis to quantify the concentration of pollutants in indoor air, the initial focus of the research involved the development of active sampling procedures for VOCs. The procedures developed focussed on sorbent filled sampling tubes to trap the pollutants from air. Active sampling was used where air is passed through the tube, using a hand-held pump, and if present, the pollutant of interest is removed from the air onto the sorbent material.

3.1 Examination of the bell chamber system

The original bell chamber used by Watt[1] was set up to provide an environment contaminated with VOCs as described in Section 2.1. The chamber was investigated as a stable, repeatable and reliable method for VOC analysis. It was vital that the method for VOC generation, sampling and analysis provided accurate concentrations of pollutants in order to use further in the testing of adsorbents as suitable pollutant scavengers.

3.1.1 Analysis of Tenax tubes by thermal desorption – gas chromatography- mass spectrometry

The system used to desorb, identify and quantify the VOCs trapped by a Tenax sorbent in the sampling tubes incorporated a thermal desorption unit, gas

chromatograph and mass spectrometer. The thermal desorption unit (TDU) was a Perkin Elmer Turbo Matrix TD. The operating conditions used when analysing VOC samples are outlined in Table 3.1. The TDU was coupled to a Perkin Elmer Autosystem XL gas chromatograph (GC). The analytes were detected by a Perkin Elmer:Turbo Mass Gold Mass Spectrometer (MS), which was coupled to the GC. The operating conditions for the GC and MS are outlined in Tables 3.2 and 3.3

Table 3.1: Operating conditions of the TDU for the desorption VOCs

Desorb flow:	19 mL min^{-1}
Desorb temperature:	300 °C
Conditioning:	Held at 320 °C for 15 minutes
Inlet split:	94 mL min^{-1}
Outlet split:	39 mL min^{-1}
Cold trap sorbent:	Tenax TA
Cold trap temperature:	Held at -30 °C, Ramped at 99 °C s^{-1} to 300 °C, Held at 300 °C for 5 min

Table 3.2: Operating conditions of the GC for the separation of VOCs

Inlet line temperature:	180 °C
Oven Temperature:	65 °C
Heating Rate:	65 °C for 5 min 65 °C for 5 min, Ramped to 90 °C at 8 °C min^{-1}, Held 90 °C for 1.87 min
Column:	Perkin Elmer, SMS Elite, (dimethylpolysiloxane (5% diphenyl)) 30 m × 0.25 mm i.d.
Carrier Gas:	Helium
Carrier Gas Flow	1 mL min^{-1}

Table 3.3: Mass spectrometer operating conditions for the detection of VOCs

Electron Energy	70 eV
Trap Emission	70 eV
Multiplier	250 V
Scan Run Time	10 min
Scan Time :	0.2 s
Inter Scan Delay:	0.1 s
m/z range:	50-300 amu
Solvent Delay	2 min

To detect the VOCs the MS was run in two different modes. First an electron impact (EI) spectrum continually scanned all mass to charge (m/z) ratios from 50-300 amu during the run producing a spectrum containing a number of peaks depending on the number of VOCs analysed, known as the total ion chromatogram (TIC). In this mode of operation, each peak represents an accumulation of all the mass fragments produced for a particular analyte. In addition, a second mode of operation was used where the MS was used to selectively monitor single ion responses (SIRs) at predetermined times. In this work, the analytes under investigation; toluene (m/z 92), ethylbenzene (m/z 91), o-xylene (m/z 91), cumene (m/z 105) or DCB (m/z 146) had retention times of 3.0-4.0, 4.0-6.5, 4.0-6.5, 6.0-7.5 or 8.0-10.0 minutes, respectively.

3.2 Experimental: Sampling validation

The sampling validation experiments conducted investigated i) the adsorption efficiency of Tenax as a VOC sampling method, ii) the suitability of the VOC bell chamber generation method and iii) reliability of the GC-MS analysis method used for the detection of VOCs.

3.2.1 Laboratory prepared Tenax tubes

To increase the number of Tenax sampling tubes available for testing new unpacked tubes (Markes, Unit D3, Llantrisant Business Park Pontyclun, UK) were packed with 200 mg of Tenax in-house. The end of the sampling tube was then tapped lightly on the bench six to eight times to settle the Tenax evenly in the tube. The 'rear/open' end of the sampling tube was then connected to an air cylinder via a mass flow controller. Air was passed through the Tenax filled tube for 5 min at a flow rate of 1 L min^{-1}, after which time a rear gauze and retaining spring were inserted and the

tubes were capped. As the sampling tubes were made of stainless steel, it was impossible to know whether the method of packing adopted was adequate or the bed length formed inside the tube. Therefore five glass tubes, with identical internal dimensions to the stainless steel commercial sampling tubes, were packed with 200 mg of Tenax using the procedure outlined above. The average Tenax bed length was measured as 36 ± 1.0 mm (2.8 % RSD). Visual examination of the packed tube, together with the consistent bed length indicated that no large voids were created during the packing procedure. The lab-packed tubes were then compared with the prepacked tubes to sample an atmosphere of VOCs. The atmospheric bell chamber system, as described in Section 2.1, was used to generate an atmosphere with known concentrations of toluene, ethylbenzene, o-xylene, cumene and DCB. The reagent suppliers are shown in Table 3.4.

Table 3.4: Addresses of analyte Manufacturer

Analyte	Manufacturer
Toluene	Bamford Laboratories, Norden, Rochdale, UK (99.5 %)
Ethylbenzene	Sigma Aldrich, Gillingham Dorset, UK (99 %)
O-xylene	Arcos Organics, New Jersey, USA (99%)
Cumene	Fisons Scientific Apparatus, Loughbrough, Leics, UK (99.5 %)
DCB	Aldrich Chemical Co. Ltd (99 %)

An injection volume of 5 μL of each analyte was then added sequentially to the chamber. The chamber was left for 1 hour to allow the VOCs to volatilise. Sampling from the chamber onto the conditioned Tenax tube was carried out for 10 s at a flow rate of 50 ml min^{-1} using a SKC sidekick pump, thereby sampling a volume of 8.3×10^{-6} m^3. The theoretical concentration, and expected masses, of each analyte trapped by sampling tubes using these conditions are given in Table 3.5. To account for any discrepancies in packing between sampling tubes, the flow rate

through each sampling tube was calibrated using a bubble meter immediately before use.

Table 3.5: Expected mass of VOCs trapped on Tenax tubes when using 5 μL injection volumes, 10 s sampling times and a pump flow rate of 50 mL min^{-1}

Analyte	Chamber concentration / mg m^{-3}	Mass of analyte trapped on Tenax / μg
Toluene	190.4	1.58
Ethylbenzene	190.4	1.58
O-xylene	192.5	1.60
Cumene	188.2	1.56
DCB	284.5	2.36

The chromatograms obtained, (Figure 3.1) indicate that similar results were obtained for the two different sets of tubes, the chromatogram for the packed tube is retarded in Figure 3.1 for clarity. The responses of the analytes obtained from the prepacked tube were only marginally higher than those obtained by the in-house packed sampling tube. For each analyte, the intensities of response when using prepacked tubes were approximately 8×10^7 greater than those produced when the in-house packed tubes were used. This equates to an increase of only 7 %. Therefore, it was assumed that the sampling beds produced by the in-house packed sampling tubes had similar absorbing efficiencies for each analyte as did the prepacked tubes. To examine the repeatability of the in-house prepacked tubes, an identical atmosphere containing known concentrations of VOCs was generated and sampled as before. Five replicate measurements were taken from the VOC chamber. On two days the average peak areas obtained for each analyte were obtained from the five chromatograms and the percentage relative standard deviation (% RSD) values were calculated (see Tables 3.6 and 3.7). For comparison, chromatographic responses were obtained using the mass spectrometer in both EI and SIR mode.

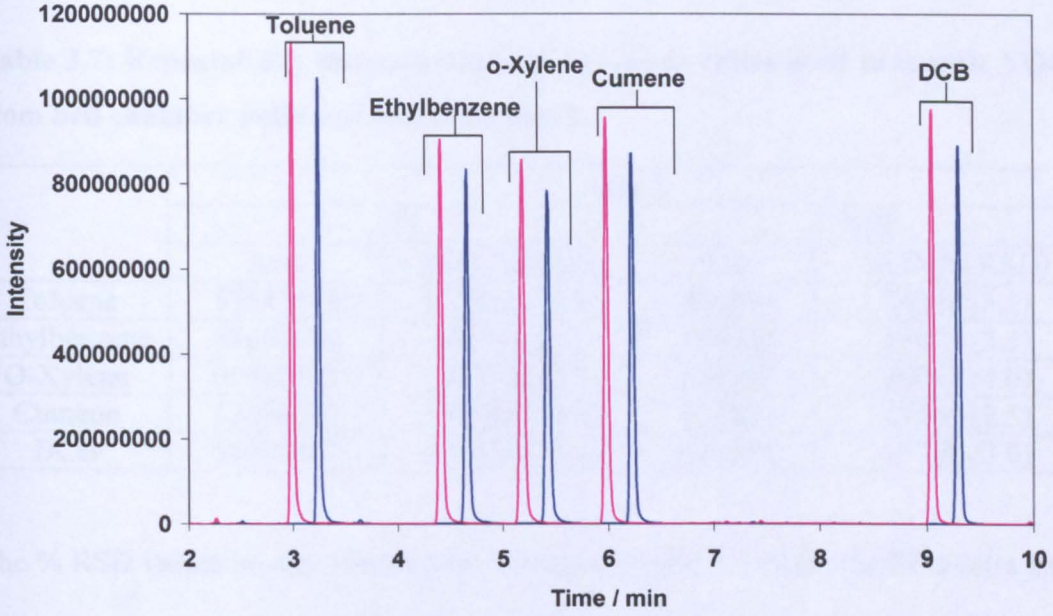

Figure 3.1: VOC EI chromatogram from a pre-packed sampling tube (—) and a VOC EI chromatogram from the lab made sampling tube (—). The packed tube has a retention shift of 15s for clarity.

Table 3.6: Repeatability measurements on lab made tubes used to sample VOC from bell chamber pollutant source on day 1.

	Day 1			
	EI		SIR	
	Ave.	STD (% RSD)	Ave.	STD (% RSD)
Toluene	47970450	1911838 (4.0)	376734	20752 (5.5)
Ethylbenzene	53205343	2319385 (4.4)	812095	40505 (5.0)
O-Xylene	52395264	2319203 (4.4)	546090	63845 (11.7)
Cumene	52116345	2283244 (4.4)	852048	50593 (5.9)
DCB	50141494	3304102 (6.6)	475615	39185 (8.2)

On day 1, the RSD values for the responses given in the EI chromatograms were within 4.0 - 6.6 %, while those obtained from the SIR peak areas were between 5.0 – 11.7 %. This amount of variation was thought to be quite high and could indicate a

variance in absorption capabilities of the in-house packed Tenax tubes. The Tenax tubes were reconditioned and the experiment was repeated.

Table 3.7: Repeatability measurements on lab made tubes used to sample VOC from bell chamber pollutant source on day 2.

	Day 2			
	EI		SIR	
	Ave.	STD (% RSD)	Ave.	STD (% RSD)
Toluene	57543549	1224701 (2.1)	444674	24348 (5.5)
Ethylbenzene	51664328	136992 (2.6)	814427	19073 (2.3)
O-Xylene	60672623	1883398 (3.1)	654367	30042 (4.6)
Cumene	53006562	1575898 (3.0)	851652	21542 (2.5)
DCB	55078477	1725543 (3.1)	521684	15701 (3.0)

The % RSD values on day 2 reduced to between 2.1 and 3.1 % for the EI spectra and 2.3 and 5.5 % for the SIR spectra. It was thought that the improvement of the % RSD values obtained on day 2 was as a result of the further conditioning of the Tenax within the tubes. The experiment was repeated with prepacked sampling tubes. The EI and SIR peak areas were obtained with the standard deviations and % RSD values calculated (see Table 3.8). The % RSD values for the prepacked tubes were between 2.3 and 4.5 % for the EI spectra and 1.7 and 5.7 % for the SIR spectra. The EI and SIR % RSD values obtained for the in-house packed tubes were comparable to the EI and SIR RSD values for the prepacked tubes.

Table 3.8: Repeatability measurements on prepacked tubes used to sample VOC from bell chamber pollutant source

	EI		SIR	
	Ave.	STD (% RSD)	Ave.	STD (% RSD)
Toluene	30411965	1004883 (3.3)	196226	3362 (1.7)
Ethylbenzene	31547967	987654 (3.1)	452058	10900 (2.4)
O-Xylene	36490251	847252 (2.3)	330219	11710 (3.6)
Cumene	31812036	906149 (2.8)	434761	12765 (2.9)
DCB	41007754	1829595 (4.5)	294824	16868 (5.7)

On this evidence it was proposed that the in-house packed sampling tubes could be used to sample VOCs from air. The main advantage of using the in-house prepared tubes was cost, as a saving of £300 was estimated if a set of 10 in-house packed sampling tubes were used rather than a set which came prepacked. From the experimental results shown above the decision was taken to use in-house packed sampling tubes in further sampling procedures. From this point on in the thesis, no distinction will be made between in-house packed and prepacked sampling tubes, they will both be referred to simply as sampling tubes.

3.2.2 Testing the sampling method for the collection of VOCs from the bell chamber

It was crucial to test the sampling conditions used to extract the VOCs from the contaminated air. In the bell chamber three variables were investigated; a) sampling time, b) chamber concentration and c) pump flow rate. Each variable was studied individually. An atmosphere containing five VOCs of known concentration was generated using the bell chamber as described in Section 3.2.1. The original sampling time used for sampling VOCs from the chamber was 10 s. Sampling times of 20, 30, 40, 50 or 60 s were therefore investigated. Increasing the sampling time that air is pumped through the tube corresponds to an increase in volume of air sampled and therefore an increase in the theoretical masses of analytes trapped by the sampling tubes, as shown in Table 3.9. The responses obtained for each analyte in the resultant SIR chromatograms are represented in Figure 3.2.

Table 3.9: Mass of analytes theoretically trapped when sampling at 50 ml min^{-1} from a chamber created using 5 µL injection using different sampling times

Analyte	Mass of analyte trapped on Tenax / µg					
	10 s	**20 s**	**30 s**	**40 s**	**50 s**	**60 s**
Toluene	1.58	3.16	4.74	6.32	7.90	9.48
Ethylbenzene	1.58	3.16	4.74	6.32	7.90	9.48
O-xylene	1.60	3.20	4.79	6.39	7.99	9.59
Cumene	1.56	3.12	4.69	6.25	7.81	9.37
DCB	2.36	4.72	7.08	9.44	11.81	14.17

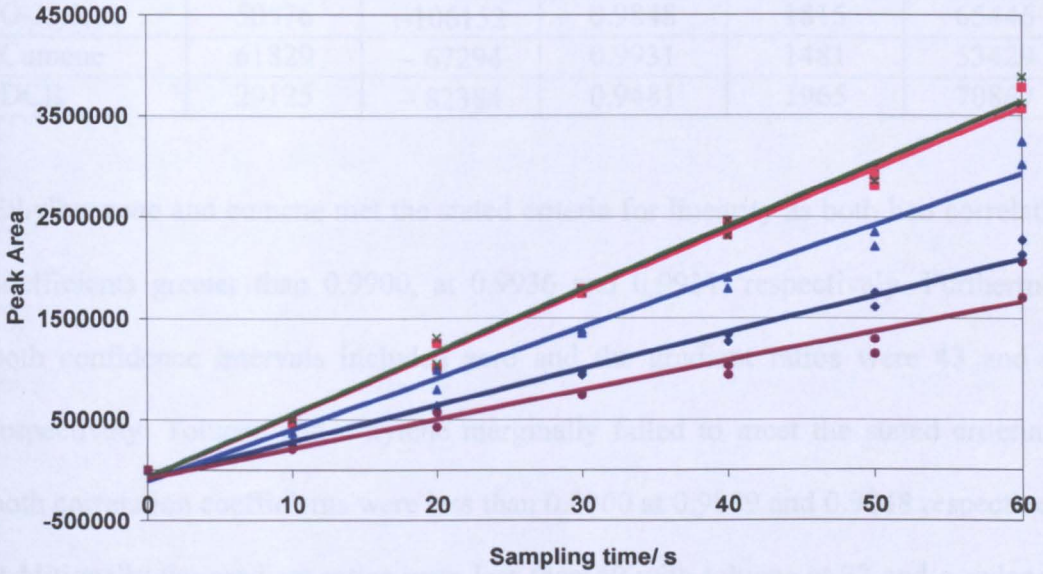

Figure 3.2: Analyte peak areas for the selected m/z ion when sampling time was increased. — Toluene, — Ethylbenzene, — O-xylene, — Cumene & — DCB

As expected there was an increase in chromatographic responses with increased sampling times. Linear regression was performed on the results and the data are given in Table 3.10. To statistically evaluate the linearity of analyte responses, the errors on the intercept and slope were examined in addition to the correlation coefficient. If a linear trend is to be confirmed it is expected that the correlation

coefficient is > 0.9900, the confidence interval of the intercept includes zero and the result of the slope divided by the slope error is > 40.[2]

Table 3.10: Statistical evaluation for the VOCs when sampling time was increased.

	Slope	Intercept	Correlation Coefficient	Error on Slope	Error on Intercept
Toluene	36217	– 85255	0.9889	1109	39999
Ethylbenzene	60827	– 70082	0.9936	1408	50787
O-Xylene	50576	–106152	0.9848	1815	65446
Cumene	61829	– 67294	0.9931	1481	53429
DCB	29125	– 82384	0.9481	1965	70867

Ethylbenzene and cumene met the stated criteria for linearity as both had correlation coefficients greater than 0.9900, at 0.9936 and 0.9931, respectively. Furthermore both confidence intervals included zero and the gradient ratios were 43 and 42, respectively. Toluene and o-xylene marginally failed to meet the stated criteria as both correlation coefficients were less than 0.9900 at 0.9889 and 0.9848 respectively. Additionally the gradient ratios were less than 40 with toluene at 32 and o-xylene at 27. However both toluene and o-xylene did meet the stated confidence interval criteria. DCB failed to meet the linearity criteria as the both the correlation coefficient and gradient ratio were well below the stated values at 0.9481 and 15, respectively. Although an increase in sampling time from 10 s to 60 s led to data which were deemed non-linear by statistical analysis it could be argued that the data fell well within analytically acceptable limits, with variations < 5 %. Thus it was thought that the sampling method was analytically valid for all 5 analytes when using sampling times between 10 – 60 s. Moreover, the results suggest that Tenax, the sampling and analysis methods were all suited to collection of toluene, ethylbenzene,

o-xylene, cumene and DCB, otherwise near-linear relationships would not be obtained.

3.2.2.1 Sampling different concentrations of VOCs.

For the sampling method to be valid for VOCs in air, the chromatographic responses of each analyte should also increase linearly with increased concentrations of VOCs. Different atmospheres of known analyte concentration were generated using the bell chamber system described in Section 3.2.1. Different liquid volumes of each analyte were injected into the system (2.5, 5 7.5 or 10 μL). The expected concentrations and masses obtained by sampling each atmosphere are given in Table 3.11. The atmospheres were sampled at 50 mL min^{-1} for 10 s. Two replicate measurements were taken for each chamber concentration. The peak areas of each analyte were taken from the SIR chromatograms and plotted against volume of analyte added to the chamber as shown in Figure 3.3.

Table 3.11: Masses of analytes theoretically trapped when sampling for 10 s at 50 ml min^{-1} from chambers of different concentrations

Analyte	Chamber concentration / mg m^{-3}				Mass of analyte trapped on Tenax / μg			
	2.5	5.0	7.5	10.0	2.5	5.0	7.5	10.0
Toluene	95.2	190.4	285.6	380.7	0.79	1.58	2.37	3.16
Ethylbenzene	95.2	190.4	285.6	380.7	0.79	1.58	2.37	3.16
O-xylene	96.3	192.5	288.8	385.1	0.80	1.60	2.40	3.20
Cumene	94.1	188.2	282.3	376.4	0.78	1.56	2.34	3.12
DCB	142.2	284.5	426.7	568.9	1.18	2.36	3.54	4.72

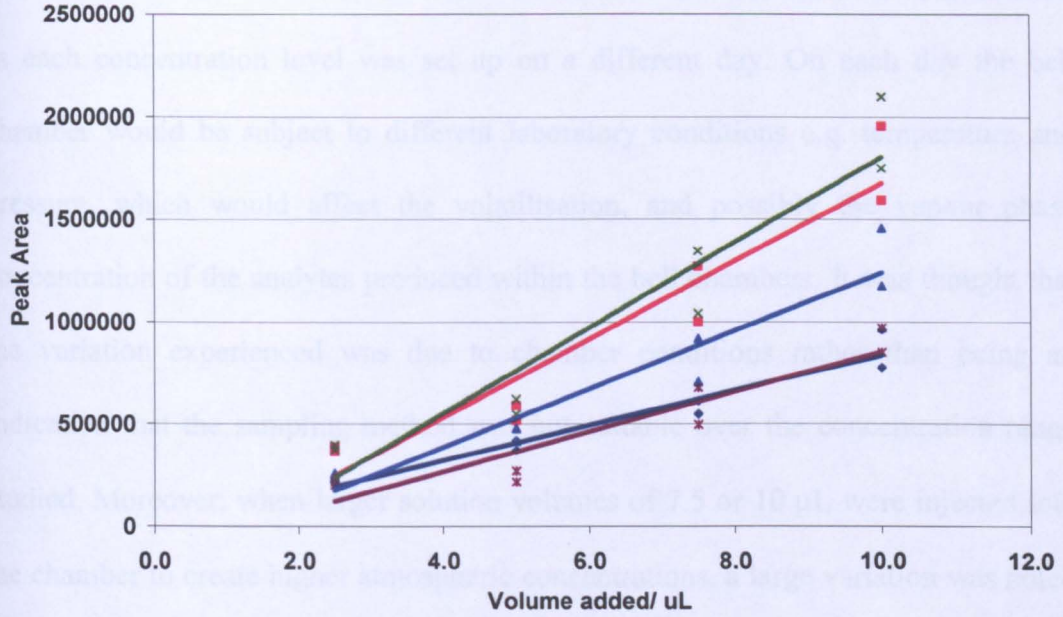

Figure 3.3: Peak area obtained from the SIR chromatogram when the atmospheric concentration was altered. —Toluene, — Ethylbenzene, — O-xylene, — Cumene & —DCB

Note that injection volume was used as the scale on the x-axis because each VOC has a different density, therefore although the volume injected was the same, the mass injected was different for each VOC therefore generating different VOC concentrations (Table 3.11). Linear regression was performed and the results are shown in Table 3.12. Using the same criteria as outlined in Section 3.2.2 the linearity of the results was assessed. All of the VOCs failed to pass the linearity criteria based on correlation coefficients of above 0.9900 and gradient ratios above 40. Toluene, ethylbenzene, o-xylene, cumene and DCB had correlation coefficients of 0.9442, 0.9103, 0.9185, 0.9128, 0.8855 and gradient ratios of 10.1, 7.8, 8.2, 7.9 and 6.8, respectively. When evaluating the confidence intervals for each VOC, the criteria was achieved as all the confidence intervals included zero. One possibility why the

results failed to meet the stated criteria was due to variation in chamber concentration as each concentration level was set up on a different day. On each day the bell chamber would be subject to different laboratory conditions e.g. temperature and pressure, which would affect the volatilisation, and possibly the vapour phase concentration of the analytes produced within the bell chambers. It was thought that the variation experienced was due to chamber conditions rather than being an indication that the sampling method was not suitable over the concentration range studied. Moreover, when larger solution volumes of 7.5 or 10 μL were injected into the chamber to create higher atmospheric concentrations, a large variation was noted for the two replicate measurements obtained. The reason for this variability was possibly due to inefficient vaporisation of the higher volume of solution used. Due to the high precision of the two measurements taken from the atmosphere created using 5 μL injection volumes, this injection volume was used for future experiments.

Table 3.12: Statistical evaluation for the VOC's linearity with respect to different chamber concentrations

	Slope	Intercept	Correlation Coefficient	Error on Slope	Error on Intercept
Toluene	85802	-19929	0.9442	8516	58302
Ethylbenzene	190977	-232233	0.9103	24481	167610
O-Xylene	142313	-181141	0.9185	17307	118490
Cumene	208789	-282113	0.9128	26345	180371
DCB	97905	-124124	0.8855	14375	98422

3.2.2.2 Assessment of different sample flow rates of air through the sampling tubes

A bubble meter was used to measure the rate of air flowing through sampling tubes. The rate of air passing through the tube is important. If it is too fast, there may not be enough time for analytes to interact with the sorbent material and be removed

from the air. If it is too slow then the sampling time becomes inefficient. Therefore atmospheres of known concentrations of VOCs were set up as described in Section 3.2.1. giving atmospheric concentrations listed in Table 3.5. Four different sampling experiments were performed with a sampling time set at 10 s and different flow rates of 25, 50, 75 or 100 mL min^{-1}. Although it was thought that tubes packed with Tenax (either in-house or pre-packed) had no obvious voids or channels through the Tenax when connected to the pump, slightly different flow rates were obtained for each tube. Therefore all tubes were individually calibrated before use. After calibration two tubes were used to sample each of the generated atmospheres. The peak area of the response on the SIR chromatograms were obtained and plotted against airflow rate (see Figure 3.4).

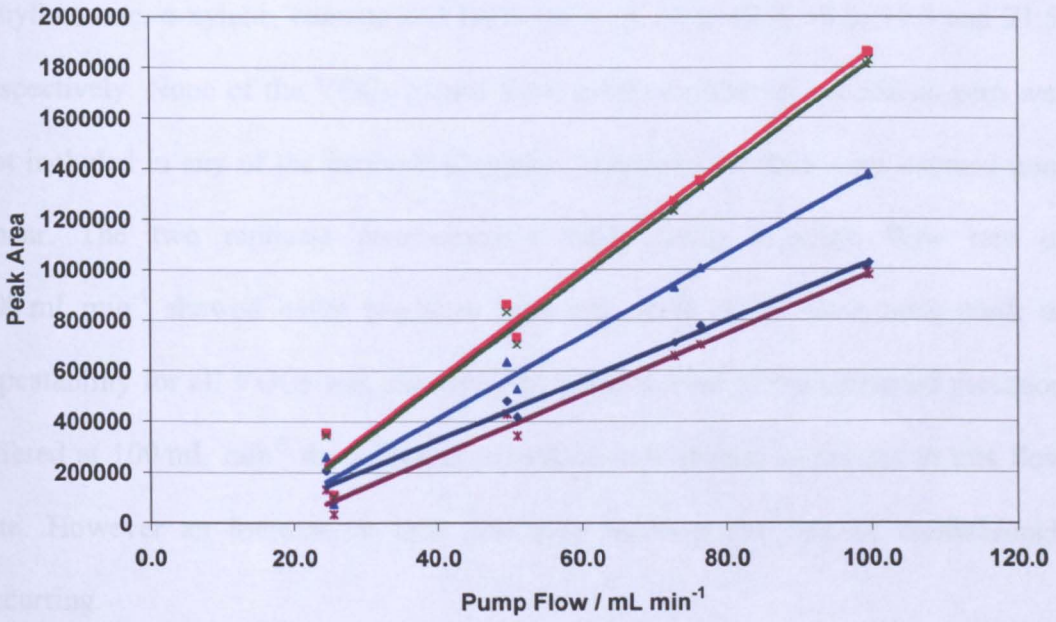

Figure 3.4: Peak area obtained from the SIR chromatogram when the pump flow rate for sampling was altered. — Toluene, — Ethylbenzene, — O-xylene, — Cumene & — DCB

Linear regression was performed and the results are shown in Table 3.13. A positive correlation was obtained between peak area and flow rate for each analyte.

Table 3.13: Statistical evaluation for the VOC's linear graphs produced by altering the pump flow

	Slope	Intercept	Correlation Coefficient	Error on Slope	Error on Intercept
Toluene	11730	-141563	0.9855	581	39725
Ethylbenzene	21698	-301938	0.9834	1151	78610
O-Xylene	16139	-233299	0.9826	877	59926
Cumene	21343	-307980	0.9836	1126	76930
DCB	12039	-218001	0.9871	561	38318

The correlation coefficients produced for each VOC were narrowly below the accepted criteria of 0.9900; between 0.9826 and 0.9871. The slope ratios produced for the VOCs were below the stated criteria of greater than 40: with toluene, ethylbenzene, o-xylene, cumene and DCB ratios of 20.1, 18.9, 18.0, 19.0 and 21.5, respectively. None of the VOCs passed the confidence interval criteria as zero was not included in any of the intervals obtained. Therefore the data were deemed non-linear. The two replicate measurements taken using a pump flow rate of 100 mL min^{-1} showed better precision than any other of the flow rates used; as repeatability for all VOCs was less then one percent. Due to the increased precision offered at 100 mL min^{-1} the sampling procedure was altered to sample at this flow rate. However an increase in flow rate may increase the risk of breakthrough occurring.

3.2.2.3 Breakthrough

It is known that sorbents have a limited capacity for absorption of a given analyte, either by saturation or chemical displacement.[3] Once this capacity has been reached

the analytes will pass through the sorbent un-absorbed. This is commonly referred to as 'breakthrough'. The point of breakthrough is identified when the concentration of analyte in the outlet stream is equal to 5 % of that in the inlet stream.[3] Breakthrough can occur when the sampling volume or concentration is too high, and the point of breakthrough can vary with air temperature. Alternatively the sorbent used may not have the retention ability for the given analyte. In this case another sorbent will have to be used.[4] To ensure that breakthrough was not occurring for an atmospheric chamber with analyte atmospheric concentrations of approximately 188-284 mg m^{-3}, two sampling tubes were connected in-line and the atmosphere was sampled at 100 mL min^{-1} for 10 s. The resultant EI chromatograms are shown in Figure 3.5. The intensities of the peaks produced on the first chromatogram range from 8.55×10^8 to 1.13×10^9. There was no evidence of breakthrough from the first sampling tube because there was no adsorption from any of the five selected VOCs onto the second Tenax tube at the appropriate retention times. The peaks present on chromatogram B do not correspond to those of the VOCs. The largest peak present in chromatogram B is only 0.1% the intensity of the toluene peak present in chromatogram A. This experiment has shown that sampling an atmosphere containing toluene, ethylbenzene, o-xylene, cumene and DCB at concentrations of 190.4, 190.4, 192.5 188.2 and 284.5 mg m^{-3} respectively, for 10 s at 100 mL min^{-1}, a total mass of 17.4 μg of VOC was absorbed onto the Tenax with no breakthrough. Therefore sampling conditions of 100 mL min^{-1} for 10 s was maintained and used throughout the rest of the experiments.

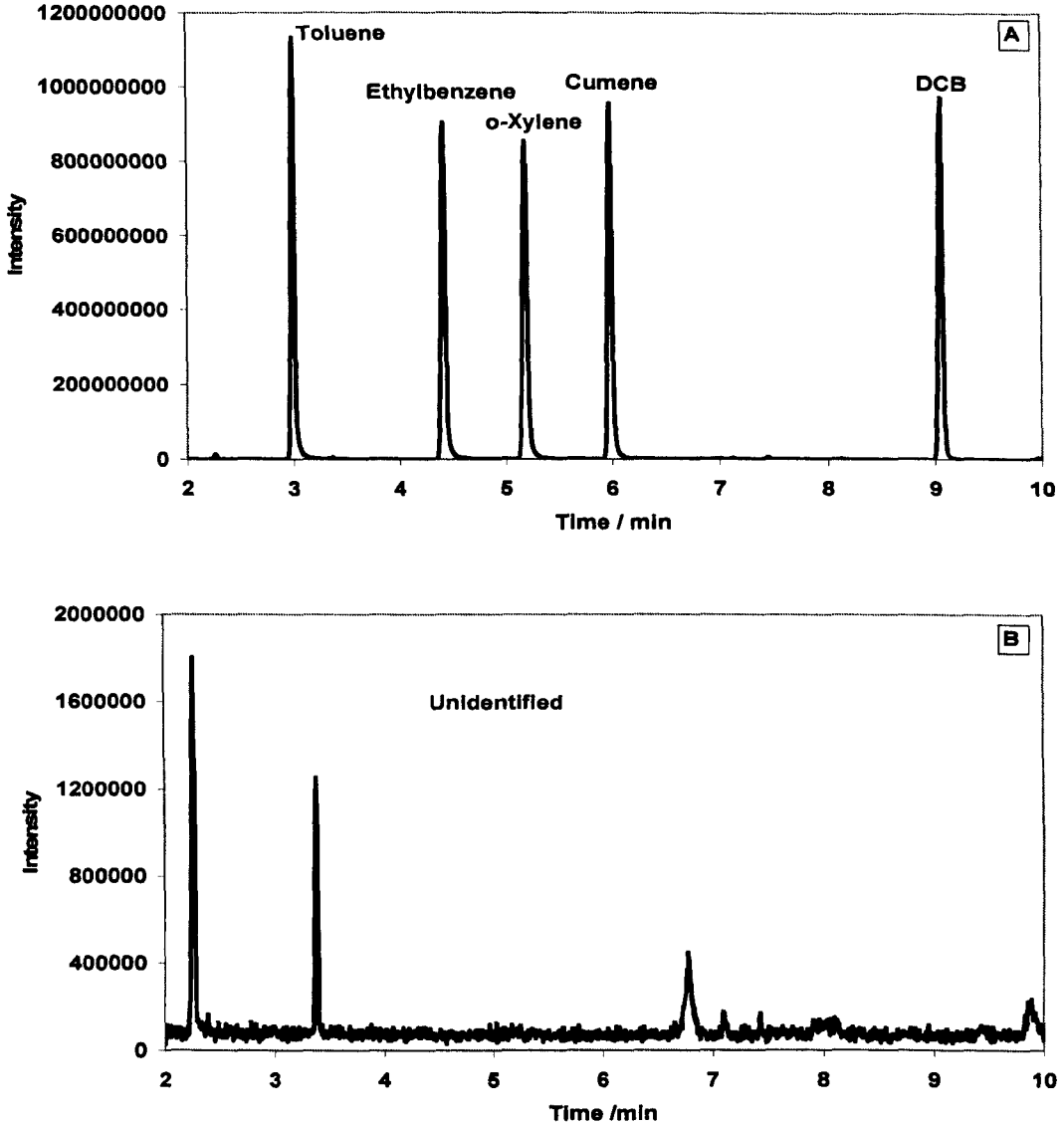

Figure 3.5: a) EI chromatogram produced from first sampling tube b) EI chromatogram produced from the second sampling tube inline.

3.2.2.4 Repeatability

The atmospheric chamber was set up as described in Section 3.2.1. The chamber was sampled for 10 s at flow rate of 100 mL min^{-1}. Five replicate measurements were taken on three separate occasions. The average peak areas, standard deviations and % relative standard deviations obtained from the EI and SIR chromatograms are listed

in Table 3.14. On day 1, the % RSD values for the average peak areas of toluene, ethylbenzene, o-xylene, cumene and DCB from the EI chromatograms were 10.5, 11.3, 11.2, 11.1 & 13.5 %, respectively, while the % RSD obtained from the SIR peak areas were 10.7, 11.8, 11.6, 11.5 & 13.7 %, respectively. This amount of variation was high and could indicate a variance in absorption capabilities of the Tenax. The % RSD values on day 2 improved to 0.97, 4.71, 4.68, 4.77 & 13.3 %, respectively, for the EI spectra and 2.9, 4.5, 6.0, 6.0 & 14.4 %, respectively, for the SIR spectra. The range of % RSD values on day 3 were improved for all analytes with values within 2.3 – 4.5 % for the EI spectra and 1.7 –5.7 % for the SIR spectra. The improvements in the % RSD values was thought to be as a result of increasing familiarity with the technique. The repeatability of tubes obtained on days 2 & 3 was within similar ranges to those obtained in Section 3.2.1. The % RSD of the packed tubes varied between 2.1 - 6.6 % for the EI spectra and 2.3 – 11.7 % for the SIR spectra. This experiment indicates that some variation is present within the sampling and analysis method. This variation may not be solely attributable to inefficient absorption of the analytes by Tenax. Contributions to the variation in the analysis may include varying chamber concentrations, inefficient desorption within the TDU or variation in the GC-MS response to the analytes. Therefore further experiments were undertaken to assess the variability of repeat injection of analyte solutions into the GC-MS.

3.2.3 Examination of repeat injection of solutions into GC-MS

Experiments were undertaken to ensure the TDU-GC-MS operating conditions used (see Section 3.1.3) were suitable to extract 100 % of trapped VOCs from sampled Tenax tubes.

Table 3.14: peak area repeatability of EI and SIR spectra when sampling VOCs under optimised conditions

	Day 1				Day 2				Day 3			
	EI		m/z		EI		m/z		EI		m/z	
	AVE	STD (%RSD)	AVE	STD (%RSD)	AVE	STD (%RSD)	AVE	STD (%RSD)	AVE	STD (%RSD)	AVE	STD (%RSD)
Toluene	34734312	3637332 (10.5)	500270	58603 (11.7)	84465752	817970 (1.0)	582951	16858 (2.9)	30411965	1004883 (3.3)	196226	3362 (1.7)
Ethyl-benzene	39432608	4446139 (11.3)	989369	116277 (11.8)	96505885	4542546 (4.7)	1345564	61364 (4.6)	31547967	987654 (3.1)	452058	10900 (2.4)
O-xylene	406880712	4545592 (11.2)	856775	99766 (11.6)	100367454	4700932 (4.7)	1009966	61138 (6.0)	36490251	847252 (2.3)	330219	11710 (3.6)
Cumene	44468465	4933262 (11.1)	1040584	119692 (11.5)	13973774	6666997 (4.8)	1844612	110455 (6.0)	31812036	906149 (2.8)	434761	12765 (2.9)
DCB	35522762	4803652 (13.5)	537845	73663 (13.7)	122086387	16199016 (13.3)	828936	119311 (14.4)	41007754	1829595 (4.5)	294824	16868 (5.7)

It was therefore thought appropriate to examine the intensity of peaks given by direct injection of solution containing a known mass of each analyte into the GC-MS. Methanolic solutions were prepared containing similar masses of VOCs as used in the previous bell chamber experiments. An autosampler was used to introduce the solutions into the GC-MS. In this 'direct injection' mode only 5% of the injected solution passed onto the chromatographic column. In comparison, when using the TDU as a sample introduction system the sample is split twice before it is introduced onto the column, passing approximately 0.43% (see Equation 2.21) of the sample onto the column. It was therefore necessary to create methanolic solutions that would introduce the same masses of analytes onto the column, after a 5 % split, as would the TDU after a 0.43 % split. Therefore, a methanolic solution containing VOCs with concentrations of approximately 0.28 $\mu g\ \mu L^{-1}$ was prepared and, using a 1 μL injection volume, equivalent masses of VOCs were introduced into the GC-MS permitting comparison of peak responses with those obtained by the TDU-GC-MS. When using the autosampler to introduce the standard VOC solution, the GC-MS was operated using an injection temperature of 250 °C. All other operating conditions for the GC-MS were similar to those listed in Tables 3.2 and 3.3. The intensities of the peaks recorded from the EI GC chromatogram are given in Figure 3.6. Included in the figure is a chromatogram recorded for a desorbed sampled Tenax tube. The toluene, ethylbenzene and o-xylene peak area intensities produced by the direct injection method were within 76-78 % of those produced by thermal desorption. The intensities of the cumene and DCB peak areas differed by 7.9 and 0.1 %. The direct injection mode experiment confirmed that the TDU-GC-MS operating conditions were acceptable.

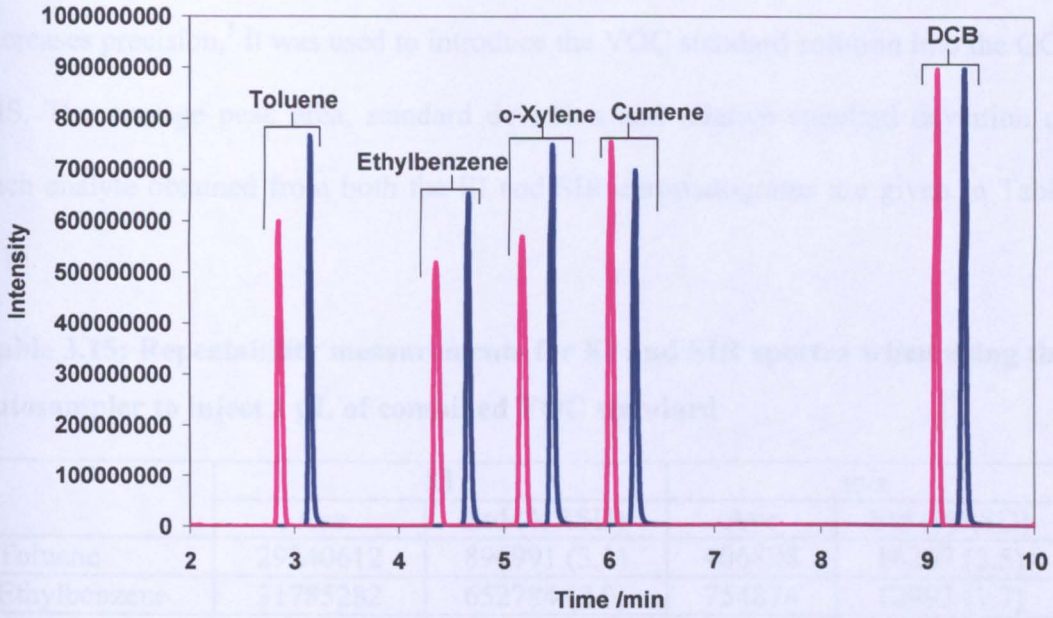

Figure 3.6: Comparison of EI chromatograms. — analytes injected on column through autosampler and — analytes injected on column through TDU

The small differences in intensities were thought to be as a result of small inaccuracies in the calculation of the TDU split. The flow rates of the inlet split, outlet split and desorb flow were all measured using a small bubble meter and stopwatch while the column flow was assumed to be 1 mL min^{-1}. If the flow rates were slightly inaccurate then this would result in a different % of analytes reaching the column, therefore a different mass of analytes reaching the column than calculated.

3.2.3.1 Repeat injection of a standard solution of VOCs into the GC-MS.

To determine the repeatability of responses when injecting a standard solution of VOCs, five 1 µL injections of the standard solution (approximately 0.28 µg µL) were

performed. As an autosampler introduction system removes operator variability and increases precision,[5] it was used to introduce the VOC standard solution into the GC-MS. The average peak area, standard deviation and relative standard deviation of each analyte obtained from both the EI and SIR chromatograms are given in Table 3.15.

Table 3.15: Repeatability measurements for EI and SIR spectra when using the autosampler to inject 1 μL of combined VOC standard

	EI		m/z	
	Ave	Std (%RSD)	Ave	Std (%RSD)
Toluene	29240612	896991 (3.1)	406898	14267 (3.5)
Ethylbenzene	31785282	652784 (2.0)	754874	12993 (1.7)
O-Xylene	35840635	571695 (1.6)	722317	13017 (1.8)
Cumene	38676292	614052 (1.6)	943469	9569 (1.0)
DCB	40006721	314999 (0.8)	595766	4940 (0.8)

The % RSD values for the EI peak areas were within 0.8 - 3.1 %, while similar % RSD values were obtained for the SIR peak areas, within 0.8 - 3.5 %. The best peak area % RSD obtained during atmospheric chamber sampling was within 2.3 - 4.5 % for EI spectrum and 1.7 - 5.7 % for the SIR spectrum, see Table 3.14. Therefore this experiment confirms that some of the variation obtained during sampling is due to instrumental variation. However not all of the variation seen during the atmospheric sampling experiments has been accounted for. Hence further experiments were undertaken to assess other sources of variation.

3.2.3.2 Injecting increasing concentrations of standard solutions into the GC-MS

To ensure that the GC-MS method had a large linear range for the VOCs of interest a range of standard solutions containing all 5 analytes were prepared between

concentrations of 0.005 and 0.3 μg μL-1. All solutions were injected by the autosampler; a 1 μL injection volume was used and solutions were injected in duplicate. The peak areas for each analyte mass were obtained from the resultant SIR chromatograms and plotted against mass (Figure 3.7). Linear regression was performed (see Table 3.16) and the average peak area, standard deviation and % RSD were calculated (shown in Table 3.17). Within the range of masses injected the SIR peak areas variation between the duplicate injections, for all analytes, was within 0.1-6.8 % with the majority between 1-4 %.

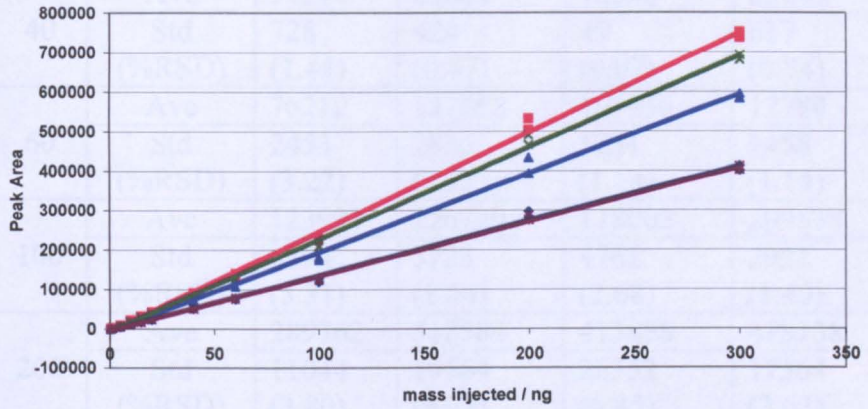

Figure 3.7: Linear graph produced when reduced masses of VOCs are injected onto the column via the autosampler.— Toluene, — Ethylbenzene, — O-xylene, — Cumene & — DCB

Table 3.16: Statistical evaluation for the VOCs when the autosampler was used to introduce the analytes to the GC-MS system.

	Slope	Intercept	Correlation Coefficient	Error on Slope	Error on Intercept
Toluene	1388	-3335	0.9969	17.2	1982.5
Ethylbenzene	2523	-6624	0.9980	25.4	2930.8
O-Xylene	2003	-5749	0.9967	25.6	2945.9
Cumene	2329	-6167	0.9981	22.8	2621.7
DCB	1375	-3232	0.9986	11.4	1315.9

Table 3.17: Peak area averages, standard deviations and %RSDs for each VOC at injection masses from 5-300 ng

Mass injected (ng)			Toluene	Ethyl-benzene	O-xylene	Cumene	DCB
	5	Ave	4779	8526	6561	7739	4681
		Std	41	25	54	79	17
		(%RSD)	(0.85)	(0.29)	(0.82)	(1.02)	(0.36)
	10	Ave	11291	20446	15616	18310	11138
		Std	79	461	144	84	116
		(%RSD)	(0.70)	(2.25)	(0.92)	(0.46)	(1.04)
	15	Ave	17616	30992	24272	28155	17250
		Std	357	672	133	463	151
		(%RSD)	(2.03)	(2.17)	(0.55)	(1.65)	(0.87)
	20	Ave	23236	42321	33234	39306	23686
		Std	463	39	274	615	193
		(%RSD)	(1.99)	(0.09)	(0.82)	(1.56)	(0.81)
	40	Ave	50274	89884	70546	83143	50008
		Std	728	424	49	617	426
		(%RSD)	(1.44)	(0.47)	(0.07)	(0.74)	(0.85)
	60	Ave	76212	137868	107936	12788	76702
		Std	2453	2835	1231	1458	861
		(%RSD)	(3.22)	(2.1)	(1.14)	(1.14)	(1.12)
	100	Ave	123997	226720	178002	209538	125121
		Std	6594	3723	4762	2932	1700
		(%RSD)	(5.31)	(1.64)	(2.68)	(1.40)	(1.36)
	200	Ave	289762	518584	413858	478138	280700
		Std	11044	19564	28352	17364	7362
		(%RSD)	(3.80)	(3.77)	(6.85)	(3.63)	(2.62)
	300	Ave	407371	744662	589768	687525	407192
		Std	7843	10125	8692	8777	6590
		(%RSD)	(1.92)	(1.36)	(1.47)	(1.28)	(1.62)

The correlation coefficients for the analytes were within 0.9967-0.9986. The gradient ratios for toluene, ethylbenzene, o-xylene, cumene and DCB were 80.7, 99.3, 78.2, 102.1 and 120.6 respectively. All the analytes included zero when evaluating the confidence intervals. Therefore the GC-MS response was deemed to be linear with respect to increasing sample concentration. Linear regression could therefore be used to determine unknown VOC concentrations within the calibration range studied.

3.2.3.3 Limit of detection of VOCs on the GC-MS

To determine the limit of detection of the GC-MS method used, a standard solution with analyte concentrations of approximately 0.001 μg μL^{-1} was prepared. Six 1 μL injections of this standard were made into the GC-MS using an autosampler. The limits of detection for each analyte were determined using peak areas from the EI spectrum. Table 3.18 shows the average values, standard deviations and % RSD calculated. The limit of detection corresponded to a 1 ng μL^{-1} injection of VOCs, which is equivalent to 50 pg of analyte reaching the detector. Using this value it is possible to back calculate and estimate the limit of detection in the corresponding atmospheric sampling method, which was approximately 0.684 mg m^{-3} (or 181.3 ppb). This corresponds to a mass of 12 ng trapped on the Tenax. It should be noted that the actual limit of detection for the atmospheric sampling method may be slightly higher than this concentration value as it is likely to include more sources of error.

Table 3.17 : Peak area averages, standard deviations and % RSD for each VOC at injection masses from 5-300 ng.

	Mass injected /ng																	
	5		10		15		20		40		60		100		200		300	
	AVE	STD (%RSD)	AVE	STD (%RSD)	AVE	STD (%RSD)	AVE	STD (%RSD)	AVE	STD (%RSD)	AVE	STD (%RSD)	AVE	STD (%RSD)	AVE	STD (%RSD)	AVE	STD (%RSD)
Toluene	4779	41 (0.86)	11291	79 (0.70)	17616	357 (2.03)	23236	463 (1.99)	50274	728 (1.44)	76212	2453 (3.22)	123997	6594 (5.31)	289762	11044 (3.8)	407371	7843 (1.92)
Ethyl-benzene	8526	25 (0.29)	20446	461 (2.25)	30992	672 (2.17)	42321	38.9 (0.09)	89884	424 (0.47)	137868	2835 (2.1)	226720	3723 (1.64)	518584	19564 (3.77)	744662	10125 (1.36)
O-xylene	6561	54 (0.82)	15616	144 (0.92)	24272	133 (0.55)	33234	274 (0.82)	70546	48.8 (0.07)	107936	1231 (1.14)	178002	4762 (2.68)	413858	28352 (6.85)	589768	8692 (1.47)
Cumene	7739	79 (1.02)	18310	84 (0.46)	28155	463 (1.65)	39306	615 (1.56)	83143	617 (0.74)	127788	1458 (1.14)	209538	2932 (1.40)	478138	17364 (3.63)	687525	8777 (1.28)
DCB	4681	16.9 (0.36)	11138	116 (1.04)	17250	151 (0.87)	23686	193 (0.81)	50008	426 (0.85)	76702	861 (1.12)	125121	1700 (1.36)	280700	7362 (2.62)	407192	6590 (1.62)

Table 3.18: Peak area average, standard deviations and % RSD for each VOC when repeatedly injecting a 1ng μL^{-1} VOC solution

	EI	
	Ave	Std (%RSD)
Toluene	55191	842 (0.8)
Ethylbenzene	43893	1825 (4.2)
O-Xylene	34358	2443 (7.1)
Cumene	36493	1380 (3.8)
DCB	30215	1652 (5.5)

3.2.4 Investigation into the introduction of volatile organic compounds onto the sampling tubes

The sampling system described in Section 2.1 involved injecting known volumes of VOC into a bell chamber and volatilisation of the VOCs at room temperature. It was hoped that complete volatilisation of all analytes occurred and that the predicted VOC atmospheric concentrations were correct. It was thought appropriate to test this by injecting a methanolic solution of known VOCs concentrations onto a Tenax sampling tube and then analysing the tube using the TDU-GC-MS. To perform the direct injection of a solution onto a Tenax sampling tube, the sample introduction system of a Perkin Elmer GC 8000 was modified as shown in Figure 3.8. An adaption union was used to connect the sampling tube to the injection port of the GC. Helium was used as a carrier gas permitting the transport of the injected analytes onto the Tenax tube. The GC oven was controlled at 25 °C. After injection of the standard solution, helium was passed over the Tenax tube for 2 minutes at a flow rate of approximately 100 mL min^{-1}. The Tenax tubes were then removed, capped and analysed by TD-GC-MS as outlined in Section 3.1.1.

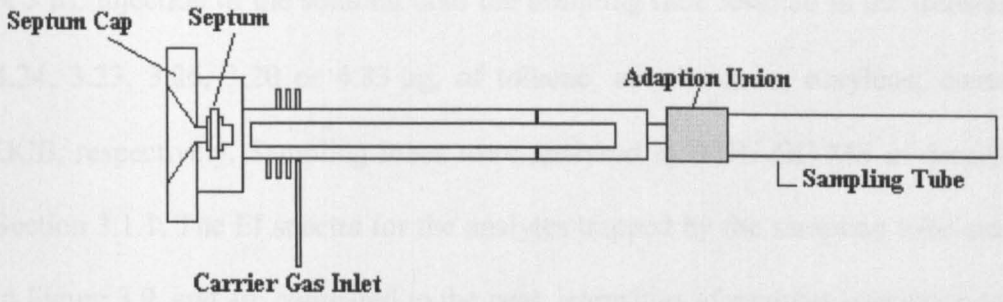

Figure 3.8: schematic of the modified Perkin Elmer GC8000 injection port used to directly inject a solution of VOCs onto a sampling tube.

3.2.4.1 Preparation of a VOC standard for direct injection

The standard VOC solution used for direct injection onto the Tenax filled sampling tube was prepared in a 10 mL volumetric flask. The final concentration of each analyte is given in Table 3.19. The concentrations of each VOC in the standard solution were chosen so that the masses injected directly onto the Tenax, via a 5 μL standard solution injection volume, were equivalent to the masses trapped in the bell chamber experiment (using 5 μL injection of each VOC into the chamber and sampling at 100 mL min^{-1} for 10 s after a 1 hour equilibration time). The final concentration of the standard required was calculated using Equation 2.1 (pg 31) to determine the theoretical concentration of analytes in the chamber.

Table 3.19: Final concentration of VOCs in the standard used for direct injection

VOC	Concentration / μg $μL^{-1}$
Toluene	0.60
Ethylbenzene	0.65
O-Xylene	0.65
Cumene	0.64
DCB	0.97

A 5 μL injection of the solution onto the sampling tube resulted in the transferral of 3.24, 3.23, 3.26, 3.20 or 4.83 μg, of toluene, ethylbenzene, o-xylene, cumene or DCB, respectively. Sampling tubes were analysed by TDU-GC-MS as described in Section 3.1.1. The EI spectra for the analytes trapped by the sampling tube are given in Figure 3.9, and are compared to the peak intensities of analytes trapped in tubes in the bell chamber experiments. Direct injection of the standard solution of toluene, ethylbenzene, o-xylene, cumene and DCB gave increased intensities of 58.7, 55.2, 40.0, 83.8 and 30.4 % respectively. The slight difference in retention time, approximately 6 s, between the two chromatograms may be due to some column degradation.

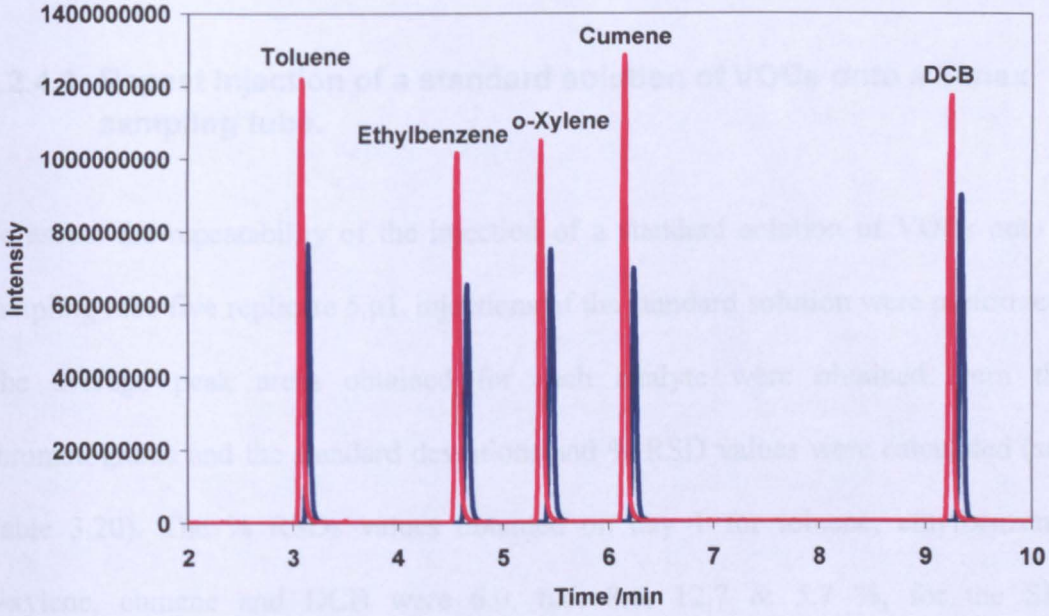

Figure 3.9: Comparison of EI chromatograms. Chromatogram in — shows analytes sampled onto Tenax from the bell chamber and the — chromatogram shows analytes injected onto Tenax via the modified GC injection port.

Previous experiments (Section 3.2.3) have shown that there is efficient adsorption/desorption of the VOC onto sampling tubes, therefore it was thought that the smaller masses of analytes trapped in the bell chamber experiment were not due to inefficient adsorption/desorption of analytes from the Tenax. Smaller masses of analytes measured during the bell chamber experiments were possibly due to i) incorrect delivery of analytes to the bell chamber due to the very small sample volume or ii) incomplete volatilisation of the analytes within the bell chamber. Both of the scenarios would result in reduced chamber concentrations. That said, the superimposed chromatograms in Figure 3.9 were of similar magnitude in intensity, considering the number of possible contributions and combinations of variability within both methods, the intensities were deemed analytically acceptable.

3.2.4.2 Repeat injection of a standard solution of VOCs onto a Tenax sampling tube.

To assess the repeatability of the injection of a standard solution of VOCs onto a sampling tube five replicate 5 μL injections of the standard solution were performed. The average peak areas obtained for each analyte were obtained from the chromatograms and the standard deviations and % RSD values were calculated (see Table 3.20). The % RSDs values obtained on day 1 for toluene, ethylbenzene, o-xylene, cumene and DCB were 6.0, 6.6, 8.6, 12.7 & 5.7 %, for the SIR chromatograms and 7.2, 5.8, 6.5, 7.4 & 6.4 %, respectively, for the EI chromatograms. When the experiment was repeated on day 2 the % RSD values were 3.5, 1.0, 3.9, 1.2 & 2.4 % for the SIR chromatograms and 1.2, 1.0, 1.1, 1.2 & 2.2 %

for the EI chromatograms. These % RSD values were analytically acceptable being less than 10%. Therefore the method of direct injection of analytes on to the sampling tube was used to calibrate atmospheric sampling experiments.

Table 3.20: Average peak areas, standard deviations and % RSD from EI and SIR spectra of VOCs repeatedly injected onto five sampling tubes

	Day 1				Day 2♦			
	EI		m/z		EI		m/z	
	Ave	Std (% RSD)	Ave	Std (% RSD)	Ave	Std (% RSD)	Ave	Std (% RSD)
Toluene	47184589	3408723 (7.2)	339544	20339 (6.0)	44464251	535461 (1.2)	372437	12965 (3.5)
Ethyl benzene	47673681	2784762 (5.8)	710936	47050 (6.6)	46454208	486403 (1.0)	769579	8269 (1.0)
O-Xylene	51721392	3373024 (6.5)	532385	45526 (8.6)	50572021	547031 (1.1)	580820	22697 (3.9)
Cumene	57697592	4281949 (7.4)	811137	102715 (12.7)	55187189	663735 (1.2)	934692	11211 (1.2)
DCB	52144365	3336318 (6.4)	462695	26206 (5.7)	51168994	1149624 (2.2)	504634	11992 (2.4)

♦*Calculated from 4 replicates due to an outlier.*

3.2.4.3 Direct injection of increasing concentrations of standard VOC solutions onto Tenax sampling tubes.

Should Tenax be an appropriate sorbent for the VOC sampling method, a linear correlation should be observed between analyte response and increasing analyte concentration. To investigate the linearity of the adsorption of the VOCs onto Tenax a range of standard solutions were prepared. The concentrations of analytes in standard solutions ranged from 0.005 – 0.40 $\mu g\,\mu L^{-1}$, 5 μL of each solution corresponding to trapped masses of 25 – 2000 ng. The peak areas for the VOC masses injected obtained for the analytes are shown in Figure 3.10. Linear regression was performed on the results giving the parameters shown in Table 3.21.

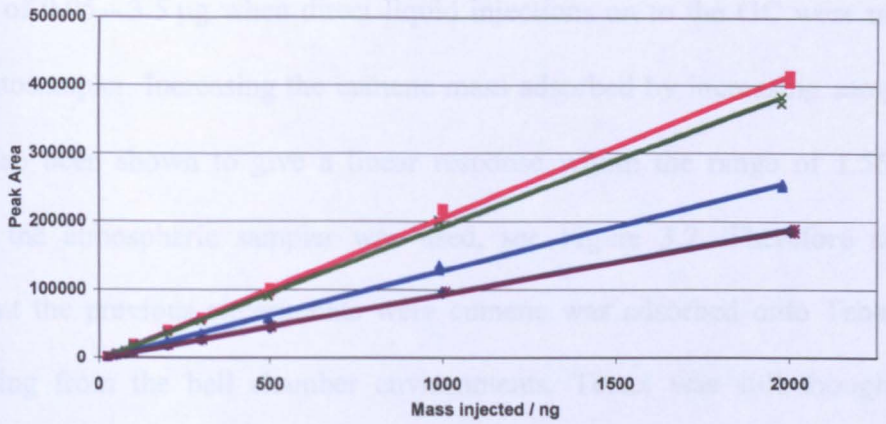

Figure 3.10: Linearity graphs produced when varying the mass injected onto the sampling tubes via the modified injection port. — Toluene, — Ethylbenzene, — O-xylene, — Cumene & — DCB.

Table 3.21: Statistical evaluation for the VOC's the direct injection manifold was used to introduce the analytes onto the sampling tubes

	Slope	Intercept	Correlation Coefficient	Error on Slope	Error on Intercept
Toluene	105.5	-4685.8	0.9929	2.1	2515
Ethylbenzene	215.8	-5432	0.9988	1.7	2172
O-Xylene	148.2	-7799.0	0.9916	3.2	4046
Cumene	250.4	-20334	0.9750	9.4	11729
DCB	92.1	181.0	0.9992	0.6	1041.3

Toluene, ethylbenzene, o-xylene and DCB had correlation coefficients of 0.9929, 0.9988, 0.9916 and 0.9992, respectively, with gradient ratios of 50.24, 126.94, 46.31 and 153.5, respectively. All of the confidence intervals included zero, therefore the responses obtained for toluene, ethylbenzene, o-xylene and DCB were deemed to be linear. Cumene responses were shown to be non-linear as it failed to meet the two of the three criteria for linearity. The slope ratio was less than 40 at 26.64 while the correlation coefficient was less than 0.9900 at 0.9750. Previous

linearity investigations have shown that cumene GC response is linear within the range of 0.05 – 3.5 μg when direct liquid injections on to the GC were made using the autosampler. Increasing the cumene mass adsorbed by increasing sampling time has also been shown to give a linear response within the range of 1.56 - 9.37 μg when the atmospheric sampler was used, see Figure 3.2. Therefore taking into account the previous experiments were cumene was adsorbed onto Tenax through sampling from the bell chamber environments. Tenax was still thought to be a suitable adsorbent for the adsorption of cumene.

3.2.5 Investigation into the development of a dynamic sampling chamber for the production of volatile organic compounds

The current system for producing VOC atmospheres involved active sampling from a static bell chamber. Volumes of 5 μL of VOC were transferred by micropipette into the 22.85 L chamber, which was sealed for one hour to allow the VOC to volatilise before sampling commenced. However the VOC concentration produced inside the bell chamber was influenced by a) lab temperature, b) lab pressure and c) accurate transfer of small volumes without analyte loss.

To eliminate some of the variation in the chamber concentration produced by the bell chamber experiments a dynamic system was designed, using Perspex atmospheric chambers see Section 2.2. First it was necessary to prepare permeation tubes that would be placed in the permeation oven. Commercial permeation tubes, which provide known and constant emission rates of VOCs into an air stream, are available for the VOCs studied in this project, however they are extremely expensive per

pollutant source (~ £800) and they have limited calibration lifetimes. Therefore an investigation was undertaken to produce in-house permeation tubes using GC autosampler vials with different sized evaporation apertures. Small GC sampling vials containing 1 mL of analyte were used. Three different apertures were made; vial 1 had a small gas syringe needle, vial 2 had two small gas syringe needles and vial 3 had a larger 18 gauge needle. Care was taken to ensure the syringe needles were not in contact with the liquid phase inside the vial. To determine the emission rate of each 'permeation vial' the vials were weighed before being placed inside the permeation oven, set at 25 °C and an air flow rate of 0.2 L min^{-1}. Over recorded periods of time the vials were removed and weighed before being re-inserted in the oven. The emission rate (ng min^{-1}) of the in-house permeation devices was determined from Equation 3.1 using the masses lost (ng) from the permeation devices over time (min).

$$E_R = \frac{mass\ loss}{time}$$

Equation 3.1

Initially toluene was examined to determine which permeation vial would be appropriate for use in the dynamic system The emission rates from the weight losses, were obtained, see Figure 3.11. Interestingly, for each vial used, the emission rate did not become relatively constant until day 8, regardless of the size of the evaporation aperture used. Permeation vial 1 contained the smallest syringe needle and consequently gave the lowest emission rate, with an average rate of 3400 ng min^{-1} (calculated from 8 days onwards). The emission rate of vial 1 was determined giving a % RSD value of 16.7 %, (n = 7), most likely associated with the error in measuring

the small weight losses (typically 10's mg) on the weighing balance. Doubling the area through which permeation occurred by doubling the number of syringe needles piercing the vial, resulted in an increase in the emission rate to 6160 ng min^{-1}. Repeat measurements were performed giving a decreased % RSD value of 4.35 % (n = 7). The largest emission rate occurred from permeation vial 3

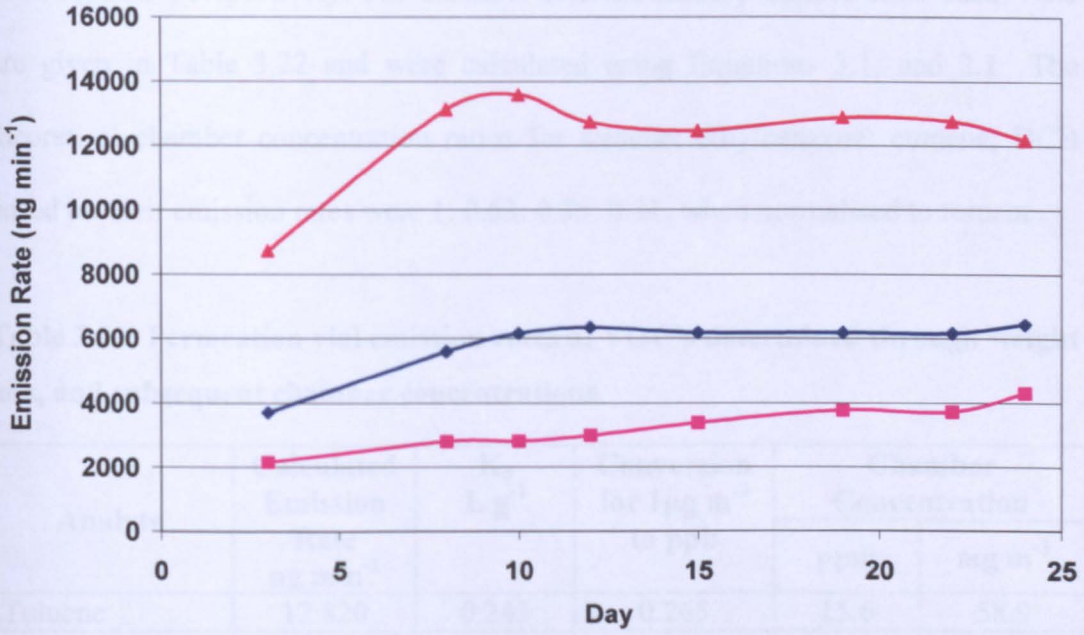

Figure 3.11: Emission rates of lab made toluene permeation tubes over a period of 24 days based on weight loss, (■) Permeation vial 1, (♦) Permeation vial 2 and (▲) Permeation vial 3

which contained the largest syringe needle, at 12 820 ng min^{-1}. Repeat measurements gave the lowest % RSD value at 3.55 % (n = 7). Therefore in order to produce the most consistent chamber concentration, and subsequently lower sampling times, the evaporation aperture associated with permeation vial 3 was chosen to create future VOC contaminated environments.

Four further permeation vials were prepared, each containing 1 mL of toluene, ethylbenzene, cumene or DCB. Note although o-xylene was examined in the original bell chamber method it was omitted here as it would dissolve the glued rubber seals of the Perspex chamber. Each VOC permeation tube was weighed and place within the chamber for a period of two weeks, the vials were then reweighed and the emission rates were measured for ethylbenzene, cumene and DCB at 8150, 4460 and 2760 ng min^{-1}, respectively. The chamber concentrations produced from each VOC are given in Table 3.22 and were calculated using Equations 3.1, and 2.1 The theoretical chamber concentration ratios for toluene: ethylbenzene: cumene: DCB based on their emission rates were 1: 0.63: 0.35: 0.21, when normalised to toluene.

Table 3.22: Permeation vial emission rates of VOC's determined through weight loss, and subsequent chamber concentrations.

Analyte	Calculated Emission Rate ng min^{-1}	K_o L g^{-1}	Conversion for 1μg m^{-3} to ppb	Chamber Concentration	
				ppm	mg m^{-3}
Toluene	12 820	0.243	0.265	15.6	58.9
Ethylbenzene	8150	0.211	0.230	8.6	37.4
Cumene	4460	0.186	0.204	4.2	20.6
DCB	2760	0.152	0.166	2.1	12.6

To determine the stability of the VOC concentrations generated in the chamber, the chamber was left to equilibrate for 1 week before sampling commenced. A sampling time of 40 s was chosen to trap 3 μg of toluene on the Tenax at a rate of 100 mL min^{-1} (to compare with the mass of toluene trapped during previous bell chamber sampling studies). However, the intensity of the toluene peak observed in the resultant chromatogram was smaller than expected, by a factor of 6. Therefore the sampling time was increased to 8 minutes. The GC chromatogram obtained then

had a toluene peak with a similar intensity to the previous bell chamber sampling method. However, the ratio of the intensities of the other VOCs were not as expected based on the theoretical chamber concentrations shown in Table 3.22 as shown in Figure 3.12.

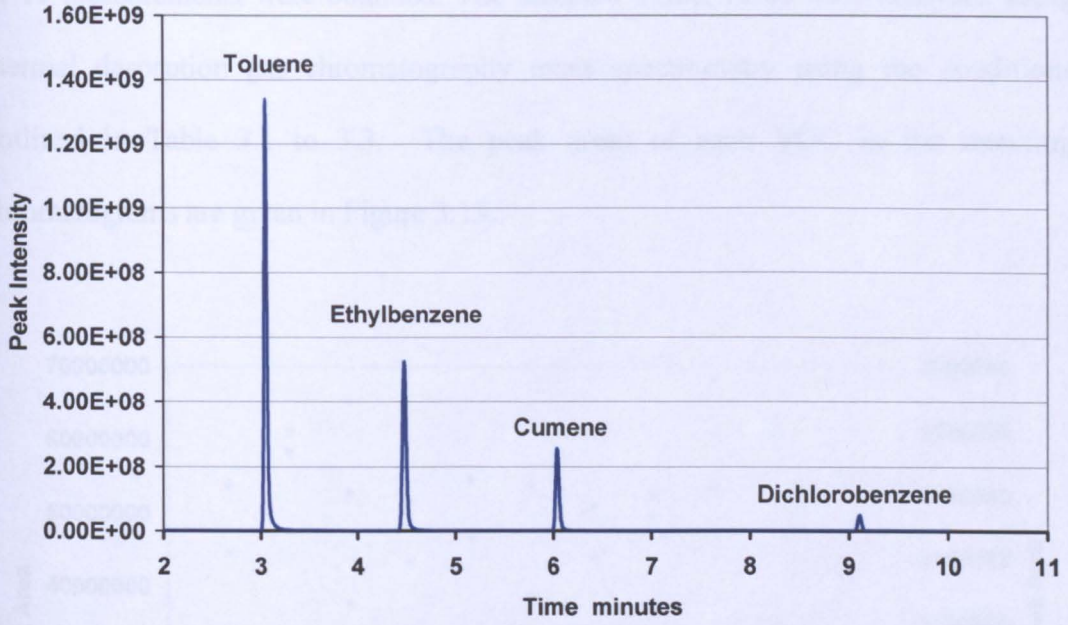

Figure 3.12: GC-MS chromatogram of VOCs obtained from atmospheric chamber generated with in-house permeation vials and sampled at a flow rate of 100 mL min^{-1}

This indicates a loss of analytes in the dynamic chamber due to adsorption onto the tubing used and Perspex chamber walls. The theoretically determined chamber concentrations should not be used to determine the concentration of VOCs within the chamber. The VOC chamber concentrations need to be determined experimentally by calibration using liquid injections of VOC standards onto Tenax via the modified injection port. However regardless of the disproportion of the intensities, expected the chamber set up would usable if the chamber concentrations were stable over time.

3.2.5.1 Examination of volatile organic compound concentrations produced over time

The VOC chamber was sampled using Tenax tubes at regular intervals for a period of 4 days, with a sampling time of 8 minutes and a flow rate of 100 mL min^{-1}. A total of 11 measurements were obtained. The sampled Tenax tubes were analysed using thermal desorption gas chromatography mass spectrometry using the conditions outlined in Table 3.1 to 3.3. The peak areas of each VOC in the resulting chromatograms are given in Figure 3.13.

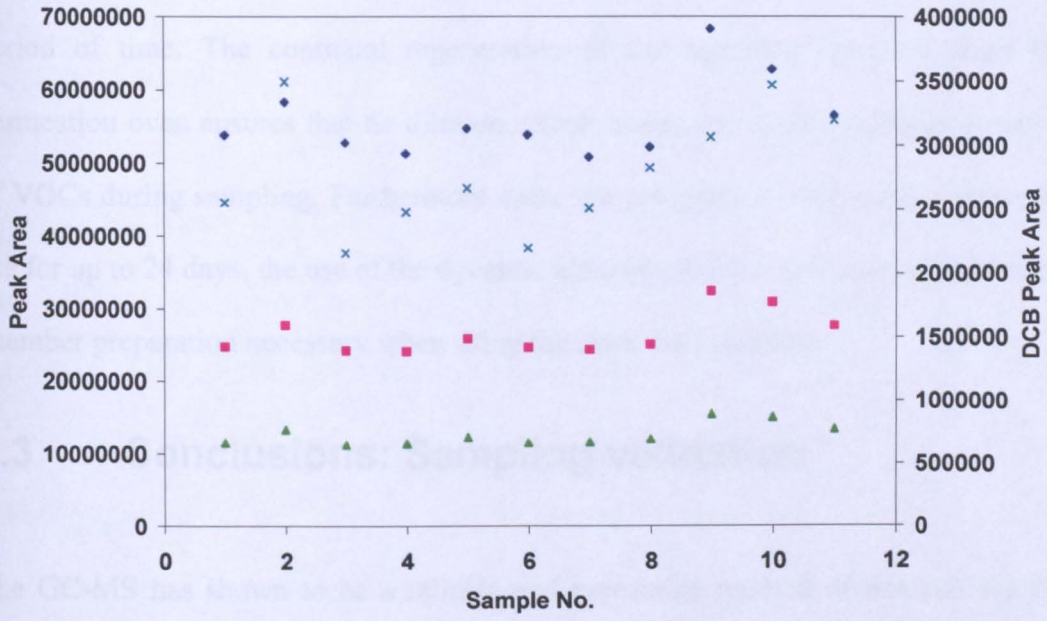

Figure 3.13: TIC peak area measurements of Tenax tubes used to sample the stability of the four chosen VOCs when produced using in-house permeation vials over a period of 4 days, (♦) Toluene, (■) Ethylbenzene, (▲) Cumene and (×) DCB

The average (n=11) peak areas for toluene, ethylbenzene and cumene were approximately 5.6×10^{-7}, 2.7×10^{-7} and 1.3×10^{-7}, respectively, all with % RSD's values between the range of 9.6 and 11.9 %. The DCB responses showed more fluctuation over the 4 days, the average peak area was $2.8 \times 10^{-6} \pm 16.9$ %. A larger variation was also noted in the DCB % RSD's values. These experiments confirm that once the dynamic chamber is prepared and left to equilibrate it can be used for at least 24 days before new permeation vials are required. Therefore continuous monitoring of a VOC chamber was possible.

Using the atmospheric chamber allows the possibility of repeated sampling over a period of time. The continual regeneration of the sampling chamber from the permeation oven ensures that no dilution effects occur due to the continual removal of VOCs during sampling. Furthermore since the permeation vials were suitable for use for up to 24 days, the use of the dynamic atmospheric chamber removed the daily chamber preparation necessary when using the static bell chamber.

3.3 Conclusions: Sampling validation

The GC-MS has shown to be a reliable and repeatable method of analysis for the determination of VOCs. It has a large dynamic range which is ideal for measuring the expected changes in the masses trapped on the Tenax when incorporating sorbents inline with the Tenax.

The accuracy, repeatability and reproducibility of the overall sampling method is greatly influenced through the generation of stable and reproducible VOC environments. The original bell chamber method for the generation of VOCs was

heavily influenced by the daily temperature, pressure and human accuracy of injecting small volumes of volatile liquids accurately within the chamber. The preparation time for the bell chambers would only allow for the generation of one chamber per day, therefore limiting the number of sampling measurements allowed before dilution effects were evident and a new chamber was required. With the variability between day to day chamber production this would not be ideal for testing adsorbents.

In developing a dynamic system it was thought that these factors would be minimised through oven temperature control and the removal of injecting small volumes of volatile liquids. However the repeatability did not improve greatly by using the dynamic system over the bell chamber method. The dynamic system set up allowed for a higher number of samples tested per day than the bell chamber method and therefore was chosen as the method to use test sorbents for their adsorption efficiency. Due to the variation in the dynamic chamber repeatability, it was determined that when testing sorbent adsorption efficiencies, a loss in mass less than 15 % of the original value was possibly due to the sampling methods used and not the capability of the sorbent tested.

The development of a liquid injection port method to introduce VOCs to the Tenax tube allowed a calibration method to be used to accurately determine the mass trapped on the Tenax. Furthermore because the use of o-xylene was not permitted within the dynamic chamber set-up the modified direct injection port could also be utilised to spike sampled Tenax tubes with o-xylene as an internal standard.

3.4 References

1 C. Watt, PhD Thesis, '*Development of novel sensors and sorbents to protect items of cultural importance in museum environments*', Department of Pure and Applied Chemistry, University of Strathclyde, Glasgow G1 1XL, 2004.

2 Personal communication with Brian Cooksey

3 M. Harper, *Journal Of Chromatography A*, 2000, **885**, 129.

4 T. Salthammer, *Organic Indoor Air Pollutants: Occurence, Measurement, Evaluation*, Wiley-VCH, Weinheim; New York, 1999.

5 E. Heftmann, *Chromatography: fundamentals and applications of chromatography and related differential migration methods. Part A:fundamentals and techniques*, 6th edn., Elsevier, Amsterdam: New York, 2004.

4 DEVELOPMENT OF A MCM-41 SYNTHETIC ROUTE AND CHARACTERISATION

Mesoporous materials are classed as inorganic solids with pore diameters of approximately 20-500 Å. They have large internal surfaces and cavities which enhance their catalytic activity. Mesoporous materials are typically amorphous, similar to silica, with an irregular atomic structure. Molecular sieves are a sub class of materials where regular arrays of uniformly sized channels are present. In 1992 a family of mesoporous molecular sieves, designated M41S, were discovered at Mobil Oil Corp in an attempt to design new porous materials that could selectively convert bulky, high molecular weight petroleum molecules into more valuable fuel and lubricant products.[1-3] MCM-41 (Mobil composite of mater) is a member of this family which is a hexagonally ordered mesoporous material with pore diameters between 1.5 - 10 nm and a surface area greater than 700 m^2g^{-1}. The surface characteristics of the mesoporous material can be tailored through the synthesis procedure.

4.1 General introduction to MCM-41 preparation

MCM-41 is prepared via a self-assembly mechanism, see Figure 4.1, where an organic structure directing agent forms micelles which are used as templates for the inorganic silica precursor. The mechanism is known as liquid crystal templating. The templating mechanism may occur via two different pathways. Either the surfactant micelles are formed before the addition of the inorganic silica precursor, or the presence of the inorganic precursor causes the surfactant micelles to form.

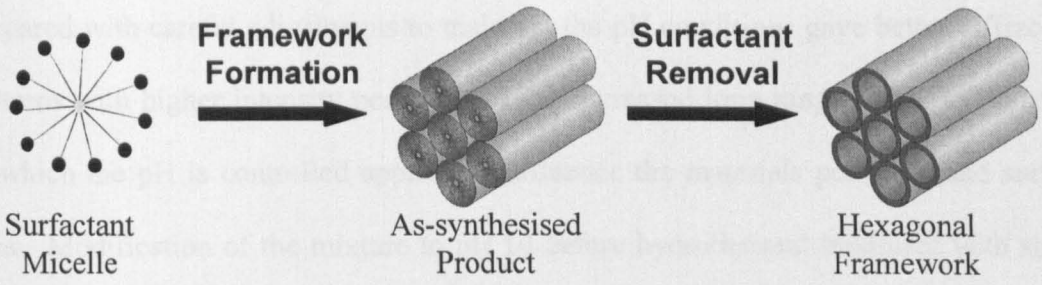

Figure 4.1: Synthesis of MCM-41 via liquid crystal templating

The basic synthesis procedure for the preparation of MCM-41 involves mixing a silica source (typically tetraethylorthosilicate or fumed silica) and an aqueous surfactant solution (e.g. cetyltrimethyl ammonium bromide) in the presence of an acid or base. The solution is matured in an oven to produce the 'as-synthesised' product. The surfactant template is then removed through calcination or acidified solvent extraction to leave a mesoporous hexagonal framework. Within this general synthesis outline there are many different procedures for producing MCM-41. Further optional steps include; pH modification; 'aging' of the as–synthesised material prior to maturing and filtration, washing and drying before surfactant extraction. It should be noted that this process of 'crystallisation' is rather poorly named as no true crystal structure is formed. Indeed the x-ray scattering contrast is not provided by atoms but rather by electron density contrast between pores and the matrix. A summary of the effects of different parameters on MCM-41 formation are given below for; pH modification, hydrothermal treatment, treatment of material before surfactant extraction or surfactant extraction. In addition the effect of surfactant type and concentration together with acidic or basic initiation of the synthesis procedure will be discussed.

4.1.1 pH modification

The pH of the as-synthesised material can be modified before the crystallisation step, either through a single addition or multiple additions of acid. Porous silicate materials

prepared with careful adjustments to maintain the pH conditions gave better diffraction patterns with higher intensity peaks indicating increased long range order.[4,5] The stage at which the pH is controlled appears to influence the materials pore size and surface area. Modification of the mixture to pH 10 before hydrothermal treatment with acetic acid resulted in a decrease in surface area from 1420 $m^2 g^{-1}$ to 1240 $m^2 g^{-1}$, repeated adjustments of the pH during the hydrothermal treatment further reduced the surface area to 1060 $m^2 g^{-1}$.[5] Interestingly modification of the pH by sulfuric acid to maintain a of pH 11 increased the surface area to 990 $m^2 g^{-1}$ compared to modification using acetic acid which resulted in a surface area of 750 $m^2 g^{-1}$.[4] Repeated adjustment of the pH to 11 with acetic acid was shown to improve the uniformity of the pores produced and improved the total pore volume of the material compared to silicate material were the pH was unmodified.[6] Modification of pH of the materials appears to result in more hydrothermally stable materials.[4] Léonard and co-workers showed that the pH of the gel produced has an influential effect on the morphologies of the final product.[7] When the pH is increased to 4 the surface of the materials becomes rough. At higher pH values submicrometer particles are present. Léonard concluded that too acidic or basic materials deeply affect the silica hydrolysis and condensation rates which in turn modifies the surfactant-silica interactions, with the formation of small submicrometer spheres a result of a fast condensation rate. Kim at al[8] modified their silicate with NaF to adjust the pH of the 'gel' to 10 before crystallisation and they found that the material produced had a higher hydrothermal stability. By adding fluoride ions, the hydroxyl groups on the surface of the silicate are replaced and are less at risk of attack by water.

4.1.2 Hydrothermal treatment

Autoclaving is generally used to age the silicate. The times used in the aging process vary from 12 h to several days.[1, 2, 4-7, 9-18] By increasing the hydrothermal crystallisation

time changes in the morphology and the surface characteristics can be induced. Moyaka[9] has shown that increasing the hydrothermal crystallisation time from 48 to 144 h at 150 °C resulted in the MCM-41 transformation from sphere shaped particles to 'rods' and 'ropes'. The increase in crystallisation time was also linked to an increase in the pore size and the wall thickness of the pores, accompanied with a decreases in surface area. Grün and co-workers[19] investigated the effect of aging on the morphology. Through x-ray diffractogram analysis it was suggested that by aging the material at 105 °C for 10 days the long range order of the material was improved, while a further increase of 55 °C resulted in a broader Bragg peak at 1.14° 2Θ suggesting the formation of a further pore system as well as maintaining the original pore array. The pore size distributions were obtained from the nitrogen adsorption isotherms. Extended hydrothermal treatment resulted in the partial collapse of the mesoporous structure and/or the formation of wider pores.[19]

4.1.3 Treatment of material before surfactant extraction

The as-synthesised silicate is generally washed in water[1, 2, 8, 10-14, 20], or washed with water then with ethanol[6, 15, 21]. The volumes of water and ethanol used to wash the as-synthesised product are often not given in the literature. When the volumes are quoted they range from 100 mL to 1 L. Before the surfactant extraction procedure the material is then dried overnight either at 100 °C[11, 13, 22] or at room temperature[1, 2, 12-14, 16, 20].

4.1.4 Surfactant extraction

Surfactant extraction through calcination generally involves heating to temperatures of approximately 550 °C at a ramp rate of 1 °C per min under a stream of air or nitrogen. Once the temperature has reached 550 °C it is held there for between 4-24 h. The

temperature at which calcination occurs can influence the material's characteristics. For example, calcination temperatures exceeding 750 °C resulted in collapse of the pore structure, causing a significant effect on the surface area of the material produced.[23] Chen[12] showed that as the calcination temperature was increased from 550 to 800 °C the surface area of MCM-41 was reduced from 1016 to 965 m^2g^{-1} and the pore diameter was reduced by 3 Å, while very little change was noted in pore volume. Shrinkage of pore diameter is also common with calcination.[4] Solvent extraction of the surfactant template is mainly performed by refluxing the as-synthesised material in acidified alcohol (e.g. HCl (37 % wt) in ethanol). Soxhlet apparatus can also be used as an alternative extraction method. It has been suggested that a calcination step should follow a solvent extraction step,[23] however this combination is not normally reported in the literature.

4.1.5 Effect of surfactant type and surfactant concentration on the characteristics of final material produced

The surfactants used to form the micelles are typically quaternary ammonium based compounds. The most common surfactants used are: cetyltrimethylammonium hydroxide/chloride or bromide. Beck at el[1] established that by increasing the carbon chain length of the surfactant from C_8 to C_{16} the pore size of the silicate approximately doubles from 18 to 37 Å. In general, increasing the chain length of the surfactant increases the pore size as the micelle diameter becomes wider. Ottaviani[24] also suggested that an increase in the chain length of surfactants resulted in a faster condensation rate of the silica. The surfactants used are typically in aqueous solution with a concentration range of 10-30 wt %. The molar ratio of the surfactants when normalised to the SiO_2 present, is usually in the range of 0.05-0.25. In general a

surfactant to silicate ratio less than one results in a MCM- 41 type product, whereas a surfactant to silicate ratio above one leads to the formation of MCM-48, due to the production of lamellar phases.[1]

4.1.6 Effect of acidic or basic initiation of the synthesis procedure on the final mesoporous silicate

Mesoporous silica formation can be initiated though an acidic or a basic route, for example quaternary alkyl ammonium hydroxides in the basic route and hydrochloric acid in the acidic route. Cai *et al.*[20] produced MCM-41 using various concentrations of ammonium hydroxide as the base source. The pH of the reaction mixtures ranged from 10.4 to over 11.4. It was shown that outside the pH range of 11.3-11.6, amorphous materials were produced while within this range MCM-41 products where obtained. The product with the highest order came from a mixture composition of TEOS: 0.125 CTAB: 69 NH_4OH: 525 H_2O. Schulz-Ekloff *et al*[17] replaced the basic initiator tetraethylammonium hyroxide with ethylacetate to gradually lower the pH of the original synthesis. During the 2 h aging process at ambient temperature the pH of the mixture dropped from 13 to 7 achieved through the hydrolysis of ethylacetate. The MCM-41 silicate produced with ethyacetate had a surface area of 1092 $m^2 g^{-1}$ whereas the surface area of the silicate prepared with tetraethylammonium hydroxide was 975 $m^2 g^{-1}$. The morphology altered from non-uniform to raspberry-like by replacing tetraethylammonium hydroxide with ethylacetate. It was postulated that the 'gradual decrease in the pH enables control of the morphology of mesoporous molecular sieves. As the decrease in pH is achieved owing to the hydrolysis of ethylacetate, local variation of pH does not occur.'

4.1.7 Summary

There is no definitive literature method routinely published to produce MCM-41. The choice of method used to produce MCM-41 is dependent on the resulting use of MCM-41 e.g. a high hydrothermal stability would be ideal when using MCM-41 as a catalyst in a thermal process with a high water content.

4.2 Results: Initial investigation into the development of a synthesis route for the production of MCM-41

The initial investigation into the use of MCM-41 as an indoor air pollutant adsorbent was conducted by Watt.[25] Watt's synthesis method used to procedure MCM-41 was adapted from a method produced by Grün[19]. An overhead stirrer was used to dissolve 2.42 g of cetyltrimethyl ammonium bromide (CTAB, Sigma-aldrich, Gillingham, UK & Steinheim, Germany) in 120 g of distilled water. To the surfactant solution 9.5 g of 25% w/w tetramethylammoniumhydroxide pentahydrate (TMAOH, Sigma-aldrich) was added. After stirring at a constant rate for 10 minutes, 10 g of tetraethyl orthosilicate (TEOS, Sigma-aldrich) was added dropwise over a further period of ten minutes. Stirring continued for a further hour. The white 'gel' produced was transferred to a bomb and placed in an autoclave for 24 hours at 100 °C. The gel was then filtered and washed before calcination. The calcination programme consisted of three steps; i) ramp from room temperature to 550 °C at a rate of 1 °C min^{-1} under a nitrogen flow, ii) hold at 550 °C for 5 hours under an air flow and iii) cool back to room temperature under an air flow. The gel produced had a molar ratio of SiO_2: 0.54 TMAOH: 0.14 CTAB: 147 H_2O, (7% CTAB). When analysed by nitrogen adsorption this method produced a material with a type IV characteristic isotherm, a BET surface area of 834 m^2 g^{-1} a total pore volume of 0.7 cm^3 g^{-1} and pore diameter of 2.9 nm. In order to develop a method

for the production of MCM-41 the method used by Watt required optimisation. The initial stage of optimisation focussed on the percentage concentration present of CTAB, therefore four materials were prepared as described with CTAB concentrations of 2.5, 5.0, 7.5 and 10.0 % CTAB. The gels produced had the following molar concentrations

i) SiO_2: 0.54 TMAOH: 0.05 CTAB: 147 H_2O (referred as MCM-41 (2.5 %)

ii) SiO_2: 0.54 TMAOH: 0.10 CTAB: 147 H_2O (referred as MCM-41 (5.0 %)

iii) SiO_2: 0.54 TMAOH: 0.15 CTAB: 147 H_2O (referred as MCM-41 (7.5 %)

iv) SiO_2: 0.54 TMAOH: 0.20 CTAB: 147 H_2O (referred as MCM-41 (10 %)

4.2.1 Analysis and characterisation of samples prepared with different concentrations of CTAB

Each material produced was characterised by nitrogen adsorption using BET analysis. A Micromeritics ASAP 2010 BET analyzer was used to determine surface area, pore volume and pore diameter. Each sample was place in the vacuum oven at 1000 mbar for at least 24 h before BET analysis. Between 300 and 400 mg was accurately weighed and transferred to a glass BET sample tube. The sample tube weight was recorded before and after the addition of the silicate material. The sample tube was attached to the degas port of the BET and degassed. When the pressure was below 100 μm Hg the sample was heated at 100 °C overnight. The sample tube was then re-weighed before the analysis commenced. During analysis difficulties were encountered with this characterisation and abnormal, or no isotherms were obtained for the four samples, for example the nitrogen isotherm obtained for MCM-41 (5%) given in Figure 4.2. The isotherm produced has some characteristics associated with a type VI isotherm, therefore the materials were suspected as nonporous. The volume of gas adsorbed should be greater than few 100 $cm^3 g^{-1}$ and not less than 2 $cm^3 g^{-1}$ as indicated. These abnormal isotherms and problems were not encountered previously when the materials

were analysed by Watt.

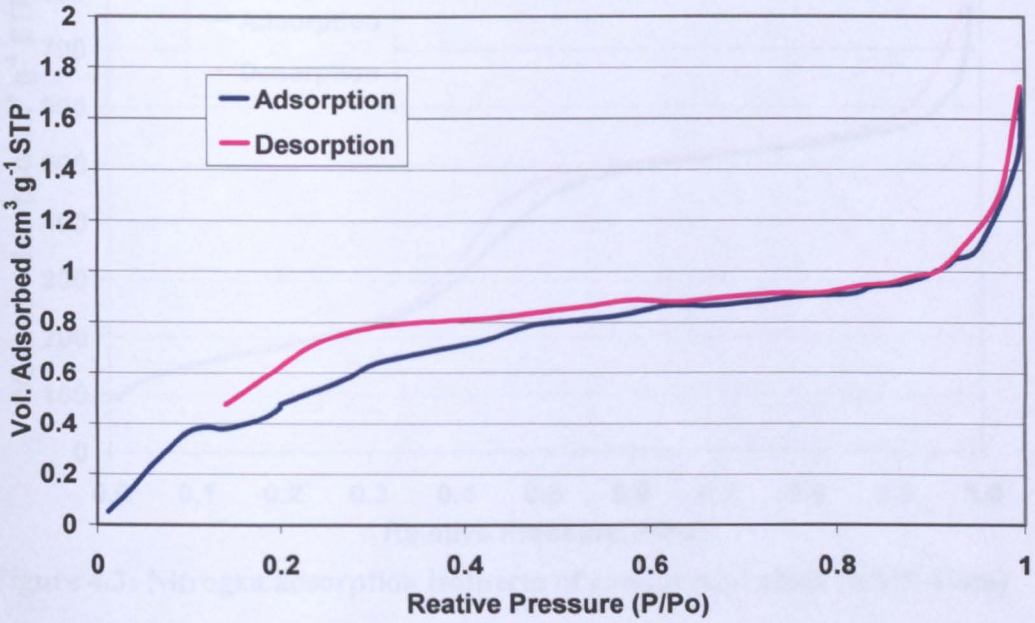

Figure 4.2: Abnormal nitrogen adsorption isotherm for MCM-41 (5% CTAB)

There were two possible explanations for not obtaining nitrogen isotherms for the samples either a) the inorganic framework was failing to form and produce mesopores or b) incorrect analysis of material by BET. Since the synthesis method had previously produced nitrogen isotherms it was originally thought that the BET was working incorrectly. Therefore in order to investigate if the BET instrument was the source of error a commercial hexagonal mesoporous silicate was purchased from Sigma Aldrich (Milwaukee, USA) and analysed by BET as a reference material. The commercial silicate was prepared as before for BET analysis. The isotherm obtained, see Figure 4.3 had mesoporous properties with type IV isotherm, a surface area of 682.9 $m^2 g^{-1}$, a pore volume of 1.24 $cm^3 g^{-1}$ and a pore diameter of 4.85 nm.

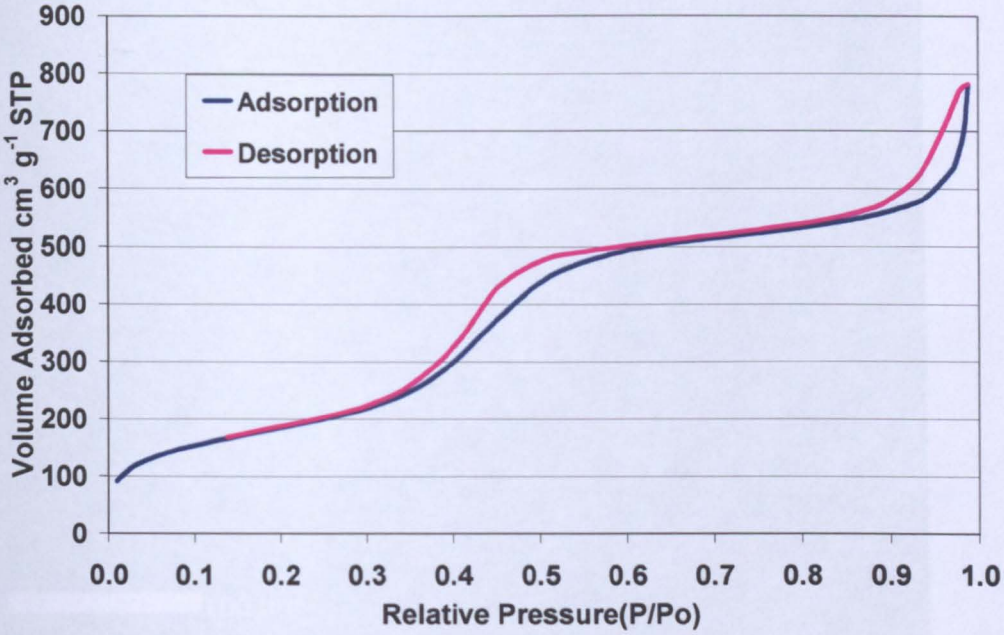

Figure 4.3: Nitrogen adsorption isotherm of commercial silica (HMS-Com)

The production of a nitrogen isotherm for the commercial mesoporous matrerial ruled out the BET as the source of the problem for the failure to produce nitrogen isotherms of the lab synthesised MCM-41. In an attempt to understand why the silicate material failed to produce nitrogen isotherms, the materials were further analysed by SEM and EDAX. To investigate the morphology and elemental composition of the materials an environmental SEM CamScan MX2500 was used. Small amount of silicate material were deposited onto a platform. The platform was mounted inside the SEM and an exploratory analysis using EDAX was conducted on a selection of silicate materials. The SEM image of sample MCM-41 (5%) is given in Figure 4.4.

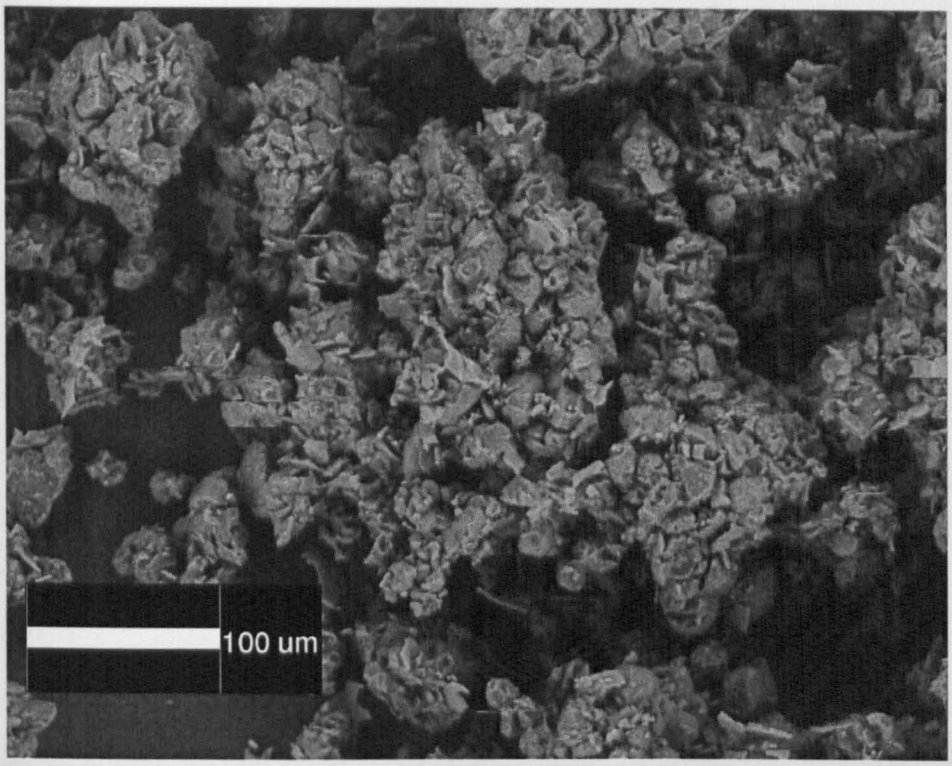

Figure 4.4: Environmental SEM image MCM-41 (5% Grun)

The image shows that the sample produced was granular, unfortunately Watt provided no SEM analysis for the material. The EDAX analysis of MCM-41 (5%) shows high levels of carbon ($K\alpha_1$ x-ray energy of 0.227 keV)[26] and bromine ($L\alpha_1$ x-ray energy of 1.480keV)[26] see Figure 4.5. The presence of carbon and bromine within a calcined product was unexpected. A possible explanation for the presence of carbon and bromine in the sample and the non mesoporous isotherms was a possible malfunction with the calcination rig during the calcination stage of the synthesis procedure, resulting in CTAB surfactant remaining within the mesopore. This theory was further strengthened when examining MCM-41 (10%) via SEM and EDAX.

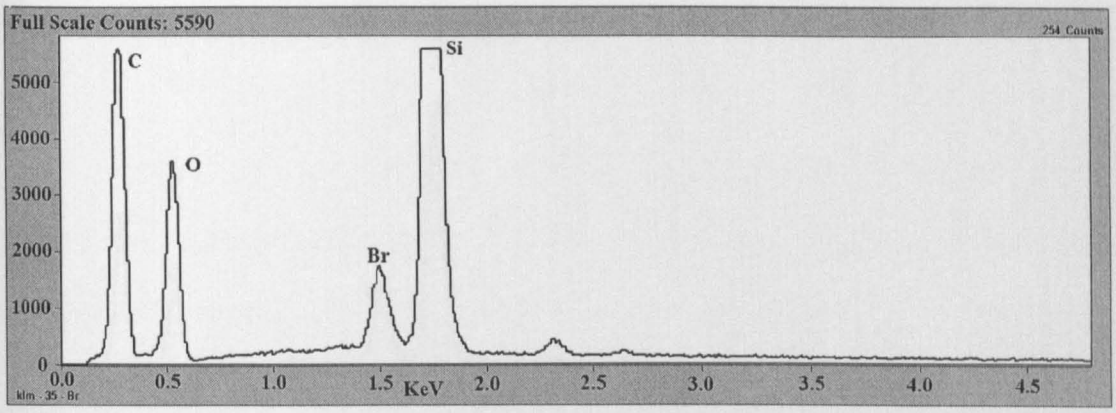

Figure 4.5: Single point EDAX analysis of MCM-41 (5% Grun)

The SEM image obtained (Figure 4.6) clearly shows a flat platelet type of material and a granular material randomly distributed throughout the silicate. EDAX spot analysis was carried out on both sections of the material for a similar number of counts.

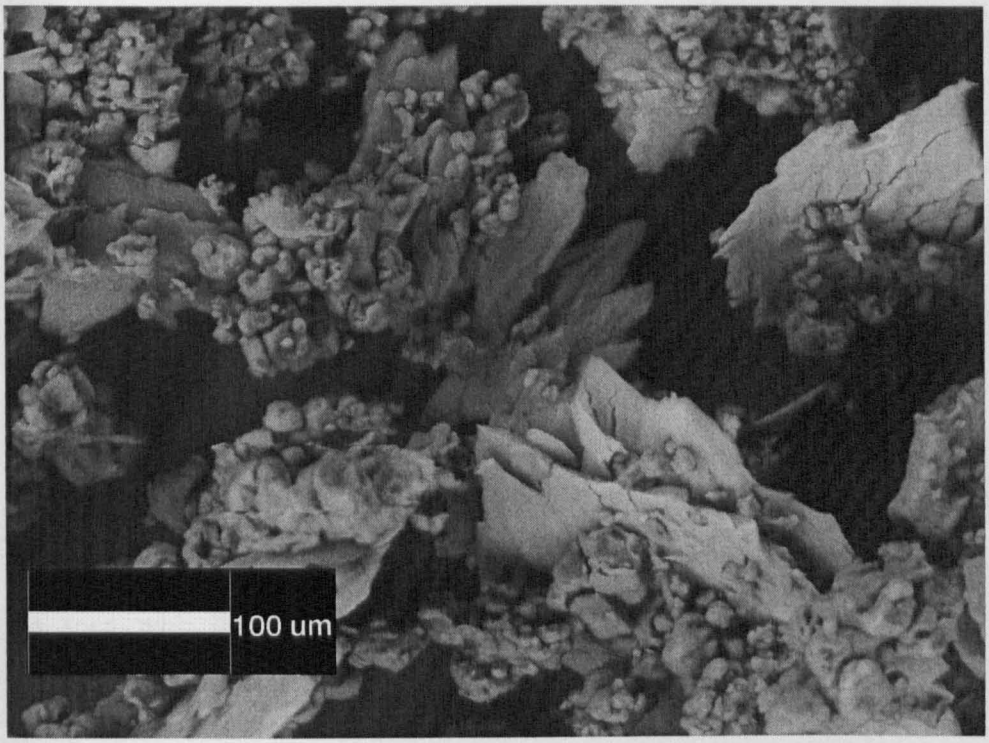

Figure 4.6: Environmental SEM image MCM-41 (10% Grun)

The granular material (Figure 4.7) has a high ratio of silica to bromine and carbon where as the platelet material (Figure 4.8) contains almost equivalent ratios of carbon, bromine and silica.

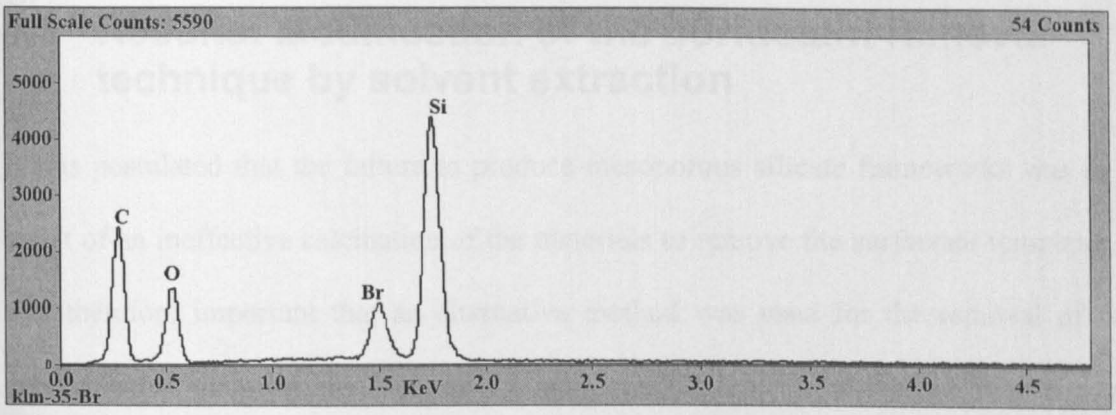

Figure 4.7: Single point EDAX analysis of MCM-41 (10% Grun)

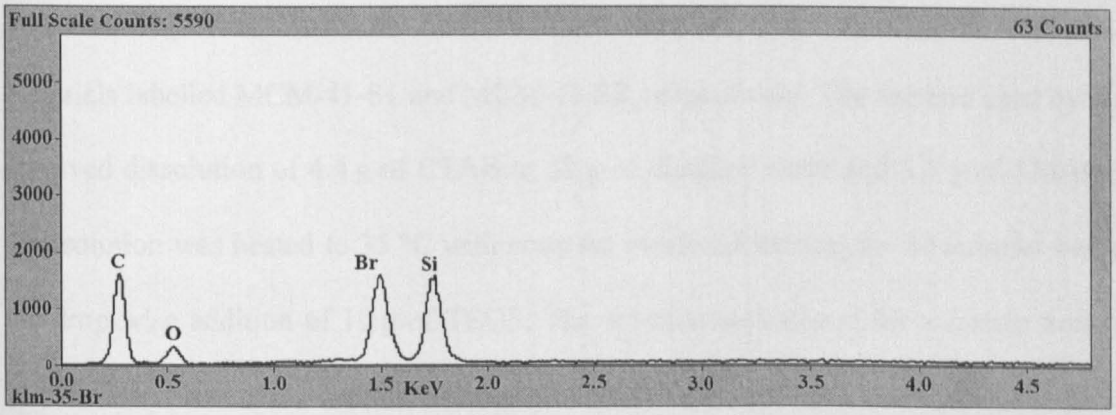

Figure 4.8: Single point EDAX analysis of MCM-41 (10% Grun) focussing on grey platelet material within Figure 4.6.

4.2.2 Summary of CTAB produced MCM-41 extracted using calcination

As seen with the MCM-41 (5%) CTAB appears in the final calcined product of MCM-41 (10%) further enhancing the theory of a malfunctioning calcination rig. Further synthesis development was therefore required in order to successfully produce mesoporous silicates.

4.3 Results: Modification of the surfactant removal technique by solvent extraction

It was postulated that the failure to produce mesoporous silicate frameworks was as a result of an ineffective calcination of the materials to remove the surfactant template. It was therefore important that an alternative method was used for the removal of the cetyltrimethyl ammonium bromide. It was clear from the literature that solvent extraction was a common alternative extraction technique to calcination that also resulted in mesoporous silicates. Two alternative synthetic procedures for MCM-41 based on the methods used by Xia[27] and Lesaint *et al*[28] were investigated to produce materials labelled MCM-41-S1 and MCM-41-S2, respectively. The method used by Xia involved dissolution of 4.4 g of CTAB in 32 g of distilled water and 3.5 g of TMAOH. The solution was heated to 35 °C with constant overhead stirring for 30 minutes before the drop wise addition of 10 g of TEOS. The solution was stirred for a further hour at 38 °C then stirred for a further two hours without heat. The silica gel produced had a molar ratio of SiO_2: 0.25 CTAB: 0.1 TMAOH: 40 H_2O. The solution was transferred without filtration or washing to a steel bomb for autoclaving at 100 °C for 24 h. This material will be referred to as MCM-41-S1.

The method used by Lesaint *et al* [28] involved the dissolution of 0.8 g of CTAB fully under stirring in 43 g of 0.1 M aqueous solution of TMAOH. The solution was heated to 45 °C before 3.81 g of TEOS was slowly added over 5 minutes. The solution was cooled to room temperature and stirring continued for a further 24 h. The molar ratio of the gel produced was SiO_2: 0.12 CTAB: 0.12 TMAOH: 130 H_2O. The gel was filtered and washed with 50 mL of distilled water. The material produced was placed on a

watchglass and heated at 70 °C for 24 h. The MCM-41 material produced via the Lesaint method will be referred to as MCM-41-S2.

Crucially the removal of the surfactant for both of the methods described above was achieved by acidified solvent extraction, 1g of silicate material was added to 25 mL hydrochloric acid (37%, Sigma Aldrich, Germany) and 300 mL ethanol (Sigma Aldrich, Germany). The mixture was then refluxed for 24 h. Once the solution was cooled the silicate material was collected by gravity filtration. The expected molar ratios of the gels produced were

i) SiO_2 : 0.25 CTAB: 0.10 TMAOH: 39 H_2O (MCM-41-S1)

ii) SiO_2 : 0.12 CTAB: 0.12 TMAOH: 130 H_2O (MCM-41-S2)

4.3.1 Analysis and characterisation of solvent extracted materials, MCM-41-S1 and MCM-41-S2

During the solvent extraction the MCM-41 material was finely distributed throughout the acidified ethanol. Gravity filtration was used to recover the fine 'dust' like product. The materials were analysed by BET and the nitrogen adsorption isotherms are given in Figure 4.9 and Figure 4.10. Both materials possess type IV nitrogen isotherms. MCM-41-S1 has a much more defined IV isotherm with a steep type H1 hysteresis loop within the P/Po region of 0.3-0.4, indicative of a narrow distribution of uniform pores. MCM-41-S2 possesses a much less defined hysteresis loop. For each of the materials produced using solvent extraction to remove the surfactant template, the volume adsorbed on the adsorption isotherms is greater then 100 cm^3 g^{-1} unlike the nitrogen adsorption isotherms (Figure 4.2) gained using the calcination technique.

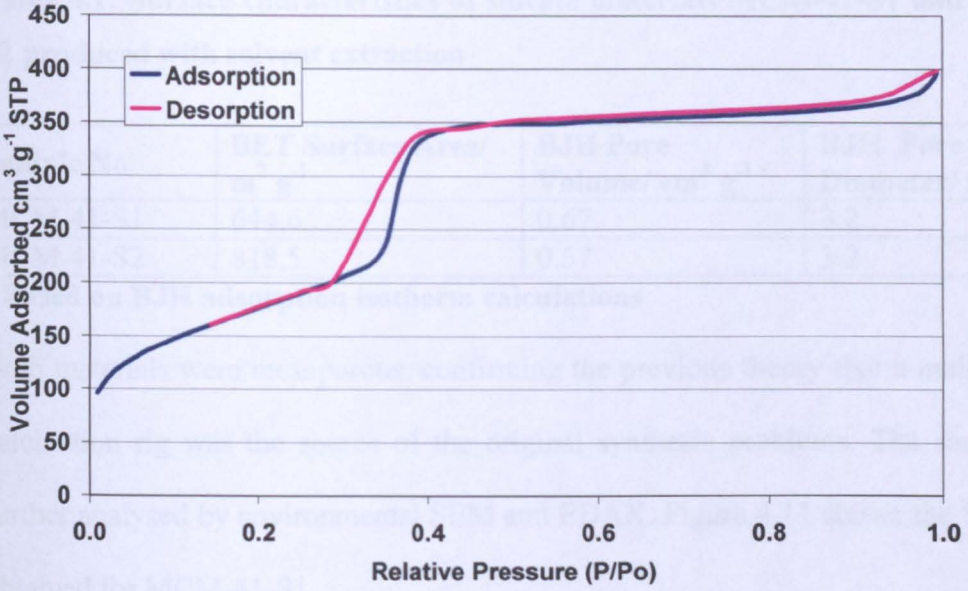

Figure 4.9: Nitrogen adsorption isotherm for MCM-41-S1

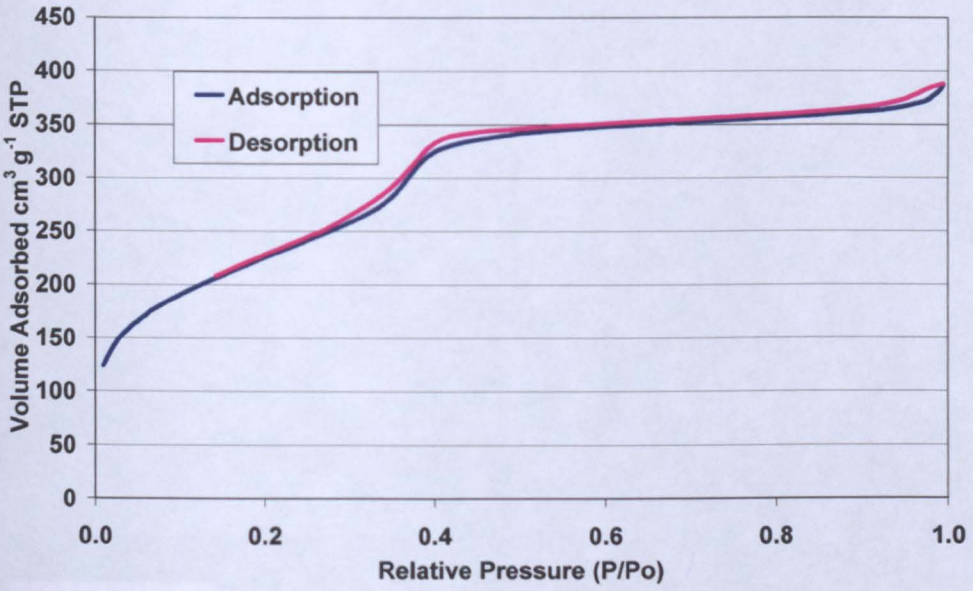

Figure 4.10: Nitrogen adsorption isotherm for MCM-41-S2

The surface characteristics of the solvent extracted materials are given in Table 4.1. Unsurprisingly the pore diameters of the materials are identical as a direct result of using the same chain length organic template in the synthesis procedures. The surface area of MCM-41-S1 was lower at 644.6 $m^2 g^{-1}$ compared to the surface area of MCM-41-S2 at 818.5 $m^2 g^{-1}$.

Table 4.1: Surface characteristics of silicate materials MCM-41-S1 and MCM-41-S2 produced with solvent extraction

Sample No	BET Surface Area/ $m^2 g^{-1}$	BJH Pore Volume/ $cm^3 g^{-1}$ •	BJH Pore Diameter/ nm •
MCM-41-S1	644.6	0.67	3.2
MCM-41-S2	818.5	0.57	3.2

• Based on BJH adsorption isotherm calculations

Both materials were mesoporous, confirming the previous theory that a malfunctioning calcination rig was the source of the original synthesis problems. The samples were further analysed by environmental SEM and EDAX. Figure 4.11 shows the SEM image obtained for MCM-41-S1.

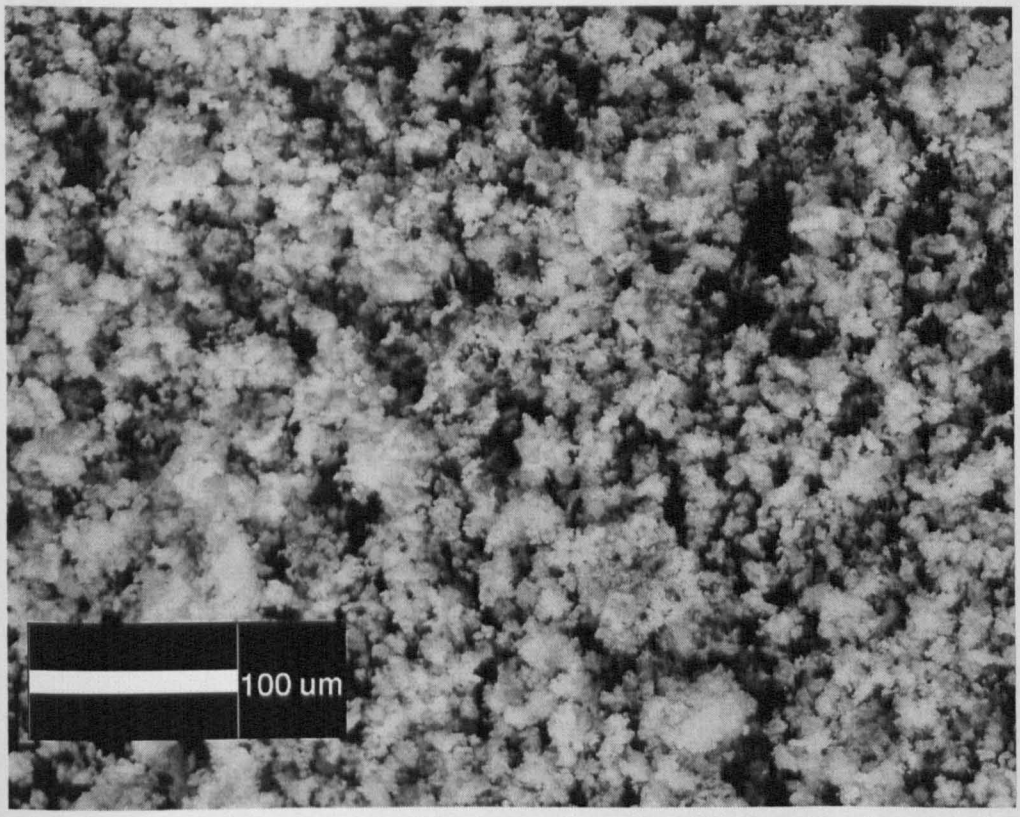

Figure 4.11: Environmental SEM image of MCM-41-S1

The material appears to be homogenous with smaller sized granules than were originally observed in the calcined products with no evidence of platelets containing bromine. The original mole gel ratio for MCM-41-S1 CTAB was calculated at 0.25 whereas for

MCM-41(10%) CTAB was calculated at 0.2. However when comparing the two EDAX results (Figures 4.7 and Figure 4.12) MCM-41-S1 was seen to contain lower values of carbon and bromine. Adding further evidence that solvent extraction was more effective at removing the surfactant template than the calcination method used.

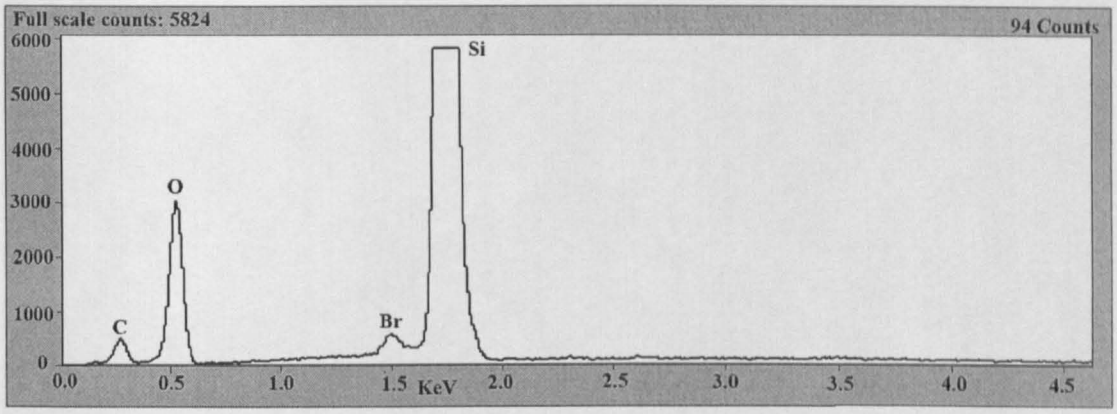

Figure 4.12: EDAX analysis of MCM-41-S1

Similar results were observed for the SEM and EDAX analysis of MCM-41-S2, Figure 4.13 and Figure 4.14. The SEM image for MCM-41-S2 contains fine granular areas as for MCM-41-S1, but the sample appears less homogeneous as there were areas with a globular 'ice' like appearance. The EDAX analysis results again shows extremely low levels of carbon and bromine.

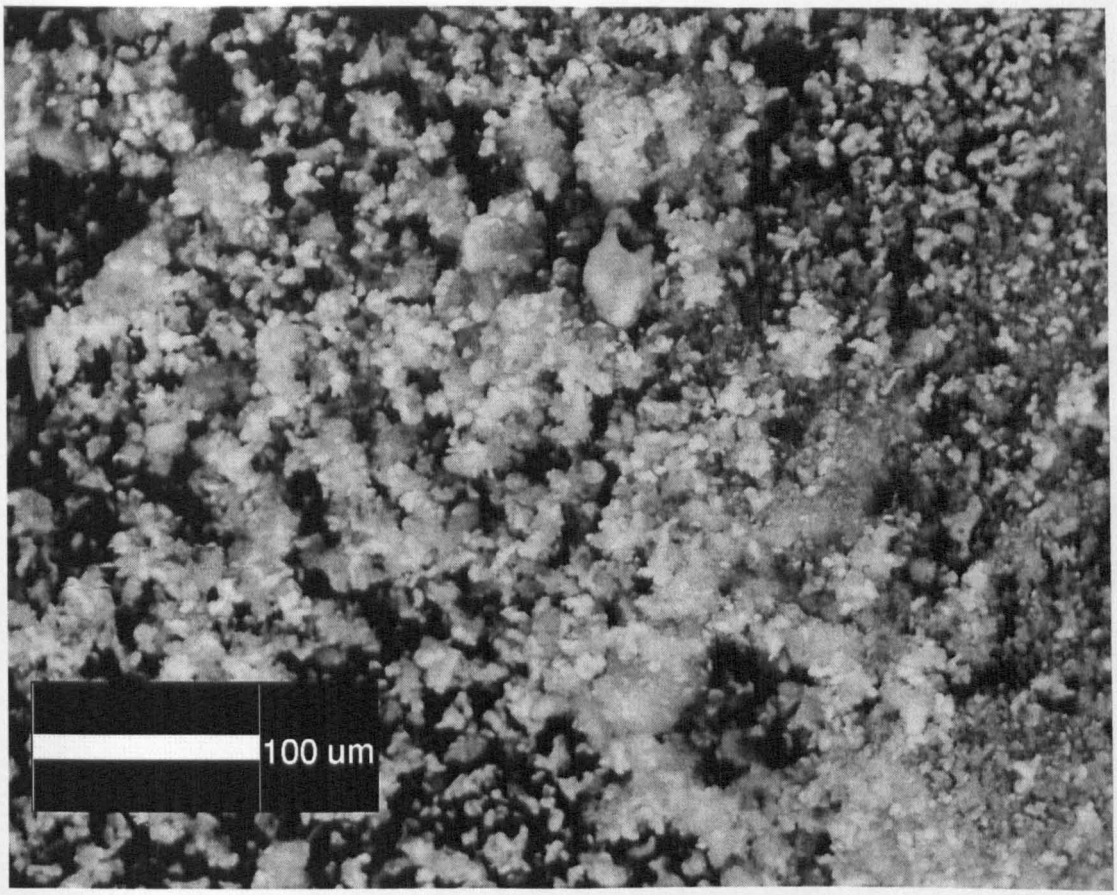

Figure 4.13: Environmental SEM image of MCM-41-S2

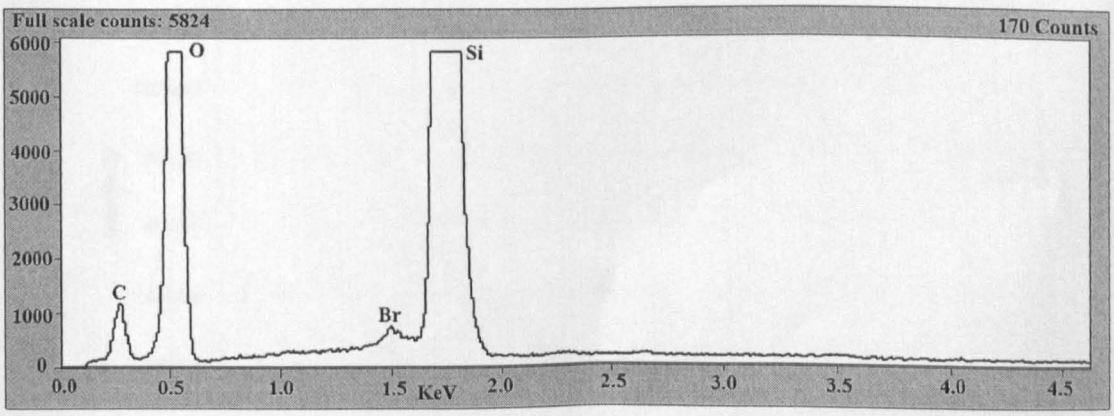

Figure 4.14: EDAX analysis of MCM-41-S2

This was conclusive evidence that the calcination rig was not removing the surfactant template leading to non-mesoporous materials containing carbon and bromine. However the solvent extraction does not remove all traces of the surfactant thereby suggesting that a further calcination step maybe required as suggested in some of the literature.

When using solvent extraction to remove the surfactant template the characterisation techniques confirmed that the material was mesoporous with typical surface characteristics for MCM-41 material. To investigate the structural regularity within the frame PXRD and TEM analysis was performed. The powder X-ray diffraction (PXRD) patterns were recorded on a Philips X'Pert diffractometer (operated at 2 kW) using Cu K_{α} radiation source and accelerator detector. The samples were prepared for analysis by grinding the sample into a fine powder. A thin layer of the sample was then prepared on the sample stage. The diffraction pattern produced for the MCM-41-S1, Figure 4.15, solvent extracted material gave sharp diffraction peaks (1 0 0), (1 1 0) and (2 0 0) that are clearly visible.

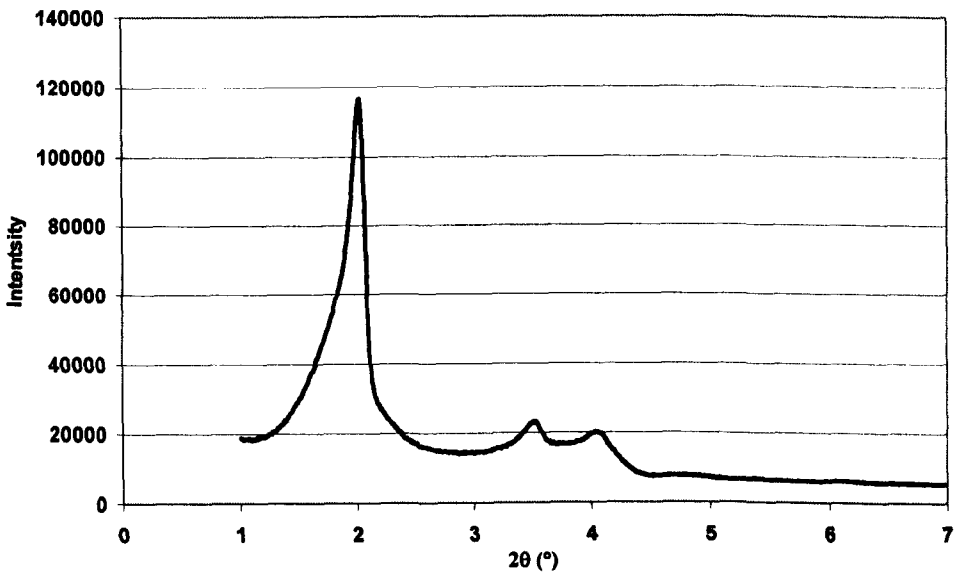

Figure 4.15: PXRD pattern of solvent extracted MCM-41-S1

The (1 0 0) diffraction peak for MCM-41-S1 was at angle 2θ of 2.007 which corresponded to a *d* spacing of 44 Å, and repeating unit (a_o) unit of 50 Å. The repeating unit includes the pore diameter and pore wall distance therefore given the BJH pore diameter the pore wall of MCM-41-S1 was determined as 18 Å. However when

MCM-41-S2 was analysed by PXRD a poor diffraction pattern was observed, see Figure 4.16, the (1 0 0) diffraction peak was at angle 2θ of 2.157, however this diffraction peak was broad and the intensity value of roughly 25 000 a.u was approximately 4.5 times less than the (1 0 0) diffraction peak of MCM-41-S1.

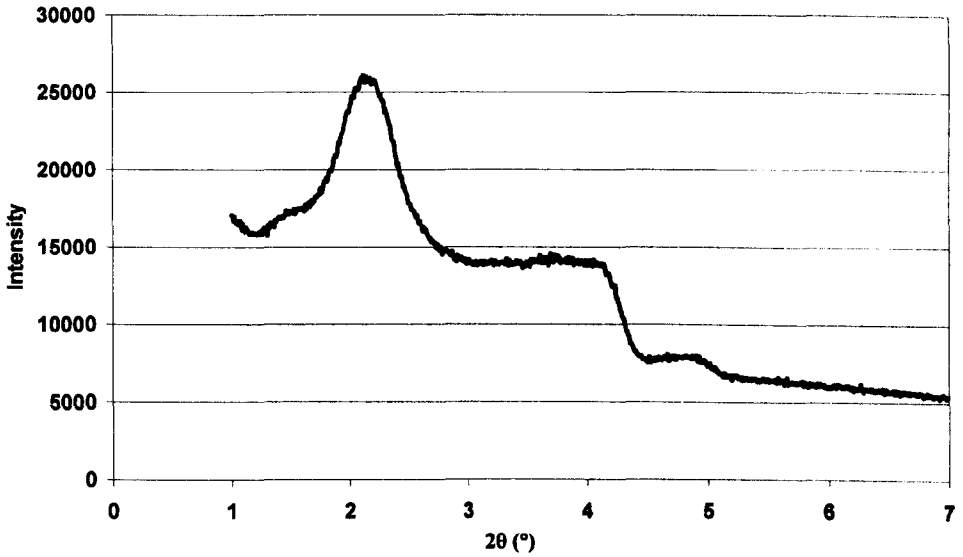

Figure 4.16: PXRD pattern of solvent extracted MCM-41-S2

Due to a shortage of instrument time only MCM-41-S1 was analysed by transmission electron microscopy based on the results from the PXRD. The transmission electron microscopy (TEM) images were taken using a JEOL-2000FX equipment operated with a 200 kV accelerating voltage. The mesoporous samples were prepared for TEM by dispersing a small quantity of the sample in ethanol and placing a drop of the mixture on a carbon – coated copper grid. TEM images of MCM-41 show a hexagonal structure were each pore is surrounded by six neighbours[1]. The areas of light contrast in the image correspond to the pores while the darker contrasted areas are the silica wall framework.

Figure 4.17 displays the TEM image for MCM-41-S1, the TEM shows the pores 'head on' with no evidence of channelling on the image. Further images of MCM-41-S1 were

taken with no channelling seen on these images either. The TEM image obtained was contradictory to the well defined PXRD pattern obtained in Figure 4.15 for the material.

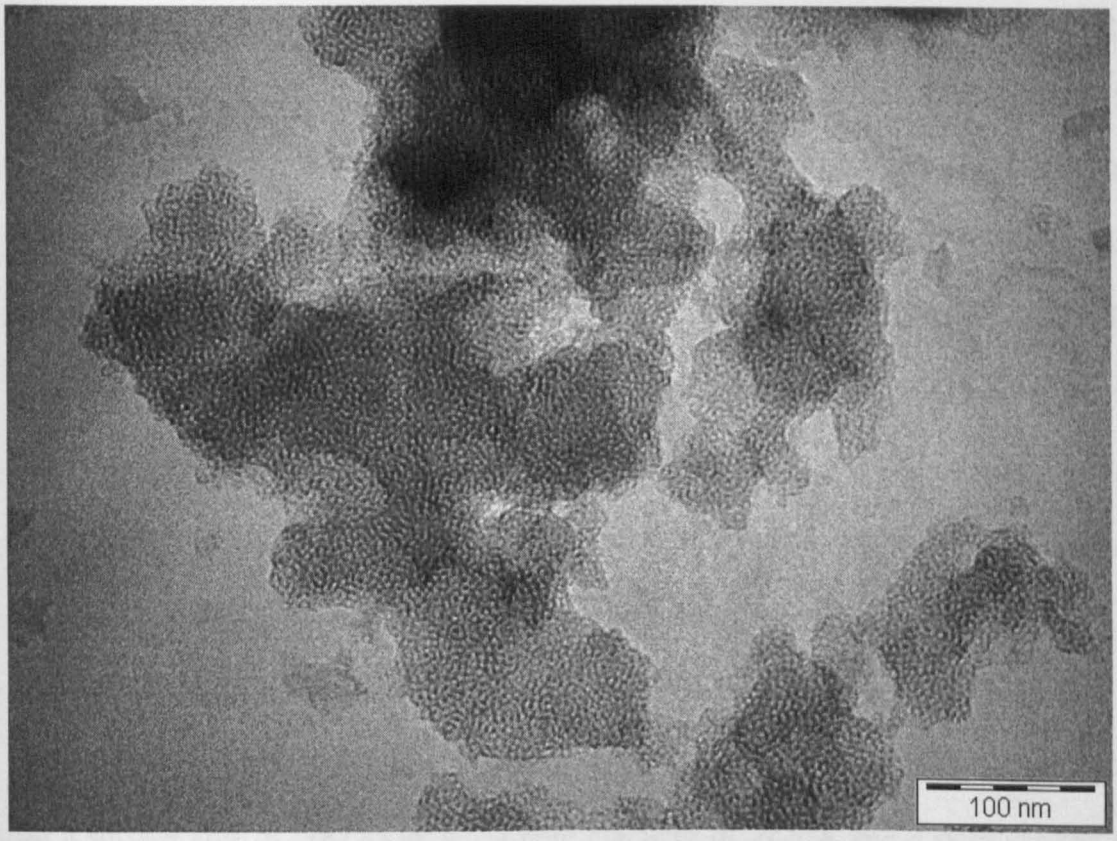

Figure 4.17: TEM for MCM-41-S1 produced via solvent extraction

4.3.2 Summary of surfactant extracted MCM-41 synthesised materials

Surfactant removal by the original calcination method proved to be ineffective in producing mesoporous silicates; the problem was resolved by using solvent extraction methods. However solvent extraction increased the preparation time and extremely fine material was produced on a small scale.

4.4 Results: Surfactant removal of CTAB with an alternative muffle furnace technique

An alternative method of removing the surfactant by 'burning out' the surfactant using a muffle furnace was investigated for two samples (MCM-41-MF1 & MCM-41-MF2). The first sample was synthesised using a modified MCM-41-S1 synthesis, 4.4 g of CTAB was dissolved in 32 g of distilled water and 4.81 mL g of 1M aq TMAOH. The solution was heated to 35 °C with constant overhead stirring for 30 minutes before the drop wise addition of 10 g of TEOS. The solution was stirred for a further hour at 38 °C then stirred for a further two hours without heat. The silica gel produced had a molar ratio of SiO_2: 0.25 CTAB: 0.1 TMAOH: 40 H_2O. The solution was transferred without filtration or washing to a Teflon bottle for autoclaving at 100 °C for 24 h. The material was washed in ethanol and water before placement in a muffle furnace at 550°C for 8 h. The material produced, referred to as MCM-41-MF1, analysed by BET, see Figure 4.18, had a surface area of 787.85 $m^2 g^{-1}$, a pore diameter of 27.5 Å and a pore volume of 1.079 $cm^3 g^{-1}$.

Compared to the material produced by solvent extraction (MCM-41-S1), MCM-41-MF1 had a reduced pore diameter of 4.5 Å, a 22 % increase in surface area and an increase in pore volume of 0.4 $cm^3 g^{-1}$. Sample MCM-41-MF1 was further analysed by PXRD and Figure 4.19 illustrates the diffraction pattern produced. The diffraction peak (1 0 0) at an angle 2θ of 1.956° corresponds to a d-spacing of 45.12 Å, indicating that the muffle furnace calcined material had a larger pore wall thickness at 24.5 Å. Compared to the solvent extracted material the intensity of the (1 0 0) peak was reduced by approximately one third.

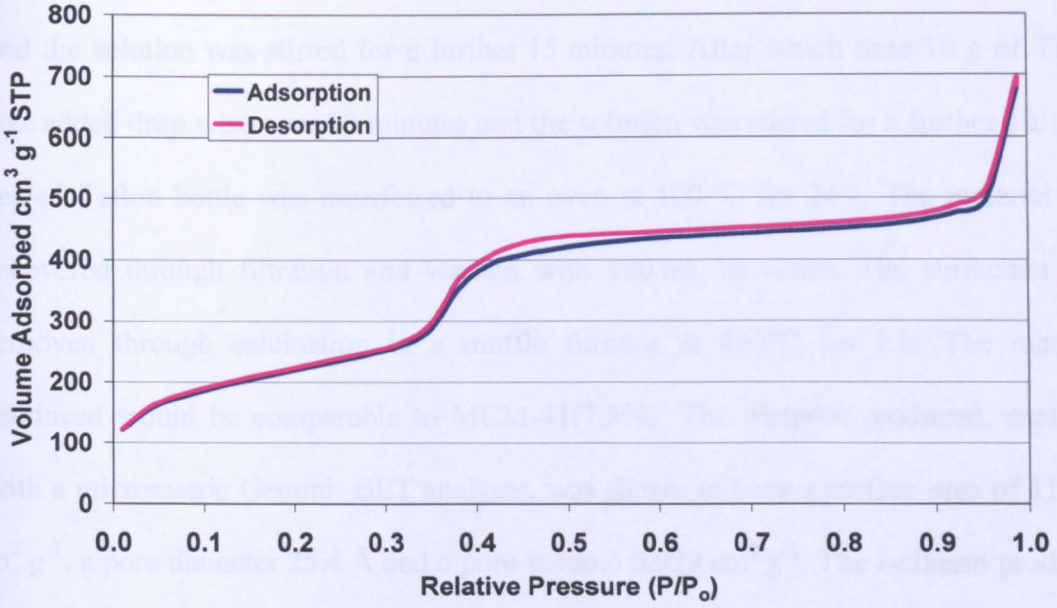

Figure 4.18: Nitrogen isotherm of MCM-41-MF1 based on the synthesis method originally used to produce MCM-41-S1

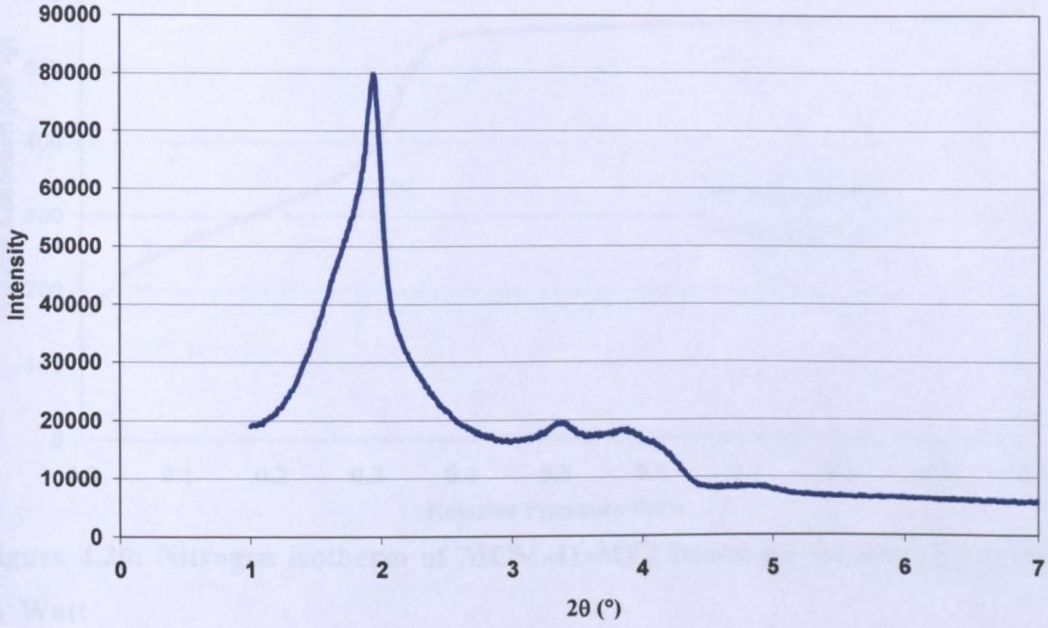

Figure 4.19: PXRD of MCM-41-MF1

As the use of the muffle furnace was encouraging a second sample (MCM-41-MF2) based on the method by Grun was analysed. The method was slightly altered, 2.41g of CTAB was dissolved in 116 g of water at 35 °C and magnetically stirred at 400 rpm in a

sealed Teflon bottle. Added to the surfactant solution was 13.5 mL of 1M TMAOH (aq) and the solution was stirred for a further 15 minutes. After which time 10 g of TEOS was added drop wise over 10 minutes and the solution was stirred for a further 1h. The sealed Teflon bottle was transferred to an oven at 100 °C for 24 h. The material was recovered through filtration and washed with 100 mL of water. The surfactant was removed through calcination in a muffle furnace at 500°C for 8 h. The material produced would be comparable to MCM-41(7.5%). The material produced, analysed with a micrometric Gemini BET analyser, was shown to have a surface area of 1155.5 $m^2 g^{-1}$, a pore diameter 25.4 Å and a pore volume 0.929 $cm^3 g^{-1}$. The isotherm produced is shown in Figure 4.20.

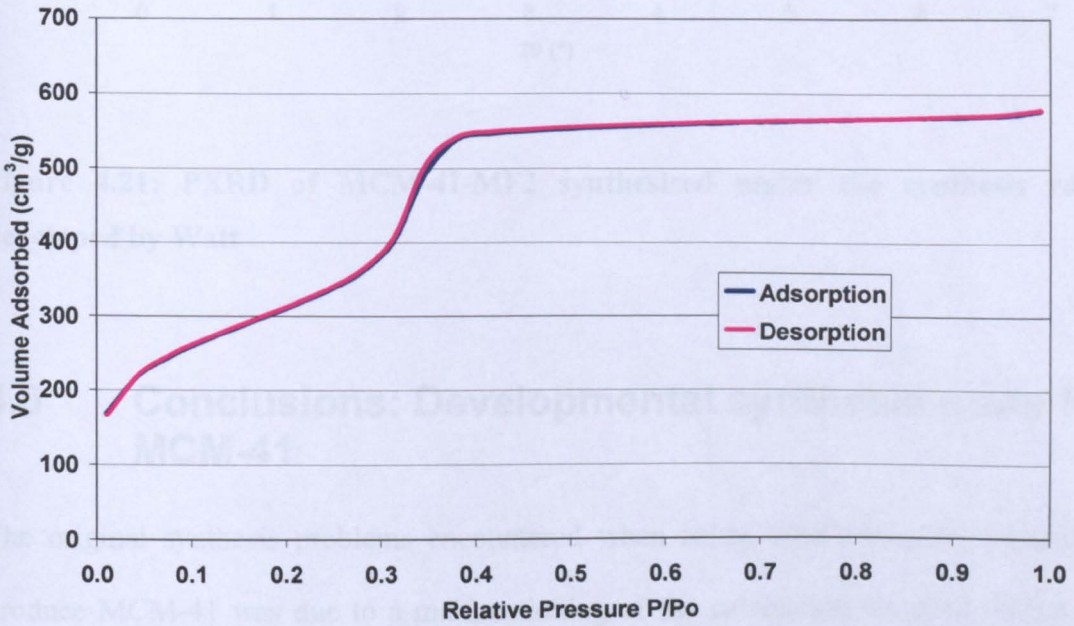

Figure 4.20: Nitrogen isotherm of MCM-41-MF2 based on the method produced by Watt

The sample labelled MCM-41-MF2 had a BET surface area of 46.6 % greater than MCM-41-MF1, however the pore size of MCM-41-24 is 2.1 Å smaller than MCM-41-MF1. The PXRD pattern of MCM-41-MF2, see Figure 4.21, gives the angle 2θ value of 2.267 °, which corresponds to a d spacing value of 39.1 Å and subsequently a pore

wall thickness of 19.7 Å. The peak (1 0 0) is similar in intensity to the peak produced for MCM-41-MF1, however the peak (1 1 0) is more defined in Figure 4.21, suggesting better long range order.

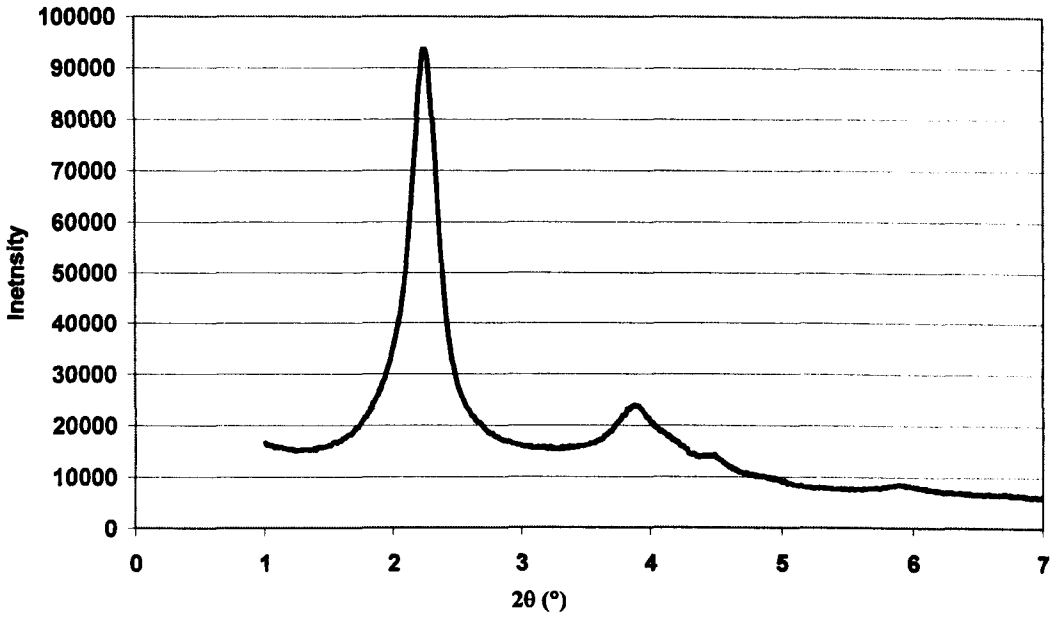

Figure 4.21: PXRD of MCM-41-MF2 synthesised under the synthesis route developed by Watt

4.5 Conclusions: Developmental synthesis route for MCM-41

The original synthesis problems encountered when using Watt's original method to produce MCM-41 was due to a malfunctioning of the calcination rig used. When the method was altered to use surfactant extraction, or calcination via a muffle furnace, mesoporous silicates were produced. None of the original 'failed' MCM-41 materials produced under the original method by Watt and the calcination rig were investigated further as indoor air pollutants. The material MCM-41-S2 was not investigated further due to the poor PXRD patterns and less defined nitrogen isotherms produced. The

materials chosen for further analysis as potential indoor air pollutant scavengers were MCM-41-S1, MCM-41-MF1 and MCM-41-MF2. From the characterisations MCM-41-S1 had the best regularity but had a smaller BET surface area than both MCM-41-MF1 and MCM-41-MF2. The largest BET surface area obtained was that of MCM-41-MF2 at 1155.5 $m^2 g^{-1}$.

4.6 References

1 J. S. Beck, J. C. Vartuli, W. J. Roth, M. E. Leonowicz, C. T. Kresge, K. D. Schmitt, C. T. W. Chu, D. H. Olson, E. W. Sheppard, S. B. McCullen, J. B. Higgins, and J. L. Schlenker, *Journal Of The American Chemical Society*, 1992, **114**, 10834.

2 C. T. Kresge, M. E. Leonowicz, W. J. Roth, J. C. Vartuli, and J. S. Beck, *Nature*, 1992, **359**, 710.

3 C. T. Kresge, J. C. Vartuli, W. J. Roth, and M. E. Leonowicz, Studies In Surface Science And Catalysis Proceedings of the meeting on mesoporous crystals and related nano-structured materials, Stockholm Sweden, 2004, p. 53.

4 K. J. Elder and J. W. White, *Chemistry of Materials*, 1997, **9**, 1226.

5 M. Kruk, M. Jaroniec, R. Ryoo, and J. M. Kim, *Microporous Materials*, 1997, **12**, 93.

6 B. Lindlar, A. Kogelbauer, P. J. Kooyman, and R. Prins, *Microporous And Mesoporous Materials*, 2001, **44**, 89.

7 A. Léonard, J. L. Blin, P. A. Jacobs, P. Grange, and B. L. Su, *Microporous And Mesoporous Materials*, 2003, **63**, 59.

8 W. J. Kim, J. C. Yoo, and D. T. Hayhurst, *Microporous And Mesoporous Materials*, 2000, **39**, 177.

9 R. Mokaya, *Microporous And Mesoporous Materials*, 2001, **44**, 119.

10 H. H. Lee, J. W. Ahn, and H. Kim, *Ceramics International*, 2004, **30**, 817.

11 J. S. Choi, D. J. Kim, S. H. Chang, and W. S. Ahn, *Applied Catalysis A-General*, 2003, **254**, 225.

12 L. Y. Chen, S. Jaenicke, and G. K. Chuah, *Microporous Materials*, 1997, **12**, 323.

13 H. P. Lin, S. Cheng, and C. Y. Mou, *Microporous Materials*, 1997, **10**, 111.

14 R. Mokaya, W. Z. Zhou, and W. Jones, *Chemical Communications*, 1999, 51.

15 M. Luechinger, L. Frunz, G. D. Pirngruber, and R. Prins, *Microporous And Mesoporous Materials*, 2003, **64**, 203.

16 J. C. Vartuli, A. Malek, W. J. Roth, C. T. Kresge, and S. B. McCullen, *Microporous And Mesoporous Materials*, 2001, **44**, 691.

17 G. Schulz-Ekloff, J. Rathousky, and A. Zukal, *Microporous And Mesoporous Materials*, 1999, **27**, 273.

18 Y. Xia and R. Mokaya, *Journal Of Materials Chemistry*, 2006, **16**, 395.

19 M. Grün, K. K. Unger, A. Matsumoto, and K. Tsutsumi, *Microporous And Mesoporous Materials*, 1999, **27**, 207.

20 Q. Cai, W. Y. Lin, F. S. Xiao, W. Q. Pang, X. H. Chen, and B. S. Zou, *Microporous And Mesoporous Materials*, 1999, **32**, 1.

21 D. Kumar, K. Schumacher, C. du Fresne von Hohenesche, M. Grün, and K. K. Unger, *Colloids And Surfaces A-Physicochemical And Engineering Aspects*, 2001, **187**, 109.

22 S. Che, Y. Sakamoto, O. Terasaki, and T. Tatsumi, *Microporous and Mesoporous Materials*, 2005, **85**, 207.

23 T. Linssen, K. Cassiers, P. Cool, and E. F. Vansant, *Advances In Colloid And Interface Science*, 2003, **103**, 121.

24 M. F. Ottaviani, A. Galarneau, D. Desplantier-Giscard, F. Di Renzo, and F. Fajula, *Microporous and Mesoporous Materials*, 2001, **44-45**, 1.

25 C. Watt, PhD Thesis, '*Development of novel sensors and sorbents to protect items of cultural importance in museum environments*', Department of Pure and Applied Chemistry, University of Strathclyde, Glasgow G1 1XL, 2004.

26 J. I. Goldstein, D. E. Newbury, P. Echlin, D. C. Joy, C. E. Lyman, C. Fiori, E. Lifshin and A. D. Romig, *Scanning Electron Microscopy and X-ray Microanalysis: a text for biologists, material scientists and geologists*, 2nd edn., Plenum Publishing Corporation, New York, 1992.

27 Y. D. Xia and R. Mokaya, *Journal Of Materials Chemistry*, 2004, **14**, 2507.

28 C. Lesaint, B. Lebeau, C. Marichal, and J. Patarin, *Microporous and Mesoporous Materials*, 2005, **83**, 76.

5 CHARACTERISATION AND DEVELOPMENT OF ALTERNATIVE MESOPOROUS SILICATES, WITH AND WITHOUT FUNCTIONALITY

Previous research within the project focussed on the synthesis and characterisation of MCM-41 as a potential mesoporous silicate used as an indoor air pollutant scavenger. Due to some of the difficulties encountered in synthesising MCM-41 with the desired physical characteristics alternative methods used to produce high surface area mesoporous silicates were investigated.

5.1 Introduction: Family of mesoporous silicates synthesised through the use of tri-block copolymers

In 1998 a family of mesoporous silicates with similar properties to MCM-41, was developed.[1, 2] In these highly ordered silicate structures non-ionic alky poly(ethylene oxide) oligomeric surfactant and poly (alkene oxide) block copolymers, or tri-block copolymers, were used in acidic media as the organic template directing agent. The silicate framework was provided by a silicate species such as TEOS. When the organic template was removed mesopores remained within the inorganic framework.

5.1.1 Formation and structure of SBA-15

The formation of a highly ordered hexagonal structured material called SBA-15 is based on an $(S^0H^+)(X^-I^+)$ pathway, see Figure 5.1. First the alkoxysilane species is hydrolysed and co-condensation steps further the formation of the silicate structure. In strongly acidic media the ethylene oxide (EO) moieties of the triblock copolymer (S^0) associates with hydronium ions (H^+). The charge on the EO units and the cationic silica species

(I^+) are assembled together by a combination of electrostatic, hydrogen bonding, van der Waals interactions. The presence of the halide ion (X^-) coordinates directly with the silicon atom.

$$Si(OEt)_4 + nH_3O^+ \rightarrow Si(OEt)_{4-n}(OH_2^+)_n + nEtOH$$

$$REO_m + yHX \rightarrow REO_{m-y}\left[(EO)H_3O^+\right]_y \ldots\ldots\ldots\ldots yX^-$$

Figure 5.1: Assembly pathway for SBA-15 (S^0H^+)(X^-I^+), where REO represents the block copolymer

Unlike MCM-41, the methods used to produce SBA-15 are more consistent. Most of the literature methods[3-9] use the original method published by Zhao and co-workers[1, 2]. The synthesis procedure involves dissolution of the tri-block copolymer P123, made from poly(ethylene oxide) (PEO) and poly(propylene oxide) (PPO) in the ratio of $PEO_{20}PPO_{70}PEO_{20}$, in water with the addition of TEOS under acidic conditions using hydrochloric acid. The mixture is stirred at 35 °C for 20 h, statically aged overnight, then the as-synthesised product is filtered, washed and air dried before calcination at 500 °C for 6 h. The structure of SBA-15 shows similarities to that of MCM-41 with the final inorganic structure demonstrating a hexagonal arrangement and a comparable surface area greater than 700 m^2 g^{-1}. There are also a number of differences. SBA-15 has a thicker wall structure compared to MCM-41 (31-64 Å) and has a uniform pore size typically100 Å. When analysed by BET, the nitrogen adsorption isotherms produced are type IV, however the point at which hysteresis takes place occurs at a higher relative pressure, generally around 0.6-0.7 P/P^o, indicative of larger pores.[3] During calcination pore shrinkage is also observed like MCM-41, a 20 % contraction has been noted for SBA-15 materials compared to 5% for MCM-41.[4, 5] One final

difference in the structure of SBA-15 compared to MCM-41 is the presence of disordered micropores within the ordered mesopores walls.

5.1.1.1 Presence of a micropores in SBA-15

When $PEO_mPPO_nPEO_m$ is dissolved in water micelles are formed where the PO (propylene oxide) blocks form the core of the micelle and the EO (ethylene oxide) blocks form the exterior of the micelle. At temperatures between 35-100 °C the PO block is strongly hydrophobic whereas the hydrophobicity of the EO block increases as the temperature increases. Therefore as the temperature increases the hydration of the EO block decreases. In 2000 Kruk and Jaroniec[6] suggested that at 35 °C the triblock copolymer micelle has extended EO blocks, like fingers, which penetrate the silica framework. Upon calcination the triblock copolymer is removed to leave a framework of mesopores, with micropores present in the framework where the EO blocks resided during the as-synthesised stage. When analysing the α_s plots calculated from the nitrogen isotherms the presence of micropores with estimated volumes of 0.12 and 0.06 $cm^3\ g^{-1}$ were recorded.[6]

The presence of micropores was further confirmed by Ryoo *et al*[3] through the organic modification of SBA-15 (discussed later in Section 5.2) with trimethylsilyl and octyldimethylsilyl. The surface area of the SBA-15 was reduced on modification from 780 to 450 and 210 $m^2\ g^{-1}$, respectively. The authors concluded that the larger octadimethylsilyl blocked all the complementary pores while the smaller trimethylsilyl blocked only a fraction of the pore,. which indicated that a large fraction of the complementary pores were sized between 1-3 nm. Ryoo *et al*[3] also suggested the possibility of connectivity between mesopores, since EO blocks of adjacent micelles may become entangled.

Galarneau and co-workers[4, 5] suggested that the presence of micropores and the connections between mesopores were as a direct result of the synthesis temperature of the SBA-15. At synthesis temperatures between 36-60 °C micropores are present but no connections between pores are present. As the temperature is increased to around 100 °C microporosity is reduced and the mesopore connections form due to the decreased interaction between the EO fingers and the silica. At 130 °C no micropores are present however bridges between structural mesopores are formed.

When comparing argon isotherms of MCM-41 and SBA-15 of identical mesopores diameter. The amount of gas adsorbed prior to capillary condensation is greater for SBA-15 than MCM-41. This was attributed to the pores present within the pore walls that increase the surface area of the material.[10]

5.1.2 SBA-16

MCM-48 is part of the M41S family to which MCM-41 belongs. It has a cubic periodic arrangement of mesoporous pores that can be replicated by a material known as SBA-16. This is a cubic cage structured mesoporous silicate also prepared with tri-block copolymers with larger EO blocks, typically F127 ($EO_{106}PO_{70}EO_{106}$). The XRD pattern produced can be indexed as (110) (200) (211) (310) (222) and (321) corresponding to a cubic structure. The nitrogen isotherm of SBA-16 is type IV and contains a hysteresis loop type H1.[1] The SBA-16 originally produced by Zhao and co-workers[1] had a pore diameter of 54 Å, a pore volume of 0.45 cm^3g^{-1} and BET surface area of 740 m^2g^{-1}. SBA-16 also contains microporosity in the walls of the mesopores.

5.1.3 Modification of the porosity of SBA-15 and SBA-16 through modification of organic templating agents

The pore size is a critical physical parameter of the material as it influences the suitability of the material for the specific task. Zhao and co-workers[1] expanded the pore size of SBA-15 through the addition of organic co-solvents such as 1,3,5-trimethylbenzene. The pore size expanded to around 260 Å while the BET surface area was 910 m^2g^{-1} and pore volume was 2.2 cm^3g^{-1}. Through altering the ratio of 1,3,5-trimethylbenzene in the reaction, mixture pore sizes between 89-300 Å were obtained. Lindlar *et al*[11] increased the mesitylene molar ratio in the as-synthesised product from 0.25 to 0.75 which resulted in an increase in both surface area, from 810 to 1190 m^2 g^{-1}, and pore diameter from 44-80 Å. Fan *et al*[12] used the addition of 1,3,5-trimethylbenzene to enlarge the mesotunnels of SBA-15 to approximately 80 Å, thereby completely interconnecting the hexagonal channels.

The tri-block copolymers can be mixed in different ratios to produce different distances of pore centre to pore centre hexagonal pore spacing.[13] These mesoporous silicates are sometimes referred to as MSU-X (Michigan State University) material where X denotes the type of poly (ethylene oxide) used.[14] The three surfactants commonly used are P65 ($PEO_{20}PPO_{30}PEO_{20}$), P85 ($PEO_{26}PPO_{39}PEO_{26}$), P123 ($PEO_{20}PPO_{69}PEO_{20}$) or F127 ($PEO_{106}PPO_{70}PEO_{106}$). The synthesis procedures reported involved dissolving approximately 1 g of solid surfactant in 1.8 g of tetramethoxysilane (TMOS), under acidic conditions. Rotory film evaporatoration was used to remove any methanol produced in the reaction. The viscous gel produced was left to condense at 40 °C for one week in a sealed flask. The template was removed from the silicate by calcination at 450 °C for 24 h. Any residual organic template was further removed by flowing a 5 % ozone stream over the dried silicate for 30 min. When pure P123, P85 and P65 were

used to produce mesoporous silicates the centre to centre distances produced were 110, 85 and 75 Å, respectively. When the tri-block copolymers were mixed with a shorter tri-block copolymer the pore centre to pore centre distance was reduced. e.g. when 100 % P123 was mixed with P65 to produce a 60:40 mixture the pore centre to pore centre distance was reduced by 21 Å to 89 Å. By mixing the ratio of copolymers used no swelling reagent was needed to change the pore size.

In 2004 Kim *et al*[15] modified the mesopores diameter and entrance size of SBA-16 by blending the ratio of co-polymers F127 and P123 present. The two tri-block copolymers were mixed to give average molar compositions of $EO_{106}PO_{70}EO_{106}$, $EO_{90}PO_{70}EO_{90}$, $EO_{80}PO_{70}EO_{80}$, and $EO_{70}PO_{70}EO_{70}$. In reducing the average length of the EO units an increase in unit cell parameter was noted.

5.1.4 Alteration of the pore size SBA-15 without changing surfactant type.

Pore size can also be controlled using supercritical CO_2. Morris *et al*[16, 17] introduced supercritical CO_2 to the silicate procedure (using P123) after the methanol had been removed via rotorevaporation. The viscous gel produced from the rotorevaporator was loaded into a 50 mL stainless steel cell which was heated to 40 °C and pressurised with CO_2 using a 260 mL Isco syringe pump and then left to stand for one week. The sample was then thermally treated at 450 °C for 24 h. The CO_2 was used to pressurise the sample from 138-482 bar. As the pressure increased the pore diameter increased in a linear manner (81-100 Å) as did the pore volume (0.76- 0.93 $cm^3\ g^{-1}$). It was noticed that a thinning of the pore wall was also associated with increasing CO_2 pressure (50-34 Å). The nitrogen isotherms produced were typical of type IV. The increase in

CO_2 pressure causes an increase in the sorption of CO_2 into the polymer core of the surfactant micelle thereby causing an expansion in the pore diameter and pore volume.

The pore size of SBA-15 can be tailored by the choice of the synthesis/ aging temperature used.[1] By increasing the temperature the EO block increases its hydrophobicity and therefore the EO block interacts less with the silica wall and creates an increased hydrophobic domain of the micelle forming larger micelles, with less microporosity.[4] Kim *et al*[15] also showed that by increasing the hydrothermal duration or temperature the pore entrance of SBA-16 could be enlarged.

5.1.5 Modification of the synthesis procedure of SBA-15

The temperature at which calcination occurs can effect both the mesopore and micropore diameter.[18] When SBA-15 is calcined between 500-800 °C silicates were produced with type IV isotherms and H1 hysteresis loops. At 500 °C SBA-15 possessed a mesopores diameter of 60 Å and a micropore diameter of 6 Å. With an increase in calcination temperature to 800 °C the mesopore diameter decreased to 4 nm while the micropore diameter increased to 1.1 nm. The micropore distribution was narrower when calcined at 500 °C compared to 800 °C. Escax *et al*[19] noted the same trend when increasing the calcination temperature from 450 to 800 °C, additionally a decrease in micropore volume from 0.03 to 0 cm^3g^{-1} and a decrease in mesopore volume from 1.51 to 0.77 cm^3g^{-1} was noted.

Recently Escax *et al*[19] have modified the porosity of SBA-15 after the calcination procedure. By treating 250 mg of SBA-15 in either 25 mL of water or aqueous ammonia (pH 11) at room temperature, or 100 °C, for 24 hours the porosity was altered. By treating SBA-15 in water at 100 °C the elimination of micropores was noted. When

treating the SBA-15 in aqueous ammonia at room temperature the presence of micropores was eliminated from 0.1 cm^3 g^{-1}, while the mesopores volume and surface area was reduced by 0.03 cm^3 g^{-1} and 268 m^2 g^{-1}, respectively. When treating SBA-15 under the harsher conditions, i.e treating with aqueous ammonia (pH 11) at 100 °C, no micropores were present however mesopores and macropores were produced with an average pore diameter of 108 Å.

5.2 Introduction: Addition of functionality to mesoporous silicates

Functionalisation of the silicate produced offers an opportunity to enhance the chemical reactivity of the silicate whilst retaining its desired structural properties. There are two ways in which organo-functionality can be added to mesoporous silicates. The first method involves post synthesis grafting (PSG) of the functionality onto the silianol groups present on the silicate after it has been prepared. The second method is referred to as the direct synthesis, co-condensation, or the one pot synthesis method. Here organo alkyl siloxane precursor is mixed with the silicate precursor during the synthesis stage.

5.2.1 Post synthesis grafting addition of organo functionality

Post synthesis grafting (PSG) adds functionality to an already present silicate framework. In general alkyl siloxanes have been added through silation and the method is traditionally carried out by refluxing the silicate, along with the alkyl siloxane, in toluene. Functional groups successfully grafted onto the silicate include: alkyl chains, [20-22] amines,[23-26] thiols,[27] cyanides.[23] After the organo-functionalised silicate forms it may be washed, filtered and dried (soxhlet procedure is often used). In the PSG method the functional group is thought to be grafted on to the inside, or opening, of the pores in

the silicate and is therefore not uniformly distributed throughout the framework. It has been suggested that almost all the organo-functionality is present on the surface of the material.[26] In general the pore size and surface area are reduced after PSG. For example, when grafting 3-aminopropyltrimethoxysilane (0.53 m mol g^{-1} of amine) onto MCM-41, Yokoi and co-workers[26] noticed a reduction in pore size from 3.64 nm to 3.10 nm, along with a surface area reduction from 1281 m^2 g^{-1} to 939 $m^2 g^{-1}$. The higher the concentration of alkylsiloxane used the greater the extent of functionalitsation through the capping of Si-OH groups, hence an even greater reduction in surface area and pore size from the original values. Secondary post synthesis grafting has also been used to end cap the remaining OH groups present with methyl groups, thereby reducing the polarity of the surface of the silicate material, a method commonly used to endcap silica stationary phases used in high performance liquid chromatography.[9, 24, 28] Mercaptopyridine has been grafted onto the surface of SBA-15 through a two step process, firstly 3-chloropropyltriethoxysilane was reacted with 2-mercaptopyrimidine and the product subsequently grafted onto SBA-15.[7]

SBA-15 has been modified with thiols and amines; as with MCM-41 modifications a reduction in surface area, total pore volume and pore size was recorded.[8] Before modification the SBA-15 had a surface area of 814 m^2 g^{-1} after modification with 3-aminopropyltriethoxysilane the surface area was reduced to 279 $m^2 g^{-1}$ and the carbon content was 9.5 %. [8]

In 2005 Luan *et al*[29] grafted 3-aminopropyltriethoxysilane onto SBA-15 using a incipient wetness impregnation technique. Here 1g of SBA-15 was added to dry toluene and dissolved 3-aminopropyltriethoxysilane and mixed for 10 min. The mixture was

then transferred to a Teflon bottle and heated at 100 °C for 24 h. The product was filtered, washed with dry toluene followed by dichloromethane, and dried at 120 °C for 12 h. An increase in the molar addition of 3-aminopropyltriethoxysilane during the synthesis stage resulted in a decrease in surface area, pore volume and pore size. When 8 % of 3-aminopropyltriethoxysilane was grafted onto the parent silica the surface area reduced from 584 $m^2 g^{-1}$ to 460 $m^2 g^{-1}$ while the pore volume decreased from 0.98 $cm^3 g^{-1}$ to 0.82 $cm^3 g^{-1}$. Lin and co workers[30] suggest that the grating procedure can be combined into one step with the surfactant removal technique, when refluxed in ethanol.

5.2.2 Addition of functionality through nitridation

Nitridation (also referred to as ammonolysis) is a process which produces porous oxynitride, or nitride materials via partial or complete displacement of silanol groups and bridging oxygen in the precursor oxides. The procedure is carried out at high temperatures under a flow of nitrogen or ammonia. Xia and Mokaya[31] recently investigated the effects of nitridation on calcined MCM-41. MCM-41 was treated with a flow of ammonia at a rate of 100 mL min^{-1}, while the temperature of the furnace was increased at a rate of 5 °C min^{-1} to the reaction temperature which was held for 20 h before cooling to 100 °C. Further cooling to room temperature was performed under a flow of nitrogen. MCM-41 was treated at temperatures of 850, 950 1050 or 1150 °C. Using nitrogen adsorption analysis they found that by increasing the reaction temperature the surface area decreased from 903 $m^2 g^{-1}$ to 743 $m^2 g^{-1}$, while the pore volume and pore size halved. All materials produced still produced type IV isotherms. It was postulated that the high treatment temperatures used induced contraction in the silica network influencing pore size and diameter more than surface area. Elemental analysis of the materials indicated that the nitrogen concentration increased from 8.6 %

to 25.1 % with increasing reaction temperature. Increasing the reaction time from 20 to 80 h also resulted in an increase in the nitrogen incorporation in the interior framework of the pores. When analysed by fourier transform infra red spectroscopy symmetric bending of NH_2 and stretching of NH bonds were visible at 1555 cm^{-1} and 3505 cm^{-1}, respectively. ^{29}Si NMR and x-ray photoelectron spectroscopy were used to confirm the presence of nitrogen in the framework. Similar trends were observed when carrying out nitridation on periodic mesoporous organo-silicas.[32]

5.2.3 Co-condensation addition of organo functionality during initial framework formation

Using the co-condensation or direct synthesis method the alkyl siloxane precursor is mixed with the silicate precursor and added to the surfactant during the initial synthesis. The material is then hydrothermally treated and the as-synthesised product can be washed before surfactant removal. To remove the surfactant template from a co-condensation produced silicate, solvent extraction must be used; generally by an acidic reflux. Calcination is not possible as the induced functionality would be removed at high temperature. All the organic groups successfully grafted via post synthesis grafting have also been successfully introduced via co-condensation.[20, 22, 27, 33-37] The direct synthesis method resulted in the functionality being distributed throughout the framework and within the pores. In addition, the functionality was more firmly bound to the surface.[38] As with adding functionality through post synthesis grafting, co-condensation reactions also decrease surface area and pore size. When Yokoi and co-workers[26] used 3-aminopropyltrimethoxysilane in a co-condensation method the surface area was reduced from 1194 $m^2\ g^{-1}$ to 1114 $m^2\ g^{-1}$, while the pore size was reduced from 3.76 nm to 3.60 nm. When the molar ratio of

3-aminopropyltrimethoxysilane to silicate increased above 0.2 the array of mesopore channels became disordered.

Direct synthesis work has been successful in bi-functionalizing MCM-41 with phenyltriethoxysilane (PTES) and either 3-aminopropyltrimethoxysilane (APTES),[39] allytrimethoxysilane or 3-mercaptopropyltriethoxysilane.[40] When MCM-41 bifunctionalised with 5 mol % PTES and 5 mol % APTES was analysed by x-ray diffraction, four diffraction peaks where observed with a unit cell length below 4 nm. The surface area of this material was determined to be 1220 m^2 g^{-1} with a pore diameter of 3.5 nm.

Saridaran *et al*[41] modified the original SBA-15 synthesis method by Zhao to directly incorporate organo functionality during the initial synthesis steps. The triblock copolymer poly(ethylene oxide)- poly(propylene oxide)-poly(ethylene oxide), and the aniline organic moiety N-[3-(trimethoxysilyl)propyl]aniline were mixed with the silicate precursor. To remove the triblock copolymer, the as-synthesised product was boiled in ethanol. The resulting organically modified SBA-15 contained a hexagonal mesoporous structure with a surface area of 289 m^2g^{-1}, a pore diameter 7.8 nm, wall thickness of 3.4 nm, mesopores volume of 0.8 cm^3 g^{-1} and a micropore volume of 0.09 cm^3 g^{-1}.

5.2.4 Co-condensation method using anionic surfactant for the addition of amino functionality

Recently amino-functionalised mesoporous silicate has been synthesised by Yokoi and co-workers[42] using a novel templating mechanism. The anionic surfactant, lauric acid sodium salt (LAS), was used as the organic template and structure directing agent. The

mechanism for the formation of the silicate-micelle framework was designated '$S^-N^+{\sim}I^-$', where S^- is the anionic surfactant, N^+ cationic amino group and I^- is the inorganic species. The organoalkoxysilane 3-aminopropyltriethoxysilane (APS) was used to add amine functionality to the silicate and as the co-structure directing agent. With a pH below 10, a large proportion of amino groups were protonated and could therefore interact with the anionic surfactant. The direct electrostatic interaction between the positively charged amino groups and the negatively charged head groups of the anionic surfactant are the driving force for the formation of the silicate micelle framework. As with ordinary co-condensation methods, removal of the surfactant must be performed by acid extraction to avoid disrupting the functionality introduced. The final amino-functionalised materials synthesised via this route have amino groups located on the surface instead of the silica wall due to the interaction between the APS cationic head group and the anionic surfactant head group, see Figure 5.2. The functionalised mesoporous silicates were produced from gels with molar ratios of x APS: (1-x) TEOS: 0.1 LAS, 180 H_2O: 20 EtOH, were x was between 0.1-0.6. The products were characterised using elemental analysis, nitrogen isotherms, ^{29}Si MAS NMR (magic angle spinning nuclear magnetic resonance) and XRD. When the APS ratio increased from 0.2-0.6 the XRD patterns produced had broader peaks indicating an increase in the disorder. However when the proportion of APS was at 0.1 a highly ordered 2D-hexagonal structure was obtained. The nitrogen isotherms produced for ratios of APS from 0.2-0.6 showed type IV isotherms. The largest surface area of 660 $m^2\ g^{-1}$ was created from APS at 0.3, with corresponding mesopore volume of 0.33 $cm^3\ g^{-1}$ and a pore radius of 3.8 nm. Solid state NMR, ^{13}C and ^{29}Si, was used to investigate the degree of condensation within the silicates produced from a typical co-condensation method and the anionic co-condensation method.

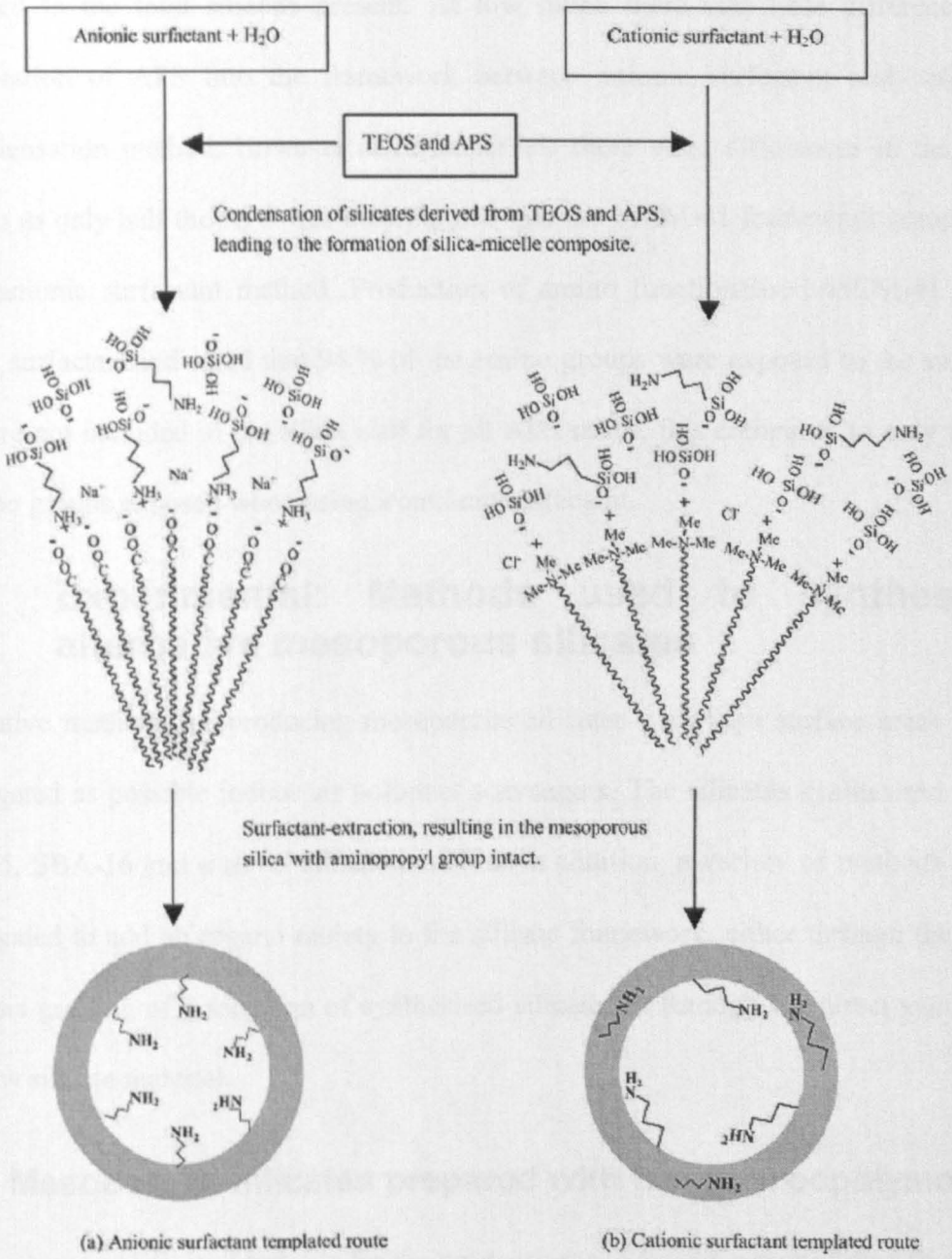

Figure 5.2:Illustration of the location of the aminopropyl group in amino-functionalized mesoporous silicas synthesised via a) the anionic templating and (b) cationic templating routes. Taken from Yokoi *et al*[42]

It was determined that the synthesis conditions were advantageous to the formation of siloxane networks when an anionic surfactant was used. The degree of incorporation of APS into the silica framework was determined by looking at the ratio of Si-C bonds

compared to the total silicons present. At low ratios there was little difference in incorporation of APS into the framework between anionic surfactant and cationic co-condensation method. However at higher levels there were differences in the two methods as only half the APS was incorporated into the MCM-41 framework compared to the anionic surfactant method. Production of amino functionalised MCM-41 with anionic surfactant indicated that 94 % of the amino groups were exposed to the surface and were not included in the silica wall for all APS ratios, this compared to only 80 % of amino groups exposed when using a cationic surfactant.

5.3 Experimental: Methods used to synthesise alternative mesoporous silicates

Alternative methods for producing mesoporous silicates with high surface areas were investigated as possible indoor air pollutant scavengers. The silicates synthesised were SBA-15, SBA-16 and a novel silicate material. In addition, a variety of methods were investigated to add an organo moiety to the silicate framework, either through the post synthesis grafting of a selection of synthesised silicates or through the direct synthesis of a new silicate material.

5.3.1 Mesoporous silicates prepared with tri-block copolymers

The mesoporous silicate synthesis for the production of SBA-15 was modified from the original method by Zhao *et al.*[1] A surfactant tri-block copolymer solution of 4 g Pluronic P123, $PEO_{20}PPO_{70}PEO_{20}$ (BASF Corporation, 3000 Continental Drive) was dissolved in 120 mL of 2 M HCl (37%) and 60 mL of distilled water in a sealed glass bottle at room temperature, and the mixture was magnetically stirred at 330 rpm. The surfactant solution was then heated to 40 °C and 11.3 g of TEOS was added and left for 24 h at 40 °C. The mixture was then placed in an oven for 5 days at 60 °C. The material was filtered and washed with water and dried overnight at 60 °C before calcination at

550 °C for 24 h. The resulting mixture had a ratio of SiO_2: 0.0032 P123: 4.4 HCl: 144 H_2O and will be referred to as SBA-15. A mesoporous silicate similar to SBA-16 was prepared using an experimental procedure based on that reported by Kim *et al*[15]. A surfactant mixture of 5 g Pluronic F127, $PEO_{106}PPO_{70}PEO_{106}$ (BASF Corporation) and 1 g Pluronic P123 was dissolved in 280 mL 1.6M HCl (37%, Sigma Aldrich) solution in a sealed Teflon bottle. The surfactant mixture was heated at 35 °C and stirred at 400 rpm using a magnetic stirrer bar. After the surfactant was fully dissolved, 22 g of TEOS was added to the mixture. The sealed silicate mixture was stirred for a further 15 min, after which the stirrer was switched off and the silicate was left to 'age' for 24 h at 35 °C. The Teflon bottle was transferred to an oven and held at 100 °C for 5 days. The white solid produced was recovered through filtration, without washing and dried overnight at 60 °C. The product was subsequently filtered, washed with ethanol, and dried before calcination in air at 550 °C for 24 h. This material will be referred to as SBA-16. The molar ratio of the silicate material produced was SiO_2:0.0037 F127: 0.016 P123: 4.4 HCl: 144 H_2O.

A novel silicate method developed by Glantreo at University College Cork was used to produce silicates with distinctive sphere morphology. To prepare the silicate material 500 mL of distilled methanol and 88 mL of distilled water were added to a 1 L glass beaker. A large magnetic stirrer was used to stir the solution before the addition of 1.25 g of CTAB. After the CTAB was dissolved in the solution at room temperature 32 mL of ammonium hydroxide (NH_4OH) was added and the beaker was covered with parafilm. After dissolution 8 mL of TEOS was then added to the mixture which was then left for 24 h. The material was Buchner filtered and washed with methanol and left to air dry overnight before calcination at 550 °C in air for 6 h. The gel ratio of the

material was SiO_2: 0.0956 CTAB: 0.17 NH_4OH: 14.59 MeOH: 136.3 H_2O. This material will be referred to as SM-01.

5.3.2 Post synthesis grafting method for the addition of propyl amine to the synthesised mesoporous silicates

The method used for post synthesis grafting (PSG) was adapted from the literature.[23, 24] Figure 5.3 displays the surface properties desired from the PSG procedure.

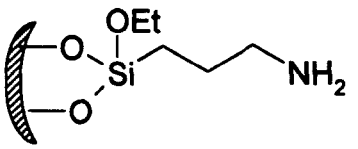

Figure 5.3: Organofunctionality grafted onto the silicate surface via post synthesis grafting

A round bottom flask was used, which was flame dried under nitrogen to ensure no moisture was introduced into the synthesis procedure. The silicate material was dried in a vacuum oven overnight. Then 0.5 g of silicate was added to 50 mL of dry toluene before 4.6 g of 3-aminopropyltriethoxysilane (3-APTEOS, Sigma-Aldrich, Steinheim Germany) was added. The mixture was refluxed for 24 hours under nitrogen. The resulting solution was rotorevaporated for approximately 1 hr to remove toluene and produce a slurry. The slurry was transferred into a soxhlet filter and washed with 100mL of 1:1 dimethylether and dichloromethane for 24 h under nitrogen, see Figure 5.4. The soxhlet filter was removed and the slurry in the round bottom flask was transferred to a fume hood to allow the remaining solvent to evaporate. The three materials modified in this way were HMS-Com, SBA-15 and MCM-41-MF1.

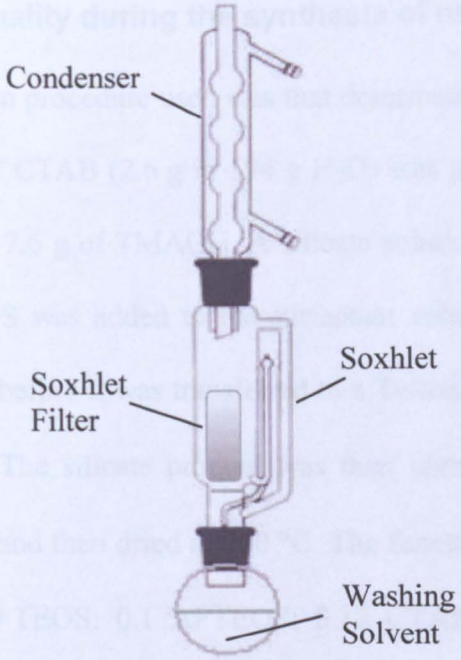

Figure 5.4: Soxhlet washing of PSG product

5.3.2.1 Nitridation method used to add functionality to silicates

Ammonia was passed over the silicate materials at high temperature. The heating consisted of a three step programme. First a drying step was used where the material was heated from room temperature to 100 °C at a rate of 5 °C min^{-1} and held at 100 °C for 30 min. The sample was then heated up to 600 °C at a rate of 5 °C min^{-1} and held for 180 min. The sample was then cooled to room temperature under a flow of nitrogen see Figure 5.5. A sample of HMS-Com was modified using this method.

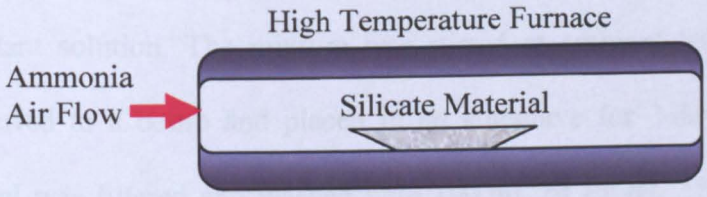

Figure 5.5: Nitridation Set Up

5.3.2.2 Co-condensation method for the addition of propyl amine functionality during the synthesis of mesoporous silicates

The co-condensation procedure used was that described by Yokoi and co-workers.[26] An aqueous solution of CTAB (2.6 g in 134 g H_2O) was prepared; the pH of this solution was adjusted using 7.6 g of TMAOH. A silicate solution containing 11 g of TEOS and 1.4 mL of APTEOS was added to the surfactant solution, and the final mixture was stirred for 2 hours, before it was transferred to a Teflon bomb and heated in an oven for 3 days at 100 °C. The silicate product was then obtained by filtration, washed with 100 mL of ethanol and then dried at 100 °C. The functionalised silicate gel had a molar composition of 0.9 TEOS: 0.1 APTEOS: 0.12 CTAB: 0.36 TMAOH: 130 H_2O. To remove the surfactant, 1 g of the as-synthesised product was stirred with 100 mL ethanol containing 9 mL of hydrochloric acid (37 wt%) at 25 °C for 4 hours. The silicate material produced will be referred to as MCM-41-cocon.

5.3.2.3 Anionic co-condensation method for the addition of propyl amine functionality during the synthesis of mesoporous silicates

The anionic co-condensation method used was modified from Yokoi and co-workers.[42] Lauric acid ((LA), SLR Grade, Fision, Loughborough, England) was used as the surfactant directing agent for the amino groups. 1.16 g of Lauric acid was dissolved in 190 g of water and 54 g of ethanol. A silicate solution with 11 g of TEOS and 1.4 mL APTEOS was prepared. The silicate solution was added slowly over 15 min to the surfactant solution. The mixture was stirred at ambient temperature for 1 hour and transferred to a bomb and placed in an autoclave for 3 days at 130 °C. The silicate material was filtered and washed with 100 mL of EtOH. The surfactant template was removed through solvent extraction then 1 g of as-synthesised material was added to a solution containing 100 mL of acetonitrile and 9 mL of HCl (37% wt) and stirred for

2 hours. The molar ratio of the material produced was 0.1 APTEOS: 0.9 TEOS: 0.1 LA: 180 H_2O: 20 EtOH. The material produced will be referred to as MCM-41-FA.

5.4 Results: Characterisation of mesoporous silicates produced using alternative methods

Where possible each of the materials produced, as described in Section 5.3 were characterised using BET, SEM, TEM or PXRD. Mesoporous materials containing carbon and nitrogen were also analysed by elemental analysis with a Perkin Elmer 2400 CHN analyser by the microanalysis service within the Department of Pure and Applied Chemistry at the University of Strathclyde.

5.4.1 Characterisation of SBA-15 and SBA-16

Samples of SBA-15 and SBA-16, prepared as outlined in Section 5.3.1, were characterised. The SEM image of SBA-15 (Figure 5.6) is notably different from the SEM obtained for MCM-41-S1 (Figures 4.11). The material obtained had a worm like morphology. The nitrogen adsorption isotherm of the SBA-15 showed type IV characteristics with an H1 hysteresis loop present at a relative pressure between 0.6-0.7 (see Figure 5.7), which corresponds to a pore diameter of 69 Å. The BET surface area of the material was 849.49 $m^2\ g^{-1}$, with a BJH pore volume of 1.01 $cm^{-3}\ g^{-1}$ and a micropore volume of 0.1346 $cm^{-3}\ g^{-1}$. The pore size distribution for the SBA-15 was between 60-90 Å, see Figure 5.8. The pore volume of SBA-15 obtained from the nitrogen isotherm analysis was larger than the previously made MCM-41 materials, therefore in order obtain the diffraction pattern a beam knife was used to avoid overloading the detector with of x-rays from the source reaching the detector as the (1 0 0) diffraction peak would be lower.

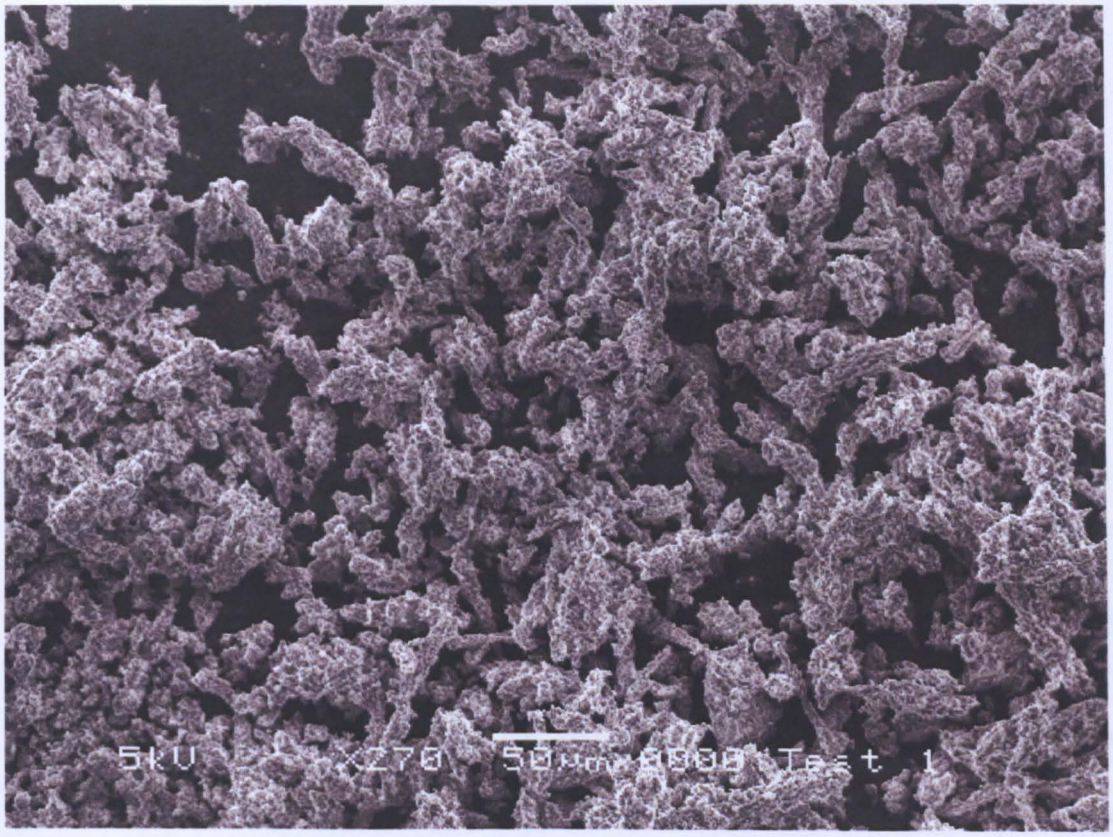

Figure 5.6: SEM image of SBA-15

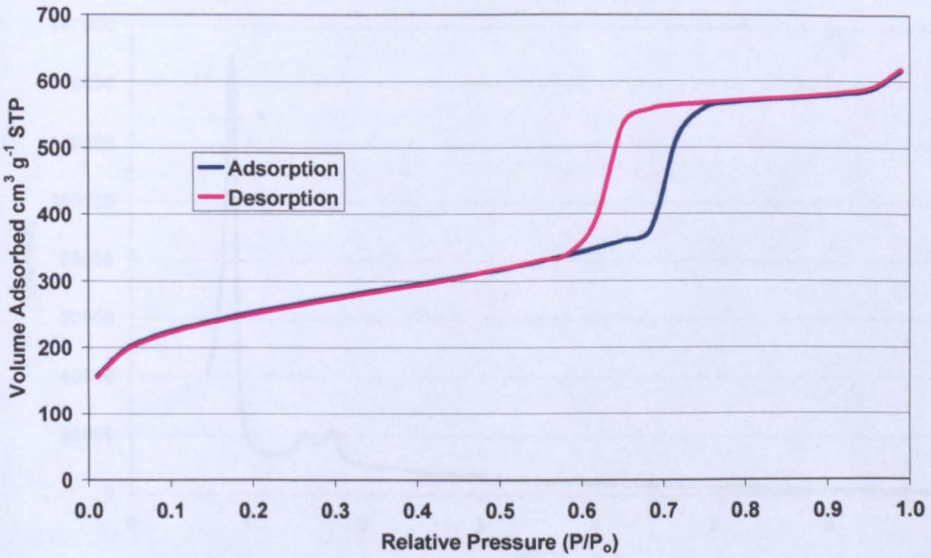

Figure 5.7: Nitrogen adsorption isotherm for SBA-15.

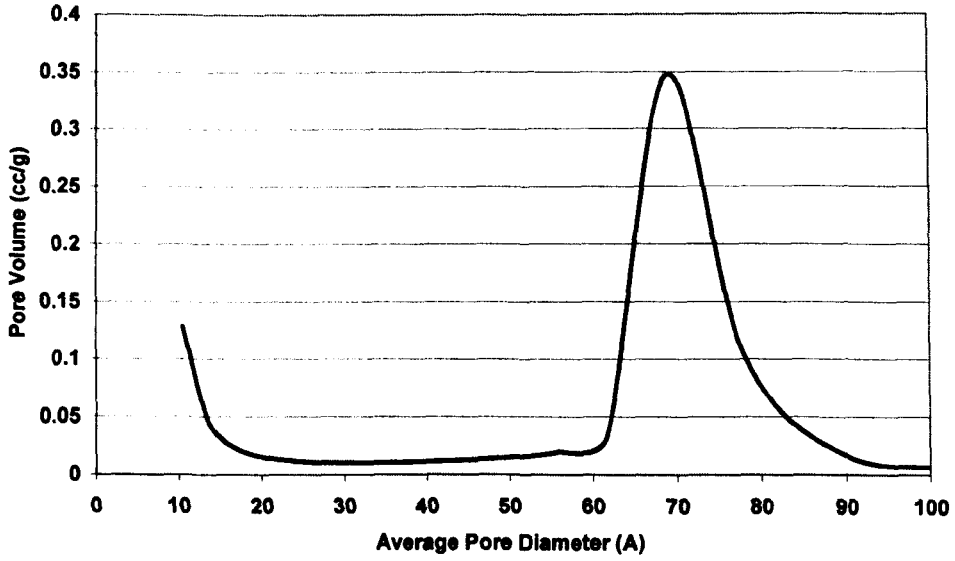

Figure 5.8: Pore size distribution SBA-15

The diffraction pattern produced for the SBA-15 sample, see Figure 5.9 was sharper than either of the MCM-41 diffraction patterns produced, with the (1 0 0) diffraction peak intensity of approximately 150 000 a.u. at an angle 2θ of 0.871. Corresponding to a d-spacing of 101 Å.

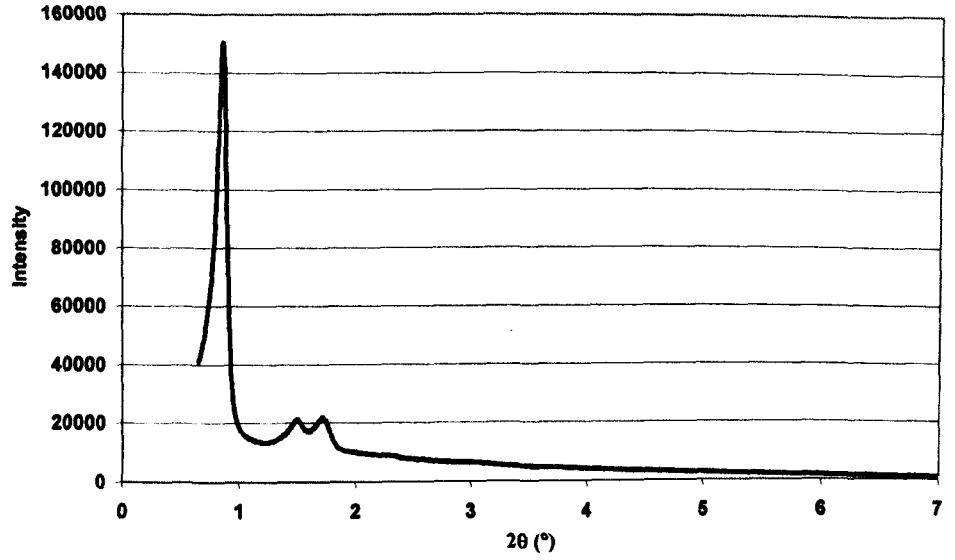

Figure 5.9: PXRD of SBA-15

The pore wall thickness was determined as 47 Å as the repeating unit was 116 Å. The TEM image of the SBA-15 sample (Figure 5.10) clearly displays areas viewing the pores 'face' on and areas where the channels are viewed perpendicular to these pores. The pore arrangement at site 'A' is hexagonal with each pore surrounded by six subsequent pores, thereby providing further evidence of structural order. The channel arrangement at site 'B' provides evidence of long range order.

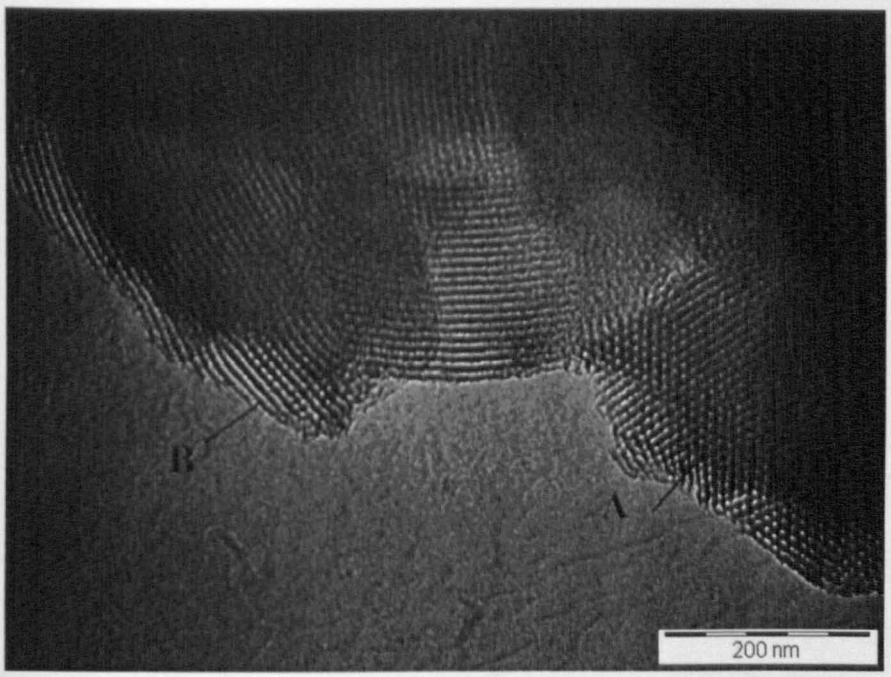

Figure 5.10: TEM of SBA-15

The nitrogen isotherm produced for the SBA-16 sample (Figure 5.11) had type IV characteristics as previously seen, however the hysteresis loop produced was classified as a type H2 because the loop was broad and the desorption branch was steeper than the adsorption branch.[43] SBA–16 had a similar surface area to previously produced materials with a BET surface area of 778.44 $m^2 g^{-1}$. The pore volume was lower than that of SBA-15 and MCM-41 at 0.7905 $cm^3 g^{-1}$. The micropore volume was also lower than that of SBA-15 at 0.049 $cm^3 g^{-1}$. The pore size distribution, given in Figure 5.12, was broad with a peak at 68 Å.

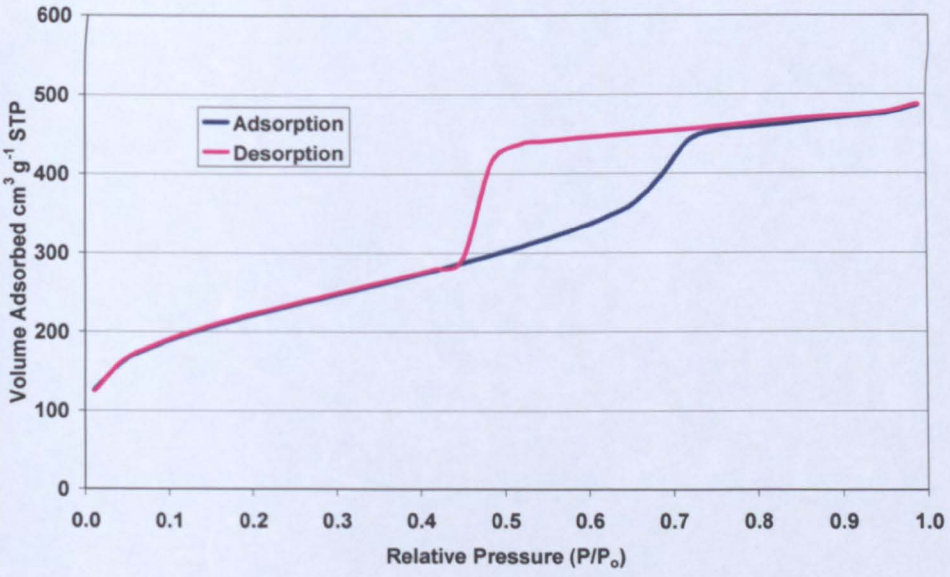

Figure 5.11 : Nitrogen adsorption isotherm of SBA-16

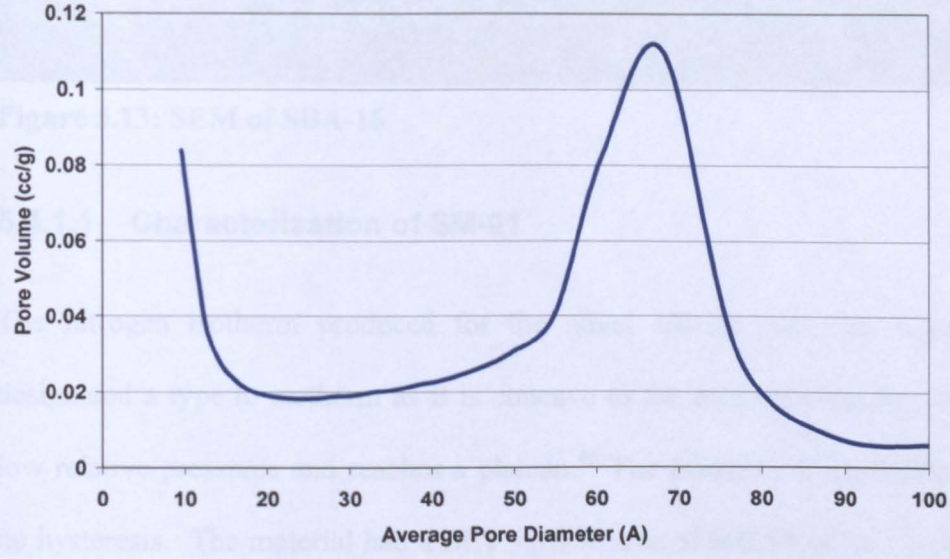

Figure 5.12: Pore size distribution of SBA-16

When SBA-16 was examined by SEM, see Figure 5.13, the material had a distinct irregular globular morphology. When analysed by PXRD no diffraction peaks were evident even though literature suggested that PXRD peaks should have been obtained.[15] No TEM analysis was conducted on the SBA-16 material due to the unavailability of the instrument.

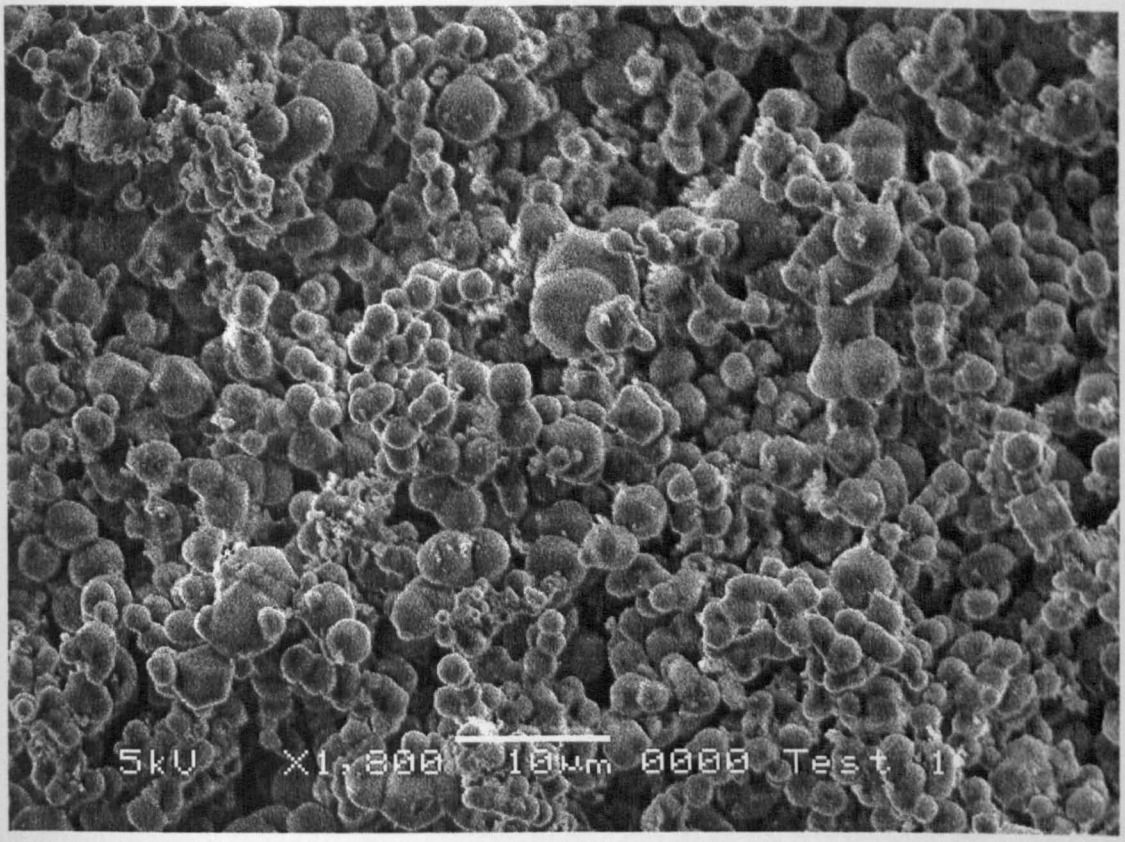

Figure 5.13: SEM of SBA-16

5.4.1.1 Characterisation of SM-01

The nitrogen isotherm produced for the novel silicate material, Figure 5.14, was designated a type Ib isotherm as it is concave to the relative pressure, rises sharply at low relative pressures and reaches a plateau.[43] The isotherm is reversible and contains no hysteresis. The material had a BET surface area of 802.94 $m^2 g^{-1}$, a pore volume of 0.4447 $cm^3 g^{-1}$ and a pore distribution less than 20 Å (Figure 5.15). The surface characteristics suggest that the material produced was microporous rather mesoporous.

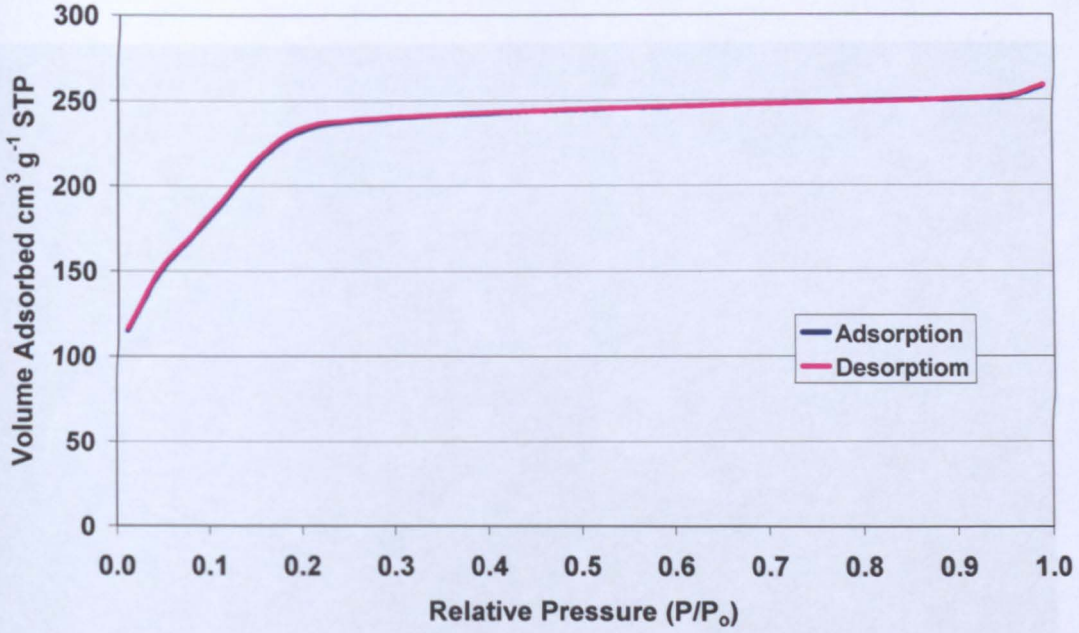

Figure 5.14: Nitrogen adsorption isotherm of sphere material

The SEM of the sphere material details a random distribution of spherical particles with diameters of approximately 1μm. PXRD diffraction was used to characterise the material however no diffraction patterns were observed.

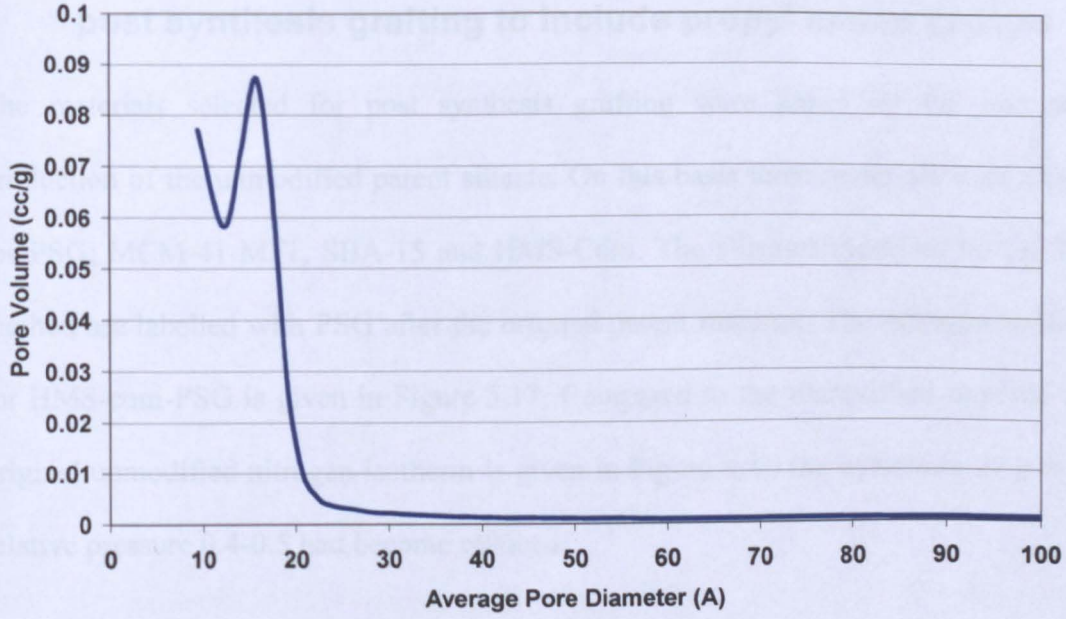

Figure 5.15: Pore size distribution SM-01

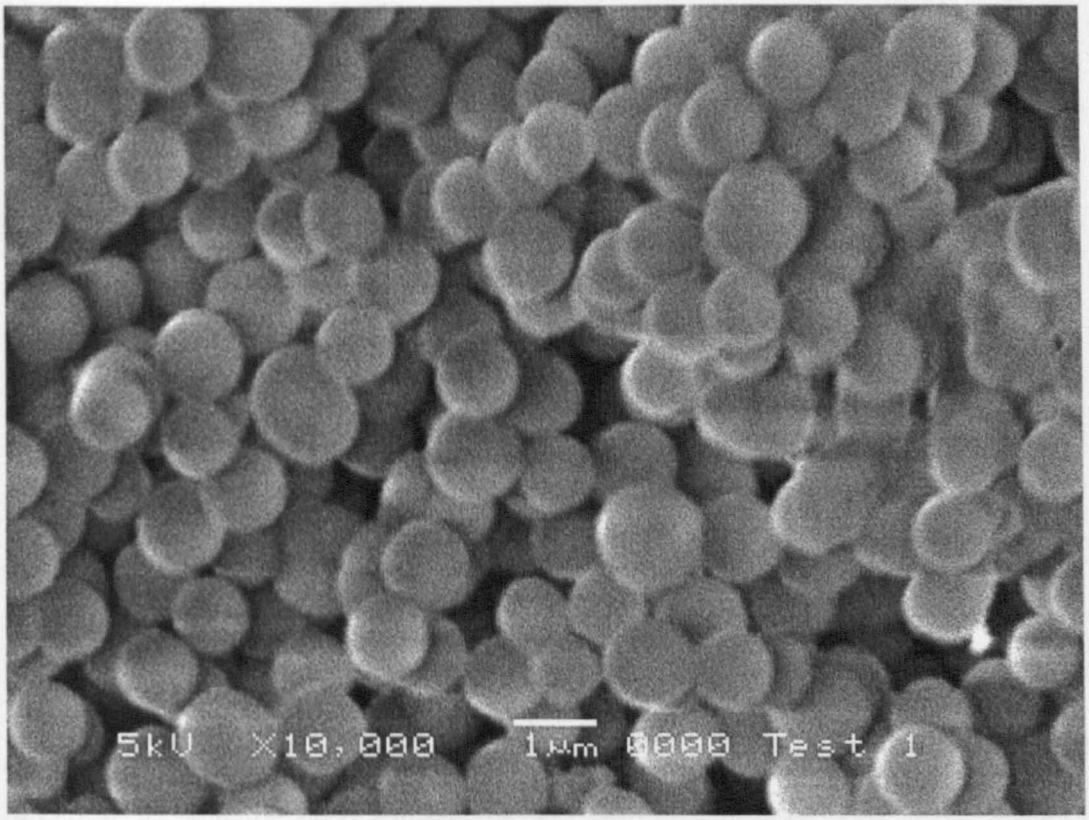

Figure 5.16: SEM of sphere material

5.4.2 Characterisation of mesoporous silicates modified using post synthesis grafting to include propyl amine groups

The materials selected for post synthesis grafting were based on the successful production of the unmodified parent silicate. On this basis three materials were chosen for PSG; MCM-41-MF1, SBA-15 and HMS-Com. The silicates modified by the PSG method are labelled with PSG after the original parent material. The nitrogen isotherm for HMS-com-PSG is given in Figure 5.17. Compared to the unmodified material (the original unmodified nitrogen isotherm is given in Figure 4.4), the hysteresis loop at the relative pressure 0.4-0.5 had become reduced.

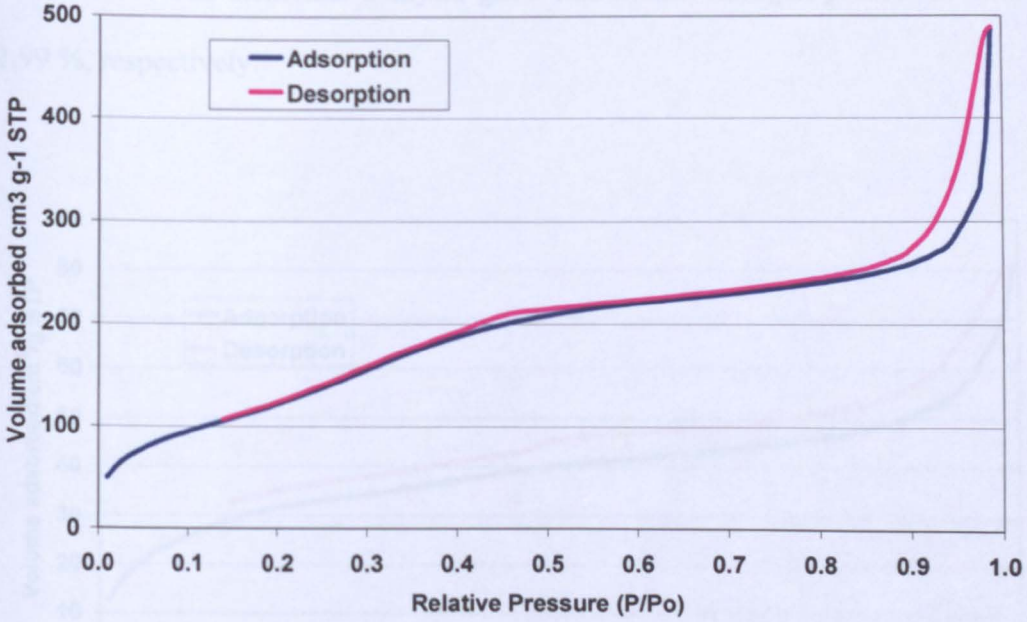

Figure 5.17: Nitrogen adsorption isotherm for HMS-Com-PSG

Additionally the BET surface area had reduced by approximately one third to 463.5 $m^2 g^{-1}$ and the pore volume had also reduced to 0.79 from 1.24 $cm^3 g^{-1}$. The reduction of surface area and the reduction of pore volume was evidence that the post grafting synthesis was successful. When HMS-com-PSG was analysed for the presence of carbon and nitrogen they were found to be present at a concentration of 9.70 and 2.91 %, respectively. The approximate ratio of 3:1 would indicate that the propyl amine groups were successfully grafted, however the nitrogen isotherm obtained had a characteristic type II isotherm indicating that the material was now non-porous. It was possible that the propyl amine was binding to the surface of the material blocking the mesopores.

When the MCM-41-MF1-PSG was analysed by BET, the surface area was greatly reduced compared to the parent MCM-41 sample at 120 $m^2 g^{-1}$, while the pore volume was reduced to 0.111$cm^3 g^{-1}$. Again the isotherm produced showed a relatively small volume of nitrogen adsorbed and the desorption branch stopped at relative pressure

around 0.15. The elemental analysis gave carbon and nitrogen present at 10.2 % and 2.99 %, respectively.

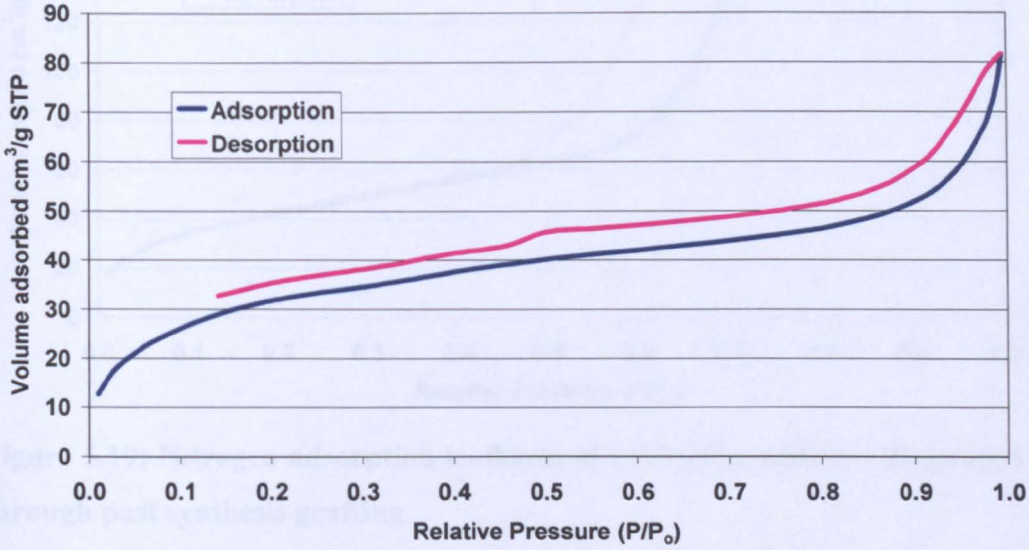

Figure 5.18: Nitrogen isotherm obtained for MCM-41-MF1-PSG

Unlike the previous two attempts to produce mesoporous materials containing propyl amine, the SBA-15-PSG material retained the Type IV isotherm with hysteresis after grafting, see Figure 5.19. However the BET surface area was reduced by almost a factor of four to 159.6 m^2 g^{-1} compared to the unmodified material. The relative pressure at which the hysteresis occurred was reduced from between 0.6-0.7, see Figure 5.7, to between 05-0.7. Elemental analysis again showed the 3:1 ratio seen in the previous two grafting attempts with carbon present at 11.5 % and nitrogen at 3.69 %. The pore volume and pore diameter were reduced at 0.265 cm^3 g^{-1} and 64 Å. Unfortunately due to lack of instrument time no SEM, TEM or PXRD was carried out on any of the three materials produced by the PSG method.

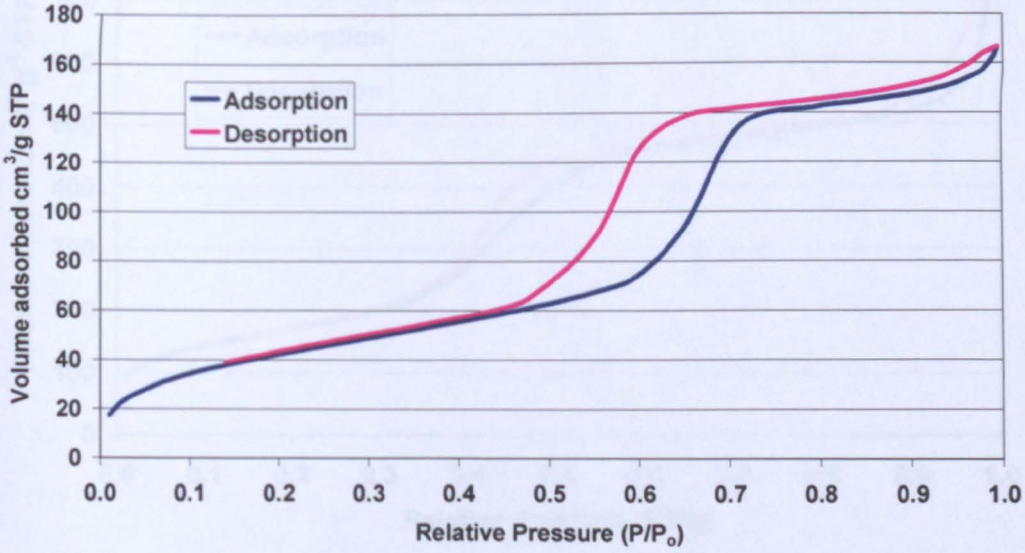

Figure 5.19: Nitrogen adsorption isotherm of SBA-15 modified with propyl amine through post synthesis grafting

5.4.2.1 Characterisation of materials modified through nitridation

The nitrogen isotherm for the HMS-com sample modified by the nitridation procedure is given in Figure 5.20. When comparing the isotherm with the parent isotherm (see Figure 4.3) it can be seen that the isotherms show similar characteristics. The surface area was 623.5 $m^2 g^{-1}$ while the pore volume and pore diameter were 1.16 $cm^3 g^{-1}$ and 4.94 nm, respectively. The elemental analysis showed that no carbon was present while nitrogen was present at 1.23 %. Unfortunately relatively little material was produced using this process, and due to lack of instrument availability at Glasgow University, no more material was synthesised and therefore an extensive adsorption testing procedure was not possible.

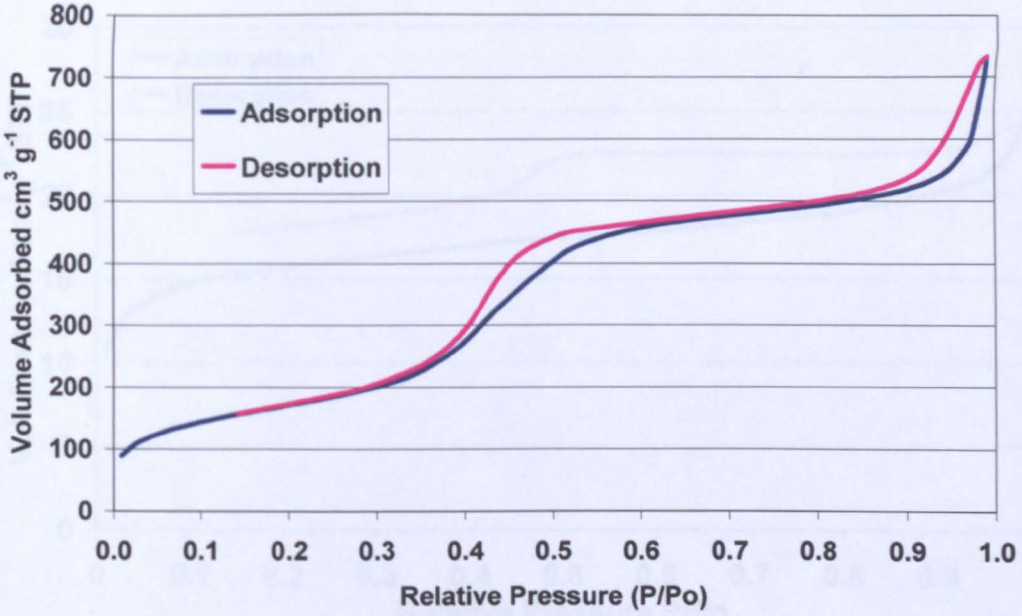

Figure 5.20: Nitrogen Isotherm of HMS-Com after nitridation

5.4.2.2 Characterisation of materials prepared through co-condensation methods

The material produced by the co-condensation method, MCM-41-cocon was characterised by BET analysis, the resulting isotherm is given in Figure 5.21. The volume of nitrogen adsorbed was small compared to other materials modified with the post synthesis grafting technique. The isotherm was difficult to distinguish with the desorption branch stopping at a relative pressure of 0.15. The isotherm possessed traits of a type I or II isotherm. The elemental analysis showed carbon and nitrogen present at a ratio of 7:1. Further elemental analysis showed the presence of bromine at 4 % and this may account for the high C:N ratio. It was possible that the method used to remove the surfactant was not as successful as the previous acidified reflux method. It was determined that the material was not mesoporous and did not have the large surface area required for an indoor air pollutant scavenger.

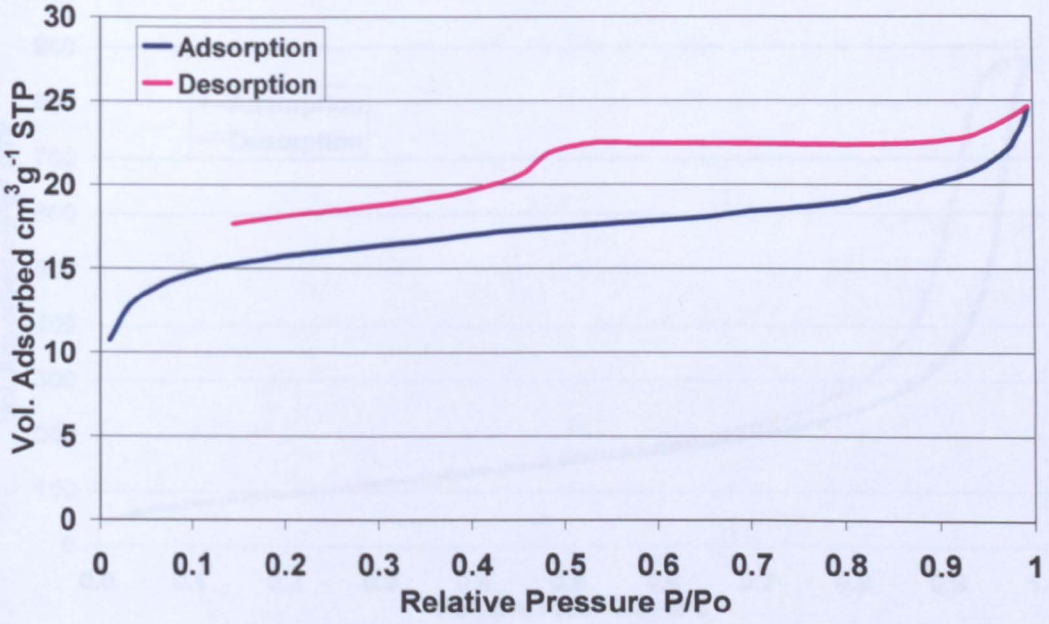

Figure 5.21: Nitrogen Isotherm of MCM-41-cocon

Figure 5.22 shows the nitrogen isotherm obtained for MCM-41-FA. The isotherm was difficult to class. The isotherm could be classed as type III as it has no point B and the isotherm is convex to the P/P° axis over the complete range.[43] The hysteresis loop at an increased relative pressure was indicative of the material containing larger diameter pores, the average pore diameter was determined at 12.6 nm. The large pore diameter was surprising considering the chain length of lauric acid is C_{11} and shorter than the chain length of CTAB at C_{16}. As a result of the increased pore diameter the surface area of the material was only 353.7 m^2 g^{-1}. The surface area obtained was larger than reported in the literature when lauric acid sodium salt was used as the anionic surfactant, 298 m^2 g^{-1}.[42] The microanalysis showed that the material contained 7.88 % carbon and 1.87 % nitrogen, giving a ratio of 4:1.

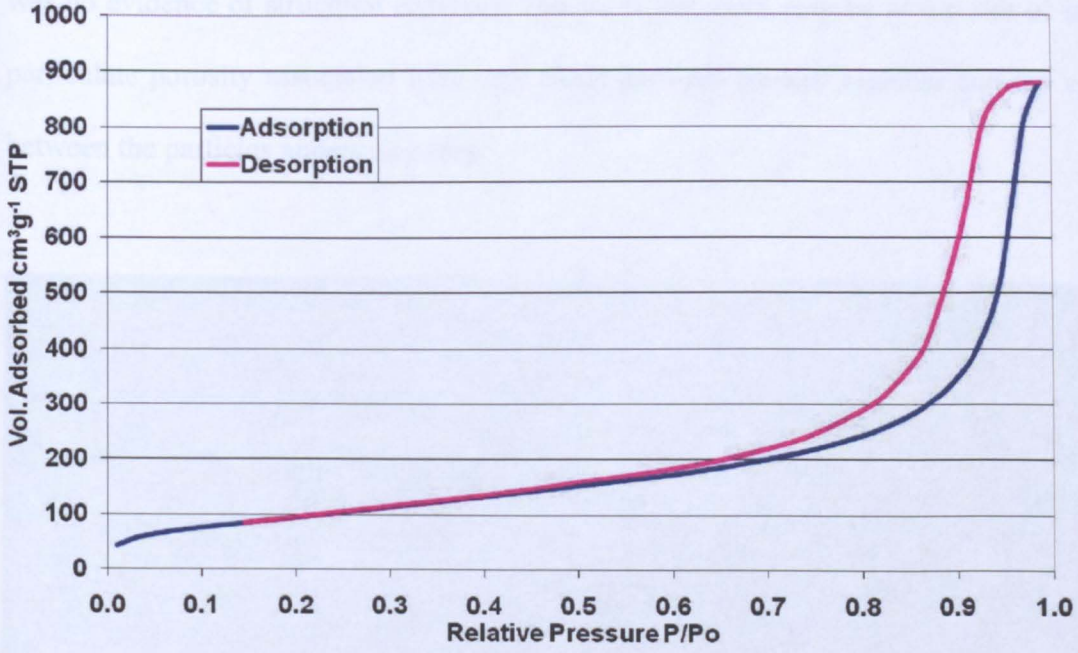

Figure 5.22: Nitrogen adsorption isotherm for MCM-41-FA

The SEM of the MCM-41-FA material shows a solid rock-like morphology, see Figure 5.23, while the TEM analysis, Figure 5.24, showed the material to be porous but there

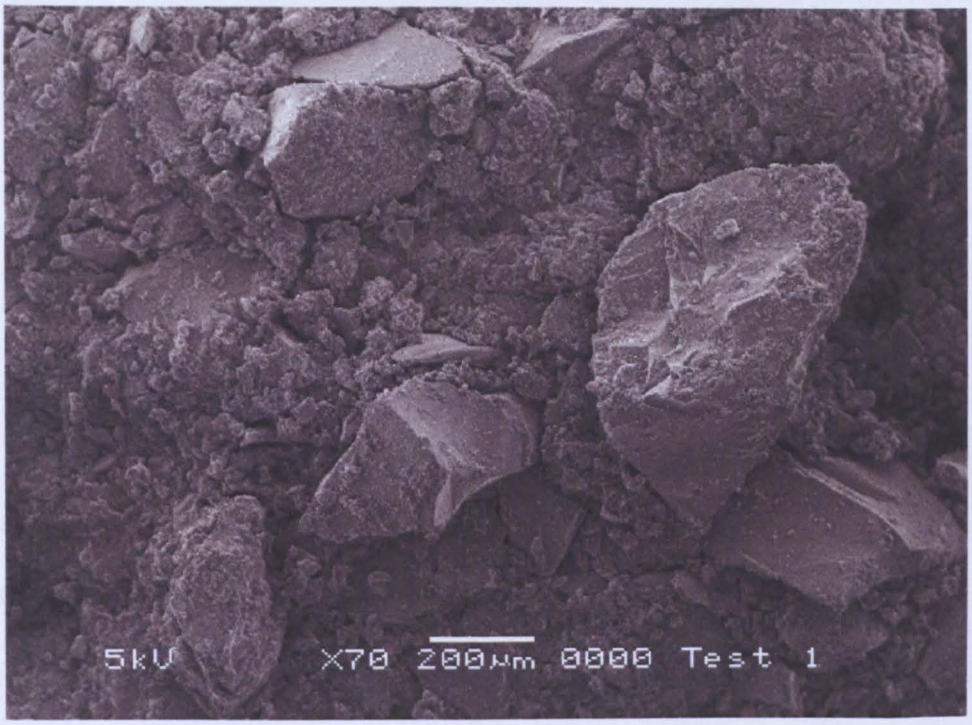

Figure 5.23: SEM of MCM-41-FA

was no evidence of structural ordering. The pores observed may be as a result of inter-particulate porosity associated with very small particles packed together and the voids between the particles appear as pores.

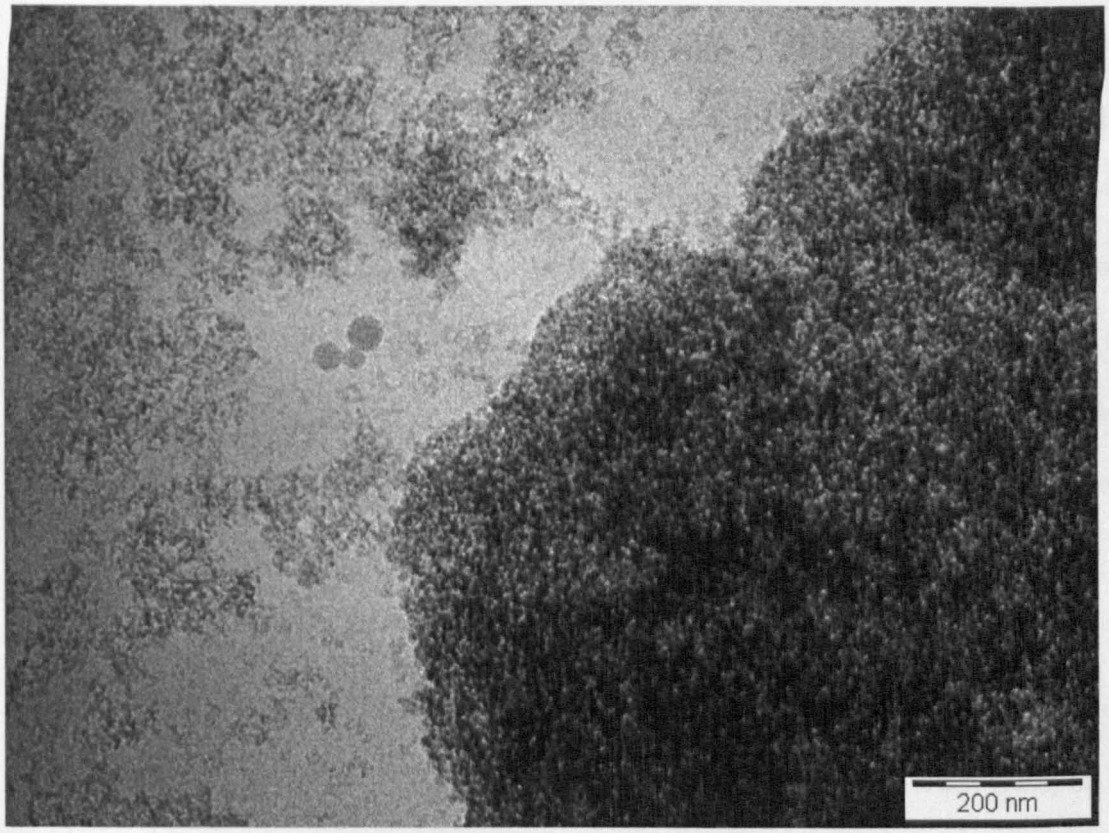

Figure 5.24: TEM of MCM-41-FA

5.5 Conclusion: Alternative synthetic routes to the production of mesoporous silicates

The goal of this synthesis section was to produce mesoporous silicates using alternative synthetic routes from the production of MCM-41. In order for the synthesised materials to be selected for further testing as indoor air pollutant scavengers successful characterisation was required. Successful characterisation included distinct nitrogen isotherms and powder diffraction patterns with typical traits of ordered mesoporous silicates.

The successful production of SBA-15 was evident from each of the techniques used to characterise the material. The presence of microporosity within the pore walls is a key difference between SBA-15 and MCM-41. Therefore SBA-15 was selected as a potential material for an indoor air pollutant scavenger. Although SBA-16 failed to show evidence of structural ordering with cubic symmetry the material was not ruled out as an indoor air pollutant scavenger based on the XRD pattern produced. Furthermore the positive characteristics of high surface area, large pore diameter and pore volume ensured that the material needed to be tested before being eliminated as an unsuitable indoor air pollutant scavenger. The novel silicate material (SM-01) provided an interesting morphology, and despite the lack of mesoporosity, the material was selected for further investigation as an indoor air pollutant scavenger.

The organic modification methods provided mixed results. Based on the elemental analysis, the post synthesis grafting of 3-aminopropyltriethoxysilane on to samples of HMS-Com, MCM-41-MF1 and SBA-15 appeared to be successful as the carbon to nitrogen ratios were close to 3:1. However on close examination of the BET analyses results it was thought that not all the silicate materials may be suitable scavengers. When grafted all the materials showed a decrease in surface area, pore size and pore volume compared to the parent material, a common characteristic when grafting organic moiety on to the surface of mesoporous silicates. However the nitrogen isotherms for HMS-com-PSG and MCM-41-MF1-PSG no longer showed the typical type IV isotherm associated with mesoporous silicates. An extensive characterisation of the post grafted materials was not possible due to the unavailability of the instruments, therefore the materials were selected for further adsorption efficiency testing.

The co-condensation method used to add 3-aminopropyltriethoxysilane to a sample failed to produce a material with definitive mesoporous characteristics. The nitrogen isotherm indicated that relatively little nitrogen was adsorbed compared to previous MCM-41 materials. This material, MCM-41-cocon, was eliminated from any further testing procedures due to the poor characterisation evidence of the presence of mesopores.

Unfortunately the production of mesoporous silicate with organic moieties directed into the pore was deemed unsuccessful. The nitrogen isotherm was not one typically associated with mesoporous materials. It was suspected that the material produced was macroscopic and the surface area small compared to other materials. The ratio of carbon to nitrogen from the elemental analysis had a higher ratio than expected at 4:1, therefore the MCM-41-FA material was no longer investigated as a potential indoor air pollutant scavenger.

Overall 6 materials were thought to possess mesoporous characteristics and therefore these materials were of interest as potential air pollutant scavengers. The selected materials were tested for their adsorption efficiency as an indoor air pollutant scavenger using generated environments containing VOCs and formaldehyde.

5.6 References

1 D. Zhao, Q. S. Huo, J. L. Feng, B. J. Chmelka, and G. D. Stucky, *Journal Of The American Chemical Society*, 1998, **120**, 6024.

2 D. Y. Zhao, J. L. Feng, Q. S. Huo, N. Melosh, G. H. Fredrickson, B. F. Chmelka, and G. D. Stucky, *Science*, 1998, **279**, 548.

3 R. Ryoo, C. H. Ko, M. Kruk, V. Antochshuk, and M. Jaroniec, *Journal Of Physical Chemistry B*, 2000, **104**, 11465.

4 A. Galarneau, N. Cambon, F. Di Renzo, R. Ryoo, M. Choi, and F. Fajula, *New Journal Of Chemistry*, 2003, **27**, 73.

5 A. Galarneau, N. Cambon, F. Di Renzo, and F. Fajula, *Langmuir*, 2001, **17**, 8328.

6 M. Kruk, M. Jaroniec, C. H. Ko, and R. Ryoo, *Chemistry Of Materials*, 2000, **12**, 1961.

7 D. Perez-Quitanilla, I. del Hierro, M. Fajardo, and I. Sierra, *Journal Of Materials Chemistry*, 2006, **16**, 1757.

8 A. M. Liu, K. Hidajat, S. Kawi, and D. Y. Zhao, *Chemical Communications*, 2000, 1145.

9 S. J. Bae, S.-w. Kim, T. Hyeon, and B. M. Kim, *Chemical Communications*, 2000, 31.

10 B. Coasne, A. Galarneau, F. Di Renzo, and R. J. M. Pellenq, *Langmuir*, 2006, **22**, 11097.

11 B. Lindlar, A. Kogelbauer, P. J. Kooyman, and R. Prins, *Microporous And Mesoporous Materials*, 2001, **44**, 89.

12 J. Fan, C. Z. Yu, L. M. Wang, B. Tu, D. Y. Zhao, Y. Sakamoto, and O. Terasaki, *Journal Of The American Chemical Society*, 2001, **123**, 12113.

13 K. M. Ryan, N. R. B. Coleman, D. M. Lyons, J. P. Hanrahan, T. R. Spalding, M. A. Morris, D. C. Steytler, R. K. Heenan, and J. D. Holmes, *Langmuir*, 2002, **18**, 4996.

14 T. Linssen, K. Cassiers, P. Cool, and E. F. Vansant, *Advances In Colloid And Interface Science*, 2003, **103**, 121.

15 T.-W. Kim, R. Ryoo, M. Kruk, K. P. Gierszal, M. Jaroniec, S. Kamiya, and O. Terasaki., *Journal Of Physical Chemistry B*, 2004, **108**, 11480.

16 J. P. Hanrahan, M. P. Copley, K. M. Ryan, T. R. Spalding, M. A. Morris, and J. D. Holmes, *Chemistry Of Materials*, 2004, **16**, 424.

17 J. P. Hanrahan, M. P. Copley, K. J. Ziegler, T. R. Spalding, M. A. Morris, D. C. Steytler, R. K. Heenan, R. Schweins, and J. D. Holmes, *Langmuir*, 2005, **21**, 4163.

18 Y. Ueno, T. Horiuchi, A. Tate, O. Niwa, H.-s. Zhou, T. Yamada, and I. Honma, *New Journal Of Chemistry*, 2005, **29**, 504.

19 V. Escax, E. Delahaye, M. Imperor-Clerc, P. Beaunier, M.-D. Appay, and A. Davidson, *Microporous And Mesoporous Materials*, 2007, **102**, 234.

20 C. Lesaint, B. Lebeau, C. Marichal, and J. Patarin, *Microporous and Mesoporous Materials*, 2005, **83**, 76.

21 Ö. Kaftan, M. Açikel, A. E. Eroğlu, T. Shahwan, L. Artok, and C. Ni, *Analytica Chimica Acta*, 2005, **547**, 31.

22 M. H. Lim and A. Stein, *Chemistry of Materials*, 1999, **11**, 3285.

23 K. Y. Ho, G. McKay, and K. L. Yeung, *Langmuir*, 2003, **19**, 3019.

24 D. Brunel, *Microporous and Mesoporous Materials*, 1999, **27**, 329.

25 A. Cauvel, G. Renard, and D. Brunel, *Journal of Organic Chemistry*, 1997, **62**, 749.

26 T. Yokoi, H. Yoshitake, and T. Tatsumi, *Journal Of Materials Chemistry*, 2004, **14**, 951.

27 A. Walcarius and C. Delacôte, *Analytica Chimica Acta*, 2005, **547**, 3.

28 G. Zhu, Q. Yang, D. Jiang, J. Yang, L. Zhang, Y. Li, and C. Li, *Journal Of Chromatography A*, 2006, **1103**, 257.

29 Z. Luan, J. A. Fournier, J. B. Wooten, and D. E. Miser, *Microporous And Mesoporous Materials*, 2005, **83**, 150.

30 H. P. Lin, L.-Y. Yang, C. Y. Mou, S. B. Liu, and H.-K. Lee, *New Journal of Chemistry*, 2000, **24**, 253.

31 Y. D. Xia and R. Mokaya, *Journal Of Materials Chemistry*, 2004, **14**, 2507.

32 T. Asefa, M. Kruk, N. Coombs, H. Grondey, M. J. MacLachlan, M. Jaroniec, and G. A. Ozin, *Journal Of The American Chemical Society*, 2003, **125**, 11662.

33 S. L. Burkett, S. D. Sims, and S. Mann, *Chemical Communications*, 1996, 1367.

34 D. J. Macquarrie, *Chemical Communications*, 1996, 1961.

35 C. E. Fowler, S. L. Burkett, and S. Mann, *Chemical Communications*, 1997, 1967.

36 D. J. Macquarrie, D. B. Jackson, J. E. G. Mdoe, and J. H. Clark, *New Journal of Chemistry*, 1999, **23**, 539.

37 S. Hamoudi, S. Royer, and S. Kaliaguine, *Microporous and Mesoporous Materials*, 2004, **71**, 17.

38 D. B. Jackson, D. J. Macquarrie, and J. H. Clark, 'Organic modification of Hexagonal Mesoporous silicas', in '*Supported Catalysts and their Applications*', ed. D. C. Sherrington and A. P. Kybett, Royal Society of Chemistry, Cambridge, 2001, p203

39 D. J. Macquarrie, *Green Chemistry*, 1999, 195.

40 S. Hall, C. E. Fowler, B. Lebeau, and S. Mann, *Chemical Communications*, 1999, 201.

41 M. Sasidharan, N. K. Mal, and A. Bhaumik, *Journal Of Materials Chemistry*, 2007, **17**, 278.

42 T. Yokoi, H. Yoshitake, T. Yamada, Y. Kubota, and T. Tatsumi, *Journal Of Materials Chemistry*, 2006, **16**, 1125.

43 F. Rouquerol, J. Rouquerol, and K. Sing, '*Adsorption by powders and porous solids: principles, methodology and applications*', Academic Press,London, 1999.

6 MESOPOROUS SILICATES AS INDOOR AIR POLLUTANT SCAVENGERS

Previous areas of the research project focussed on two objectives. First the generation of stable polluted environments and the methods used to detect and quantify VOCs and formaldehyde, see Chapter 3. Second was the synthesis of mesoporous silicates with the physical characteristics that had the potential to become indoor air pollutant scavengers. The remainder of the project focussed on assessing the adsorption capabilities of a selection of synthesised sorbents for VOCs and formaldehyde.

6.1 Introduction to mesoporous silicates as adsorbents

Mesoporous sorbents have been developed as adsorbents for a range of different processes.

6.1.1 Mesoporous silicates as water pollutant scavengers

Boron removal from waters has been achieved using modified MCM-41.[1] Using the PSG method, propyl bromide was grafted onto the surface and was subsequently reacted with N-methylglucamine to produce a tertiary amine. To test the adsorption, the modified MCM-41 was added to an aqueous solution containing 10 mg L^{-1} of boron for 30 minutes. The silicate recovered was analysed by inductively coupled plasma optical emission spectroscopy and the sorption efficiency for the silicate containing 1.5 mmol g^{-1} of propyl bromide was shown to be higher than the alternative unmodified commercial resin Amberlite IRA 743. The modified silicate was shown to extract almost 100 % of the boron (using 200 mg of sorbent) while a commercial resin required double the mass to produce the same percentage sorption

efficiency. MCM-41 was also modified to remove dyes from waste water.[2] The material was post synthesis grafted to incorporate amine or carboxylic acid functional groups. The modified materials were used to adsorb Acid blue 25 and Methylene blue from a 100 mL aqueous solution. Amine modified MCM-41 had a higher adsorption capacity for Acid blue 25 than Methylene blue. The adsorption capacity was determined at 250 mg of Acid blue 25 per gram of amine modified MCM-41. Alternatively Methylene blue had a good affinity for the carboxylic acid modified MCM-41. The adsorption capacity was determined at 0.3 mmol of Methylene blue dye per gram of carboxylic acid modified MCM-41.

6.1.2 Mesoporous silicates modified for the adsorption of transition metals

MCM-41 has also been used to adsorb metals as well as organics. Pérez-Quitanilla *et al*[3] investigated the use of modified MCM-41 for the removal of Hg^{2+} from waste water. MCM-41 was post synthesis grafted using a two-step process to add the organo functional group propylsulfanyl pyridine. A sample of 0.2 g of modified MCM-41 material was suspended in 30 mL of aqueous solution. A 5 mL solution of Hg^{2+} 0.1M was added to the mixture. The sorbent was removed by filtration and the remaining Hg^{2+} concentration in the solution was analysed. The adsorption capacity of the material was determined to be 0.12 mmol of Hg^{2+} per gram of sorbent. Mesoporous silicates modified with amino groups have been used as ligands to trap Co^{2+} cations in an octahedral complex parallel to the functionalised surface.[4] Unmodified MCM-41 showed negligible adsorption of Co^{2+} while amino functionalised silicas produced via the traditional co-condensation and anionic surfactant co-condensation methods both adsorbed Co^{2+}. When these silicate

materials, containing the same molar ratio of 3-aminopropyltriethoxysilane, were compared, the adsorption of larger amounts of cation occurred on the co-condensation MCM-41 produced via the anionic surfactant method, possibly as a result of the higher content of amino groups on the surface of the material. Amino functionalised silicates have also been used to adsorb Fe^{3+} cations.[5] Co-condensation amino functionalised silicate, molar ratio 0.6 TEOS: 0.4 APTES: 0.12 CTAB: 0.36 TMAOH: 130 H_2O, adsorbed more Fe^{3+} ions at 0.56 mmol g^{-1} compared to 0.27 mmol g^{-1} of Co^{2+}.

Liu *et al*[6] functionalised SBA-15 with 3 mercaptopropyl and 3-aminopropyl through post synthesis grafting. The thiol and amino modified SBA-15 was investigated as a sorbent for Hg^{2+}, Cu^{2+}, Zn^{2+}, Cr^{3+} and Ni^{2+} from waste water. A sorbent mass of 100 mg was used to remove the metal ions with concentration ranges between 10.2 and 5.1 ppm in 10 mL of water. The thiol functionalised SBA-15 removed Hg ions to below the detection limit of the inductively coupled plasma spectroscopy detector, however was ineffective in the removal of the other metal ions under investigation. In comparison the amino functionalised SBA-15 showed the reverse trend to the thiol functionalised SBA-15. The difference in adsorption capacity was based on the formation of stable complexes of the metal ions with the grafted ligands. Softer transition metals, e.g. Hg are prone to form stronger complexes with softer donor ligands, e.g. S, while harder metals, e.g. Cu form stronger complexes amine donors.

In 2006, SBA-15 functionalised with 2-mercaptopyrimidine was tested for the adsorption of cadmium.[7] The maximum adsorption of cadmium was 0.99 mmol g^{-1}

for the modified material compared to 0.04 mmol g^{-1} for the unmodified material. The adsorption efficiency was affected by the pH; at pH's lower than 6 the adsorption was limited, as coordination could only occur through the sulfur atom. Co-ordination was possible through both the sulfur and the nitrogen atom at pH 6, therefore increasing the binding capacity.

6.1.3 Mesoporous silicates as air pollution adsorbents

In 1998 Zhao and co-workers[8] predicted that MCM-41 would be a promising adsorbent for the removal of VOCs as it has a larger pore volume than hydrophobic zeolites and pure-silica ZSM-5. Through the adsorption isotherm of benzene, MCM-41 was shown to have the highest saturation mass at approximately 700 mg g^{-1} while the zeolite and ZSM-5 had saturation masses of 350 and 275 mg g^{-1}, respectively. Similar trends were seen with carbon tetrachloride and *n*-hexane. When adsorption isotherms were determined with water MCM-41 had a significantly bigger saturation mass at approximately 800 mg g^{-1} while for the zeolite and ZSM-5 the adsorption saturation mass was less than 200 mg g^{-1}. This was thought to be a potential problem when sampling VOC's from environments with a high relative humidity. Serrano and co-workers[9] have shown that through modification of the synthesis procedure MCM-41 materials may exhibit different organophilic and hydrophobic properties which influence the adsorption behaviour for VOC removal. MCM-41 materials produced via the sol-gel method (without an oven heating step) gave higher adsorption masses and adsorption strength for toluene. Recently[10] MCM-41 synthesised with a pore size of 29 Å has been used to trap VOC's, with carbon ranges from 3-12 (including toluene, ethylbenzene, o-xylene and cumene) from the air. MCM-41 was packed into sampling tubes and retained using glass wool. Glass

beads were used to enhance the polluted air flow through the sampling tube by inter dispersing the fine silica powder. The VOC's absorbed onto the MCM-41 were then desorbed and analysed via a TDU-GC-MS. MCM-41 preferentially absorbed larger VOC's, typically larger than C_8. The trapping ability for smaller molecules within the range of C_3-C_5 was poor.

When Serrano and co-workers[9] studied SBA-15 as an adsorbent for toluene they noted that SBA-15 adsorbs a lower amount of toluene compared to MCM-41 produced under various different methods. However the temperature at which desorption occurs was higher than the MCM-41 sorbents indicating a higher strength of adsorption. This higher desorption temperature was linked to the higher temperature release of toluene in the micropores compared to the toluene released from the mesopores. The lower amount of toluene adsorbed was directly linked to the limited micropores available for adsorption.

Unmodified SBA-15 has been shown to have a preferential adsorption rate for CO_2 over CH_4 and N_2.[11] This preferential adsorption results in SBA-15 separating CO_2 from a gas stream containing CH_3 and N_2. Aminosilane functionalised SBA-15 has also been investigation for the adsorption of CO_2[12] where various aminosilanes were grafted onto SBA-15. When the SBA-15 was functionalised with 3-aminopropyltriethoxysilane the adsorption capacity for CO_2 increased from 0.05 to 0.15 mmol g^{-1}. When the amino content increased, the amount of CO_2 adsorbed increased, e.g. 0.15 to 0.52 mmol g^{-1}. Hiyoshi *et al*[12] suggested that the adsorption of CO_2 onto the SBA-15 resulted in the production of an alkylammonium carbamate,

see Figure 6.1. Interestingly the adsorption capacity of the sorbents were not effected by the presence or absence of water.

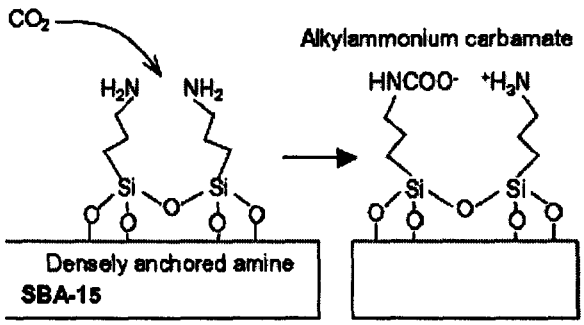

Figure 6.1: Adsorption of CO_2 onto densely situated amine functionalised SBA-15 to produce alkylammonium carbamate.[12]

SBA-16 functionalised with N'-[3-(trimethyoxysilyl)propyl] ethylenediamine has also been used successfully for the adsorption of CO_2, at a pressure of 30 bar, with an adsorption capacity of 6 mmol g^{-1}.[13]

Ueno and coworkers[14] have investigated the adsorption characteristics of SBA-15 for the aromatic hydrocarbons toluene and benzene. When a calcination temperature of 773 K was used the resulting SBA-15 showed an absorption selectivity for benzene over toluene. The selectivity was a result of the uniform micropore distribution created at the calcination temperature of 773 K. The micropores were suitable for the adsorption of benzene and not the larger toluene molecule, therefore micropore structure can exhibit selectivity of aromatic hydrocarbon gases. However in this study further investigation was required to determine the effect of non-bonding interactions.

In 2007 Kosuge *et al*[15] investigated the effect of pore structure of mesoporous silicas on the adsorption of VOCs. Kosuge determined that the presence and number of

micropores were essential contributing factors to achieving a large VOC adsorption capacity. The adsorption capacity of toluene and benzene was directly compared for MCM-41 and SBA-15. The SBA-15 was prepared under three different methods to induce different extents of microporosity and various morphologies. The adsorption behaviour was investigated by looking at the breakthrough curves produced from a mixed gas flow of 500 ppm. For SBA-15 with a fibre like morphology breakthrough was noted after 60 min for toluene and 20 min for benzene, while MCM-41 breakthrough occurred after 20 and 5 min, respectively. The SBA-15 materials prepared with rod like morphology showed similar trends to that of MCM-41. MCM-41 had a lower breakthrough capacity despite its larger pore volume of 0.75 mg g^{-1} and surface area of 1154 m^2 g^{-1}, compared to 0.63 mg g^{-1} and 730 m^2 g^{-1} of the fibre like SBA-15. Kousuge states that "the presence of micropores directly leads to an increase in the dynamic capacity for these VOCs and is therefore an essential factor in determining the dynamic capacity of the adsorbents".

6.2 Experimental: Investigation of synthesised sorbents as indoor air pollution scavengers

To identify the synthesised sorbent suitable for the application of an indoor air pollutant scavenger, a range of testing was carried out through the use of polluted environments.

6.2.1 Materials to be examined as indoor air pollutant scavengers

A selection of the materials prepared in Chapters 4 and 5 were selected, based on their favourable physical characteristics, for further testing as indoor air pollutant scavengers. A summary of the materials selected and preparation methods used are

given in Table 6.1. Atmospheric chambers were used to create VOC and formaldehyde environments for testing, (see Section 2.1). The VOC environment was created using four in-house permeation vials as described in Section 3.2.5. To create the formaldehyde environment a second similar independent chamber was set up with a conventional commercial formaldehyde permeation vial as the pollutant source.

6.2.1.1 Packing of materials for efficiency testing

In order to actively sample from the polluted chambers it was essential that the sorbents were suitably packaged to allow active sampling to occur. The sorbents were packed into glass tubes 10 cm in length with dimensions of 5 mm internal diameter and an 8 mm outer diameter. Each glass tube was packed with 100 mg of sorbent inter-dispersed with 1.5 g of glass beads (750-1000 μm), contained within two plugs of glass wool as shown in Figure 6.2. The glass beads were incorporated within the sampling tubes to reduce the backpressure within the tube and enable the flow rate required. This method of adding glass beads to reduce the impedance in air flow has previously been used by Wu *et al*[10]. Each sorbents' adsorption efficiency was tested using two packed sampling tubes. Blank sampling tubes were prepared in the absence of any sorbent for control measures. Sampling tubes were re-prepared with fresh sorbent for each experiment.

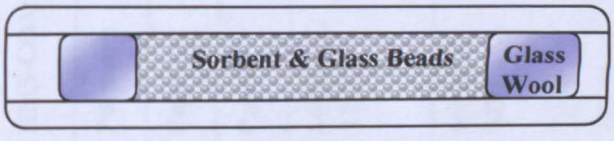

Figure 6.2: Sorbent packed within glass sampling tubes inter-dispersed with glass (750-1000 μm) plugged with glass wool

Table 6.1: Summary of methods used to produce the materials of interest for testing

Sample Number	Preparation Method				Characterisation			
	Synthesis	Hydro thermal	Filtration	Extraction	BET	SEM	TEM	PXRD
HMS-COM	Commercial Products				✓	✗	✗	✗
Puracarb					✗	✗	✗	✗
Purakol					✗	✗	✗	✗
Purafil					✗	✗	✗	✗
MCM-41-S1	4.4g CTAB dissolved in 32g H_2O with 3.5g of TMAOH. Stir 30min. Add 10g of TEOS. Stir for 1h at 38°C	Statically heated to 100 °C for 24 h in a steel bomb	No Filtration	1g refluxed in 25mL HCl in 300mL EtOH for 24 h	✓	✓	✓	✓
MCM-41-MF1	4.4g CTAB dissolved in 32g H_2O with 3.5g of TMAOH. Stir 30min. Add 10g of TEOS. Stir for 1h at 38°C	Statically heated to 100 °C for 24 h in a sealed Teflon bottle	No Filtration	Calcined at 500 °C in a muffle furnace for 24 h	✓	✗	✗	✓
MCM-41-MF2	2.41g of CTAB dissolved in 116g of Water at 35 °C. 13.5mL of 1M TMAOH stirred for 1 h. 10g of TEOS added over 10min	Statically heated to 100 °C for 24 h in a sealed Teflon bottle	Filtered and washed with 100mL H_2O	Calcined at 500 °C in a muffle furnace for 24 h	✓	✗	✗	✓

Table 6.1 : continued

Sample Number	Preparation Method				Characterisation			
	Synthesis	Hydro thermal	Filtration	Extraction	BET	SEM	TEM	PXRD
SBA-15	4 g P123, 120 mL 2M HCl, 60 mL H_2O, 330 rpm at rm tp (until dissolved). Heat to 40 °C , 11.3 g TEOS	24 h at 40 °C (Static) 5days at 60 °C	Filter. Wash with H_2O. Dry overnight at 60 °C.	Calcined in air at 550 °C for 24 h	✓	✓	✓	✓
SBA-16	5 g F127, 1 g P123, 280 mL 1.6 M HCl, 22 g TEOS, Stir 15 min at 400 rpm.	24 h at 35 °C (Static) 5days at 100 °C	Filter. Oven dried over night at 60 °C. Filter & Wash EtOH	Calcined in air at 550 °C for 24 h	✓	✓	✗	✓
Sphere Material	500 mL MeOH, 88 mL H_2O 1.25 g CTAB, 32 mL NH_4OH, 8 mL TEOS	24 h at 16 °C	Filtered and washed with MeOH. Air dried overnight	Calcined in air at 550 °C for 24 h	✓	✓	✗	✓
	Synthesis	Modification Method						
HMS-Com -PSG	Commercial Product	0.5g of material added to 50mL dry Toluene with 4.6 g 3-APTEOS. Refluxed for 24 h under N_2. Soxhlet washed in 100mL dimethyl ether and dichloromethane under N_2 for 24 h			✓	✗	✗	✗
MCM-41-MF1- PSG	As MCM-41-MF1				✓	✗	✗	✗
SBA-15 PSG	As SBA-15				✓	✗	✗	✗

N/A- Characterisation absent due to instrument unavailability

6.2.2 The preparation of contaminated environments

The dynamic VOC chamber was set up as outlined in Section 2.2. Permeation vials were used as pollutant sources for toluene, ethylbenzene, cumene and DCB as described in Section 3.2.5. The permeation oven temperature was set at 25 °C with an oven flow of 200 mL min^{-1}. The relative humidity within the chamber was set at zero. The VOC chamber was actively sampled using Tenax TA filled thermal desorption tubes at a rate of 100 mL min^{-1} for 8 minutes. The formaldehyde atmosphere was generated inside an identical 20 L Perspex chamber, outlined in Section 2.2. The commercial permeation tube used to create the formaldehyde concentration stream has an emission rate (E_R) of 981 ng min^{-1} and a K_o value of 0.746 L g^{-1}. The chamber conditions were set with a oven temperature of 80 °C and a flowrate of 0.2 L min^{-1} with a 0.1 L min^{-1} relative humidity flow. The theoretical concentration within the chamber was calculated using Equation 2.5 at 4478 μg m^{-3}. To determine the concentration of the formaldehyde chamber C_{18} cartridges loaded with 2,4-DNPH were used to actively sample the chamber at a rate of 50 mL min^{-1} for 40 minutes.

6.2.2.1 Determination of formaldehyde vapour concentration

The solution used to trap formaldehyde consisted of 0.1g recrystallised 2,4-DNPH (Aldrich, Gillingham, UK) dissolved in 49.5 mL acetonitrile (HPLC grade, Sigma Aldrich, Steinheim, Germany) and 0.5 mL orthophosphoric acid (BDH Laboratory supplies). Immediately before sampling each cartridge was flushed with 10 mL of acetonitrile and air-dried. The Sep Pak C_{18} cartridge (Waters Corporation, 34 Maple Street, Massachusetts) was then loaded with 2 mL of 2,4 DNPH solution, at a rate of 1 mL min^{-1}, and dried for 10 min under a stream of nitrogen. After sampling was

completed each cartridge was immediately eluted with 5 mL of acetonitrile. The solutions were analysed by HPLC consisting of a Jasco PU-980 Intelligent Pump and a Jasco UV-975 Intelligent UV/VIS detector. Injections were made manually through a rheodyne valve with a 10 μl injection loop. The peak area results were printed on a ChromJet integrator. A calibration graph was produced using 2, 4, 8, 12, 16, & 20 ng μL^{-1} F-DNPH standards (Aldrich, Milwaukee, US) in acetonitrile, created from a 200 ng μL^{-1} stock solution. The mobile phase used was acetonitrile:water at a ratio of 40:60. A flow of 1.5 mL min^{-1} was passed through an APEX II ODS C_{18} column, 15 cm in length with a 4.6 mm internal diameter. The concentration of F-DNPH present from the eluted C_{18} cartridges was determined from the calibration graphs.

6.2.2.2 Stability of formaldehyde atmospheric chamber

The stability of formaldehyde concentration produced by the commercial permeation tube was assessed over 4 days. Although the permeation tube had a calibrated emission rate of 981 ng min^{-1} this was most likely inaccurate as it was no longer within its calibration period. In order to increase the emission rate of the tube the oven temperature was increased from 70 °C to 80 °C. C_{18} cartridges loaded with 2,4-DNPH were used to sample the formaldehyde chamber at a flow rate of 50 mL min^{-1} for 40 min. The experimental chamber concentration was calculated to be approximately 1470 μg m^{-3} ± 6.8 % RSD, whereas the theoretical concentration, with the oven temp set at 70 °C, was 4478 μg m^{-3}. From the average chamber concentration detected, the emission rate of the permeation tube was estimated to be 482 ng min^{-1}, approximately half the original value. The formaldehyde chamber stability was thought to be suitable for the determination of adsorption efficiency of

the sorbents, with replicate measurements of concentration (n equal to 14) giving an RSD value less than 7 %.

6.2.3 Calculation of adsorption efficiency for volatile organic compounds, or formaldehyde, extracted from polluted air

Evaluation of the pollutant stream concentration was critical in the determination of the adsorption efficiency of the synthesised sorbents. To test the adsorption efficiencies of synthesised materials for the target pollutants the following steps (a-c) were adopted.

a) First the dynamic sampling chamber, described in Section 3.2.5, was used to generate a known concentration of VOCs or formaldehyde. The atmospheres were then actively sampled, using specific flow rates and sampling times, onto Tenax tubes or modified C_{18} cartridges, respectively. Sampling tubes were then analysed to determine the mass of the pollutants trapped by the sampling tube. These masses will be referred to as '$mass_A$'

b) The dynamic sampling system was then modified by placing the material to be tested in the outlet flow immediately before the Tenax sampling tube or modified C_{18} cartridge (see Figure 6.3). The sampling procedure described above was then repeated. Sampling tubes were again analysed and the mass of pollutants trapped by the sampling tubes is denoted '$mass_B$'.

c) Finally the sorbents were removed from the outlet flow and the sampling experiment was repeated for a third time as described in (a) above. Trapped masses will be referred to as '$mass_C$'

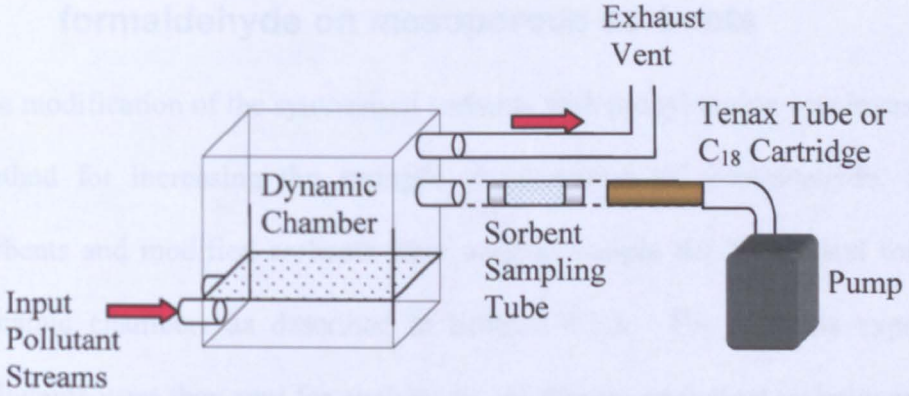

Figure 6.3: Sampling set up to test the adsorption efficiencies of the selected sorbents

To determine the percentage adsorption of pollutant mass retained by the sorbent (the percentage adsorption efficiency) the following calculation was used

$$\%\,\text{Sorbent Efficiency} = \left(1 - \left(\frac{\text{mass}_B}{\frac{1}{2}(\text{mass}_A + \text{mass}_C)}\right)\right)100$$

Equation 6.1

The VOC chamber was sampled for 8 minutes using a flow rate of 100 mL min^{-1} through both the sorbent sampling tube and Tenax tube. The flow rate and sampling time used to determine the formaldehyde efficiency was altered to 50 mL min^{-1} and 40 minutes, respectively. Each sorbent was independently assessed for their adsorption efficiency of the selected VOCs and formaldehyde. In addition to synthesised materials previously mentioned, three commercially available sorbents

known as Puracarb, Purakol and Purafil (Purafil, 2654 Weaver Way, Georgia, U.S.A.) were also investigated for their adsorption properties.

6.2.4 Preliminary investigation into adsorption mechanism of formaldehyde on mesoporous sorbents

The modification of the synthesised sorbents with propyl amine was investigated as a method for increasing the strength of adsorption of formaldehyde. Synthesised sorbents and modified sorbents were used to sample the VOCs and formaldehyde dynamic chambers as described in Section 6.2.3. The sorbents exposed to the pollutants were then sent for analysis by the thermo analytical techniques of thermal volatisation analysis mass spectrometry (TVA-MS) and thermo gravimetric analysis mass spectrometry (TGA-MS). Attempts were made to identify the mechanism of adsorption of the sorbent, however the results proved inconclusive. Therefore a preliminary experimental method was developed in-house to help investigate the strength of adsorption of formaldehyde on the synthesised sorbents.

To compare the adsorption strength of modified and unmodified mesoporous silicates for formaldehyde, the following steps (a-c) were adopted.

a) First a formaldehyde sampling chamber, described in Section 3.2.5, was generated. The atmosphere was then actively sampled with a modified C_{18} cartridge at a rate of 50 mL min^{-1} for 40 min. The cartridge was then eluted with 5 mL of acetonitrile and analysed by HPLC as described in Section 6.2.2.1. The mass of formaldehyde trapped by the cartridge was then calculated and will be referred to as '$mass_D$'.

b) The formaldehyde sampling system was then modified by placing either a packed sampling tube of SBA-15 or SBA-15-PSG in the outlet flow immediately before the modified C_{18} cartridge (see Figure 6.3). The sampling procedure and analysis described above was then repeated. The mass of formaldehyde trapped by the modified C_{18} cartridge was denoted '$mass_E$'. To determine the mass on the sorbent, $mass_F$, the following Equation 6.2 was used.

$$\text{Formaldehyde mass on sorbent } (mass_F) = mass_D - mass_E$$

Equation 6.2

c) Each of the packed and sampled sorbent tubes was then further 'backflushed' under a reverse flow of nitrogen through the sorbent at rate of approximately 100 mL min^{-1} for a period of 20 minutes, where any *exiting formaldehyde* from the sorbent was trapped by a fresh C_{18} cartridge, as shown in Figure 6.4. These secondary C_{18} cartridges were eluted with 5 mL of acetonitrile and analysed with HPLC to determine the mass of formaldehyde on the cartridge ($mass_G$) and therefore the formaldehyde retained by the sorbent ($mass_H$) was determined using Equation 6.3.

$$\text{Mass retained by sorbent } (mass_H) = mass_F - mass_G$$

Equation 6.3

The greater the mass of formaldehyde retained by the sorbent after the backflushing was indicative of a greater strength of adsorption of formaldehyde by the sorbent.

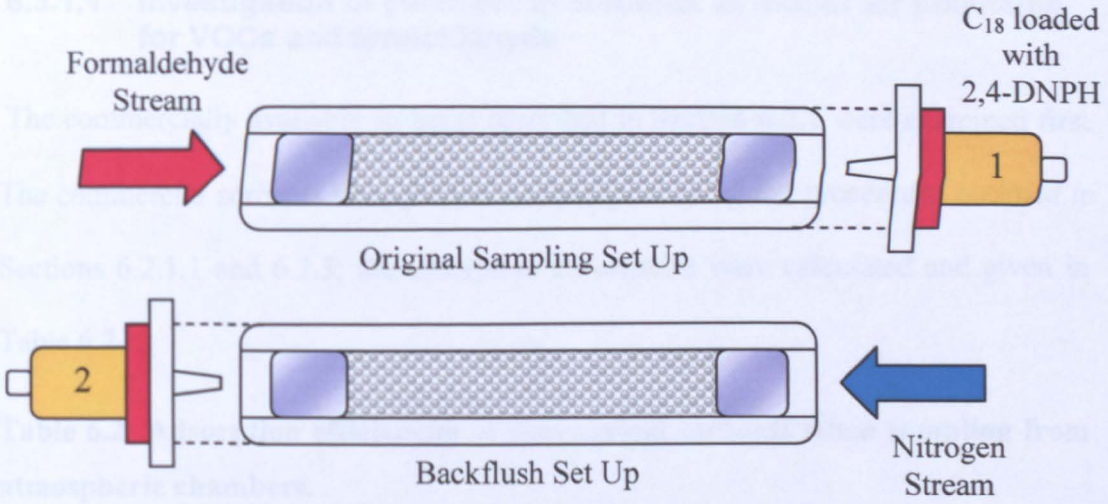

Figure 6.4: Sampling set up schematic to investigate the strength of formaldehyde adsorption.

6.3 Results: Development of an indoor air pollutant adsorbent

6.3.1 Determination of sorbent efficiency for volatile organic compounds or formaldehyde extracted from polluted air

Selected sorbents, listed in Table 6.1, were tested for their adsorption efficiency for VOCs and formaldehyde. Each sorbent was packed into glass sampling tubes as described in Section 6.2.1.1, and placed in a sampling stream containing either formaldehyde or VOCs. Before the sorbents were tested a tube containing glass beads was placed inline in the system. It was shown that neither formaldehyde nor any of the VOCs studied were adsorbed onto the control glass beads, therefore the adsorption efficiencies calculated for tested sorbents were solely attributed to the sorbents themselves.

6.3.1.1 Investigation of commercial sorbents as indoor air pollutants for VOCs and formaldehyde

The commercially available sorbents described in Section 6.2.1 were examined first. The commercial sorbents were packed and sampled using the procedures outlined in Sections 6.2.1.1 and 6.2.3; the adsorption efficiencies were calculated and given in Table 6.2.

Table 6.2: Adsorption efficiencies of commercial sorbents when sampling from atmospheric chambers.

Commercial Sorbent	% Adsorption Efficiency				
	Formaldehyde	Toluene	Ethyl-benzene	Cumene	DCB
Puracarb	72.0	99.9	100.0	100.0	100.0
Purakol	76.1	100.0	100.0	100.0	100.0
Purafil	83.5	4.0	17.7	38.2	8.2

Purcarb's active ingredient is potassium hydroxide and is generally used for the removal of hydrogen sulfide gas via chemisorption.[16] Therefore it was surprising that it adsorbed the VOCs at 100 % and had reasonable formaldehyde adsorption efficiency at 72.0 %. Purakol is a premium grade activated carbon that can adsorb hydrocarbons, nitrogen oxides and volatile organic compounds. Unsurprisingly the Purakol absorbed the VOC's at 100 % efficiency. The adsorption of formaldehyde was 76.1 %. Purafil removes sulfur oxides, organic acids and aldehydes by chemisorption with impregnated potassium permanganate. This explains why Purafil had the highest commercial sorbent adsorption efficiency for formaldehyde at 83.5 %. However Purafil adsorbed the lowest amount of any of the VOCs studied with the highest adsorption efficiency obtained for cumene at less than 40 %. The results indicate that there was no one commercial sorbent with 100 % adsorption efficiency for both formaldehyde and the VOCs studied. Therefore the synthesised

mesoporous silicates were investigated as possible alternatives to the commercial sorbents available. The mesoporous pore size of the silicates makes them ideal for the adsorption of VOCs while the possibility of organo functionality allows the specific targeting of formaldehyde. The adsorption efficiency of the most suitable sorbent produced would ideally have a high adsorption efficiency for both target groups.

6.3.1.2 Investigation of synthesised materials as indoor air pollutant scavengers for VOCs and formaldehyde

A selection of sorbents synthesised in Sections 4 & 5 were chosen to sample VOCs and formaldehyde based on their suitable structural characteristics. Each sample was packed into sampling tubes and used to sample formaldehyde and the VOC chambers independently as outlined in Section 6.2.3. The adsorption efficiencies calculated are displayed in Table 6.3.

The adsorption efficiencies of HMS-COM for the indoor air pollutants was between 97.6-100 % for the VOCs while the adsorption efficiency for formaldehyde was less than 25 %. This high VOC adsorption efficiency of between 98.0-100 % was also obtained for MCM-41-MF1 and SBA-15. However unlike HMS-Com the adsorption efficiency for formaldehyde using the synthesised mesoporous silicates of MCM-41-MF1 and SBA-15 was much improved at 83.1 and 95.1 %, respectively. The material SM-01 had a high adsorption efficiency for the VOCs selected however none of the adsorption efficiencies were determined at 100 % and the adsorption efficiencies were lower than for MCM-41 and SBA-15.

Table 6.3: Adsorption efficiencies of a selected range of mesoporous silicates used to sample polluted environments

Sorbent	% Adsorption efficiency of sorbents				
	Toluene	Ethyl-benzene	Cumene	DCB	Formaldehyde
HMS-COM	97.5	99.9	100	100	23.2
MCM-41-S1	n.a.f	n.a.f	n.a.f	n.a.f	n.a.f
MCM-41-MF1	98.0	99.9	100	100	83.1
MCM-41-MF2	n.a.f	n.a.f	n.a.f	n.a.f	n.a.f
SBA-15	99.6	99.8	100	100	95.1
SBA-16	n.a.f	n.a.f	n.a.f	n.a.f	n.a.f
SM-01	77.2	88.7	94.8	94.2	85.8

n.a.f = no air flow obtained through the sampling tube to allow adsorption efficiency testing to occur.

The corresponding formaldehyde efficiency for SM-01 was similar to the ethylbenzene efficiency at 85.8% and the MCM-41 formaldehyde adsorption efficiency at 83.1 %. From these results the indication was that either MCM-41 or SBA-15 was suitable for the adsorption of VOCs and formaldehyde. However problems were noted for a number of sorbents tested where it was impossible to achieve an air flow over the sorbent (indicated by 'n.a.f' in Table 6.3). It was therefore imperative that a method was created to increase the particle size of the sorbents used for air sampling purposes.

6.3.2 Improved design for the flow of polluted air through mesoporous silicates

To overcome the aforementioned sampling difficulties selected sorbents were pressed into pellets, using a hydraulic press and half inch die at a load pressure of 25 tonnes for 5 min. The pellets were subsequently crushed with a mortar and pestle and

sieved with mesh sizes of 300 and 425 μm and the sorbents were re-examined for formaldehyde and VOC adsorption under identical conditions as the previous testing method. The results are given in Table 6.4.

Table 6.4: Adsorption efficiency for sorbents with particle sizes 300-425 μm

Sorbent	% Adsorption Efficiency				
	Toluene	Ethyl-benzene	Cumene	DCB	Formaldehyde
HMS-COM	94.0	99.9	100.0	100.0	N/A
MCM-41-S1	42.4	68.8	83.9	85.1	N/A
MCM-41-MF1	98.0	99.0	99.4	99.6	78.5
MCM-41-MF2	86.2	98.6	99.6	99.8	92.7
SBA-15	88.6	99.7	100.0	100.0	94.0
SBA-16	92.8	100.0	100.0	100.0	82.5
SM-01	92.8	98.0	99.0	99.5	93.9

N/A – no analysis results due to sorbent shortage for secondary analysis

The pelletisation, crushing and sieving procedures to produce particle sizes of 300-425 μm solved the problems encountered when trying to draw 50 and 100 mL min^{-1} of air through the sorbent sampling tubes. If this method of sorbent sampling was to be used throughout the rest of the research project as it was important that the method of producing the sorbent with particular sizes of 300-425 μm was not detrimental to the adsorption efficiency of the synthesised sorbents. Comparing the adsorption efficiency for SBA-15 in Table 6.3 with the adsorption efficiency of the 300-425 μm, the difference for each of the VOCs was by less than 1 %, except for toluene which was reduced by 11 %. The reduction of the toluene adsorption efficiency was not in evidence for the other mesoporous silicates, MCM-41-MF1 and SM-01, that were sampled as 300-425 μm and un-pelletised sampling.

From the adsorption efficiency testing investigation of these mesoporous silicates it was apparent that the mesoporous silicates were suitable for the adsorption of indoor air pollutants. It was unpractical to continue testing each of the sorbents in further experiments and therefore one sorbent was selected for continual investigation. To select the sorbent for continual investigation its physical characteristics and adsorption efficiencies for VOCs and formaldehyde were taken into account. MCM-41-S1 and MCM-41-MF1 were eliminated based on their poorer adsorption efficiencies of VOCs and formaldehyde, respectively. SBA-15, MCM-41-MF2, SBA-16 and SM-01 all showed promising adsorption properties and therefore could not be ruled out of the investigation based on these results.

SM-01 had the best adsorption efficiency for VOCs and formaldehyde however the physical characterisation suggests that the material is microporous in nature and no PXRD patterns were observed indicating no long range order. Therefore SM-01 was not investigated further. Due to lack of evidence of long range order SBA-16 was also eliminated at this stage. Based on the literature evidence which suggests the importance of the presence of microporosity within the mesopores for an enhanced adsorption capacity SBA-15 was chosen for future testing over MCM-41-MF2.[9]

6.3.3 Investigation into the use of post synthesised mesoporous silicates as indoor air pollutant scavengers

Surface modification of the silanol groups present on the silicate sorbents was investigated as a possible method to enhance the strength of adsorption of

formaldehyde from the air. Surface modification was attempted through the post grafting synthesis of propyl amine groups onto the silicate as described by the method in Section 5.3.2.1, to produce materials MCM-41-MF1-PSG and SBA-15-PSG. Each of the sorbents were pressed and sieved to produce particle sizes between 300-425 nm and the sorbents were then packed into the glass sampling tubes as described in Section 6.2.1.1. Each of the modified materials was tested for formaldehyde and VOC adsorption using the sampling procedure and chamber set up as outlined in Section 6.2.2 & 6.2.3. The adsorption efficiency for MCM-41-MF1-PSG and SBA-15-PSG for both formaldehyde and VOCs is given Table 6.5.

Table 6.5: Adsorption efficiencies of organically modified synthesised sorbents for indoor air pollutants

Modified Sorbent	% Adsorption Efficiency				
	Toluene	Ethyl-benzene	Cumene	DCB	Form-aldehyde
SBA-15-PSG	-10.8	19.6	38.1	78.6	97.6
MCM-41-MF1-PSG	-44.6	44.0	73.0	92.8	92.2

The adsorption efficiency for ethylbenzene, cumene and DCB was reduced from the unmodified parent materials, which had adsorption efficiencies of approximately 100 %. The increase in the toluene mass trapped on the Tenax was most likely the result of residual toluene used in the modification process. For each of the modified materials the adsorption efficiency for formaldehyde was similar to the adsorption efficiencies gained from the parent material. The results indicate that propyl amine modified mesoporous material is suitable for the adsorption efficiency for formaldehyde however reduced adsorption efficiencies were observed for the

selected VOCs. This reduction may result from the decrease in pore size and pore volume of the mesoporous silicates compared to the original parent silicates.

6.3.3.1 Strength of adsorption of formaldehyde on organically modified mesoporous silica

To compare the adsorption strengths of modified and unmodified mesoporous siliates for formaldehyde, SBA-15 and SBA-15-PSG sampling tubes were prepared and used to sample a formaldehyde environment under previously stated conditions (see Section 6.2.4). C_{18} cartridges were placed immediately after the sorbent tubes to ensure there was no breakthrough of formaldehyde. Both sorbent sampling tubes were then 'backflushed' under a flow of nitrogen at rate of approximately 100 mL min^{-1} for a period of 20 minutes, where any exiting formaldehyde within stream was trapped by a further C_{18} cartridge. Table 6.6 contains the masses of formaldehyde trapped on each C_{18} cartridge.

Table 6.6: Mass trapped on modified and unmodified SBA-15, and the masses of formaldehyde remitted from the sorbent after sampling through backflushing

	Mass of formaldehyde trapped (μg)			
	On C_{18} cartridge	Suspected on sorbent	Re-emitted by sorbent under backflushing	Retained by sorbent after flushing
No Sorbent	9.74	n/a	n/a	n/a
SBA-15	1.25	8.48	6.24	2.24
SBA-15-PSG	0.32	9.43	0.29	9.14

Under the chosen conditions, 9.74 μg of formaldehyde was trapped onto a C_{18} cartridge. When the sorbents SBA-15 or SBA-15-PSG were placed immediately before the C_{18} cartridges and the sampling repeated, the masses of formaldehyde trapped was reduced to 1.25 and 0.32 μg respectively. Therefore the masses of

formaldehyde trapped on the sorbents were calculated to be 8.48 and 9.43 μg, respectively. To asses how strongly bound the formaldehyde was to each sorbent the sorbents were immediately backflushed with nitrogen and the eluents passed over a C_{18} cartridge. The masses trapped by the C_{18} cartridges were 6.24 μg for the SBA-15 sorbent and 0.29 μg for the SBA-15-PSG sample.

6.4 Conclusion: Development of an indoor air pollutant adsorbent

The initial testing regime was flawed due the problems encountered when trying to draw polluted air through some of the fine particulate material produced. In an effort to overcome the air flow problems the preparation method used to pack the sorbent into the sampling tubes was altered. The production of 325-400 μm particulate material from crushed pellets alleviated the air flow problems. From the second set of efficiency testing carried out using the modified packing procedure several of the sorbents were shown to be potential candidates for further investigation as indoor air pollutant scavengers. Based on the adsorption efficiency testing and the physical characterisation of each of the sorbents SBA-15 was selected for further detailed adsorption experiments.

It was hoped that mesoporous silicates modified with propyl amine groups would chemisorb formaldehyde from air. The SBA-15-PSG appeared to absorb the formaldehyde suggesting possible chemisorption. This would provide a very strong pollution adsorbent as formaldehyde would be eliminated from the environment. However toluene, used in the modification procedure, was released from the SBA-15-PSG material. The release of toluene into the environment is undesirable if

the sorbents were to be used to reduce the occurrence of SBS. However if the modified and unmodified materials were used in combination to produce a multi-bed sorbent, where the modified material was placed inline before the unmodified material, then the released toluene would be adsorbed by the unmodified material. Alternatively the solvent used in the method to graft propyl amine to the silicate parent material must be changed or the cleaning stage used after the grafting is completed must be improved to remove the suspected residual toluene within the pores which is released during testing.

6.5 References

1. Ö. Kaftan, M. Açikel, A. E. Eroğlu, T. Shahwan, L. Artok and C. Ni, *Anal. Chim. Acta*, 2005, **547**, 31-41.

2. K. Y. Ho, G. McKay and K. L. Yeung, *Langmuir*, 2003, **19**, 3019-3024.

3. D. Pérez-Quintanilla, I. Del Hierro, M. Fajardo and I. Sierra, *Microporous and Mesoporous Materials*, 2006, **89**, 56-68.

4. T. Yokoi, H. Yoshitake, T. Yamada, Y. Kubota and T. Tatsumi, *Journal Of Materials Chemistry*, 2006, **16**, 1125-1135.

5. T. Yokoi, H. Yoshitake and T. Tatsumi, *Journal Of Materials Chemistry*, 2004, **14**, 951-957.

6. A. M. Liu, K. Hidajat, S. Kawi and D. Y. Zhao, *Chemical Communications*, 2000, 1145-1146.

7. D. Perez-Quitanilla, I. del Hierro, M. Fajardo and I. Sierra, *Journal Of Materials Chemistry*, 2006, **16**, 1757-1764.

8. X. S. Zhao, Q. Ma and G. Q. Lu, *Energy and Fuels*, 1998, **12**, 1051-1054.

9. D. P. Serrano, G. Calleja, J. A. Botas and F. J. Gutierrez, *Industrial & Engineering Chemistry Research*, 2004, **43**, 7010-7018.

10. T.-M. Wu, G.-R. Wu, H.-M. Kao and J.-L. Wang, *Journal of Chromatography A*, 2006, **1105**, 168.

11. X. Liu, J. Li, L. Zhou, D. Huang and Y. Zhou, *Chemical Physics Letters*, 2005, **415**, 198-201.

12. N. Hiyoshi, K. Yogo and T. Yashima, *Microporous And Mesoporous Materials*, 2005, **84**, 357-365.

13. C. Knöfel, J. Descarpentries, A. Benzaouia, V. Zeleňák, S. Mornet, P. L. Llewellyn and V. Hornebecq, *Microporous And Mesoporous Materials*, 2007, **99**, 79-85.

14. Y. Ueno, T. Horiuchi, A. Tate, O. Niwa, H.-s. Zhou, T. Yamada and I. Honma, *New Journal Of Chemistry*, 2005, **29**, 504-508.

15. K. Kosuge, S. Kubo, N. Kikukawa and M. Takemori, *Langmuir*, 2007, **23**, 3095-3102.

16. Purafil®, *Product Selection Guide for Purafil Media*, www.purafil.com/literature/Media%20Application%20Guide.pdf Accessed 17th May 2006.

7 SIMULATED USE OF MESOPOROUS SILICATES SAMPLING INSIDE A CLOSED CABINET

In Chapter 6 preliminary experiments were carried out to identify a suitable mesoporous silicate as an indoor air scavenger. From the adsorption efficiency investigation, in combination with the sorbents characterisation, SBA-15 was selected as the sorbent which showed the most potential as an indoor air pollutant scavenger. To further investigate the suitability of SBA-15 as an indoor air pollutant scavenger a series of experiments were designed to simulate closed environments.

7.1 Experimental: Preparation of simulated environments

To simulate the extraction of pollutants by the sorbents in a real polluted environment a 100 L Perspex chamber was used to contain a low concentration of VOCs. A pump connected to a sampling tube containing SBA-15 was placed inside the 100 L chamber as shown in Figure 7.1.

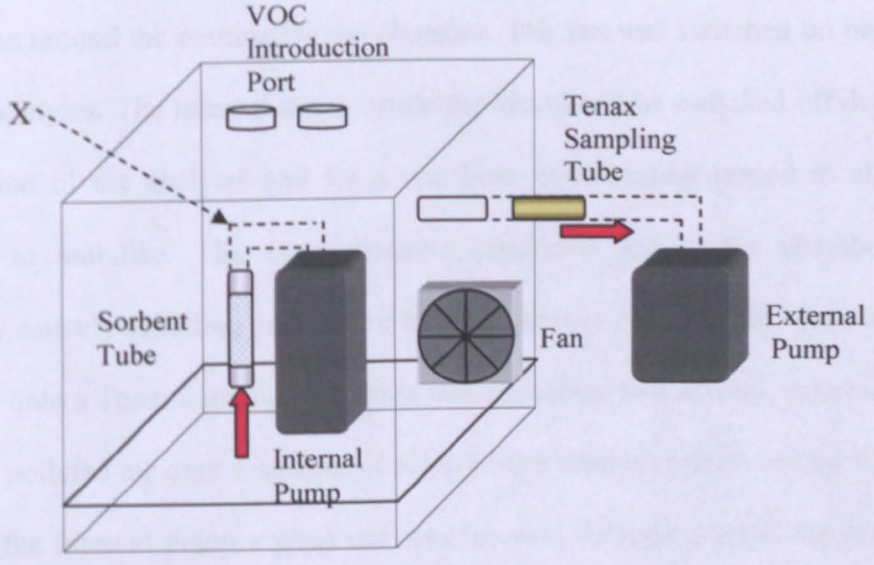

Figure 7.1: Experimental set up for sampling inside a closed environment

The internal pump was set to pull air through the sorbent tube at a flow rate of 100 mL min^{-1}. To create the VOC environment a 20 μL liquid injection volume of each VOC, was added through a sampling port situated on top of the 100 L chamber. The initial VOC concentrations generated are given in Table 7.1. To restrict the loss of analyte through the door seals the edges were coated in Vaseline.

Table 7.1: Theoretical concentrations of VOCs inside the 100L Perspex chamber from VOC injection volumes 20 μL and corresponding theoretical masses trapped on Tenax sampling tube given a sampling time of 10 s at 100 mL min^{-1}

	Theoretical Concentration/μg m^{-3}	Mass trapped on Tenax /μg
Toluene	174 000	2.87
Ethylbenzene	174 000	2.87
Cumene	172 000	2.84
DCB	260 000	4.29

To ensure mixing was achieved inside the 100 L chamber a small d.c. powered fan was added to the chamber before the addition of any VOC analytes. The power cables to the fan exited the chamber via the door, to stop analyte loss the power cables were coated with Vaseline around the entrance to the chamber. The fan was switched on before the addition of analytes. The internal pump inside the chamber was switched off during the initial addition of the analytes and for a one hour equilibration period to allow the atmosphere to stabilise. The concentrations generated inside the chamber were measured by actively sampling 16.7 mL of air, sampling at 100 mL min^{-1} for 10 s, from the chamber onto a Tenax sampling tube that was connected to a second, external pump. To pass the polluted air over a sample of SBA-15 the internal pump was switched on. To activate the internal pump a glass rod was inserted through a small sampling port (1.1 cm dia.) on the roof of the chamber. After the contaminated air passed over the sorbent for 2 hours, active sampling was performed to reassess the pollutant concentration inside the chamber. Any decrease in the pollutant concentrations was

attributed to the successful extraction of analytes onto the sorbent. The internal pump was left to run for 8 hours with reassessment of the pollutant concentrations every 2 hours.

To determine the masses of VOCs trapped on the external Tenax sampling tube a set of three calibration standards were used. Each calibration standard contained the VOCs toluene, ethylbenzene, cumene and DCB at equal concentrations. The standards were prepared in methanol at concentrations levels of 0.1, 0.4 and 1.0 μg μL^{-1}. For calibration 5μL of each standard was injected directly onto individual Tenax tubes, via the direct injection port shown in Figure 3.8 and analysed by TDU-GC-MS. Prior to analysis 5 μL of 0.4 μg μL^{-1} o-xylene was added to each Tenax tube to act as an internal standard in the calibration experiments. Tenax tubes used in the sampling experiments were also spiked with o-xylene prior to analysis.

7.1.1 Simulated environments with reduced volatile organic compounds

An identical 100 L chamber experiment was set up with a reduced VOC concentration using the method discussed in Section 7.1. To create the reduced VOC concentrations the liquid injection volume for each VOC was reduced to 1 μL. The theoretical concentrations generated within the chamber are given in Table 7.2. Due to the reduced chamber concentration the sampling time was increased to 60 s. The theoretical masses trapped by the Tenax are given in Table 7.2.

To determine the mass of VOCs trapped on the external Tenax sampling tube a new set of calibration standards were required. Methanolic standards with concentrations of 25, 44, 77, 130, 160 and 200 ng μL^{-1} were prepared. The internal standard of o-xylene was reduced to 100 ng μL^{-1}.

Table 7.2: Theoretical concentrations of VOCs inside the 100L Perspex chamber from VOC injection volumes 1 μL and corresponding theoretical masses trapped on Tenax sampling tube given a sampling time of 60 s at 100 mL min^{-1}

	Theoretical Concentration /μg m^{-3}	Mass trapped on Tenax /μg
Toluene	8700	0.870
Ethylbenzene	8700	0.870
Cumene	8600	0.860
DCB	13 000	1.284

To determine the mass of VOCs trapped on the external Tenax sampling tube a new set of calibration standards were required. Methanolic standards with concentrations of 25, 44, 77, 130, 160 and 200 ng μL^{-1} were prepared. The internal standard of o-xylene was reduced to 100 ng μL^{-1}.

7.1.2 Passive adsorption

To investigate the effectiveness of SBA-15 as a passive adsorbent a static 20 L atmospheric chamber was used to generate a VOC environment. The chamber was sealed with Vaseline and unused sampling ports were plugged and sealed with Vaseline. A VOC injection volume of 1 μL of each VOC was used to create the atmosphere. The VOC concentration generated inside the 20 L chamber would be approximately five times greater than the previous reduced VOC 100 L chamber experiments, see Table 7.3.

Table 7.3: Theoretical concentrations of VOCs inside the 20L Perspex chamber from VOC injection volumes 1 μL and corresponding theoretical masses trapped on Tenax sampling tube given a sampling time of 10 s at 100 mL min^{-1}

	Theoretical Concentration/μg m^{-3}	Mass trapped on Tenax /μg
Toluene	44 000	0.73
Ethylbenzene	44 000	0.73
Cumene	43 000	0.72
DCB	65 000	1.08

After introduction of the VOC solutions the chamber was left for a further hour to allow the VOC concentrations to equilibrate. The chamber was sampled at 10 s and 100 mL min^{-1} to determine the experimental VOC concentration. A mass of 500 mg of SBA-15 sorbent was then loaded into a passive sampling tube and introduced to the chamber system from a sampling port on the roof of the chamber. After the addition of the SBA-15 sorbent the chamber concentration was measured twice every two hours for a period of 8 hours.

To determine the masses of VOCs trapped by the external Tenax tubes methanolic calibration standards with concentrations of 25, 44, 77, 130, 160 and 200 ng μL^{-1} were used in conjunction with a methanolic o-xylene internal standard of 0.1 $\mu g\ \mu L^{-1}$. The preparation of calibration tubes and spiking of the sampling tubes with the internal o-xylene standard used the direct injection port as described in Section 3.2.4.

7.2 Results: Simulated use of mesoporous silicates sampling inside a closed environment

Two types of experiments were designed to reduce VOC concentrations within a closed environment. The sorbent SBA-15 was used to reduce VOC concentrations in both active and passive mode.

7.2.1 Sampling inside a closed environment

Before a 100 L Perspex chamber could be used to assess the efficiency of selected sorbents as pollutant scavengers (see Section 7.1 and Figure 7.1) the 'goodness' of seal was tested to ensure that any significant loss of analytes during simulated testing was due to the action of the chosen sorbent and not to leakage of the analyte from the closed environment. A polluted environment was created, using the method similar to that of

the bell chamber set up; a four-fold increase in VOC injection volume was used to compensate for the approximate four fold increase in chamber size. Therefore a 20 μL aliquot of each VOC solution was injected into the chamber. During this experiment the internal pump and the sorbent filled sampling tube, shown in Figure 7.1, was omitted. The theoretical concentrations expected from the 20 μL liquid injection volumes are given in Table 7.1. To determine the VOC chamber stability Tenax sampling tubes were used to measure the chamber concentration levels by sampling the chamber from the active sampling port at 100 mL min^{-1} for 10 s. The chamber was monitored at 1, 22 and 48 h after the addition of the VOCs to the system. To determine if there was a chamber leak, the VOC peak areas obtained after the one hour equilibration time were compared to the VOC peak areas obtained after 22 and 48 h and the % loss calculated, the results are given in Table 7.4.

Table 7.4: % Loss of VOCs from 100L chamber over a 48 h period

Time/h	Toluene		Ethylbenzene		Cumene		DCB	
	TIC	SIR	TIC	SIR	TIC	SIR	TIC	SIR
22	-8	-9	-5	+2	-4	-3	-1	-1
48	+9	+14	+2	+1	+1	-2	-6	-10

Over the 48 h the analyte losses were determined to be less than 10 % however, increases in VOC concentration were also noted up to 14 %. This was attributed to the variation in atmospheric concentrations due to room temperature fluctuations.

7.2.1.1 Sampling of a closed environment using glass beads

A control experiment was carried out using the same 20 μL VOC injection volume to create the polluted environment. A sampling tube was prepared containing only glass beads and was connected to the internal sampling pump, as shown in Figure 7.1, see Section 7.1 for the method used to asses the chamber concentration. The theoretical

masses trapped on the Tenax sampling tube are given in Table 7.1. After the chamber was produced and equilibrated it was monitored over 8 h with the external pump and samples were taken from the chamber at 2 h intervals at a sampling rate of 100 mL min^{-1} for 10 s. A set of three calibration standards were used to quantify the masses of analyte trapped on the Tenax sampling tube through use of the direct injection procedure, see Section 3.2.4. The concentrations of VOCs used in the direct injection standards were 0.1, 0.4 and 1.0 μg μL^{-1}, made in methanol; 5 μL of each calibration standard was used to load Tenax tubes. The experimental mass trapped on each Tenax tube at each time interval is shown Figure 7.2.

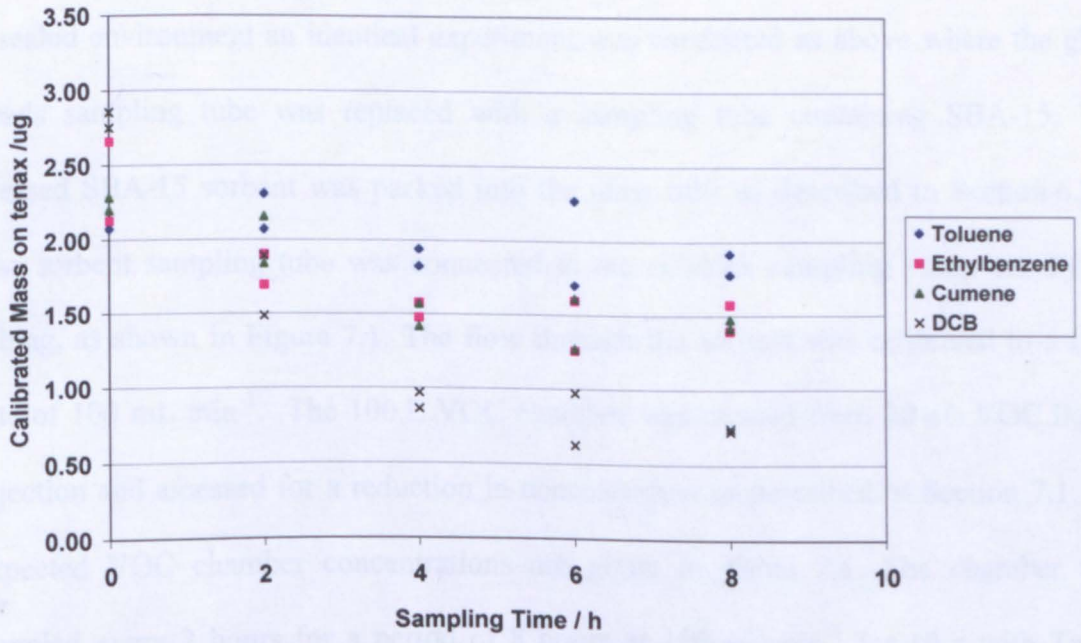

Figure 7.2: The calibrated VOC mass on each Tenax tube when sampling from a 100 L chamber made from 20 μL VOC injections containing a sampling tubes of glass beads.

After the equilibration time the masses of toluene, ethylbenzene, cumene and DCB trapped on the Tenax were 2.1, 2.4, 2.2 and 2.8 μg, therefore the chamber concentrations of the VOCs at 0 h were 126 000, 144 000, 132 000 and 168 000 μg m^{-3},

respectively. The chamber concentrations for each of the VOCs and their masses trapped on the Tenax tubes were lower than the theoretical calculated values in Table 7.1. After 4 h of sampling through the glass beads a decrease in all VOC masses trapped was evident. The largest loss in analyte mass trapped was DCB with the mass trapped decreasing from 2.8 μg to below 1 μg. The decrease in the masses trapped was thought to be due to surface adsorption of VOCs onto the glass beads. Theoretically 1.5 g of glass beads have an approximate surface area of 41.4 cm^2

7.2.1.2 Sampling inside a closed environment with SBA-15 present to reduce the VOC concentration

To determine the influence of 100 mg of SBA-15 had on the VOC concentration inside a sealed environment an identical experiment was conducted as above where the glass beads sampling tube was replaced with a sampling tube containing SBA-15. The pressed SBA-15 sorbent was packed into the glass tube as described in Section 6.2.1. The sorbent sampling tube was connected to the sidekick sampling pump via Tygon tubing, as shown in Figure 7.1. The flow through the sorbent was calibrated to a flow rate of 100 mL min^{-1}. The 100 L VOC chamber was created from 20 μL VOC liquid injection and assessed for a reduction in concentration as described in Section 7.1, the expected VOC chamber concentrations are given in Table 7.1. The chamber was sampled every 2 hours for a period of 8 hours at 100 mL min^{-1} for 10 s with Tenax sampling tubes, see Figure 7.3. To calibrate the exact masses of VOCs trapped by the Tenax tubes, VOC standards were used as described in Section 3.2.4. The concentration of the calibration standards and internal standard used are given in Section 7.1. When the chamber was sampled for 10 s at a rate of 100 mL min^{-1} the expected masses trapped onto the Tenax were 2.87, 2.87, 2.84 and 4.29 μg for toluene, ethylbenzene, cumene and dichlorobenzene, respectively. Experimentally the masses

trapped on the Tenax at 0 h for toluene, ethylbenzene, cumene, and dichlorobenzene were determined at 1.9, 1.6, 1.4 and 1.5 μg, respectively, giving starting chamber concentrations of 114 000, 96 000, 84 000, and 90 000 μg m^{-3}, respectively.

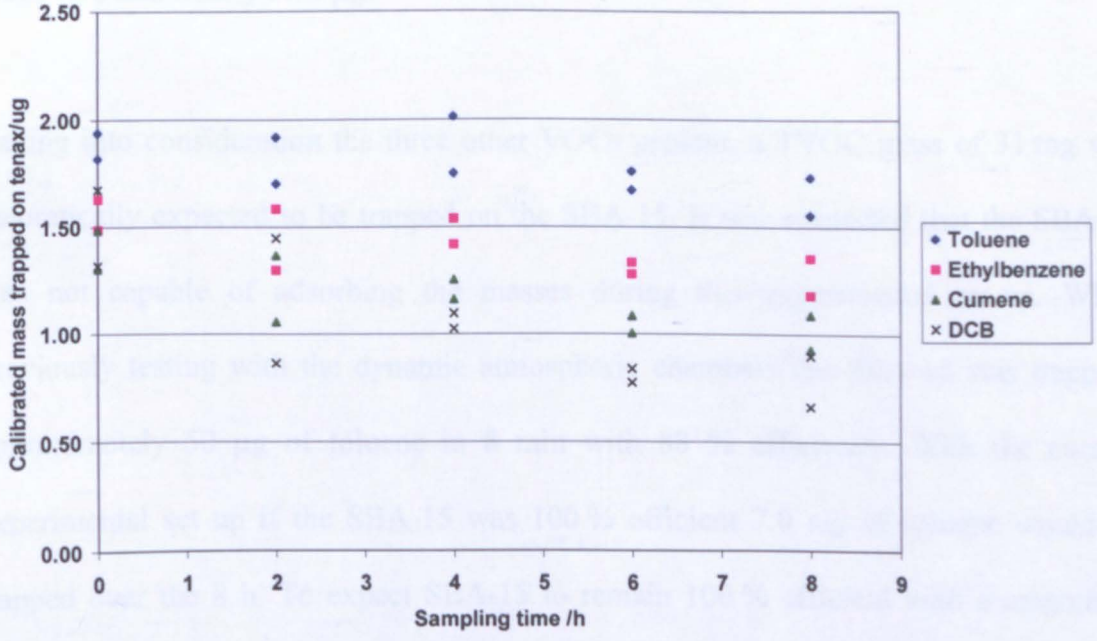

Figure 7.3: Masses of VOCs trapped on Tenax sampling tubes when sampling from a 100 L polluted environment generated for 20μL VOC injections within which SBA-15 was used to reduce the concentration.

The initial VOC environment had lower analyte concentrations than was generated in the previous glass beads experiment (see Figure 7.2). The reduction in chamber concentration was possibly due to either an incorrect injection of 20 μL into the sampling chamber or different environmental lab effects of temperature and pressure. Since all of the masses trapped are lower it was more likely to be the later.

Based on the initial atmospheric set-up concentrations, sampling conditions and the assumption that the SBA-15 sorbent was working at 100 % efficiency, predictions were made as to the expected masses trapped on the Tenax tubes, see example calculation in the Appendix. It was calculated that in each 2 h period the mass of toluene adsorbed

was 2.09, 1.84, 1.62, to 1.42 mg. As this mass of toluene would be removed from the chamber it would therefore lower the concentration within the chamber. Hence, the expected toluene masses trapped on the Tenax tubes should have reduced to 2.90, 2.55, 2.25, 1.98 and finally 1.74 μg.

Taking into consideration the three other VOCs present, a TVOC mass of 31 mg was theoretically expected to be trapped on the SBA-15. It was suspected that the SBA-15 was not capable of adsorbing the masses during this experimental set-up. When previously testing with the dynamic atmospheric chambers the SBA-15 was trapping approximately 50 μg of toluene in 8 min with 88 % efficiency. With the current experimental set up if the SBA-15 was 100 % efficient 7.0 mg of toluene would be trapped over the 8 h. To expect SBA-15 to remain 100 % efficient with a magnitude increase in the masses trapped was an overestimation of the capabilities of the sorbent therefore a reduced chamber concentration was required.

7.2.1.3 Sampling inside a closed cabinet with low VOC concentration with SBA-15

To reduce the VOC 100 L chamber concentrations, 1 μL injection volumes were used giving theoretical concentrations of 8700, 8700, 8600 and 13 000 μg m^{-3} for toluene, ethylbenzene, cumene and dichlorobenzene respectively. With lower VOC concentrations it was essential to increase the sampling time from 10 s to 60 s to collect a sufficient mass of analyte for analysis. With the decreased chamber concentrations a new range of calibration standards were required, and standards were prepared in the range 25 – 200 ng μL^{-1} while the internal standard was 100 ng μL^{-1}. To load the Tenax tubes with the calibration standards and to spike both the calibration tube and sampling tubes with an internal standard the direct injection port was used, see Sections 3.2.4 and

7.1 for details. When the chamber was sampled for 60 s at a rate of 100 mL min^{-1} the expected masses trapped onto the Tenax was 870, 870, 860, 1300 ng for toluene, ethylbenzene, cumene and dichlorobenzene, respectively. Experimentally the masses trapped on the Tenax at 0 h for toluene, ethylbenzene, cumene, and dichlorobenzene were determined at 540, 600, 744 and 630 ng, respectively, giving starting chamber concentrations of 5300, 5950, 7300 6200 µg m^{-3} respectively. The chamber was monitored over 8 h with one sample taken every two hours after the pump was started. The masses trapped on the Tenax tubes are given in Figure 7.4. The experimentally corrected theoretical losses based on the initial masses trapped at 0 h are also displayed in Figure 7.4.

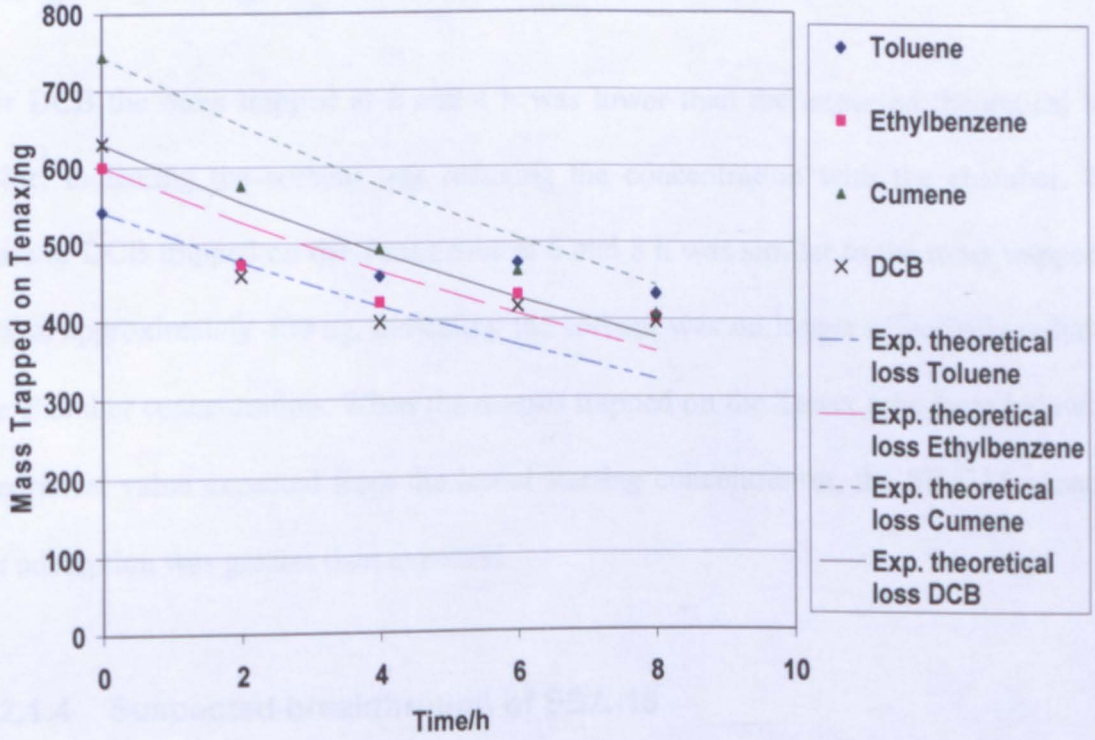

Figure 7.4: Mass of VOC trapped on Tenax when sampled from a 100 L chamber, created from 1µL VOCs injections and sampled for 60 s at 100 mL min^{-1}.

For toluene the mass trapped on the Tenax tube matches the theoretical loss after 2 h however after this two hour period the masses trapped are consistently higher than the theoretical value with the mass trapped of 478 ng, suggesting that toluene breakthrough of the SBA-15 had occurred. For ethylbenzene the masses trapped on the Tenax tube at 2 and 4 h was lower than expected indicating the sorbent was 100 % effective at reducing the concentration within the chamber. At 6 and 8 h the mass of ethylbenzene trapped on the Tenax was similar to the mass trapped at 4 h at approximately 400 ng, indicating the sorbent was no longer reducing the concentration within the chamber. For cumene the masses trapped on the Tenax tube at each 2 h interval were below the theoretical loss masses calculated indicating that the SBA-15 was effectively reducing the chamber concentration of cumene for the duration of the experiment, absorbing a total mass of 0.30 mg.

For DCB the mass trapped at 2 and 4 h was lower than the expected theoretical loss value, indicating the sorbent was reducing the concentration with the chamber. The mass of DCB trapped on the Tenax tube at 6 and 8 h was similar to the mass trapped at 4 h, at approximately 400 ng, indicating the sorbent was no longer effectively reducing the chamber concentration. When the masses trapped on the Tenax tube were below the theoretical value expected from the initial starting concentration, the SBA-15 capacity for adsorption was greater than expected.

7.2.1.4 Suspected breakthrough of SBA-15

It was suspected that breakthrough may be occurring during the VOC sampling experiment with low VOC concentrations. To examine this hypothesis a Tenax tube was placed inline behind the SBA-15 sampling tube during the experiment, indicated with an x in Figure 7.1. The experimental chamber was set up with 1 μL injections of VOCs.

The experimentally derived concentrations of toluene, ethylbenzene, cumene and dichlorobenzene generated inside the chamber were approximately 5900, 6200, 4200 and 8300 μg m^{-3}. The internal pump was started and the chamber was sampled for a 10 minutes. Initially a short sampling time was chosen to protect the GC-MS from overloading if saturation of SBA-15 was obtained quickly. The chamber was vented over night and the Tenax tube was removed and analysed. The TVOCs obtained on the Tenax tube were quantified as 0.65 μg giving the SBA-15 an adsorption efficiency of 97.4%. Since breakthrough did not occur at the low sampling time the experiment was repeated with an increased sampling time of 2 h. The VOC chamber concentrations and the Tenax trapped masses are detailed in Table 7.5. The chamber concentrations for toluene, ethylbenzene and cumene were similar therefore the total masses of each VOC passing over the sample of SBA-15 were approximately 80.8 μg. The masses of each VOC that passed through the SBA-15 and trapped on the subsequent Tenax tube varied greatly between the three VOCs of similar concentration.

Table 7.5: Mass of VOCs adsorbed on Tenax as breakthrough analytes from SBA-15

	Original Chamber conc. (μg m^{-3})	Mass on SBA-15 assuming 100% Efficiency (μg)	Mass trapped on Internal Tenax tube (μg)	% Efficiency of SBA-15	Chamber conc. after 2h (μg m^{-3})
Toluene	6787	81.4	53.0	35.0	6260
Ethylbenzene	6705	80.4	8.5	89.4	5682
Cumene	6721	80.7	0.1	99.9	5492
DCB	10157	121.9	2.7	97.7	7716
TVOC	**30370**	**364.5**	**64.3**	**82.4**	**25150**

The largest un-retained VOC was toluene which attributed 82.4 % of the TVOCs present on the Tenax. The total theoretical mass available for trapping, based on the original chamber concentrations, was 364.5 μg. The total mass detected on the breakthrough Tenax tube was only 64.3 μg, therefore 300.2 μg of VOCs were adsorbed on the 100 mg of SBA-15. The data suggests that after 2 hours of sampling the sorbent was not working at the capacity expected for toluene or ethylbenzene. The breakthrough data suggests that competitive adsorption may be taking place with the more polar analytes preferentially absorbing on the SBA-15.

7.2.2 Passive adsorption of VOCs by SBA-15

The investigation into the passive adsorption of VOCs by SBA-15 required a different experimental set up than used previously, see Section 7.1.2. Here a sealed 20 L chamber was used and 1 μL injection volumes were used to create the VOC atmosphere. The VOC concentrations of the chamber are given in Table 7.3. A 500 mg sample of SBA-15 was added to the chamber through the sampling port located at the top of the chamber. After a one hour equilibration time sampling occurred at a rate of 100 mL min^{-1} for 10 s. The chamber was sampled every 2 h over a period of 8 h. Each of the sampling tubes was spiked with o-xylene and the mass trapped on the Tenax tubes was determined from the calibration standards used as described in Section 3.2.4. The calibrated VOC masses trapped on the Tenax sampling tubes over the 8 h sampling time are displayed in Figure 7.5.

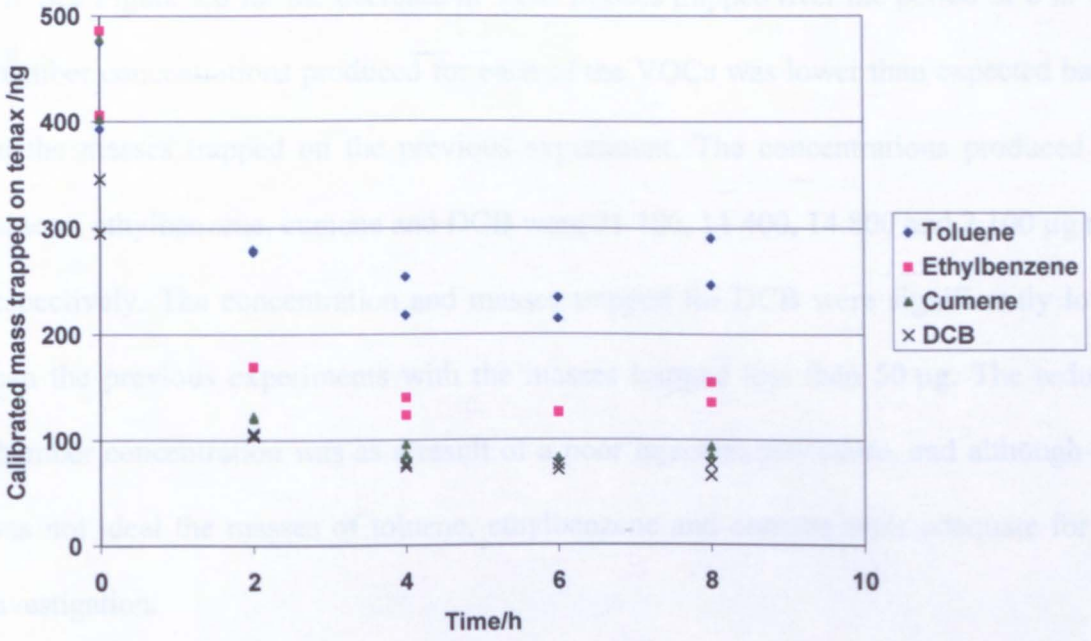

Figure 7.5: Passive adsorption of VOCs by SBA-15.

At time 0, before the addition of SBA-15, the VOC concentrations of toluene, ethylbenzene, cumene and DCB were 26 100, 26 800, 26 400 and 19 200 μg m^{-3} respectively. As indicated from Figure 7.5 there was a reduction in VOC concentration during the first two sampling periods. After 4 hours it was suspected that saturation had occurred with the mass of analytes trapped on the Tenax for toluene, ethylbenzene, cumene and DCB levelling of at around 240, 135, 88 and 74 ng, respectively. Given these trapped masses the chamber concentration for toluene, ethylbenzene, cumene and DCB was reduced to 14 400, 8 100, 5 300, 4 400 μg m^{-3}, respectively If the reduction of VOCs was due to the passive adsorption onto the SBA-15 then a second addition of SBA-15 would show another stepwise reduction of the VOC masses trapped on the Tenax. The experiment was repeated with a double addition of 500 mg SBA-15. The experiment was set up as previously described. The first addition of SBA-15 occurred after the 1 hour equilibration time. The chamber was sampled after 2 and 4 h, before the second addition of 500 mg of SBA-15. The chamber was again sampled after 6 and

8 h. See Figure 7.6 for the decrease in VOC masses trapped over the period of 8 h. The chamber concentrations produced for each of the VOCs was lower than expected based on the masses trapped on the previous experiment. The concentrations produced for toluene, ethylbenzene, cumene and DCB were 21 100, 11 400, 14 800 and 2 100 μg m^{-3}, respectively. The concentration and masses trapped for DCB were significantly lower than the previous experiments with the masses trapped less than 50 μg. The reduced chamber concentration was as a result of a poor injection procedure, and although this was not ideal the masses of toluene, ethylbenzene and cumene were adequate for the investigation.

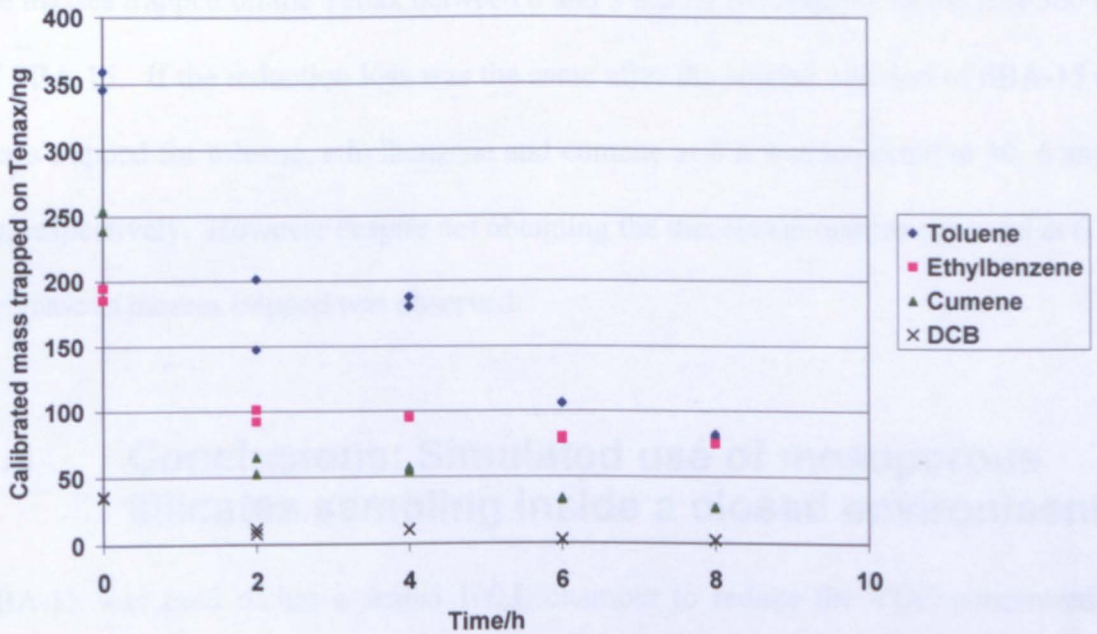

Figure 7.6: Passive adsorption of VOCs after a double addition of 500 mg of SBA-15

After 2 hours from the addition of SBA-15 a clear reduction in the masses trapped of toluene, ethylbenzene and cumene was evident. The masses trapped of these VOC reduced from 352, 190 and 246 ng to 172, 98 and 59 ng, respectively. The masses trapped after 4 h were similar to the masses trapped after two hours, the concentration of

toluene, ethylbenzene and cumene were reduced to 11 400, 5 900, 3 500 μg m^{-3}, respectively. If the observed loss in the masses trapped between the start time at 0 h and 2 h was due to the presence of the SBA-15 then a similar decrease in masses trapped would be expected from the periods of 4 to 6 h. At 6 h the masses trapped on the Tenax for toluene, ethylbenzene and cumene were 102, 80 and 33 ng, respectively. The masses trapped after 8 h for toluene, ethylbenzene and cumene were 80, 76 and 27 ng, respectively, giving a final chamber concentration of 4 800, 4 600 and 1600 μg m^{-3}. The observed decrease in masses trapped on the Tenax between 4 and 6 h, after the second addition of SBA-15, was not as prevalent as expected based on the reduction in the masses trapped on the Tenax between 0 and 2 h after the addition of the first 500 mg of SBA-15. If the reduction loss was the same after the second addition of SBA-15 the mass trapped for toluene, ethylbenzene and cumene at 6 h was expected at 30, 6 and 0 ng, respectively. However despite not obtaining the theoretical masses expected at 6 h a decrease in masses trapped was observed.

7.3 Conclusions: Simulated use of mesoporous silicates sampling inside a closed environment

SBA-15 was used within a sealed 100 L chamber to reduce the VOC concentration. When the chambers were created from VOC injection volumes of 20 μL the expected reduction in chamber concentration was not evident due to the increased adsorption capacity expected of the 100 mg sorbent. When the chamber was created with lower VOC concentration using 1 μL injections the expected mass losses were in evidence. This was further in evidence when a Tenax tube was attached to the rear of a SBA-15 sampling tube. When sampling the chamber for two hours relatively little mass of ethylbenzene, cumene and DCB were seen on the Tenax sampling tube; further

evidence that the SBA-15 was suitable for the adsorption of VOCs. However the adsorption of toluene by SBA-15 is not as efficient as the other VOCs used in the investigation. The difference in adsorption may be due to a preferential adsorption of more polar molecules by SBA-15. Further evidence is required to substantiate this theory. The reduction in VOC chamber concentrations was also in evidence when using the SBA-15 to passively adsorb the VOCs.

8 CONCLUSIONS AND FUTURE WORK

The overall aim of this project was to produce a mesoporous silicate as an indoor air pollutant scavenger for the deployment in museums and indoor environments such as offices and households. In order to achieve this, future work will have to be carried out on the mesoporous silicates in conjunction with the atmospheric chamber sampling system. The generation of VOC environments from the liquid injection of small volumes of VOCs proved to be problematic due to the inconsistent VOC chamber concentrations associated with changes in atmospheric temperature, pressure and the difficulties associated in the transfer of small volumes of volatile liquid accurately. Despite those difficulties, a sampling method has been validated and can produce linear relationships for the VOCs studied. Using a 10-60 s sampling period, the VOC sampling method was valid for collection of VOCs between 1.58 and 14.17 μg. A drawback of using the bell chamber system involved the daily generation of the VOC environment and the limited number of samples allowed before the requirement of a new chamber. The development of a dynamic chamber overcame these drawbacks. The use of pierced permeation vials containing 1 mL volume of analyte was a low cost alternative for the creation of a range of VOCs within one environment. The VOC concentrations calculated from the theoretical equations was inaccurate, most likely due to wall loss, therefore to precisely determine the exact VOC chamber concentrations the use of calibration standards were required. In order to use calibration standards the direct injection port has shown to be an appropriate method for the deployment of the calibration standards on to the Tenax sampling tubes. The use of the direct injection port allowed for the VOC masses between 25 to 2000 ng to be deposited linearly on the Tenax tubes with a repeatability of less than 10 %.

Mesoporous silicates were successfully prepared using TEOS with either CTAB or triblock copolymers as surfactant templating agents. The resultant sorbents were characterised by nitrogen adsorption, x-ray diffraction, SEM and TEM. The sorbents were packed into glass tubes which provided a suitable method for active sampling. When the sorbent materials were directly packed into the glass housings sampling problems occurred with air flow restrictions. To compensate the sorbents were pressed and crushed to particle sizes 325-400 μm, before packing. VOCs were actively sampled from the atmospheric chambers onto the sorbent. A number of improvements should be made to the packing of sorbents for sampling. The optimal particle size should be determined along with the optimal bed length and sorbent mass to glass bead ratio required to maximise the sorbents adsorption efficiency. Once the packing has been optimised further optimisation of the sampling flow rates through the sorbent is required. After the optimisation of the packing and sampling empty Tenax sampling tubes could be employed to house the mesoporous silicate. This would allow the sampled silicates to be introduced into the TDU-GC-MS, therefore quantification of VOCs trapped on the mesoporous silicate to be validated. Furthermore this method could help examine the adsorption process that occurred.

From the initial testing of the percentage adsorption efficiencies several of the mesoporous materials produced were shown to be possible candidates as an indoor air pollutant scavengers, principally SBA-15, MCM-41-MF2, SBA-16 and SM-01. However there are many mesoporous silicates that have not been investigated here which could be potential indoor air pollutant scavengers. Further investigation into the strength of the adsorption of the VOCs onto the mesoporous silicates would be beneficial in determining the most appropriate silicate as an indoor air pollutant scavenger. From the combination of most desirable mesoporous characteristics and the

adsorption efficiency obtained from the initial testing SBA-15 was further investigated as an indoor air pollutant scavenger.

SBA-15 was used to extract analytes from a closed polluted environment with VOC concentrations between 5300 and 7300 $\mu g\ m^{-3}$. The VOC concentrations generated were the lowest possible levels within the experimental design of chambers used in this project, and were only 5 times greater than the concentrations associated with SBS. The SBA-15 sorbent was shown to reduce the concentration of the polluted environment by examination of the masses trapped on Tenax. The levels of reduction in toluene, ethylbenzene, cumene and DCB concentrations varied, with the concentration of toluene least reduced. Some toluene was observed when checking for breakthrough of SBA-15. The results obtained on this thesis have shown the novel use of mesoporous silicate materials as alternative low cost VOC sorbent materials, performing, in some cases, as well as commercially available materials. Further investigation is required to determine if competitive adsorption is occurring between the selected VOC analytes studied.

Furthermore before SBA-15 can be used as an indoor air scavenger an investigation into the maximum adsorption of the sorbent must be undertaken, therefore when problem environments have been identified and the pollutant levels quantified the mass of sorbent and exposure time can be estimated for reduction or elimination of the problematic pollutants. The determination of breakthrough masses is critical for the chosen mass of sorbent.

Functionalisation of the sorbent with propyl amine has shown to be beneficial to the strength of adsorption of formaldehyde. However residual toluene remains from the grafting process which is released during active sampling. Therefore if the functionalised sorbent is used to remove formaldehyde a secondary sorbent is required

to adsorb the released toluene. Alternatively, the possibility of toluene removal after grafting and before sampling should be investigated. Functionalised mesoporous silicates have shown potential as sorbents for the removal of indoor air pollutants however more investigations will have to be carried out into the optimised surface coverage and other types of functionalisation possible for the adsorption of formaldehyde i.e. thiols and metals. The investigation into alternative functionalisation may lead to the future use of mesoporous silicates as adsorbents for acetic and formic acid although a multi sorbent bed may be required to target all the pollutants in the museum environment. Currently, no other commercially available sorbent removes formaldehyde with the same efficiency as the functionalised mesoporous materials synthesised in this project.

Functionalised and unfunctionalised silicate materials offer a viable alternative to the commercial sorbents currently used by museum curators. Sorbents such as charcoal have several problems associated with their use, which would be eliminated through the use of silicate sorbents. Charcoal is difficult to handle due to its black colourisation and the potential contamination of displays with charcoal particulates is a problem for curators. Charcoal has the additional problem associated with the re-release of trapped pollutants into the environment from a change of temperature or relative humidity. The use of silicate sorbents offers an alternative solution for curators.

APPENDIX: THEORETICAL LOSS CALCULATION

A 20 μL (0.02 mL) injection volume of toluene was transferred to the 100 L chamber. The density of toluene is 870 mg mL^{-1}, so the total mass of toluene transferred to the chamber was 17.4 mg, giving an initial chamber concentration of 0.174 mg L^{-1}. At that time (see t_0 in Table A.1) the chamber was actively sampled using Tenax and an external pump (100 mL min^{-1} for 10 s) thereby removing 0.0167 L of polluted air from the chamber. During active sampling, 0.0029 mg of toluene would be removed from the air reducing its vapour phase concentration to 0.173971 mg L^{-1}.

At the beginning of the next time period (see t_2 in Table A.1) a pump inside the chamber was switched on and the polluted air was drawn over a sorbent for 120 min at a sampling rate of 100 mL min^{-1}; drawing 12 L of polluted air over the sorbent. If the sorbent was 100 % efficient it would have removed 2.0877 mg of toluene from the air, reducing the toluene vapour phase concentration to 0.1530969 mg L^{-1}. To measure the reduced concentration of toluene in the chamber active sampling was again performed using Tenax and the external pump (100 mL min^{-1} for 10 s). If the chamber concentration had been successfully reduced to 0.1530969 mg L^{-1}, the mass of toluene trapped during active sampling would be 0.002552 mg. After active sampling, the concentration of toluene inside the chamber would have reduced slightly to 0.153069 mg L^{-1}.

This process of active sampling before and after extraction of toluene from the air was repeated 3 times, each time the extraction process lasted 2 hours. The chamber concentrations and masses expected before and after each extraction process (labelled t_4,

t_6, and t_8) are given in Table A.1. Similar calculations were also performed for the extraction of ethylbenzene, cumene or dichlorobenzene and the masses and concentrations obtained are given in Tables A.2 – A.4, respectively.

Table A.1: Toluene masses and concentrations used in the theoretical loss experiment.

Sampling time	Initial chamber concentration (mg L^{-1})	Expected mass trapped by synthesized sorbent (assuming 100% Efficiency) (mg)	New reduced chamber concentration (mg L^{-1})	Mass removed from system by Tenax (mg)	Adjusted chamber concentration (mg L^{-1})
t_0	0.174000	N/A	N/A	0.002900	0.173971
t_2	0.173971	2.087652	0.153094	0.002552	0.153069
t_4	0.153069	1.836828	0.134791	0.002245	0.134678
t_6	0.134678	1.616139	0.118517	0.001975	0.118497
t_8	0.118497	1.421965	0.104277	0.001738	0.104260

Table A.2: Ethylbenzene masses and concentrations used in the theoretical loss experiment.

Sampling time	Initial chamber concentration (mg L^{-1})	Expected mass trapped by synthesized sorbent (assuming 100% Efficiency) (mg)	New reduced chamber concentration (mg L^{-1})	Mass removed from system by Tenax (mg)	Adjusted chamber concentration (mg L^{-1})
t_0	0.174000	N/A	N/A	0.002900	0.173971
t_2	0.173971	2.087652	0.153094	0.002552	0.153069
t_4	0.153069	1.836828	0.134791	0.002245	0.134678
t_6	0.134678	1.616139	0.118517	0.001975	0.118497
t_8	0.118497	1.421965	0.104277	0.001738	0.104260

Table A.3: Cumene masses and concentrations used in the theoretical loss experiment.

Sampling time	Initial chamber concentration (mg L^{-1})	Expected mass trapped by synthesized sorbent (assuming 100% Efficiency) (mg)	New reduced chamber concentration (mg L^{-1})	Mass removed from system by Tenax (mg)	Adjusted chamber concentration (mg L^{-1})
t_0	0.172000	N/A	N/A	0.002867	0.171971
t_2	0.171971	2.063656	0.151335	0.002522	0.151310
t_4	0.151310	1.815715	0.133152	0.002219	0.133130
t_6	0.133130	1.597563	0.117155	0.001953	0.117135
t_8	0.117135	1.405621	0.103079	0.001718	0.103062

Table A.4: DCB masses and concentrations used in the theoretical loss experiment.

Sampling time	Initial chamber concentration (mg L^{-1})	Expected mass trapped by synthesized sorbent (assuming *100%* Efficiency) (mg)	New reduced chamber concentration (mg L^{-1})	Mass removed from system by *Tenax* (mg)	Adjusted chamber concentration (mg L^{-1})
t_0	0.260000	N/A	N/A	0.004333	0.259957
t_2	0.259957	3.119480	0.228762	0.003813	0.228724
t_4	0.228724	2.744685	0.201277	0.003355	0.201243
t_6	0.201243	2.414920	0.177094	0.002952	0.177065
t_8	0.177065	2.124776	0.155817	0.002597	0.155791